THE ROLE OF MUSCLE-ENRICHED MICRORNAS AS MARKERS OF FAILED MYOCARDIAL REPERFUSION

By

Jose Anselmo Coelho Lima Junior, MD

Thesis submitted for the degree of
Doctor of Philosophy

Institute of Cellular Medicine

October 2018

Abstract

The advent of primary percutaneous coronary intervention (PPCI) for the treatment of ST-elevation myocardial infarction (STEMI) has significantly reduced mortality rates in this population. However, coronary artery disease remains a leading cause of morbidity and death worldwide. This may be a consequence of inadequate myocardial reperfusion despite reestablishment of coronary artery patency following PPCI. Failed myocardial reperfusion is associated with worse prognosis but usually passes undetected, as current diagnostic methods are not routinely available. The aim of my PhD was to investigate the plasmatic kinetics of muscle-enriched micro ribonucleic acids (microRNAs) following PPCI as well as their association with cardiac damage, function and the phenomenon of failed myocardial reperfusion.

Firstly, I retrospectively analysed the prognostic importance of cardiac troponins, which are established markers of myocardial injury, in a large cohort (n = 4,914) of STEMI patients treated with PPCI. Troponin levels routinely measured at 12 hours post-reperfusion were not associated with mortality, highlighting the need for identification of new prognostic markers in this population. To overcome methodological issues for microRNA quantification in plasma samples from STEMI patients, I validated an endogenous microRNA (miR-425-5p) as a control for real-time polymerase chain reaction (RT-qPCR) data normalisation. Subsequent microRNA screening and kinetics analyses revealed that the muscle-enriched miR-1 and miR-133b are rapidly released into the circulation following PPCI, reaching an initial peak at 30min and a second peak at 90min post-PCI. The presence of a second peak seemed to be associated with a higher index of microvascular resistance, a surrogate marker of failed myocardial reperfusion. In addition, miR-1 and miR-133b levels at 30min and 90min post-PPCI were associated with microvascular obstruction measured by cardiac MRI, another parameter of unsuccessful myocardial reperfusion. Finally, miR-1 and miR-133b levels were significantly elevated in a subgroup of STEMI patients with larger infarcts and worse left ventricular function and remodelling 3 months after PPCI. These findings suggest a potential new role for muscle-enriched microRNAs as tools for early identification of failed myocardial reperfusion and prognostic stratification in STEMI patients.

Declaration

This thesis is submitted for the partial fulfilment of the requirements for the degree of Doctor of Philosophy at Newcastle University. The research here described was conducted at the Institute of Genetic Medicine, Newcastle University between September 2014 and September 2017 under the supervision of Professor Ioakim Spyridopoulos. I declare that all of the work here described is my own, except where otherwise acknowledged in the text. My studies were funded by a PhD overseas scholarship from CAPES Foundation.

I certify that none of the material offered has been previously submitted by me for a degree or other qualification at this or any other university.

Jose Anselmo Coelho Lima Junior
October 2018

Acknowledgements

First, I would like to thank my supervisors for all the support and encouragement they provided me with. This work would not be possible without you. In particular, I would like to thank Prof Ioakim Spyridopoulos, who has been a true mentor and inspiration for me and with whom I have the utmost pleasure to directly work with and learn from. Also, a special thanks to Prof Simi Ali, who has always been extremely kind and helpful in supervising my work. In addition, I would like to thank my co-supervisors Prof John Kirby and Dr Jeremy Palmer for their support and valuable input.

My PhD studies were funded by the CAPES Foundation, Brazilian Ministry of Education, for which I will be forever grateful.

I would also like to thank all the colleagues who enormously contributed to this work: Dr Ashfaq Mohammed, Dr Suzanne Cormack, Adnan Ali, and Samuel Jones. They recruited the participants and collected the blood samples here analysed. Particularly, Samuel and Adnan who helped with the work described in chapters 4 and 5. In addition, I would like to thanks Prof Kimon Stamatelopoulos and Dr Giorgios Giorgiopoulos for their fundamental assistance with the statistical analysis described in chapter 3. The PhD can be a very daunting experience and my colleagues from IGM definitely made the journey smoother. Thank you Lilia, Emily, Anna, Kate, and Lauren!

Lastly, but not least importantly, I would like to thank my family and my friends, for all the support and understanding when I could not be present. I dedicate this work for you! No words would ever be able to express my gratitude to you!

Publications

Manuscripts

1. **Coelho-Lima J**, Mohammed A, Cormack S, Jones S, Das R, Egred M, Panahi P, Ali S, Spyridopoulos I. Overcoming heparin-associated RT-qPCR inhibition and normalization issues for microRNA quantification in patients with acute myocardial infarction. *Thromb Haemost*, 2018. In press. DOI: 10.1055/s-0038-1660437

2. Richardson GD, Sage A, Bennaceur K, Al Zhrany N, **Coelho-Lima J**, Dookun E, Draganova L, Saretzki G, Breault DT, Mallat Z, Spyridopoulos I. Telomerase mediates lymphocyte proliferation but not the atherosclerosis-suppressive potential of regulatory T-cells. *Arterioscler Thromb Vasc Biol*, 2018; 38 (6): 1283 – 1296. DOI: 10.1161/ATVBAHA.117.309940

3. **Jose Coelho-Lima**, Ioakim Spyridopoulos. Non-coding RNA regulation of T cell biology: implications for age-associated cardiovascular diseases. *Exp Gerontol*, 2017. In press. DOI: 10.1016/j.exger.2017.06.014

4. **Jose Lima Junior**, Jonathan A Batty, Hannah Sinclair, Vijay Kunadian. MicroRNAs in ischemic heart disease: from pathophysiology to potential clinical applications. *Cardiol Rev*, 2017; 25 (3):117 - 125. DOI: 10.1097/CRD.0000000000000114

5. Batty JA, **Lima Jr JAC**, Kunadian V. Direct cellular reprograming for cardiac repair and regeneration. *Eur J Heart Fail*, 2016; 18(2):145 – 156. DOI: 10.1002/ejhf.446

6. **Jose Lima Jr**, Vijay Kunadian. Vitamin D: evidence for an association with coronary collateral circulation development? *Postep Kardiol Inter*, 2015; 11, 3(41): 174-176. DOI: 10.5114/pwki.2015.54008

7. **Jose Coelho-Lima**, Javed Ahmed, Georgios Georgiopoulos, Syeda E.R. Adil, David Gaskin, Fareen Ahmed, Haaris Ahmed, Alan Bagnall, Konstantinos Stellos, Kimon Stamatelopoulos, Ioakim Spyridopoulos. Pre-procedural cardiac troponin predicts outcome in patients with ST elevation myocardial infarction undergoing primary PCI. (*Manuscript submitted to Annals of Internal Medicine*)

8. **Jose Coelho-Lima**, Ashfaq Mohammed, Suzanne Cormack, Samuel Jones, Adnan Ali, Pedram Panahi, Alan Bagnall, Simi Ali, Ioakim Spyridopoulos**.** Cardiac-enriched microRNA kinetics analysis unveils potential new markers of failed myocardial reperfusion in STEMI patients. (*Manuscript submitted to Clinical Chemistry*).

Table of Contents

List of Figures

List of Tables

List of Abbreviations

3'UTR	3' untranslated region
AGO-2	Argonaute 2
ANOVA	Analysis of variance
BD	Becton Dickinson
CABG	Coronary artery bypass grafting
CAD	Coronary artery disease
cDNA	Complementary DNA
CI	Confidence interval
Cq	Quantification cycle
cTn	Cardiac Troponin
cTnI	Cardiac Troponin I
cTnT	Cardiac Troponin T
CV	Coefficient of variation
DGCR8	DiGeorge syndrome critical region 8
DNA	Deoxyribonucleic acid
EC	Endothelial cell
ECG	Electrocardiogram
EDTA	Ethylenediaminetetraacetic acid
EDV	End diastolic volume
ELISA	Enzyme-linked immunosorbent assay
ESV	End systolic volume
FACS	Fluorescence activated cell sorting
FITC	Fluorescein isothiocyanate
FSC	Forward scatter
g	Grams
HAEC	Human aortic endothelial cells
h	Hours
HR	Hazard ratio

HUVEC	Human umbilical vein endothelial cells
ICAM-1	Intercellular adhesion molecule 1
IL	Interleukin
IMH	Intramyocardial haemorrhage
IMR	Index of microvascular resistance
IQR	Interquartile range
IS	Infart size
kg	Kilograms
KLF	Krüppel-like factors
LAD	Left anterior descending artery
LDL	low density lipoprotein
LGE	Late gadolinium enhancement
LV	Left ventricular/ventricular
LVEF	Left ventricular ejection fraction
MACE	Major adverse cardiovascular events
mg	Milligrams
MI	Myocardial infarction
min	Minutes
miRISC	miRNA-induced silencing complex
miR / miRNA	MicroRNA
ml	Millilitres
mmol	Millimoles
MP	Microparticle
MRI	Magnetic resonance imaging
mRNA	Messenger RNA
MVO	Microvascular obstruction
ng	Nanograms
nm	Nanometer
nt	Nucleotide
NHS	National Health Service
NSTEMI	Non-ST elevation myocardial infarction

OSS	Oscillatory shear stress
oxLDL	oxidized low density lipoprotein
PBS	Phosphate buffered saline
PCI	Percutaneous coronary intervention
PCR	Polymerase Chain Reaction
PPCI	Primary percutaneous coronary intervention
Pre-cTn	Pre-procedural cardiac troponin
Post-cTn	Post-procedural cardiac troponin
REC	Research ethics committee
RNA	Ribonucleic acid
RT-qPCR	Reverse transcription polymerase chain reaction
SD	Standard deviation
SEM	Standard error of the mean
SPECT	Single-photon emission computerized tomography
SSC	Side scatter
SSFP	Steady-state free precession
STEMI	ST-elevation myocardial infarction
STIR	Short inversion time inversion recovery
TASH	Transcoronary ablation of septal hypertrophy
TIMI	Thrombolysis in Myocardial Infarction
TR	Repetition time
VAMP8	Vesicle-associated membrane protein 8
VCAM-1	Vascular cell adhesion molecule 1
VSMC	Vascular smooth muscle cells
µl	Microlitres
µm	Micrometer

Chapter 1. Introduction

1.1. Preamble

Despite recent advances in cardiovascular research and development of modern therapeutic strategies for cardiovascular disease, coronary artery disease (CAD) remains the leading cause of mortality worldwide (Moran et al., 2014a, Moran et al., 2014b, Moran et al., 2014c). Coronary artery disease encompasses a spectrum of clinical syndromes that share atherosclerosis-related myocardial ischaemia as a common pathophysiological mechanism. At the most serious end of this spectrum is ST-elevation myocardial infarction (STEMI), which is characterised by irreversible cardiomyocyte injury due to acute and sustained myocardial ischaemia. Current treatment for STEMI aims to urgently re-establish coronary blood flow by implantation of intra-vascular stents via percutaneous coronary intervention (PCI). Despite achievement of optimal coronary perfusion, a failure of myocardial reperfusion can occur in up to 50% of STEMI patients undergoing PCI and is associated with worse clinical outcome. Failed myocardial reperfusion is not routinely assessed as the available imaging and invasive techniques that can be used to detect it are not presently feasible for daily clinical practice. The focus of this thesis will be the investigation of a potential role for circulating microRNAs (miRNAs) as non-invasive, biochemical markers of failed myocardial reperfusion in STEMI patients.

1.2. Acute Myocardial Infarction

1.2.1. Socio-economic burden of coronary artery disease

Coronary artery disease is an important public health problem worldwide. Mortality rates associated with CAD have increased in the last decades (>7 million in 2010 vs. 4.5 million in 1980), despite a trend in reduction of deaths in high-income nations (Moran et al., 2014a). This is partially explained by increasing mortality numbers in medium to low-income regions, especially in Eastern Europe, central and south Asia and Middle Eastern countries. Also, with the population ageing phenomenon, the group in which CAD death rates increased the most was that comprised by individuals ≥ 80 years old (Moran et al., 2014a). In the United Kingdom, CAD was the leading cause of mortality in 2010 and the average number of years of life lost due to CAD was greater than the average of the original 15 European Union members, USA, Canada, Australia, and Norway combined (Murray et al., 2013). Nevertheless,

the burden of CAD is not only associated with mortality but also with morbidity. As an increasing number of individuals are living with the disease, CAD impact on morbidity and quality of life is very significant. Between 1990 and 2010, it has been reported a global increase of 29% in disability-adjusted life years, a measure of years of disability lived with 3 non-fatal CAD sequelae: non-fatal acute myocardial infarction, angina pectoris, and ischaemic heart failure (Moran et al., 2014a). In the UK, the prevalence of individuals living with some form of CAD was estimated to be 2.3 million in 2013 (Townsend et al., 2014). Consequently, the costs associated with the management of the disease are very high.

The economic burden of CAD on healthcare systems around the globe is enormous. In 2012/2013, the estimated expenditure of the NHS on the treatment of CAD, including all levels of care, was £1.597 billion (Townsend et al., 2014). In developing countries, where the percentage of the gross domestic product (GDP) destined to healthcare is usually smaller than that of developed countries, the relative burden of CAD can be even worse. For instance, in South Korea the total cost of acute myocardial infarction management alone was estimated to be USD1.177 billion in 2012 (Seo et al., 2015). Therefore, advances in the understanding of the disease pathophysiology and improved prognostic stratification strategies could not only help to decrease the mortality and morbidity figures but also to optimise the expenditure of public funds with CAD.

1.2.2. Coronary artery disease pathophysiology

Atherosclerosis is the cornerstone pathological mechanism of CAD. Atherosclerosis is defined as a chronic low-grade inflammatory process of the *tunica intima* of medium and large arteries (Libby, 2002). Atherogenesis initiates with the trafficking of circulating inflammatory cells, such as monocytes and T lymphocytes, into the arterial walls (Hansson and Libby, 2006). This process is triggered by various stimuli (e.g. dyslipidaemia, hyperglycaemia, pro-inflammatory cytokines released by the adipose tissue, bacterial products, and oscillatory shear stress), which ultimately induce the expression of leukocyte adhesion molecules on the luminal surface of endothelial cells. Once in the intima, these leukocytes orchestrate a series of pro-inflammatory signals with the adjacent cells in their microenvironment, i.e. endothelial cells and vascular smooth muscle cells (VSMC). Mediators of inflammation and immunity, such

as leukotrienes, prostanoids, cytokines, and histamine, regulate vascular tone, increase vascular permeability, promote more circulating leukocyte recruitment, and migration of VSMCs from the tunica media to the intima (Libby and Theroux, 2005). In the intima, VSMCs proliferate and generate a complex extracellular matrix (EM). Some components of the EM, for instance proteoglycans, bind to lipoproteins and prolong their permanence in the intima, increasing lipoprotein susceptibility to oxidative modifications (Williams and Tabas, 1998). Oxidized-lipoproteins are internalized by macrophages, generating lipid-enriched cells, the so-called foam cells. Foam cells apoptosis in atherosclerotic lesions results in release of tissue factor and lipids to the extracellular space, which can coalesce and form the lipid or "necrotic" core of atherosclerotic plaques (Bogdanov et al., 2003). Furthermore, with the lesion progress, calcification can occur by mechanisms similar to osteogenesis (Demer, 2002).

Atherosclerotic lesions development can alternate periods of slow and fast growth. Plaques do not necessarily grow towards the arterial lumen. Actually, by most of their development time plaques grow outwards, due to a vascular remodelling mechanism (Clarkson et al., 1994). Therefore, a significant burden of disease may exist and be undetected by coronary angiography, as the technique can only evaluate the inner vascular wall. This observation has changed the concept of atherosclerosis as being a delimited, focal process to be understood as a systemic, diffuse process. In fact, it has been described that only when the plaque volume reaches 40% the arterial lumen begins to narrow (Ambrose et al., 1988). Intraluminal coronary narrowing caused by these large, stable atherosclerotic plaques results in transient inappropriate blood supply to the myocardium in times of increased oxygen demand, e.g. exercise, which is clinically manifested as stable angina pectoris.

1.2.3. Acute coronary syndromes

Some atherosclerotic lesions are characterized by a thin, fibrous cap and abundant lipid core with high number of inflammatory cells and lower number of VSMCs, the so-called vulnerable plaques or thin-capped fibroatheromas (Davies, 1996). Eventually, these vulnerable plaques can suffer rupture, erosion or haemorrhage, exposing their pro-thrombotic content to the blood stream, triggering the formation of an intracoronary thrombus (Davies and Thomas, 1985, Falk et al., 2013). Several

mechanisms contribute to thrombogenesis following plaque rupture: (i) platelet activation, followed by adhesion and aggregation, promoted by the contact with collagen present in the EM of disrupted plaques; (ii) coagulation cascade activation by macrophage and VSMC-released tissue factor; (iii) pro-coagulant conditions, such as obesity and diabetes, which increase circulating levels of plasminogen activator inhibitor-1 (PAI-1) (Libby and Theroux, 2005). The thrombus can suffer spontaneous lysis, or cause incomplete or complete coronary obstruction, in this case leading to severe acute ischemia distal to the site of blockage, clinically manifested as acute coronary syndromes (ACS).

Depending on the duration, location, and extent of coronary blockage, ACS can present as three distinct clinical entities: (i) unstable angina (UA); (ii) non-ST elevation myocardial infarction (NSTEMI); and (iii) STEMI. In UA, acute coronary occlusion provokes clinical symptoms of myocardial ischemia, such as chest pain, and ischemic changes on the electrocardiogram (ECG), e.g. T wave inversion, but it is usually associated with partial or transient coronary obstruction, which is not sufficient to cause the release of myocardial necrosis biomarkers, such as cardiac troponins (cTn). Acute myocardial infarction is characterised by the present of clinical symptoms of myocardial ischemia associated with detectable release of myocardial necrosis biomarkers (Ambrose and Singh, 2015). Electrocardiographic changes distinguish between NSTMI and STEMI, as NSTEMI patients usually present ST segment depression (>2mm in at least two contiguous leads) and T wave changes whereas the ECG pattern of STEMI is ST elevation (in two or more contiguous leads ≥ 0.2 mV in V1-V3 or > 0.1 mV in the other leads) or new onset left bundle branch block (Alpert et al., 2000).

1.2.4. Diagnostic criteria and clinical classification of acute MI

The European Society of Cardiology recently published the 4th Universal definition of myocardial infarction, which outlines the criteria for clinical diagnosis and classification of myocardial infarction (Thygesen et al., 2018). Myocardial infarction is defined by the presence of acute myocardial injury [as evidenced by rise and/or fall of cTn with at least one value > 99th percentile of the upper reference limit (URL)] in the setting of myocardial ischaemia (Thygesen et al., 2018). Acute myocardial ischaemia requires at least one of the following criteria: symptoms (e.g. chest pain, dyspnoea,

sweating, vomiting), new ischaemic ECG changes, development of pathological Q waves, imaging evidence of loss of viable myocardium or wall motion abnormalities, and/or identification of a coronary thrombus by angiography or post-mortem autopsy (Thygesen et al., 2018). Apart form the electrocardiographic criteria described in the previous section, MI can also be classified according to the underlying pathological mechanism or clinical scenario into 5 types (Thygesen et al., 2018):

- Type 1: caused by atherothrombotic CAD, usually following atherosclerotic plaque rupture or erosion
- Type 2: the underlying pathological mechanism is an imbalance between myocardial oxygen supply and demand. For example, stressors such as acute bleeding (with a drop in haemoglobin levels) or sustained tachyarrhythmia may precipitate MI type 2 due to reduced oxygen availability or increased demand in an already ischaemic myocardium
- Type 3: defined by cardiac death in patients with ischaemic symptoms or ECG but who died before blood samples could be obtained or changes in cTn levels could be identified or when MI is diagnosed by autopsy
- Type 4: percutaneous coronary intervention-related MI. Defined by elevation > 5 times the 99th cTn percentile URL in patients with normal cTn prior to the procedure or > 20% rise in cTn if baseline levels were already > 5 times the 99th cTn percentile URL
- Type 5: coronary artery bypass graft (CABG)-associated MI. Diagnosis requires a cTn value > 10 times the 99th cTn percentile URL in the initial 48h following CABG in the presence of normal baseline cTn values

1.2.5. Clinical complications and prognosis of MI

In recent years, prognosis following MI, especially regarding mortality, has significantly improved with the development and wider employment of new therapeutic strategies (Menees et al., 2013, Pedersen et al., 2014). Nonetheless, whilst more patients are surviving MI the number of individuals living with its complications is also increasing (Moran et al., 2014a).

In the acute phase following MI, left ventricular (LV) dysfunction represents one of the most common complications. The incidence of LV dysfunction varied between 17% and 28% during hospitalisation due to MI or in the 90 days thereafter in large

population studies (Hung et al., 2013, Gjesing et al., 2014, Desta et al., 2015). Acute LV dysfunction can occur due to a combination of cardiomyocyte loss, myocardial stunning, acute mitral regurgitation secondary to papillary muscle dysfunction, and decompensation of pre-existing heart failure (Cahill and Kharbanda, 2017). It is a strong, independent predictor of clinical outcome, including major adverse cardiovascular events (re-infarction, congestive heart failure) and death, following MI (van Kranenburg et al., 2014, Desta et al., 2015).

Myocardial infarction can also lead to the development of chronic heart failure. Chronic heart failure is a clinical syndrome characterised by progressive impairment in the ventricle ability to fill or eject blood due to any structural or functional cardiac disorder (Yancy et al., 2013). In the healing phase that follows MI, the interplay between several factors such as inflammation, fibrogenesis, and neurohormonal activation leads to an adaptive process of ventricular remodelling to restore cardiac function (Cahill and Kharbanda, 2017). This may, however, results in a pathological remodelling, with alterations in ventricular structure, wall thinning, and further cardiomyocyte loss, that will ultimately lead to a decline in cardiac function (Sun, 2009).

Another complication of MI is the occurrence of cardiac arrhythmias. Atrial fibrillation (AF), the most common arrhythmia detected in clinical practice, may occur in up to 6% - 21% of patients with MI (Cappato, 2009). Development of AF during hospitalisation for STEMI has been shown to be associated with higher risk on in-hospital (Crenshaw et al., 1997, Rathore et al., 2000, Lehto et al., 2005) as well as follow-up (Kinjo et al., 2003) mortality. In addition, the incidence of ventricular arrhythmias ranges from 5.2% to 11.6% in patients post-MI (Henkel et al., 2006, Mehta et al., 2012, Jabbari et al., 2015a) and it was associated with higher 30-day mortality in STEMI patients (Jabbari et al., 2015b).

1.2.6. Therapeutic management of myocardial infarction

The goal of the therapeutic management of MI is to maintain or restore myocardial perfusion whilst decreasing myocardial oxygen demand and increasing myocardial oxygen supply. General supportive measures involve administration of supplemental

oxygen to tackle hypoxia and opiates, such as morphine, for pain relief in patients with severe chest pain (Roffi et al., 2016, Ibanez et al., 2018).
Considering the relevance of thrombus formation in the pathogenesis of MI, anti-thrombotic therapy is one of the pillars of both STEMI and NSTEMI pharmacological management. Combined administration of anti-platelet medications such as acetylsalicylic acid and $P2Y_{12}$ receptor inhibitors (e.g. ticagrelor, clopidogrel or prasugrel) is recommended for all patients by the most recent guidelines (Roffi et al., 2016, Ibanez et al., 2018). Other anti-platelet agents such as glycoprotein (GP) IIb/IIIa inhibitors (e.g. tirofiban, abciximab) may be indicated in patients who need to undergo invasive procedures (Ibanez et al., 2018). In addition, anticoagulants, e.g. low-molecular weight heparins, may also be indicated, especially for NSTEMI patients (Roffi et al., 2016).

In NSTEMI patients, early administration of beta-blockers is recommended to all patients without contra-indications as it reduces myocardial oxygen consumption by decreasing heart rate, blood pressure, and myocardial contractility (Roffi et al., 2016). In STEMI patients, early administration of beta-blockers should be considered in haemodynamically stable patients only (Ibanez et al., 2018).

1.2.7. Reperfusion therapy

The major difference in the management of NSTEMI and STEMI is the urgent need to restore blood flow in the culprit coronary artery in the latter (Ibanez et al., 2018). Total coronary artery occlusion is observed in most cases of STEMI and therefore re-establishment of vessel patency is paramount to achieve myocardial reperfusion. The first modality of reperfusion therapy to be developed, namely thrombolysis, aims to dissolve the intracoronary thrombus by intravenous administration of pharmacological agents that promote fibrinolysis (e.g. tenecteplase, alteplase, or reteplase) (Ibanez et al., 2018). Thrombolysis significantly decreases mortality in STEMI patients (Group, 1994), especially in high-risk groups (e.g. elderly) and when it is administered within 2 hours of symptom onset (Boersma et al., 1996, White, 2000). Nonetheless, thrombolysis efficacy decreases with time elapsed from symptom onset (Pinto et al., 2011) and it presents some absolute contra-indications, such as previous haemorrhagic stroke, trauma, surgery or gastrointestinal bleeding in the past month, or known bleeding disorders (Ibanez et al., 2018).

1.2.8. Primary percutaneous coronary intervention

Reperfusion therapy for STEMI has evolved with the advent of and continuous improvements in primary percutaneous coronary intervention (PPCI) over the last 2 decades. This procedure entails direct opening of the occluded coronary artery via a technique known as angioplasty, in which a wire is inserted via the radial or femoral artery and advanced into the coronary artery (Mann et al., 2015). Once the wire passes the site of occlusion, a balloon attached to the wire is inflated to open the vessel. In most cases, a small metallic scaffold, called stent, is placed at that site to prevent re-occlusion (Mann et al., 2015). Primary PCI is superior to thrombolysis in reducing re-infarction, stroke, and mortality (Zijlstra et al., 1999, Keeley et al., 2003, Andersen et al., 2003). Therefore, PPCI is the preferred modality of reperfusion therapy in STEMI patients with less than 12h of symptom onset, provided the procedure can be performed by an experienced team within 120 minutes of the diagnosis (Ibanez et al., 2018). Otherwise, patients should receive thrombolysis first and then be referred to a PCI centre (Ibanez et al., 2018).

1.3. Failed myocardial reperfusion

1.3.1. Definition

Primary PCI results in successful restoration of normal or near-normal coronary blood flow, as indicated by angiographic thrombolysis in myocardial infarction (TIMI) flow grades 2 and 3, in more than 90% of STEMI patients (Luman, 2014). Despite re-establishment of epicardial coronary artery perfusion, myocardial function does not entirely recover in approximately 50% of reperfused STEMI patients due to an impairment in microvascular flow, which consequently results in inadequate myocardial reperfusion (Wu, 2012). This impairment in microvascular flow, termed 'no-reflow' phenomenon, was firstly observed in animal models of myocardial ischaemia and reperfusion (Kloner et al., 1974) and, subsequently, in human patients treated with PCI (Rezkalla et al., 2010).

The pathological bases of the no-reflow phenomenon are still poorly understood but it can effectively hinder the benefits of reperfusion therapy (Rezkalla et al., 2010). An initial hypothesis that it could be associated with blockage of the coronary microcirculation by distal embolization of microthrombi and atheroma fragments was strongly suggested by the findings from pathological, imaging, and interventional studies (Falk, 1985, Limbruno et al., 2005, Sakuma et al., 2003, Wu et al., 2011b, Haeck et al., 2009). Reinforcing this hypothesis, serial cardiac magnetic resonance imaging (MRI) studies using late gadolinium enhancement showed core areas of hypoencement within hyperenhanced infarct regions (Wu, 2012), which were referred to as microvascular obstruction (MVO) to reflect the hypothesis of microvascular blockage in the pathogenesis of the no-reflow phenomenon. Later advancements in cardiac MRI protocols allowed the *in vivo* identification of intramyocardial haemorrhage (IMH) due to paramagnetic effects evoked by haemoglobin metabolites (Amabile et al., 2012). This revealed that areas of MVO and IMH substantially overlap and collectively represent areas of myocardial tissue with vascular damage and erythrocyte extravasation, instead of microvascular occlusion (Robbers et al., 2013). Therefore, the current understanding is that failed myocardial reperfusion initially manifests as MVO in the core infarct zone followed by severe microvascular injury and IMH in 40% of the cases (**Figure 1.1**) (Robbers et al., 2013).

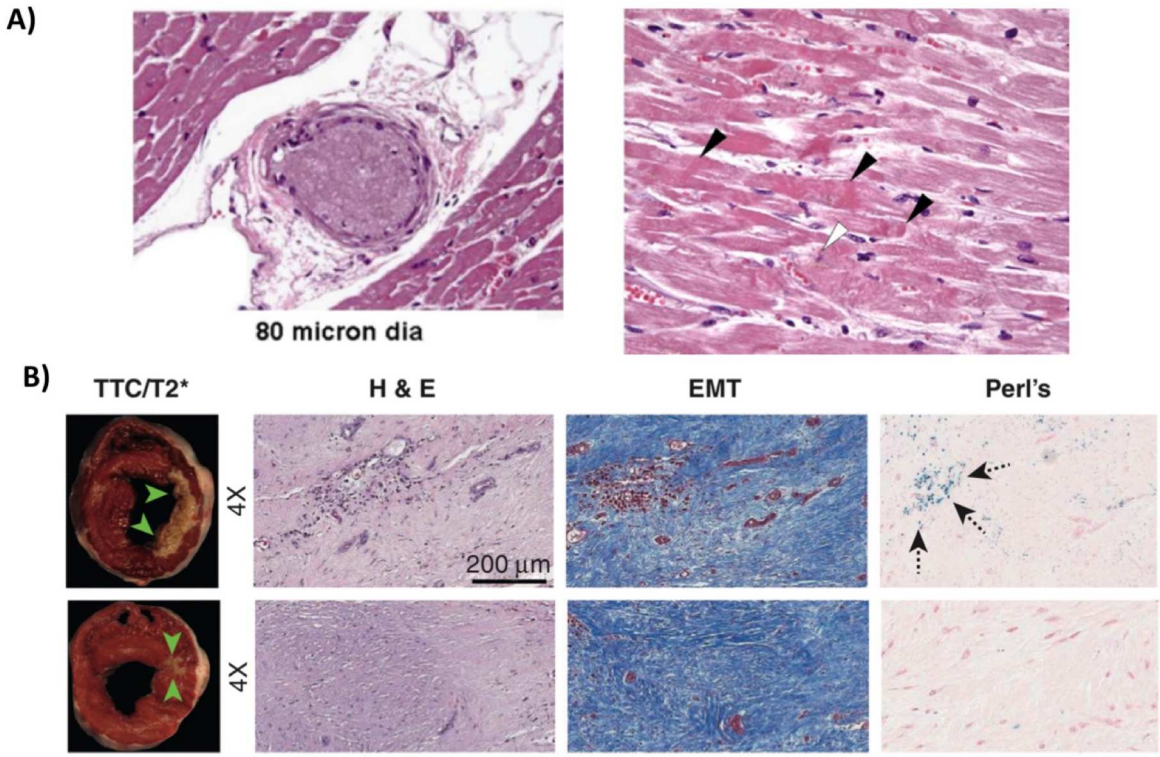

Figure 1.1. Histopathological findings associated with coronary microvascular obstruction and intramyocardial haemorrhage in the infarct zone. A) obstructed coronary microvessel (left panel) and areas of contraction band necrosis (black areas) and coagulative necrosis (white arrows) distal to obstructed microvessels. **B)** myocardial sections stained with triphenyltetrazolium chloride (TTC) localising the infarct area (green areas) and corresponding histological sections stained with haematoxylin and eosin (H&E) for tissue damage, elastin masson trichome (EMT) for fibrosis, and Perl's for iron. Note that presence of iron (haemorrhage) is more prominent in the larger infarct area compared to a smaller infarct. Adapted from: (Schwartz et al., 2009, Wang et al., 2019)

1.3.2. Pathophysiological mechanisms of failed myocardial reperfusion

A complex interaction between factors associated with ischaemia, reperfusion, and atherothrombotic microembolization has been implicated in the pathophysiology of failed myocardial reperfusion (Niccoli et al., 2016, Betgem et al., 2015).

The seminal study by Kloner et al. (Kloner et al., 1974) demonstrated for the first time the histopathological alterations associated with failed myocardial reperfusion in a canine model of transient coronary occlusion (90 min) followed by reperfusion. Using the fluorescent stain for endothelium thioflavin S, they observed that some areas of the myocardium inside the infarct zone did not uptake the marker despite reperfusion

of the corresponding coronary vessel (Kloner et al., 1974). In these regions, electron microscopy ultrastructural analysis showed endothelial cell protrusion, subsarcolemmal blebs and adherent inflammatory cells to the endothelium contributing to narrowing of the lumen (Kloner et al., 1974, Reffelmann and Kloner, 2006). Presence of cardiomyocyte swelling and interstitial oedema seems to further aggravate capillary obstruction by external compression (Kloner et al., 1974, Schwartz and Kloner, 2012). Additionally, release of vasoconstrictor substances, such as endothelin-1, has also shown to be associated with microvascular obstruction in STEMI patients (Eitel et al., 2010). Hypoxic conditions also lead to loss of endothelial integrity, which may contribute to intramyocardial haemorrhage following microvascular injury. Indeed, reduction in endothelial cell density, disruption in the endothelial lining, increase in paracellular permeability, and extravasation of erythrocytes have been described as effects of ischaemia on the vasculature (Kloner et al., 1974, Maxwell and Gavin, 1991, Goddard and Iruela-Arispe, 2013).

Although essential for myocardial salvage, coronary reperfusion also leads to microvascular damage. Reperfusion triggers a cascade of events culminating in plugging of neutrophils and platelets, erythrocyte aggregation, and further injury to the endothelial glycocalix (Bekkers et al., 2010, Maksimenko and Turashev, 2012). Together, these factors aggravate obstruction and damage of coronary microvessels by a mechanical effect or release of inflammatory mediators. In addition, neutrophil influx into vascular walls following reperfusion and subsequent release of reactive oxygen species and matrix-metaloproteinases provokes disintegration of the basal membrane, allowing erythrocytes to escape from the intravascular compartment into the interstitial space (Kloner et al., 1991). Finally, it has been suggested that activation of the inflammatory and coagulation cascades after reperfusion might lead to thrombosis in the microvessels and subsequent consumption of coagulation factors, worsening the haemorrhage. (Robbers et al., 2013)

A wealth of evidence from experimental and clinical studies has linked coronary microembolization with microvascular obstruction. Microemboli originate from the erosion or rupture of atherosclerotic plaques, spontaneously or after manipulation during PCI (Virmani et al., 2006). Intracoronary infusion of microspheres in experimental models provokes an immediate decrease in coronary blood flow and regional contractile dysfunction (Skyschally et al., 2002, Dorge et al., 2000). In

addition, a post-mortem study of patients who died from ACS has shown distal microembolization of thrombus and atheromatous material (Falk, 1985). In the clinical scenario, angiographic and intracoronary imaging studies have demonstrated an association between the no-reflow phenomenon and the atherosclerotic burden in the culprit coronary artery (Wu et al., 2011b, Limbruno et al., 2005). Also, circulating microparticles from thrombotic material have been shown to be associated with surrogate electrocardiographic and angiographic markers of microvascular obstruction (Porto et al., 2012).

1.3.3. Detection of failed myocardial reperfusion

Microvascular obstruction can be detected by invasive and non-invasive methods, with varying degrees of sensitivity among them. Therefore, incidence of MVO in STEMI patients has been reported to range from as low as 10% using angiographic methods up to 60% in studies that employed cardiac MRI (Niccoli et al., 2013).

Invasive methods of MVO determination include the index of microvascular resistance (IMR) and the TIMI flow grade. The IMR is determined by a pressure- and temperature-sensitive coronary wire in the culprit coronary artery at the end of PPCI (Carrick et al., 2016a). It is defined as the distal coronary pressure multiplied by the mean transit time of three consecutive bolus injections of room temperature saline (3 mL) during maximal coronary adenosine-induced hyperaemia (Carrick et al., 2016a). Higher IMR values have been associated with microvascular pathology, including both MVO and IMH (Carrick et al., 2016a). The challenges with using this method are the need for special equipment, trained personnel, and use of additional pharmacological interventions (e.g. adenosine) (Niccoli et al., 2016). The TIMI flow grade is an angiographic description of the blood flow rate in epicardial vessels, ranging from no flow (grade 0) to normal flow (grade 3). TIMI flow < 3 following angioplasty has been associated with MVO (Morishima et al., 2000). However, as previously mentioned, the sensitivity of this method for MVO detection is very low.

Microvascular obstruction can be non-invasively detected by the electrocardiogram, echocardiography, positon-emission tomography (PET), and by magnetic resonance imaging. In the ECG, maximum ST elevation at baseline (McLaughlin et al., 2004) and incomplete ST-segment resolution in relation to baseline (Infusino et al., 2014)

have been shown to be markers of MVO. However, there is no consensus regarding which leads to analyse, at which time point ECG analysis should be performed, and whether it should be serial (Niccoli et al., 2016). Myocardial contrast echocardiography employs ultrasound to detect contrast microbubbles whose flow through the coronary microcirculation resembles that of red blood cells and therefore infer about the occurrence of microvascular obstruction (Galiuto et al., 2008). Nonetheless, it presents several limitations including operator-dependency and only partial coverage of the left ventricle, providing only a semi-quantitative assessment of MVO (Niccoli et al., 2016). Cardiac PET scan can inform about infarct size, myocardial tissue perfusion state, as well as metabolic and inflammatory changes after reperfusion but requires further validation in human patients (Lautamaki et al., 2009).

Cardiac MRI is the current gold-standard technique for assessment of MVO. It provides reproducible, detailed tissue characterization and spatial resolution, allowing accurate MVO identification, quantification and localization relative to the entire left ventricle (Hundley et al., 2010). Detailed tissue assessment is possible due to the distinct ways in which the various tissues affect two MRI signal components (T1, T1 relaxation time; and T2, T2 relaxation time) (Biglands et al., 2012). For tissue characterization in the context of myocardial infarction, a contrast agent known as gadolinium is intravenously injected prior to image acquisition (Hundley et al., 2010). Gadolinium has a short T1, meaning that an enhanced signal is observed on T1 weighted images in tissues where it is concentrated. Gadolinium is an extracellular agent and has well-known clearance kinetics after administration: it passes through the coronary arteries into the myocardium in just a few seconds and then through the normal myocardium after approximately 10 to 15 minutes. In areas of myocardial necrosis, where the extracellular space is relatively expanded, gadolinium takes longer to be cleared (Hundley et al., 2010, Perazzolo Marra et al., 2011). Therefore, when T1-weighted images are acquired after 10-15 min of gadolinium administration an enhanced signal is still observed in infarct zones compared to the surrounding myocardium. This is a MRI imaging acquisition technique called late gadolinium enhancement (LGE), which is used to determine the infarct core (Hundley et al., 2010). In areas of microvascular flow obstruction, gadolinium passage to the extracellular space is delayed as it occurs via passive diffusion instead of perfusion (Saeed et al., 2010). Using this principle, MVO can then be detected as: (i) a lack of

gadolinium enhancement during first pass (< 2 min), termed early MVO; and (ii) a hypoenhanced area within the hyperenhanced infarct core identified by LGE, called late MVO (Wu, 2012). Thus, current cardiac MRI protocols allow both a qualitative as well as quantitative assessment of MVO, i.e. detection of presence of MVO as an area of hypoenhancement as well as estimation of the mass of myocardial tissue affected by MVO in relation to the total myocardial mass. Hypoenhanced areas (MVO) in the MRI correlate with histological characteristics of microvascular damage (Driesen et al., 2012). Cardiac MRI has also been validated for detection of IMH, especially in the first week after reperfusion (O'Regan et al., 2010, Pedersen et al., 2012, Kumar et al., 2011, Payne et al., 2011). Although all T1 and T2 sequences can be used, T2 sequence has shown greater diagnostic performance for IMH (Payne et al., 2011).

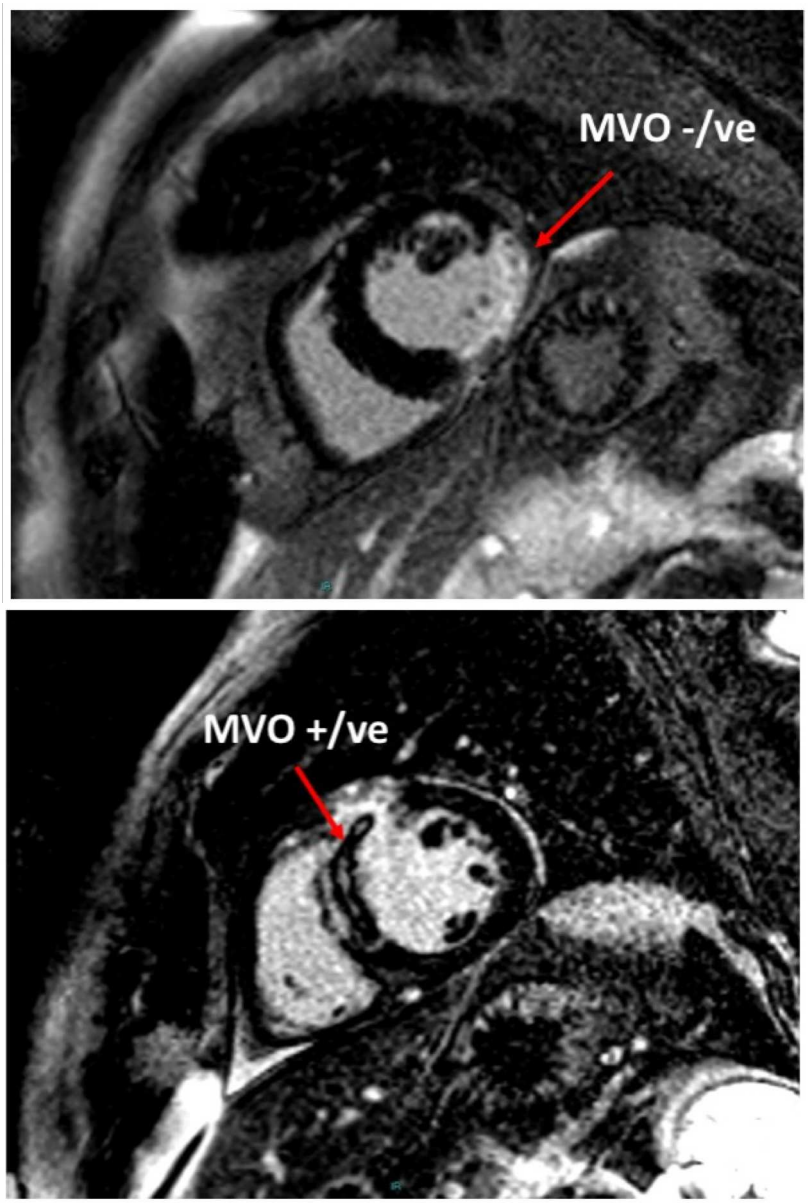

Figure 1.2. Microvascular obstruction as detected by late-gadolinium enhancement cardiac magnetic resonance imaging. The upper panel depicts an area of hyperenhancement correspondent to a large myocardial infarction. The lower panel shows an area of hypoenhancement within an hyperenhanced core, correspondent to microvascular obstruction.

1.3.4. Prognostic implications

Failed myocardial reperfusion is clinically relevant as the occurrence of MVO and IMH has been associated with adverse outcomes. Detection of MVO is associated with larger IS, lower LVEF, and adverse left ventricular remodelling (Lombardo et al., 2012, Hombach et al., 2005). In addition, it increased mortality in STEMI patients (de Waha et al., 2010, Eitel et al., 2014). In fact, MVO provided independent and incremental prognostic prediction value for a composite of all-cause death, re-infarction, and heart failure after 1 year of PPCI in addition to clinical scores and LVEF in a large multicentre observational study including 738 STEMI patients (Eitel et al., 2014). Furthermore, IMH has also been associated with larger IS, impaired LV function, LV remodelling, and increased risk of major adverse cardiac events and death (Ganame et al., 2009, Beek et al., 2010, Amabile et al., 2012).

1.3.5. Therapeutic approaches for MVO

Despite intensive pharmacological research aiming to target MVO, there is currently no therapeutic strategy that has been unequivocally shown to be efficient in either preventing or treating MVO (Niccoli et al., 2016). Several trials testing anti-inflammatory agents (Armstrong et al., 2007), integrin receptor blockers (Faxon et al., 2002), anti-oxidants (Chan et al., 2012), calcium-channel blockers (Bar et al., 2006), and cyclosporine (Cung et al., 2015), for example, have failed to show any clinical benefits. Some promising results were obtained with administration of high doses of statins prior to PCI (Kim et al., 2010) or prolonged infusion of gpIIb/IIIa after PCI (Petronio et al., 2005), however these need to be tested in larger trials with defined end-points. Henceforth, treatment of MVO remains an unmet clinical need.

1.4. Cardiac troponins and myocardial damage

1.4.1. Molecular aspects and spatial distribution

Troponin is a protein complex formed by 3 subunits (C, I, and T) that, along with actin and tropomyosin, constitute the thin filament of striated muscle (Filatov et al., 1999). Troponin regulates the calcium-mediated interaction between actin and myosin that results in muscle contraction in both skeletal and cardiac muscular tissues (Gomes et al., 2002). In this context, Troponin C binds to calcium, Troponin I inhibits the enzyme actin-activated myosin Mg^{2+}ATPase, and Troponin T is the subunit that is bound to tropomyosin (Gomes et al., 2002). Cardiac troponins I and T occur in 3 distinct isoforms in slow and fast skeletal muscle and in cardiomyocytes. In contrast, the cardiac subunit C has the same aminoacid sequence as the skeletal muscle subunit (Barton et al., 1992). The cardiac isoforms of troponin I (cTnI) and troponin T (cTnT) can be detected by monoclonal antibodies targeting their myocardial-specific epitopes and used as markers of cardiac damage.

In cardiomyocytes, most of the cTn is bound to the contractile complex whereas a small portion is found free in the cytoplasm (3 – 8% of cTnI; 6 – 7% cTnT) (Katus et al., 1991, Bleier et al., 1998). The spatial distribution of cTn in the heart varies (Swaanenburg et al., 2001). The concentration of cTn is higher in the left ventricle compared to the right ventricle and the atria (Swaanenburg et al., 2001). There seems to be no difference in cTn concentration between the right and left atria (Swaanenburg et al., 2001). In the left ventricle, cTn is uniformly distributed although presenting substantial inter-individual variability (Swaanenburg et al., 2001).

1.4.2. Release kinetics after irreversible cardiac injury

In the context of MI, prolonged ischaemia leads to irreversible myocardial necrosis. Disruption of the cellular membrane integrity results in release from intracellular contents (Wu, 2017). For macromolecules, such as proteins, size directly influences release kinetics, i.e. the smaller the protein the quicker it appears in the circulation (Wu, 2017). In terms of cardiac protein biomarkers, the first to be detected in the blood stream is myoglobin, followed by troponin, creatine kinase, and lactate dehydrogenase (Wu, 2017). Proteins that are only present in the cytoplasm display a

monophasic release pattern whereas those that are part of the structural cellular scaffold present a delayed release (Wu, 2017). Because cTn has both cytoplasmic and structural distribution, it has a biphasic release pattern, characterized by initial liberation of the cytosolic pool followed by a gradually declining plateau phase that represents the degradation of the structural cTn component (Katus et al., 1991, Bertinchant et al., 1996).

Coronary reperfusion markedly affects cTn plasmatic kinetics. In non-reperfused patients, cTn release steadily increases in the circulation reaching a peak at day 3 or 4 post-MI (Katus et al., 1991, Bertinchant et al., 1996). With reperfusion, an early peak occurs at around 8h to 12h post-reperfusion, reflecting a rapid washout of the cytosolic cTn pool (Katus et al., 1991, Bertinchant et al., 1996). Kinetics of cTn after 24h does not seem to be affected by coronary reperfusion as it reflects the slow degradation and release of the structural cTn pool (Katus et al., 1991, Bertinchant et al., 1996).

1.4.3. Correlations with the extent of cardiac damage

There is strong evidence demonstrating the correlation between cTn circulating levels post-MI and IS derived from multiple studies (Hallen, 2012). Although different studies used distinct methods for IS determination [e.g. single-photon emission computed tomography (SPECT) and cardiac MRI], they were unanimous in reporting positive relationships between cTn and IS, with coefficients of correlation ranging from 0.60 to 0.75 (Omura et al., 1993, Ohlmann et al., 2003, Giannitsis et al., 2008, Tzivoni et al., 2008, Vasile et al., 2008, Hallen et al., 2009). There seems to be no difference between cTnI and cTnT in their correlation with IS (Chia et al., 2008). Importantly, the timing of cTn measurement affects such correlations, as admission cTn levels had weak association with IS. Later time points, especially after 24h after symptom onset, seem to better estimate IS (Chia et al., 2008, Steen et al., 2006). In fact, measurement at a single time point after 24h, notably 72h, was as effective as peak levels or the area under the curve derived from serial cTn measurements (Chia et al., 2008, Bohmer et al., 2009).

1.4.4. Evidence for association with failed myocardial reperfusion

Considering the established correlation between cTn and myocardial damage, a few studies assessed their association with MVO (Younger et al., 2007, Hallen et al., 2011, Mayr et al., 2012, Pernet et al., 2014, Nguyen et al., 2015a). In a cohort of 93 STEMI patients who received thrombolytic therapy, Younger et al. observed higher cTnI levels at 72h post-reperfusion in patients with late MVO ($p < 0.005$) however no association was found for 12h levels ($p = 0.13$) (Younger et al., 2007). In contrast, correlation between 12h cTnI and the extent of MVO ($r = 0.67$, $p < 0.0001$) was found to be superior than that for 72h ($r = 0.42$, $p = 0.040$) in a cohort of 51 consecutive STEMI patients treated with PCI (Pernet et al., 2014). Considering that cTn washout is quicker with PCI than with thrombolysis, the discrepant results between these 2 studies might be explained by the effect of the different reperfusion therapy modalities on cTn kinetics. Levels of cTnI at 24h and 48h post-reperfusion have also been found to be independently associated with MVO in a cohort of 175 STEMI patients (Hallen et al., 2011). As for cTnT, strong correlations with late MVO were reported at 8h, 16h, 24h, 48h, 72h, and 96h post-reperfusion, with the strongest ($r = 0.738$, $p < 0.005$) at the 96h time point in a cohort of 118 STEMI patients (Mayr et al., 2012). In another study, moderate correlations were observed between 24h ($r = 0.420$, $p < 0.001$) and 48h ($r = 0.400$, $p < 0.001$) cTn levels and late MVO ($n = 201$) (Nguyen et al., 2015a). Taken together, these findings point towards a relationship between cTn post-reperfusion levels and MVO, especially at time points of the plateau phase.

1.4.5. Prognostic relevance

Cardiac troponins correlate with surrogate markers of worse prognosis, such as larger IS, MVO, impaired LVEF, and adverse LV remodelling (Mayr et al., 2011, Hallen et al., 2010). Nevertheless, in the modern era of PPCI, there is little evidence of an independent association between cTn levels and clinical outcomes in STEMI patients. Conflicting results in terms of outcome prediction have been reported for cTn post-reperfusion levels (Boden et al., 2013, Buber et al., 2015, Hall et al., 2015, Cediel et al., 2017). As for admission cTn, small studies have suggested independent prognostic prediction for major adverse cardiac events and mortality (Giannitsis et al., 2001, Wang et al., 2014a). Therefore, the prognostic role of cTn in PCI-reperfused STEMI patients is yet to be elucidated.

1.5. MicroRNAs: small molecules with a big potential as disease markers

1.5.1. Non-coding RNAs

In the past 15 years, with the development of array and RNA-sequencing technologies, it was possible to verify that approximately 85% of the human genome is transcribed into RNA and that most of the transcriptome does not code proteins (Hangauer et al., 2013, Djebali et al., 2012, Elliot and Ladomery, 2016). In humans, the proportion of non-coding to coding RNA transcripts is 47:1. Non-coding RNAs comprise a heterogeneous group of RNA species arbitrarily divided into short [<200 nucleotides(nt)] and long (>200 nt) ncRNAs. These RNA species present distinct spatiotemporal expression and exert their functions at all gene regulatory levels (Cech and Steitz, 2014).

MicroRNAs belong to a class of small non-coding RNAs (approximately 20 to 23 nt in length) that post-transcriptionally inhibit gene expression. The first miRNA, lin-4, was identified in *Caenorhabditis elegans* in 1993 (Lee et al., 1993). To date, over 1,500 miRNAs have been identified in humans with evidence supporting their involvement in the regulation of all known cellular processes (Berezikov, 2011).

1.5.2. MicroRNA biogenesis and function

MicroRNA encoding-sequences can be found in intergenic or intragenic regions of the genome. Transcription of these sequences, regulated by RNA polymerase II, generates single or multiple hairpin structures, known as primary microRNA transcripts (pri-miRNAs). Transcription of intergenic miRNA genes is controlled by specific promoters whereas intragenic miRNA genes can be processed by their own promoters (if anti-sense oriented) or by their host-gene promoters (if sense-oriented). The hairpin region of pri-miRNAs is recognized by a microprocessor complex, a multi-protein complex comprised of Drosha and double-stranded RNA-binding protein DiGeorge syndrome critical region 8 (DGCR8) (Gregory et al., 2004). The pri-miRNAs are cleaved by the microprocessor complex cleaves into smaller hairpin structures of approximately 70 – 100 nt, named precursor miRNAs (pre-miRNAs). Intragenic pri-miRNAs require other splicing enzymes (spliceosome) to complement the microprocessor complex mechanism. In contrast, an unconventional class of

intragenic miRNAs, known as mirtrons, entirely escape the Drosha-mediated process to be transformed into pre-miRNAs solely by the splicing machinery. The nuclear protein Exportin 5 transports pre-miRNAs to the cytoplasm, where they are processed by the RNase III enzyme Dicer into smaller (~22-23 nt) double-stranded miRNAs (Chendrimada et al., 2005) (**Figure 1**).

Double-stranded miRNAs contain a guide or mature strand and a passenger strand. The mature strand is incorporated into a miRNA-induced silencing complex (miRISC) whereas the passenger strand is degraded. This traditional concept has nonetheless been challenged by reports that show that the miRNA passenger strand can be biologically active and modulate the gene expression in thyroid and lung cancer, for instance (Misono et al., 2018, Jazdzewski et al., 2009) In humans, miRISC binds to the 3' untranslated region (3'-UTR) of target mRNAs by imperfect base-pairing (Gregory et al., 2005). However, for the binding to be effective there must exist perfect complementarity between the target mRNA and miRNA nucleotides 2 to 8. This results in mRNA translational repression and/or degradation, and therefore post-transcriptional gene silencing. The function of miRISC relies mainly on its proteins Argonaute 2 (AGO-2), which interacts directly with the mRNAs, and glycine-tryptophan protein of 182 kDa (GW182), which mediates mRNA degradation by deadenylation (Eulalio et al., 2008). In addition, repression efficiency can be influenced by factors such as the number of target sites for the same or multiple miRNAs in the mRNA 3'-UTR and mRNA secondary structure (Pillai et al., 2007).

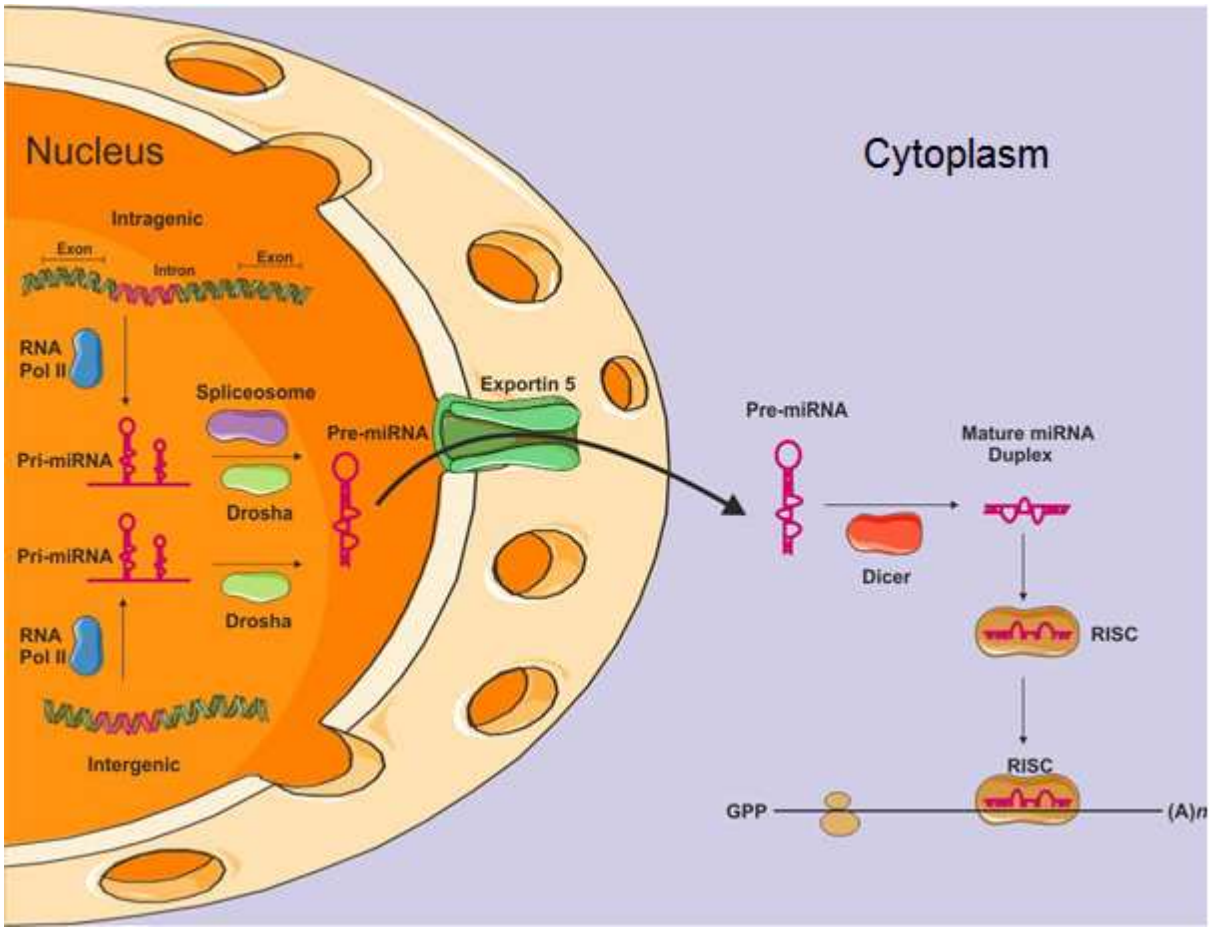

Figure 1.3. MicroRNA biogenesis and function. Intragenic and intergenic miRNA-encoding sequences are transcribed by RNA Polymerase II (RNA Pol II) into primary miRNA (pri-miRNAs) transcripts, which are processed by the microprocessor complex and splicing enzymes (intragenic-derived pri-miRNAs), into precursor miRNAs (pre-miRNAs). Pre-miRNAs are transported to the cytoplasm by Exportin 5, where are further processed by the enzyme Dicer to form the mature miRNA duplex. The mature strand of the duplex is incorporated by the RNA-induced silencing complex (RISC), which binds to the 3'UTR of target mRNAs, causing mRNA translational repression and/or degradation. *From*: (Lima et al., 2017)

1.5.3. MicroRNA regulation of atherothrombosis

MicroRNAs have been shown to regulate multiples mechanisms associated with atherothrombosis, including vascular inflammation, atherogenesis, plaque rupture, and platelet reactivity.

Atherosclerosis preferentially develops at sites of disturbed blood flow (e.g. arterial curvatures and bifurcations), where the endothelium is exposed to oscillatory shear stress (OSS) (Caro, 2009). In such areas, LDL deposition and its subsequent

oxidation (to oxidized LDL; oxLDL) triggers an inflammatory response that results in cellular trafficking into the arterial wall and plaque formation (Weber and Noels, 2011). Expression of some miRNAs is affected by OSS, with functional consequences. For example, OSS led to miR-10 downregulation in the aortic arch and aorto-renal branches of pigs (Fang et al., 2010), which was associated with activation of the IκB/NF-κB-mediated inflammatory pathway in human aortic endothelial cells (HAECs). Furthermore, OSS promoted miR-21 overexpression in cultured human umbilical vein endothelial cells (HUVECs), inducing the expression of adhesion molecules such as vascular cell adhesion molecule 1 (VCAM-1) and monocyte chemotactic protein-1 (MCP-1), with augmented monocyte adhesion to endothelial cells (ECs) (Zhou et al., 2011). Furthermore, regulation of Krüppel-like factors (KLFs), a family of transcription factors induced by atheroprotective laminar flow which anti-inflammatory, anti-proliferative, and anti-thrombotic effects in ECs (Atkins and Jain, 2007), by miRNAs has been shown by many studies (Wu et al., 2011a, Fang and Davies, 2012, Loyer et al., 2014a, Hergenreider et al., 2012). For example, miR-92 was shown to inhibit KLF2 (Wu et al., 2011a) and KLF4 (Fang and Davies, 2012) *in vitro* an *in vivo*. In addition, *in vivo* inhibition of miR-92a in LDL-receptor knockout (LDL-$R^{-/-}$) mice reduced endothelial inflammation and atherosclerotic plaque size (Loyer et al., 2014a).

It has been demonstrated that oxLDL regulates the expression of miRNAs, such as miR-155 and miR-342-5p, in atherosclerotic plaque macrophages, which can modulate the inflammatory response and atherosclerosis progression by modulation of the NF-κB and interleukin-6 (IL-6) signalling, respectively (Nazari-Jahantigh et al., 2012, Wei et al., 2013). MicroRNA regulation of adhesion molecules that facilitate the infiltration of inflammatory cells into the arterial walls has also been shown (Harris et al., 2008, Sun et al., 2012). Induced *in vitro* inhibition of the EC-expressed miR-126 results in increased VCAM-1 expression and augmented leukocyte adhesion to ECs (Harris et al., 2008).

Furthermore, miRNAs are also involved in atherosclerotic plaque destabilization. One of the cardinal features of a vulnerable plaque is a thin fibrous cap. Two miRNAs, miR-24 and miR-29, seem to regulate fibrous cap thinning by enhancing macrophage apoptosis-associated metalloproteinase 14 proteolytic activity and reducing the production of extracellular matrix (Di Gregoli et al., 2014, Boon et al., 2011). Also,

expansion of the necrotic core, which predisposes plaque rupture, was shown to be enhanced by miR-155 and miR-21, which promote increased intra-plaque macrophage apoptosis and impaired clearance of necrotic core contents (Ghorpade et al., 2012, Das et al., 2014). Finally, plaque erosion was shown to be promoted by miR-712 and miR-223 via fragmentation of the proteoglycan versican and EC apoptosis, respectively (Son et al., 2013, Pan et al., 2014).

Platelet activation is fundamental for thrombus formation following plaque rupture. Platelets, although anucleate, possess the required biomachinery to convert pre-miRNAs into mature miRNAs. Platelets have functioning Dicer and AGO-2 proteins, which allow platelet miRNAs to post-transcriptionally regulate gene expression e.g. AGO2-miR-223 complex can regulate the expression of P2Y12 receptors (Landry et al., 2009). This observation opened new avenues for the study of microRNAs as modulators of platelet function. Kondkar et al. (Kondkar et al., 2010) measured platelet reactivity in 288 healthy individuals and reported increased levels of the vesicle-associated membrane protein 8 (VAMP8), a protein involved with platelet granule secretion, in hyperactive platelets. VAMP8 was identified as a target of miR-96, which overexpression decreased VAMP8 levels. Similarly, Nagalla et al. (Nagalla et al., 2011) confirmed inhibition of mRNAs (PRKAR2B, KLHL5, and CLOCK*)* by platelet miRNAs (miR-200b, miR-495 and miR-107*)* and showed that PRKAR2B$^{-/-}$ platelets presented reduced reactivity, suggesting that miRNA target genes regulate platelet function.

1.5.4. MicroRNA release and transport in biological fluids

The potential of miRNAs as disease biomarkers was unveiled by reports that circulating microRNAs are released in the body fluids within extracellular vesicles (Valadi et al., 2007), and, to a less extent, bound to HDL-cholesterol particles (Vickers et al., 2011) or AGO-2 protein (Turchinovich and Burwinkel, 2012), conferring high stability against circulating RNAses. Indeed, miRNAs display characteristics of ideal biomarkers as they can be reliably detected in biofluids even after years of sample storage and repeated freezing-thaw cycles (Moldovan et al., 2014). Furthermore, miRNA content in extracellular vesicles differs from that of their maternal cells, suggesting the existence of a selective packing process during the

their formation (Diehl et al., 2012), which could be specifically associated to pathological states.

Cells release membrane vesicles under basal or stress conditions. Extracellular vesicles differ in size, biogenesis and cellular release mechanism (Raposo and Stoorvogel, 2013). Although there is no consensus in the literature with regards to the classification and nomenclature of extracellular vesicles, the current most accepted terminology includes three different subtypes: (i) exosomes; (ii) microvesicles or microparticles; and (iii) apoptotic bodies (Witwer et al., 2013). Exosomes, the smallest, have a size range of 40 to 100nm; microparticles size ranges from 100 nm to 1000nm; and apoptotic bodies, the largest vesicles, hae a size of approximately 1- 5um. With regards to the biogenesis and cellular release mechanism, exosomes are formed in intracellular compartments, known as multivesicular bodies, which fuse to the cellular membrane to release exosomes to the extracellular space. In contrast, microvesicles are shed directly from the cellular membrane, especially under stress conditions (Vion et al., 2013). Finally, apoptotic bodies are formed during the last stages of apoptosis (Loyer et al., 2014b).

Mostly due to their size, the contents of the different types of extracellular vesicles also differ. Apoptotic bodies, for example, contain intracellular organelles and cytoplasmic material, including proteins, DNA, and RNAs. Microvesicles contain parent cells' surface proteins and some cytoplasmic content. Exosomes carry some proteins, lipids, DNA, and miRNAs, despite their small size (Loyer et al., 2014b). Interestingly, it has been demonstrated that the miRNA cargo within exosomes is an active, not random process. Specific motifs in miRNA sequences are recognized by the heterogeneous nuclear protein ribonucleoprotein A2B1 (hnRNPA2B1), which guides miRNA loading into exosomes (Villarroya-Beltri et al., 2013).

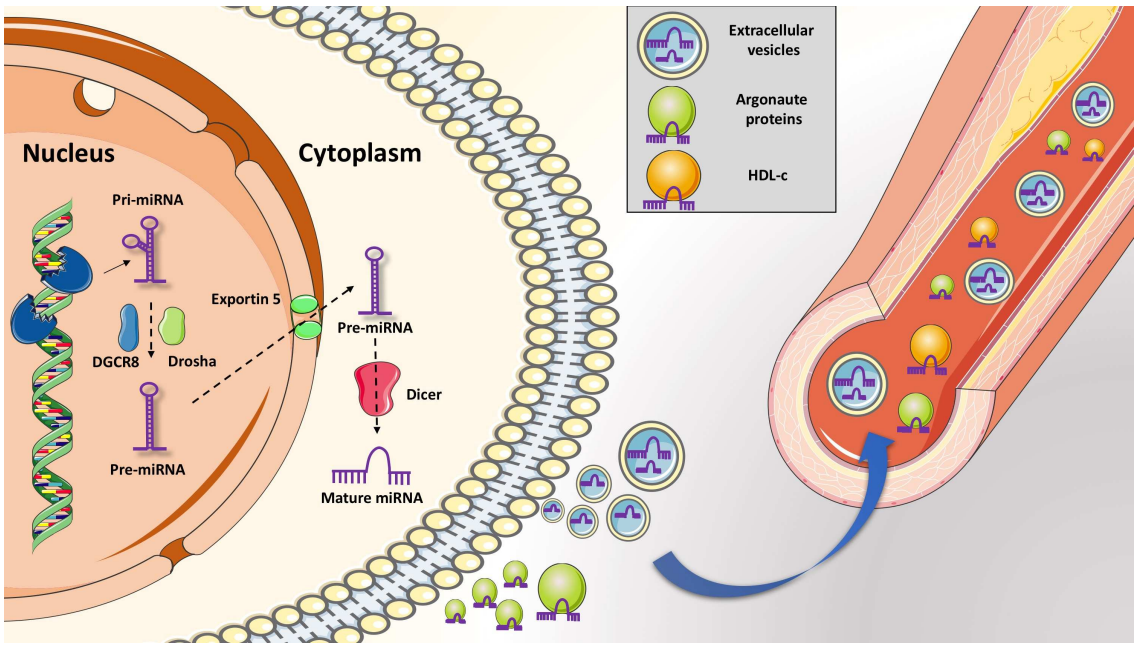

Figure 1.4. – MicroRNA release from cells and transport in biological fluids.

In addition, it has been shown that extracellular vesicles can deliver their genetic information to other cells. This newly described mechanism of intercellular communication suggests that circulating miRNAs could also have biological roles, as these miRNAs can be internalized by recipient cells and influence the expression of target genes. In the context of cardiovascular biology, some evidence already reinforces this hypothesis (Hergenreider et al., 2012, Loyer et al., 2014b, Wang et al., 2014b, Bang et al., 2014). For instance, miR-143 and miR-145, found in microvesicles secreted by KLF2-stimulated HUVECs, were internalized by vascular smooth muscle cells (VSMCs), where they regulated target genes expression (Hergenreider et al., 2012). Administration of such microvesicles to apolipoprotein E knockout ($ApoE^{-/-}$) mice reduced atherosclerotic plaque size (Hergenreider et al., 2012). These findings suggest an important role of miRNA-containing extracellular vesicles in the mechanism of intercellular communication between the endothelium and VSMCs.

In addition to platelet function regulation, it has been suggested that platelet miRNAs may also play a role in the cross-talk between circulating cells and the endothelium. Gidlof *et al*. (Gidlof et al., 2013b) reported downregulation of miRNA-22, -185, -320b, and -423-5p in platelets from STEMI patients. These miRNAs were upregulated in the supernatant of aggregated platelets and in thrombi obtained from these patients, suggesting miRNA transfer from platelets to the site of thrombus formation. Transfer

of such miRNAs between platelets and ECs and their biological functionality in the recipient cells were confirmed by the observation that miR-320b targeted intercellular adhesion molecule 1 (ICAM-1) in ECs, decreasing its cellular expression. Similarly, Laffont *et al*. (Laffont et al., 2013) observed that thrombin-activated human platelets released microvesicles containing miR-223. These vesicles were internalized by HUVECs and regulated the expression of target genes. These results point towards an interesting role for platelet-derived miRNAs in the interaction between circulating cells and the vasculature.

1.5.5. Circulating miRNAs deregulated in STEMI

Most studies that addressed the role of miRNAs in the diagnosis of ACS focused in their ability to discriminate myocardial infarction (Viereck and Thum, 2017). Cardiac muscle-specific circulating miRNAs, such as miR-208 (Wang et al., 2010), miR-1, miR-133a, miR-133b, and miR-499-5p(D'Alessandra et al., 2010), were shown to be upregulated whereas miR-122 and miR-375 were downregulated in STEMI patients (D'Alessandra et al., 2010). Wang *et al.* (Wang et al., 2010) demonstrated that miR-208 levels were elevated after 4 hours of the symptoms onset in 100% of a subset of 20 STEMI patients, in contrast to 85% detection of cardiac troponin I. ROC curve analysis revealed 90.9% sensitivity and 100% specificity of miR-208 to discriminate patients with acute MI, suggesting that it could be used as a biomarker for early diagnosis of MI. A meta-analysis on the use of circulating miRNAs in the diagnosis of MI demonstrated that when used as a single test the diagnostic performance of miRNAs compares to that of troponin (Lippi et al., 2013). Nevertheless, substantial variability in the settings and miRNAs measured among studies as well as broad heterogeneity were reported (Lippi et al., 2013). In addition, slightly elevated levels of muscle-enriched miRNAs (miR-133a, miR-208a) were detected in patients with stable CAD (Fichtlscherer et al., 2010), which raises questions about the specificity of such miRNAs in detecting ACS. In this context, Zeller *et al*. (Zeller et al., 2014) reported a high discriminatory power of miR-132, miR-150, and miR-186 for unstable angina (AUC: 0.910; CI: 84-0.98), which biomarker-guided diagnosis is still an important clinical challenge. Although the evidence points towards a promising role of miRNAs as markers of cardiac injury, little is known about their release kinetics following STEMI and there is very scarce evidence of their correlation with

myocardial damage assessed by imaging techniques (Eitel et al., 2012). Furthermore, there are

The prognostic value of circulating miRNAs in predicting the risk of MI (Zampetaki et al., 2012) or major adverse cardiac events (MACE) (Jansen et al., 2014) has also been evaluated. In the cohort of the Bruneck study (n=820), which was followed up for 10 years (1995 to 2005), baseline levels of miR-126 were associated with increased risk of MI whereas miR-197 and miR-223 were associated with decreased risk. Platelets were identified as the major source of such circulating miRNAs (Zampetaki et al., 2012). In addition, extracellular vesicles levels of miR-126 and miR-199a were shown to predict MACE in patients with stable CAD followed up for 6 years. This effect was not observed for freely circulating miRNAs. Moreover, platelets and endothelial cells were the main sources of miRNA-containing microvesicles (Jansen et al., 2014).

Interestingly, circulating miRNA levels seem to be influenced by medications, such as antiplatelet therapy (de Boer et al., 2013, Willeit et al., 2013). Reduction of highly expressed platelet miRNAs, such as miR-223, miR-126, miR-191, and miR-150, was observed in healthy individuals receiving prasugrel and increasing doses of aspirin for 3 weeks and in patients with carotid atherosclerosis receiving antiplatelet therapy (Willeit et al., 2013). Also, miR-126 plasma levels were decreased by aspirin treatment in type 2 diabetes mellitus patients (de Boer et al., 2013). These findings generated a new concept that circulating miRNAs could potentially monitor antiplatelet therapy efficiency. However, these findings also highlight the need for studies to report data regarding the interaction between medications and miRNA levels, as this might introduce bias on data interpretation.

In sum, there is a strong body of evidence linking circulating miRNA levels to cardiovascular pathology, including STEMI. However, current aspects limit the introduction of circulating miRNAs in clinical practice. First, miRNA quantification relies on real-time quantitative polymerase chain reaction (RT-qPCR) for which there is no standardised, unequivocally accepted normalization strategy, which is a critical issue when it comes reproducibility among studies (Santovito and Weber, 2017). In addition, most studies in STEMI patients have selected small sets of miRNAs based on previous literature or experience of the authors, therefore perhaps overlooking

potential new circulating miRNA markers of cardiac injury (Santovito and Weber, 2017).

1.6. Aims of this study

The overall aim of this PhD project was to investigate a potential role of circulating microRNAs as markers of failed myocardial reperfusion and myocardial damage in STEMI patients.

In addition, specific aims included:

- To evaluate the prognostic relevance of routinely measured cardiac troponins prior to and 12 hours post-PCI for prediction of mortality in STEMI patients
- To identify an endogenous circulating miRNA control for RT-qPCR data normalization in STEMI patients
- To investigate the post-PCI plasmatic kinetics of candidate miRNA markers of failed myocardial reperfusion
- To validate whether these candidates are deregulated in a second STEMI cohort
- To evaluate the association between candidate miRNAs and cardiac MRI parameters of myocardial injury (infarct size and MVO)
- To assess the association between candidate miRNAs and cardiac functional recovery after PPCI

Chapter 2. Methods

2.1. Retrospective STEMI cohort

2.1.1. STEMI cohort 1 database

For retrospective analysis of the prognostic relevance of cTn in STEMI patients, a local coronary artery disease (CAD) database (Dendrite), which contains prospectively collected data from 5,288 consecutive STEMI patients treated with PPCI at the Freeman hospital (Newcastle upon Tyne, UK) between January 2008 and December 2014, was used. Baseline demographics, clinical presentation, procedure details and procedural complications were recorded at the end of each PCI and hospital stay by the attending physician. Post-procedural complications, troponin and other laboratory measurements, clinical data and discharge medications were updated on discharge by Freeman hospital database managers. Data regarding variables of interest were extracted from this master database by two medical students, Syeda Adil and David Gaskin. Data quality control analysis and data coding for statistical analysis were performed by me.

As previously published by our group, the diagnosis of STEMI was based on the presence of chest pain suggestive of myocardial ischaemia lasting longer than 30 minutes accompanied by ST-segment elevation or new left bundle branch block on the ECG (Boag et al., 2015). Patients were considered for PPCI if they presented within 12h of symptom onset. STEMI patients were given 300 mg of aspirin and were transferred directly to the cardiac catheterization laboratory. On arrival, either 600 mg of clopidogrel, 60 mg of prasugrel or 180 mg ticagrelor loading dose were administered along with standard doses of heparin or bivalirudin according to international guidelines. Glycoprotein (GP) IIb/IIIa inhibitors were administered by discretion of the operator during PPCI. Patients who did not have cTn quantified prior to (n = 310, 5.8%) or after PPCI (n = 64, 1.2%), either because they were in cardiogenic shock, under cardiopulmonary resuscitation conditions, or cTn measurement was omitted by treating physician, were excluded from the analysis, resulting in a total of 4,914 patients for data analysis. When patients were admitted several times for PPCI, only data from their first presentation was included for analysis.

2.1.2. Cardiac troponin measurement

Serum samples were obtained from arterial blood collected from radial or femoral sheath directly prior to the start of PPCI (pre-procedural) as well as from venous blood samples collected 12 hours post-PPCI as per routine clinical protocol by the attending physician. Cardiac troponin measurements were performed by pathology department staff at the Freeman Hospital. Cardiac troponin I (cTnI) was measured in 1,809 (36.8%) patients with the Siemens cTnI assay on a point-of-care Stratus CS analyser (Siemens Healthcare Diagnostics, Germany) whereas cardiac troponin T (cTnT) was quantified in 3,105 (63.2%) individuals with the Roche Elecsys high-sensitivity cTnT (hs-cTnT) assay on the Cobas e601 module (Roche Diagnostics, United Kingdom). According to manufacturer information, the Siemens Stratus CS cTnI assay has a limit of detection (LoD) of 30 ng/L and imprecision of 10% coefficient of variation (CV) at 60 ng/L. The hs-cTnT assay has a LoD reported at 2.05 ng/L and CV <10% at the 99th percentile (14 ng/L). Considering the high correlation between these two assays in patients with acute chest pain (r=0.758) (Haaf et al., 2014), a linear transformation of cTnI values to the cTnT scale was performed to pool all measurements and group patients according to cTn quartiles.

2.1.3. Follow-up and mortality data

The median follow-up time was 62 months. Mortality data were provided by the Office of National Statistics, which records all deaths in the UK. This information was linked to the Dendrite database using the National Health Service (NHS) patient unique identification number (NHS number). The cut-off date for mortality assessment in every patient was the 20th of June 2017. The prognostic end-points were (i) all-cause mortality during hospitalisation and (ii) longer-term all-cause mortality, which included only deaths occurred after hospital discharge.

2.1.4. Statistical analysis

Patients were assigned to quartiles according to their pre-procedural cardiac troponin (Pre-cTn) levels. Data normality was assessed using the Shapiro-Wilk test. As data did not pass the normality test, comparisons between pre-procedural troponin quartile groups were performed with the Kruskal-Wallis test with Dunn's correction for

multiple comparisons for continuous variables or with the Chi-square test for categorical variables. Following univariate Cox-regression analysis, variables that were associated with in-hospital or longer-term mortality ($p < 0.01$) were selected for identification of core models of independent predictors of mortality by Cox-regression analysis. Multivariate analysis was performed using backwards conditional stepwise Cox regression and a *p* value equal or lower than 0.01 was considered significant. The association of cTn with mortality was assessed by Kaplan Meier analysis and multivariate Cox regression over the core models. The percentage of missing values for the confounders included in the multivariate Cox regression analysis was all below 5%.

The additive predictive value of pre-cTn as a dichotomous variable (upper versus lower quartiles) over baseline predictors for in-hospital and longer-term mortality was assessed by implementing Receiver Operating Characteristic (ROC) analysis and comparing corresponding Area(s) Under the Curve (AUCs) for nested multivariable logistic regression models (i.e. the core model with pre-cTn versus the core model alone). A significant increase in the AUC ($p < 0.05$) was considered a measure of discrimination ability between the prediction models. In addition, we calculated the Harrell's C-index for censored time-to-event data (Harrell et al., 1996). Harrell's c of inverse hazard ratio was used as a measure of the predictive power of survival regression models and statistics were derived with the STATA procedures "somers d" and "lincom" (Newson, 2010).

The incremental reclassification value of pre-cTn over conventional predictors of in-hospital and longer-term mortality was estimated by categorized NRI (catNRI) (Pencina et al., 2011, Pencina et al., 2012). Categorical NRI quantifies the correctness of upward and downward reclassification into correct pre-defined risk categories (4). For in-hospital mortality, catNRI was calculated across risk categories of <2%, 2% to 5%, and ≥5%, according to the estimated probability of death during acute coronary syndrome (ACS) hospitalization by the GRACE Score v2.0 available at https://www.outcomes-umassmed.org/grace/grace_risk_table.aspx (Fox et al., 2014). For longer-term mortality, risk categories were <15%, 15-20% and ≥20%. On the basis of non-existing pre-defined risk categories of all-cause mortality in STEMI patients for the specific duration of the follow-up period, event rates were taken into account to derive the optimal cut-offs implemented in the catNRI analysis. For the

Cox-regression, ROC, and NRI analyses, only patients that had no missing values for any clinical variable were included, hence why the number of events displayed in these analyses is lower than the true total. The ROC and NRI analyses were performed by Prof Kimon Stamatelopoulos and Dr Giorgio Giorgiopoulos, from the National and Kapodistrian University of Athens. All tests were two-tailed. Statistical analysis was performed by SPSS software v22.0 (IBM, New York, USA) or STATA package, version 11.1 (StataCorp, College Station, Texas, USA). Graphs were produced using GraphPad Prism version 7 (GraphPad Software, San Diego, USA). Statistical significance was deemed at $p < 0.05$, unless stated otherwise.

2.2. STEMI cohort 2

2.2.1. Recruitment, inclusion and exclusion criteria

A second STEMI patient cohort (n = 20) was prospectively recruited between January 2017 and June 2017 for the study of miRNA release kinetics post-PPCI by Dr Ashfaq Mohammed at the Freeman Hospital. The study was approved by the local ethics committee (REC reference: 16/NE/0405). As described above, patients presenting with chest pain suggestive of myocardial ischaemia with ST-segment elevation or new left bundle branch block on the ECG and indication of PPCI (<12h of symptom onset) were included. Exclusion criteria comprised clinically unstable patients (haemodynamically unstable, shocked, or unconscious patients) and previous myocardial infarction. As per current clinical guidelines, patients received 300 mg of aspirin and 600 mg of clopidogrel, 60 mg of prasugrel or 180 mg ticagrelor loading dose along with standard doses of heparin (70 units/kg) or bivalirudin (0.75mg/kg) at admission to the cardiac catheterization laboratory. Administration of GPIIb/IIIa inhibitors was at the discretion of the attending interventional cardiologist during PPCI. In addition, one patient undergoing transcoronary ablation for septal hypertrophy (TASH) was also recruited as part of this study as a positive control for optimal coronary artery perfusion. Finally, 6 healthy individuals were also included as negative controls.

2.2.2. Blood sampling

At the start of the PCI procedure, a total of 10 mL of arterial blood was drawn into 3 x 4mL ethylenediaminetetraacetic acid (EDTA)-coated tubes [Becton Dickinson (BD) Biosciences, USA, cat. no. 367844] when the arterial sheath was inserted. These samples represented the pre-reperfusion time point. The procedure was then carried out as usual and the exact time of reperfusion was recorded. Reperfusion was defined by restoration of TIMI 2 or 3 flow and/or occurrence of reperfusion arrhythmias. Blood samples were then collected in additional 12 different time points post-reperfusion (5, 10, 20, 30, 40, 50, 60, 75, 90, 120, 180 min and 24h; 10mL of blood was drawn per time point). Samples were taken from a central arterial source up to 90 min post-reperfusion using a 6F radial artery sheath left in since the PCI procedure. At 120 min, 180 min, and 24h post-reperfusion, samples were collected by venepuncture from a peripheral venous source (antecubital vein). At each interval of 60 min, samples collected up to that point were transported at room temperature to the laboratory for plasma isolation. Blood sampling in the TASH patient followed the same approach, except that the exact time of ethanol injection, rather than reperfusion, was recorded and used as the temporal reference for further blood sampling. Only one blood sample was collected from each healthy donor from the antecubital vein using a vacutainer b;ood collection set (BD, USA, cat. no. 368652).

2.3. STEMI cohort 3

2.3.1. Recruitment, inclusion and exclusion criteria

Cryopreserved plasma samples from a third STEMI cohort were used to validate candidate miRNAs and to assess their correlation with MVO, cardiac damage and function parameters. This cohort included participants of the CAPRI trial (n = 50), which evaluated the effect of cyclosporine infusion at the start of PPCI on myocardial ischaemia and reperfusion injury. This clinical trial was approved by the local ethics committee and verbal consent was obtained once patients met inclusion criteria, followed by written consent post procedure (REC reference: NE/14/1070; EudraCT number: 2014-002628-29). The study included patients presenting within 6h of chest pain onset, ST-segment elevation, and with a major (at least 3mm) culprit coronary artery occluded (TIMI flow grade 0-1) at the time of admission coronary angiography.

Exclusion criteria comprised clinically unstable patients, presence of immunological, neoplastic, hepatic, or kidney disorders, patients with an open (TIMI flow > 1) culprit coronary artery at the time of angiography, previous MI, or contra-indications to cardiac MRI. Patients received standard pharmacological therapy as per current international guidelines and were randomized to have a bolus dose of cyclosporine or placebo at the start of PCI. In addition, demographic, clinical and laboratorial data were recoded. All patients underwent cardiac MRI assessment during hospitalisation and after discharge.

2.3.2. Blood sampling

Sample collection was performed exactly as described for STEMI cohort 2, except that blood was taken only at pre-reperfusion and at 5, 15, 30, and 90 min post-reperfusion. Samples were kept upright, at room temperature, until the last one (90 min) was collected and then were immediately taken to the laboratory for plasma isolation. Plasma was isolated using the same protocol as described for STEMI cohort 2 and was stored as 250μL aliquots in cryopreservation tubes at -80°C until analysis.

2.4. Plasma isolation

2.4.1. Standard plasma isolation

Blood samples were centrifuged at 1,500 x *g* and room temperature for 15 min and the top two thirds of the supernatant obtained at the end of the centrifugation were collected without disturbing the red cell pellet, transferred in 250μL aliquots to cryopreservation tubes and stored at -80°C until analysis. Time of sample storage until analysis varied between 6 months and 1 year.

2.4.2. Platelet-poor plasma isolation

Platelet-poor plasma was isolated from STEMI cohort 2 patient (n = 10) blood samples collected prior to and at 30 min and 90 min post-reperfusion as well as controls (n = 3) for the purposes of circulating microparticle quantification, as

standard plasma contains residual platelets that might interfere with MP analysis (Dey-Hazra et al., 2010, Mitchell et al., 2016). Isolation of platelet-poor plasma comprised two centrifugation steps: (i) whole blood was centrifuged at 1,500 x *g* and room temperature for 15 min, after which the top two thirds of the supernatant (standard plasma) were collected and transferred to a new polypropylene tube; (ii) whole plasma was then centrifuged again at 1,500 x *g* and room temperature for 15 min, the top two thirds (platelet-poor plasma) were transferred to a fresh polypropylene tube, and stored at -80°C until analysis.

2.5. Circulating microparticle isolation

Circulating microparticles were isolated from fresh platelet-poor plasma samples, as plasma cryopreservation has been shown to result in ex-vivo MP generation from residual platelets upon freezing and thawing (Dey-Hazra et al., 2010, Mitchell et al., 2016). In brief, 250μL of platelet-poor plasma were transferred to a polypropylene tube and diluted (1:4) with 750μL of phosphate buffered saline (PBS) (Gibco, by life technologies, catalogue number. 1829993). Subsequently, samples were centrifuged at 20,000 x *g* and 4°C for 30 min. The supernatant was carefully aspirated leaving the MP pellet in 20μL of the solution. Samples were immediately processed for downstream RNA extraction or flow cytometry analysis (**Figure 2.1**).

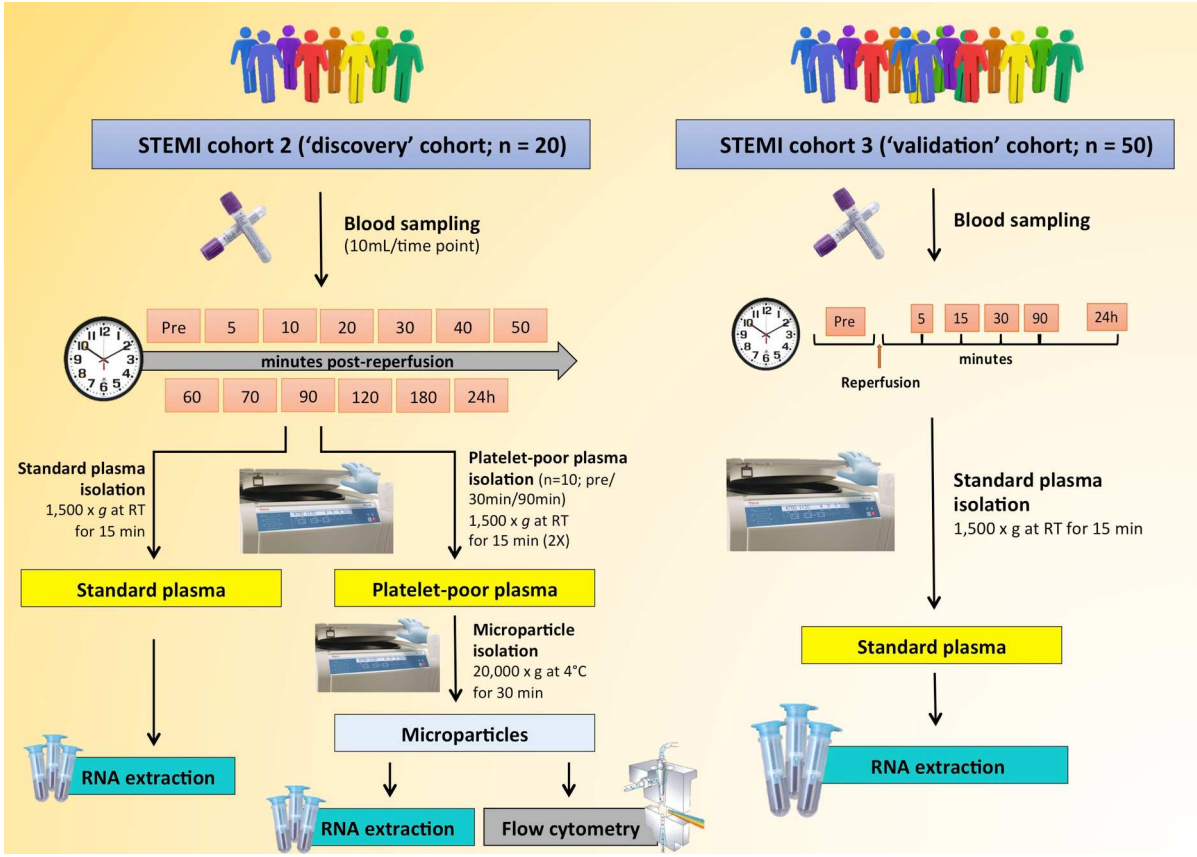

Figure 2.1. Blood sampling and processing strategy in prospectively recruited STEMI cohorts. Blood samples were collected from 2 STEMI cohorts at different time points prior to and post-PCI. The 'discovery' cohort samples were used for microRNA screening, kinetics, and plasmatic transport analyses. The 'validation' cohort samples were used to validate results observed in the 'discovery' cohort and to assess microRNA levels correlations with cardiac MRI parameters.

2.6. RNA extraction

2.6.1. RNA extraction from plasma

Plasma samples were quickly thawed at 37°C for 2 min and centrifuged at 1,900xg and room temperature for 10 min to avoid formation of cryoprecipitate and remove residual cells and debris (Cheng et al., 2013). Total RNA was isolated from 200µL of plasma using the miRNeasy serum/plasma kit (Qiagen, Germany, cat. no. 217184), according to the manufacturer's protocol. In brief, 200µL of each plasma sample were mixed with 1000µL of the Qiazol lysis reagent in 2mL polypropylene tubes and incubated at room temperature for 5 min. During the incubation period, 3.5µL (1.6 x 10^8 copies/µL) of synthetic cel-miR-39 (Qiagen, Germany, cat. no. 219610) were added to all samples. In samples used for miRNA screening, the cel-miR-39-3p RNA spike-in template (Exiqon, Denmark, cat. no. 203202) was added instead. Then,

200μL of chloroform were added to each tube, the mixture incubated for 3 minutes at room temperature, and centrifuged for 15 min at 12,000 x g and 4°C. The upper aqueous phase (500μL) was carefully collected without disturbing the interphase and transferred to a new 2mL polypropylene tube. Subsequently, 750μL of 100% ethanol were added to the aqueous phase, the mixture (750μL) was transferred to an RNeasy MinElute spin column, and centrifuged for 30 sec at 10,000 x g and room temperature. The flow-through was discarded and the procedure repeated with the remaining 500μL of the mixture. Serial washes of the column were then performed by quick centrifugation with buffer RWT (700μL), buffer RPE (500μL), and 80% ethanol (500μL) for 30 sec (buffers RWT and RPE) and 2 min (80% ethanol) at 10,000 x g and room temperature. After the serial washes, the column's membrane was dried by centrifugation for 5 min at 10,000 x g and room temperature. Finally, 60μL of RNAse-free water were added to the centre of the membrane to elute the RNA and this was collected in a fresh tube by centrifugation for 1 min at 10,000 x g and room temperature.

Following RNA extraction, assessment of total RNA concentration and integrity was performed by a 2100 Bioanalyzer instrument using the RNA 6000 Pico Kit (Agilent technologies, Germany, cat. no. 5067-1513), according to the manufacturer's protocol. RNA samples were then stored at -80°C until analysis.

2.6.2. RNA isolation from microparticles

Immediately after microparticle isolation, the 20μL MP pellet was resuspended in 180μL of PBS. The 200μL suspension was then subjected to the same RNA extraction process described in the previous section. RNA samples were stored at -80°C until analysis.

2.7. Enzyme-linked immunosorbent assay (ELISA)

Heparin was measured in pre-reperfusion plasma and plasma-derived RNA samples from the same STEMI patients (n = 10) using a competitive enzyme-linked immunosorbent assay (ELISA) kit (BlueGene, China, cat. no. E07H0247). The ELISA plate wells were already pre-coated with monoclonal anti-porcine heparin antibody.

Plasma (100µL) and RNA (10µL; diluted in 90µL of PBS to a final volume of 100µL) samples were incubated with a heparin-horseradish peroxidase (HRP) conjugate in the pre-coated wells for 1 hour at 37°C. Phosphate buffered saline (PBS) only (100µL) was added to blank control wells. Standards (100µL) containing six serial concentrations of heparin (range: 0pg/mL – 2,500pg/mL) were added to wells in duplicates to generate a standard curve for heparin concentration calculation in STEMI samples. After the incubation period, the sample-conjugate solution was removed and wells were washed with 200µL of washing buffer 6 times. A substrate for HRP (100µL) was then added to each well, including the blank wells, and incubated for 15 minutes at 37°C. Finally, a stop solution was added to the wells and absorbance was immediately measured at 450nm wavelength by spectrophotometry (Varioskan lux, Thermo Fisher Scientific, USA). A standard curve (**Figure 2.2**) was generated using a four-parameter logistic (4-PL) curve-fit. Heparin concentration in the samples was calculated based on the standard curve and dilution factor (RNA samples) by the SkanIt software (Thermo Fisher Scientific, USA).

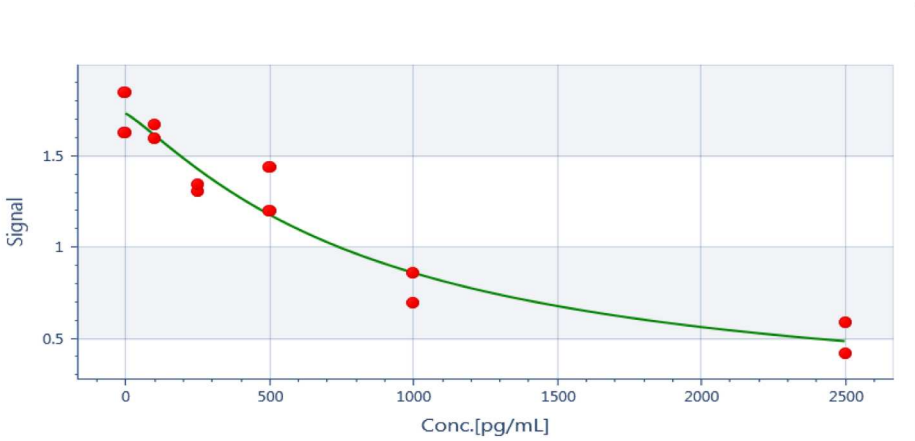

Figure 2.2. Heparin ELISA standard curve. A standard curve was generated using a four-parameter logistic (4-PL) curve-fit according to the readings obtained from standards with known heparin concentration (0; 50; 100; 500; 1000; and 2500pg/mL). The equation that describes the curve [y = 1.73465 + ((0.135615 - 1.73465) / (1 + (x/858.255)^-1.1809))], with R^2 = 0.967, was used by the SkanIt software to calculate heparin concentration in the tested RNA and plasma samples.

2.8. RNA sample treatment with heparinase

To test whether *in vitro* heparin inhibition with heparinase had any effect on miRNA detection by RT-qPCR, 5µL of heparin-contaminated RNA samples from STEMI patients (n = 3) were incubated with serial doses (0U, 0.1U, 0.25U, 0.5U, 1U) of heparinase I from *Flavobacterium heparinum* (Sigma-Aldrich, Germany, cat. no. H2519) for 1 hour prior to reverse transcription (RT) reaction set up. Along with heparinase, samples were also incubated with some of the components of the TaqMan® microRNA reverse transcription kit (Applied Biosystems, USA, cat. no. 4366597), as previously described by Johnson ML et al. (Johnson et al., 2003) and Li S et al. (Li et al., 2017) and shown in **Table 2.1**. To validate this, all samples from STEMI cohorts 1 and 2 (n = 70) were treated with a single heparinase dose (0.3U) and miRNA expression was compared with heparin-contaminated samples from the same patients.

Reagents	Volume (µL/per reaction)
RNA sample	5
Heparinase	1
10X RT buffer	1.5
RNAse inhibitor	0.19
Total reaction volume	**7.69**

Table 2.1. RNA sample treatment with heparinase

2.9. Reverse transcription

2.9.1. Universal reverse transcription

For miRNA screening experiments, 4µL of total RNA were reverse transcribed using the Universal cDNA synthesis kit II (Exiqon, Denmark, cat. no. 203301). RNA samples were mixed with the components of the kit in nuclease-free 0.2mL polypropylene tubes on ice, as indicated in **Table 2.1**. A spike-in miRNA (UniSp6) was also added across all samples to control for variations in complementary DNA (cDNA) synthesis (**Table 2.2**). Reverse transcription (RT) reactions were carried out

in a thermocycler with the settings: (i) incubation at 42°C for 60 min; (ii) inactivation at 95°C for 5 min.

RT reaction components	Volume (µL/per reaction)
RNA sample	4
5X Reaction buffer	4
Enzyme mix	2
UniSp6 spike-in	1
Nuclease free water	9
Total reaction volume	**20**

Table 2.2. Universal reverse transcription reaction components

2.9.2. Taqman-based reverse transcription

Reverse transcription for each target miRNA in cohorts 2 and 3 were performed using 5µL of RNA, TaqMan® microRNA reverse transcription kit (Applied Biosystems, USA, cat. no. 4366597) and stem-loop specific 5X TaqMan microRNA assays (Applied Biosystems, USA, cat. no. 4427975). Reverse transcription in all samples from cohorts 2 and 3 were performed without prior RNA treatment with heparinase and with heparinase treatment to test the effect of in vitro heparin inhibition on miRNA detection by RT-qPCR. In samples not treated with heparinase, 5µL of RNA were mixed with the components of the kit and the 5X microRNA assay in nuclease-free 0.2mL polypropylene tubes on ice, as indicated in **Table 2.3**. In RNA samples that had been treated with heparinase, the remaining components of the RT kit were added as described in **Table 2.4**. No reverse transcriptase control reactions containing all reagents but reverse transcriptase were also included to control for genomic DNA contamination. Reverse transcription was carried out in a thermocycler with the settings: (i) incubation at 16°C for 30 min; (ii) incubation at 42°C for 30 min; (iii) inactivation at 85°C for 5 min.

RT reaction components	Volume (µL/per reaction)
RNA sample	5
dNTPs	0.15
Reverse transcriptase	1
10X RT buffer	1.5
RNAse inhibitor	0.19
Nuclease-free water	4.16
TaqMan 5X miRNA assay	3
Total reaction volume	**15**

Table 2.3. Reverse transcription reaction set up for heparin-contaminated RNA samples.

RT reaction components	Volume (µL/per reaction)
RNA sample	5
Heparinase	1
dNTPs	0.15
Reverse transcriptase	1
10X RT buffer	1.5
RNAse inhibitor	0.19
Nuclease-free water	3.16
TaqMan 5X miRNA assay	3
Total reaction volume	**15**

Table 2.4. Reverse transcription reaction set up for heparinase-treated RNA samples. Note that the final reaction volume is the same as for the RT reaction for heparin-contaminated RNA samples due to 1µL less of nuclease-free water to compensate for the addition of 1µL of heparinase.

2.10. Effect of heparin and bivalirudin on miRNA detection

2.10.1. Effect of in vitro heparin addition to RNA samples

To assess the effect of *in vitro* heparin addition to RNA samples on miRNA detection by RT-qPCR, serial doses (0U, 0.005U, 0.05U, 0.1U, 0.25U, 0.5U, 1U, and 2U) of heparin sodium 1,000 IU/mL (Wockhardt, UK, cat. no. FP1079) were added to 5µL

heparin-free RNA samples from STEMI patients (*n* = 3) and the components of the TaqMan® microRNA reverse transcription kit, as shown in **Table 2.5**. Reverse transcription was performed using the same settings as mentioned in the previous section. The difference in quantification cycle (Cq) values (ΔCq) to the heparin-free samples from the same STEMI patients were calculated after RT-qPCR.

RT reaction components	Volume (µL/per reaction)
RNA sample	5
Heparin	1
dNTPs	0.15
Reverse transcriptase	1
10X RT buffer	1.5
RNAse inhibitor	0.19
Nuclease-free water	3.16
TaqMan 5X miRNA assay	3
Total reaction volume	**15**

Table 2.5. Reverse transcription reaction set up for experiments testing the effect of *in vitro* heparin addition to RNA samples on miRNA detection.

2.10.2. Effect of in vitro bivalirudin addition to RNA samples

To investigate whether *in vitro* addition of bivalirudin (Sigma-Aldrich, Germany, cat. no. SML1051) to RNA samples would have any effect on cel-miR-39 or the endogenous miRNA control expression, 0.1 and 1 µg/µL of bivalirudin were added to bivalirudin-free RNA samples from stable CAD patients (*n* = 3) just prior to reverse transcription (**Table 2.6**). Then, the ΔCq between bivalirudin-free and bivalirudin-treated RNA samples from the same patients with stable CAD were determined after RT-qPCR.

RT reaction components	Volume (µL/per reaction)
RNA sample	5
Heparin	1
dNTPs	0.15
Reverse transcriptase	1
10X RT buffer	1.5
RNAse inhibitor	0.19
Nuclease-free water	3.16
TaqMan 5X miRNA assay	3
Total reaction volume	**15**

Table 2.6. Reverse transcription reaction set up for experiments testing the effect of *in vitro* bivalirudin addition to RNA samples on miRNA detection.

2.11. Real-time quantitative polymerase chain reaction

2.11.1. SYBR-based qPCR

Only fresh cDNA samples were used for PCR quantification. Screening of 179 circulating miRNAs was performed using human serum/plasma focused miRNA PCR panels (Exiqon, Denmark, cat. no. 339325) and the Exilent SYBR Green master mix (Exiqon, Denmark, cat. no. 203421). Each miRNA PCR panel comprised 2x 96-well plates pre-coated with LNA miRNA primers for target miRNAs, for the spike-in miRNAs added cel-miR-39, UniSp6, and UniSp3 as well as blank wells. For each plate, 10µL of cDNA were mixed with 500µL of the Exilent SYBR Green master mix and 490µL of nuclease-free water in a 2mL polypropylene tube. Subsequently, 10µL the mixture was added to each well on ice. The plate was covered with an optical adhesive film (Applied Biosystems, USA, cat. no. 4311971), briefly centrifuged, and loaded into a 7500AB PCR instrument (Applied Biosystems, USA). The PCR reaction was carried out with the following settings: (i) polymerase activation at 95°C for 10 min; (ii) denaturation (40 cycles) at 95°C for 10 sec; (iii) annealing/extension at 60°C for 60sec; (iv) melting curve analysis.

2.11.2. SYBR-based qPCR data quality control

Data quality control assessment was based on the Cq values obtained for cel-miR-39, UniSp6, and UniSp3 templates across all samples. These spike-in miRNAs had been added to samples prior to RNA extraction (cel-miR-39), cDNA synthesis (UniSp6), or were included in the PCR plate (UniSp3) to control for variations in each of these experimental steps.

2.11.3. TaqMan-based qPCR

Target microRNA quantification using hydrolysis probes was performed with freshly synthesised cDNA only. Each PCR reaction for individual miRNAs was prepared in nuclease-free 0.2mL polypropylene tubes on ice, by mixing 4.8µL of cDNA sample, 3.6µL of 20X TaqMan small RNA assay, 36µL of the SensiFAST probe Hi-ROX master mix (Bioline, UK, cat. no. BIO-82005), and 27.6µL of nuclease-free water to a total volume of 72µL. Subsequently, 20µL of the mixture were transferred to a 96-well PCR plate in triplicates. No cDNA template control and no reverse transcription control reactions for each target miRNA were also added in triplicate. The plate was covered with an optical adhesive film, briefly centrifuged, and loaded into a 7500AB PCR instrument (Applied Biosystems, USA). The PCR reaction was carried out with the following settings: (i) polymerase activation at 95°C for 10 min; (ii) denaturation (40 cycles) at 95°C for 15 sec; (iii) annealing/extension at 60°C for 60sec.

2.11.4. TaqMan assay efficiency

Efficiency of TaqMan small RNA assays for each of the 7 miRNAs quantified by TaqMan-based RT-qPCR in this study was assessed. Reverse transcription was carried out using each assay as described in section 3.9.1 and a serial cDNA dilution in nuclease-free water (dilution factor = 4) was performed. Real-time qPCR was then carried out in triplicates using the different cDNA dilutions and a fixed 20X small RNA assay volume (3.6µL), as described in the previous section, to produce a calibration curve based on the Cq values obtained for each cDNA dilution for estimation of assay efficiency. Assay efficiency (E%) was calculated as a function of the calibration curves slopes: $E = 10^{(-1/slope)}$. All assays presented E% between 95% and 105% as

well as coefficient of determination (R^2) > 0.98, indicating optimal qPCR amplification (**Figure 2.3**).

2.11.5. Data analysis and normalisation

In the miRNA screening experiments, inter-plate calibration was performed to minimize PCR inter-run variability. A calibration factor for each plate was determined as the difference between the average Cq of UniSp3 triplicates in that plate and the overall UniSp3 Cq average for all plates. Inter-plate calibration was performed by correcting the target miRNA Cq in each plate according to the calibration factor. The global miRNA mean expression was calculated as the geometric mean of Cq values obtained for all miRNAs, excluding miRNAs with Cq > 35. In both SYBR- and TaqMan-based PCR experiments, the comparative Cq (ΔΔCq) method was used to determine Cq values and real-time qPCR data was analyzed using the 7500 software v2.0.5 (Applied Biosystems, USA). Fold changes were calculated using the $2^{-\Delta\Delta Cq}$ method.

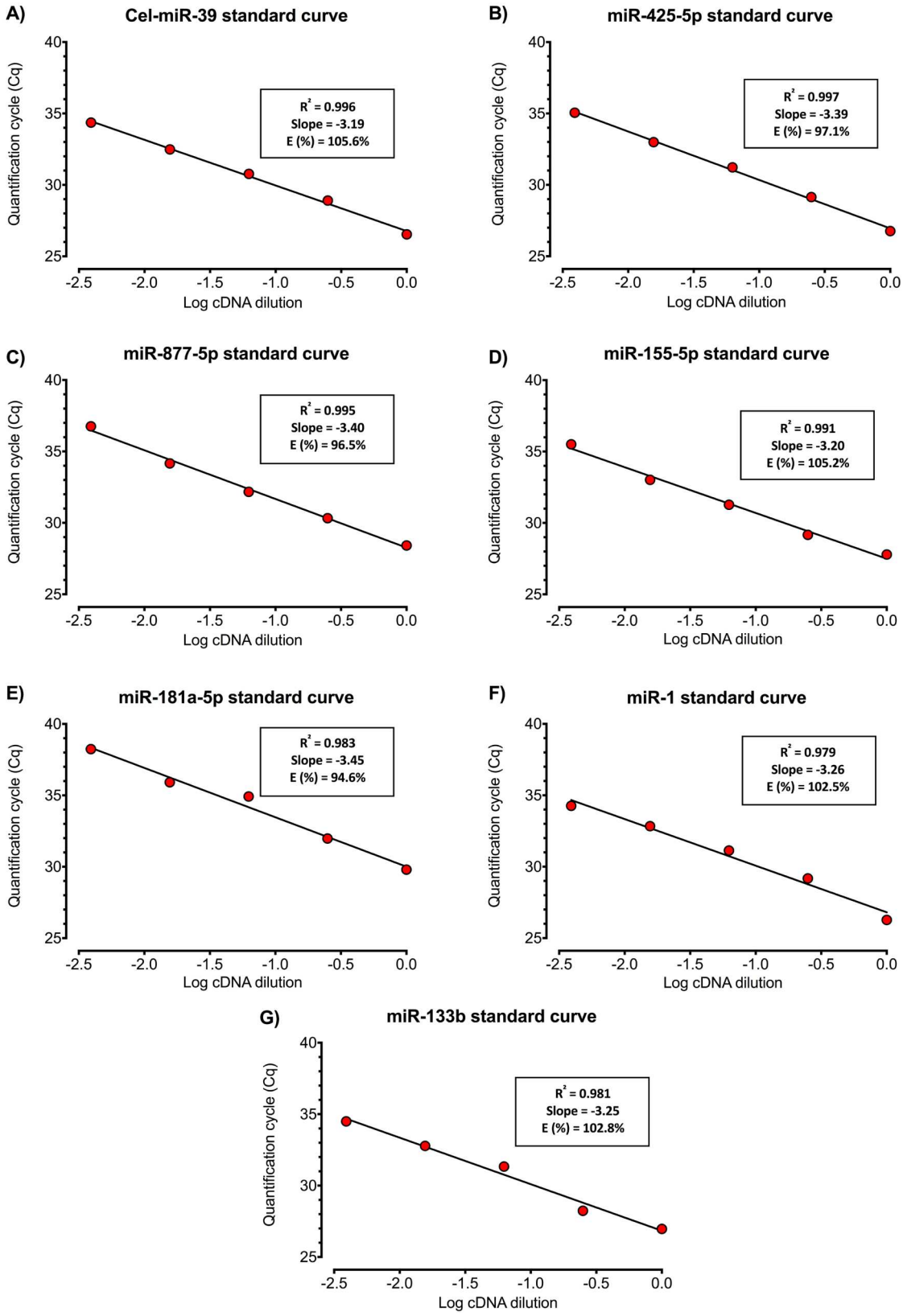

Figure 2.3. TaqMan small RNA assay calibration curves. Serial cDNA template dilutions (dilution factor = 4) were performed and calibration curves were plotted. The coefficient of determination (R^2) and slope for each curve are displayed. Primer efficiency (E%) was calculated as a function of the slope, $E = 10^{(-1/slope)}$. Quantification cycle (Cq) values are displayed as the average of 3 technical replicates.

2.12. MicroRNA expression stability assessment

In order to validate an endogenous miRNA control for RT-qPCR normalization, expression stability of each candidate microRNA across different samples was determined by calculation of the coefficient of variability (CV) and by the NormFinder v20 (Andersen et al., 2004), geNorm v3.5 (Vandesompele et al., 2002), and BestKeeper (Pfaffl et al., 2004) software. The CV was calculated as the ratio between the standard deviation and mean of the Cq values obtained for each miRNA across all samples and then multiplied by 100. The Cq values for candidate miRNAs obtained in each sample were simultaneously input in the software applications for determination of expression stability. Each software applications utilize a different statistical algorithm to determine the variation in expression of multiple candidate normalisation genes across different samples. Lower stability scores in NormFinder (*S* score), geNorm (*M* score), and BestKeeper [standard deviation - SD (±crossing point)] are expected for more stable miRNAs. Therefore, results from these different software were analysed in combination in order to find the most stably expressed endogenous miRNA in STEMI patients.

2.13. Flow cytometry

2.13.1. Microparticle staining with annexin-V

Circulating microparticles obtained as described in section 2.5 were processed for quantification by flow cytometric analysis. The microparticle pellet was resuspended in 100µL of 1X annexin-V binding buffer (10nM HEPES, pH 7.4, 140nM NaCl, 2.5nM $CaCl_2$,) (BD Biosciences, USA, cat. no. 51-66121E), which had been diluted in 1:10 with distilled water. The MP suspension was then incubated with 5µL of FITC annexin-V or 5µL of a FITC isotype control (FITC mouse IgG2b κ isotype control, Biolegend, cat. no. 401205) for 30 minutes, protected from light, at room temperature. At the end of the incubation period, MP samples were washed with 500µL of PBS and centrifuged at 20,000 x *g* and 4°C for 20 minutes. The supernatant was carefully aspirated and the MP pellet was resuspended in 500µL of 1X annexin-V buffer. The MP suspension was then transferred to TruCount™ tubes (BD biosciences, USA, cat. no. 340334). The tubes were gently vortexed for 5 seconds and incubated at room temperature in the dark for 20 minutes, as per the

manufacturer's recommendation. Samples were then taken immediately for quantification by flow cytometry.

2.13.2. Microparticle gating strategy

Because of MP's very small size, flow cytometric MP analysis requires working conditions very close to the lowest limit of detection of current flow cytometers. Therefore, adequate MP quantification relies on the optimal balance between MP detection and signal background exclusion. To achieve this, Megamix-Plus SSC (BioCytex, France, cat. no. 7803) were employed to calibrate the flow cytometer and establish a gate for MP sample analyses. Megamix-Plus SSC are fluorescent beads of varied diameters (0.16µm, 0.20µm, 0.24µm, and 0.5µm) that are equivalent to the size range of MP (0.3 to 1µm) when using side scatter (SSC) as a size-related parameter. Briefly, 500µL of the beads suspension were transferred to a cytometric tube, which was vortexed and positioned in a BD FACS Canto II cytometer for calibration using the FACSDiva software (BD Biosciences, San Jose, CA, USA). The cytometer settings were adjusted according to BioCytex's recommendations and bead acquisition was performed in the lowest available speed. Gating strategy comprised 3 steps (**Figure 2.4A**):

1. Adjustment of the FITC detector voltage so that the 0.5µm bead population is at the beginning of the 5th decade (**Figure 2.4A left upper panel**).
2. Determination of MP region boundaries. On a SSC-H count histogram, the number of events and SSC-H median parameters were calculated for each of the 4 bead populaitons. The lowest MP gate boundary was determined by the formula: Low SSC-H lelvel = Md 0.16 + (0.3 x (Md 0.20 – Md 0.16)), where Md 0.16 represented the median SSC-H for the 0.16µm bead population and Md 0.20 represented the median SSC-H for the 0.20µm bead population. The highest boundary corresponded to the end of the 0.50µm SSC-H peak (**Figure 2.4A middle upper panel**). Another boundary was also set at centre of the gap between the 0.20µm and 0.24µm peaks, which corresponds to differentiate small (< 0.50µm) and large (≥ 0.50µm) MP.
3. Setting the MP gate in dual scatter. Once the MP gate boundaries were defined on the SSC (log) scale, the corresponding regions were created on a dual scatter plot (SSC-H x FSC-H), which was used for later MP analysis

Figure 2.4A right upper panel). This calibration procedure was repeated regularly to minimise variability across different samples.

To confirm whether the MP gate was indeed able to separate 'true' annexin-V events from the instrument background noise the following samples were analysed under the same settings (n = 3 for each): (i) filtered 1X annexin-V binding buffer only (**Figure 2.4B**); (ii) unstained MP (**Figure 2.4C**); (iii) MP sample with FITC isotype control (**Figure 2.4D**); (iv) annexin-V-stained MP (**Figure 2.4E**).

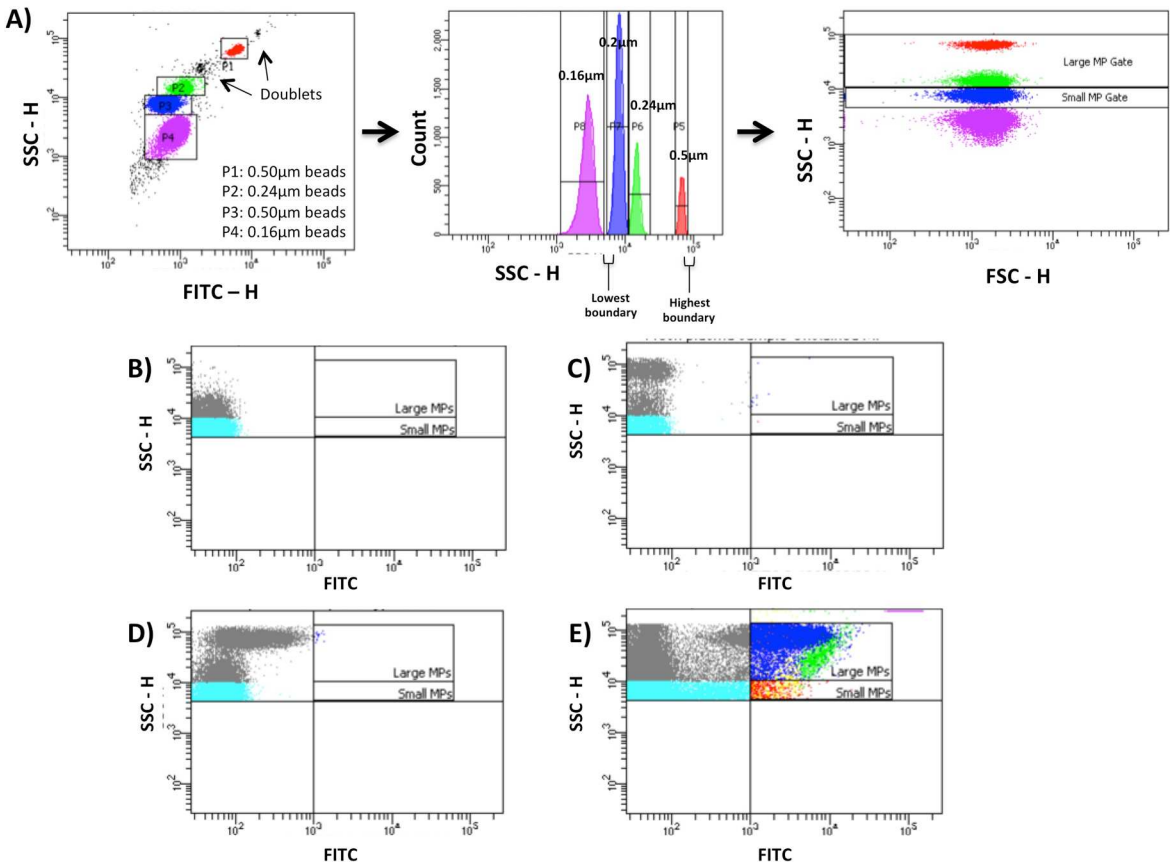

Figure 2.4. Gating strategy for circulating microparticle quantification by flow cytometry. (A) Microparticle gate boundaries determination with Megamix-plus SSC fluorescent beads. **(B)** Filtered 1X annexin-V binding buffer only; **(C)** unstained MP sample; **(D)** MP sample stained with FITC IgG isotype control; **(D)** Annexin-V-stained MP sample.

2.13.3. FACS analysis and microparticle quantification

TruCount™ tubes contining microparticle samples stained with FITC annexin-V or FITC IgG isotype control were gently vortexed prior to analysis to mix contents well. All samples were analysed at low speed until 10,000 TruCount™ beads were acquired using the BD FACS Canto II cytometer and the FACSDiva software. Microparticles were considered as annexin-V positive events detected within both the large and small MP gate. Considering that the number of TruCount™ beads in each tube is accurately determined by the manufacturer and was known in each case, the absolute MP count (MP/µl) in each 250µL plasma sample could be determined by comparing the number of positive events in the MP gate, with the number of TruCount™ bead events. This was calculated using the formula:

$$\text{MP count (MP/µl)} = \frac{\#\text{events in MP gate}}{\#\text{TruCount bead events}} \times \frac{\#\text{beads/tube}}{\text{volume plasma/test(µl)}}$$

2.14. Additional methods

2.14.1. Cardiac magnetic resonance imaging

Cardiac magnetic resonance imaging was performed in patients from cohort 3 at 1-7 days post-MI (average of 3 days; 'baseline MRI') as well as at 3 months post-MI ('follow-up' MRI) with a Siemens Avanto 1.5 Telsa MRI scanner using a phased array body coil combined with a spine coil. In brief, according to the CAPRI trial protocol, cine images of the heart in 2, 3 and 4 chamber views were obtained using a steady state free precession pulse (SSFP) sequence (repetition time [TR]: set according to heart rate, image matrix 144x192, echo time (TE): 1.19ms, flip angle: 80°). T2 weighted STIR (short inversion time [TI] inversion recovery) images were obtained in the same projections, using a black-blood segmented turbo spin echo technique (TR according to heart rate, TE 47ms, flip angle 180°, TI 140ms, image matrix 208x256). Gadobutrol, a contrast agent (Gadovist, Bayer Schering Pharma AG, Berlin, Germany), was administered intravenously at a dose of 0.1mmol/kg, and after 10 minutes short axis end-diastolic LGE images (in corresponding locations to cine and

STIR images) were obtained using an inversion recovery (IR) segmented gradient echo sequence (TR: according to heart rate, TE: 3.41ms, flip angle: 25°, image matrix: 196x256). Imaging analysis was carried out using the cvi42 software (Circle Cardiovascular Imaging Inc., Calgary, Canada) by a trained research fellow involved in the CAPRI trial, Dr Ashfaq Mohammed. Epicardial and endocardial borders were traced automatically on each end-systolic and end-diastolic short axis cine frame with manual correction where necessary, allowing automated calculation of left ventricular mass, dimensions and ejection fraction (LVEF). For infarct size and MVO determination, LGE images taken at the end of diastole were used. Areas of enhancement with signal > 5 standard deviations above normal myocardial areas (infarction) were identified and quantified automatically. Regions of hypoenhancement within a hyperenhanced zone (MVO) were also identified and semi-automatically quantified. To prevent bias, miRNA measurements were performed in a blind fashion in relation to cardiac imaging data.

2.14.2. Index of microvascular resistance

The index of microvascular resistance (IMR) was invasively determined immediately after stent deployment in the infarct-related artery using a combined temperature and pressure coronary wire sensor (Certus, ST. Jude Medical). Hyperaemia was induced by intracoronary adenosine injection. IMR was determined as the distal coronary pressure multiplied by the mean transit time of three consecutive bolus injections of room temperature saline (3 mL) during maximal coronary adenosine-induced hyperaemia.

2.15. Statistical analysis

Statistical analysis was performed with the SPSS software v22.0 (IBM, New York, USA). Data normality was assessed using the Shapiro-Wilk test. Gaussian-distributed data were analyzed using parametric tests (t test with Welch's correction; paired *t*-test; or one-way ANOVA, where appropriate) and non-Gaussian data using non-parametric tests (Mann Whiteny U test; Wilcoxon matched-pairs signed rank test). Correlations between variables were analyzed with the Spearman's correlation test. Data are presented as mean and standard error of the mean and standard

deviation (SD) or median and interquartile ranges (IQR) where appropriate and a $p < 0.05$ was considered statistically significant, unless stated otherwise.

Chapter 3. Prognostic Value of Cardiac Troponin in STEMI patients

3.1. Introduction

Cardiac troponins (cTn) are established markers of myocardial damage. In response to STEMI, a small pool of cytoplasmic troponins is quickly released from cardiomyocytes into the circulation followed by a sustained, myofibril degradation-associated cTn release (Wu, 2017). In STEMI patients treated with reperfusion therapy, circulating cTn levels reach a peak between 8-12h post-reperfusion (Katus et al., 1991, Solecki et al., 2015, Laugaudin et al., 2016). This peak is higher in amplitude and occurs earlier when compared to non-reperfused patients (Katus et al., 1991, Solecki et al., 2015, Laugaudin et al., 2016). Some studies have shown an association between post-reperfusion cTn levels and failed myocardial reperfusion, as evidenced by the presence of microvascular obstruction on cardiac MRI (Younger et al., 2007, Hallen et al., 2011, Mayr et al., 2012, Pernet et al., 2014, Nguyen et al., 2015a). This observation suggests that cTn may provide useful prognostic information in this population.

Nonetheless, there is scarce and conflicting evidence regarding the prognostic relevance of current cTn assays for prediction of mortality in STEMI patients undergoing PPCI (Cediel et al., 2017, Boden et al., 2013, Buber et al., 2015, Hall et al., 2015, Nguyen et al., 2016). Considering that the reperfusion process significantly affects cTn release, I hypothesized that pre-procedural cTn (pre-cTn) may be a stronger predictor of mortality as compared to post-PCI, peak cTn. This chapter aimed to assess the prognostic power of pre-PCI as well as 12h post-PCI cTn levels for mortality prediction in a large cohort of consecutive STEMI patients treated with PPCI.

3.2. Results

3.2.1. Patient baseline and peri-procedural characteristics

Both pre-cTn and post-procedural cTn were available for 4,914 (92.9%) patients and were used for analysis. Cohort baseline characteristics are displayed in **Table 3.1**. In summary, patients with higher pre-cTn levels were more likely to be female and older but had lower prevalence of traditional cardiovascular risk factors (current smoking, family history of CAD, hypercholesterolaemia, and obesity) and prior history of CAD. Furthermore, patients in the highest pre-cTn quartile were more often admitted following inter-hospital transfer than directly from ambulance ($p < 0.001$) and presented with greater incidence of cardiogenic shock (Killip class IV; $p < 0.001$), higher heart rate ($p < 0.001$), longer symptom-onset-to-reperfusion time ($p < 0.001$) and door-to-balloon (dtob) time ($p < 0.001$), and greater frequency of anterior myocardial infarction ($p < 0.001$) (**Table 3.1**).

In terms of periprocedural parameters (**Table 3.2**), patients in the highest pre-cTn quartile required more frequent femoral access ($p < 0.001$), received greater volumes of contrast media ($p < 0.001$), and received GPIIb/IIIa inhibitors more often ($p < 0.001$). Furthermore, this group of patients displayed a higher incidence of angiographic coronary 'slow flow' phenomenon ($p < 0.001$) and were less likely to achieve TIMI flow 3 post-PPCI ($p < 0.001$) (**Table 3.2**).

Variable	Entire cohort	1st cTn quartile* (< 34 ng/L)	2nd cTn quartile* (34 – 124.9 ng/L)	3rd cTn quartile* (125 – 669.2 ng/L)	4th cTn quartile* (> 669.2 ng/L)	*p* value
Sample size, n (%)	4,914 (100%)	1,246 (25.4)	1,217 (24.8)	1,223 (24.9)	1,228 (25)	
Gender (male), n (%)	3,485 (70.9)	911 (73.1)	871 (71.6)	825 (67.5)	878 (71.6)	**0.015**
Age [years, mean (SD)]	62 (13)	60.6 (12.3)	62.5 (12.7)	64.6 (12.8)	63.8 (13.7)	**<0.001**
Risk factors, n (%)						
Smoking status						
Never smoked	1,190 (25.9)	285 (24.2)	296 (25.8)	327 (28.5)	282 (25.1)	0.104
Ex-smoker	1,296 (28.2)	308 (26.2)	354 (30.8)	304 (26.5)	330 (29.6)	**0.034**
Current smoker	2,109 (42,9)	583 (49.6)	498 (43.4)	516 (45)	512 (45.6)	**0.021**
Family history of CAD	2,097 (45.8)	583 (49.1)	526 (46)	518 (44.9)	470 (42.8)	**0.022**
Hypertension	2,164 (44)	553 (44.4)	559 (45.9)	544 (44.5)	508 (41.4)	0.140
Diabetes Mellitus	587 (12.1)	151 (12.3)	144 (11.9)	132 (10.9)	160 (13.3)	0.356
Hypercholesterolemia	1,774 (36.1)	483 (38.8)	461 (37.9)	430 (35.2)	400 (32.6)	**0.006**
Obesity	1,202 (27.1)	343 (29.6)	318 (28.2)	275 (25.2)	266 (25)	**0.032**
Medical history of CAD, n (%)						
Previous angina	890 (18.3)	254 (20.6)	259 (21.5)	189 (15.6)	188 (15.6)	**<0.001**
Previous MI	569 (11.7)	179 (14.5)	147 (12.2)	119 (9.9)	124 (10.4)	**0.001**
Previous PCI	311 (6.3)	110 (8.8)	73 (6)	60 (4.9)	68 (5.6)	**<0.001**
Previous CABG	89 (1.8)	23 (1.8)	28 (2.3)	19 (1.6)	19 (1.6)	0.466
Clinical characteristics on admission						
Heart rate, bpm [median (IQR)]	74 (62 – 87)	70 (60 – 81)	73 (62 – 87)	77 (65 – 89)	78 (65 – 92)	**<0.001**
Systolic BP, mmHg [median (IQR)]	128 (110 – 148)	126 (110 – 146)	128 (110 – 148)	130 (110 – 150)	127 (108 – 148)	0.310
Cardiogenic shock, n (%)	198 (4.1)	30 (2.4)	35 (2.9)	55 (4.5)	78 (6.4)	**<0.001**
Admission route, n (%)						
Emergency services	3,508 (71.4)	1,018 (81.7)	889 (73)	802 (65.6)	799 (65.1)	**<0.001**
Inter-hospital transfer	1,406 (28.6)	228 (18.3)	328 (27)	421 (34.4)	429 (34.9)	**<0.001**
Door to balloon, min [median (IQR)]	24 (18 – 34)	24 (18 – 33)	24 (18 – 35)	23 (18 – 32)	26 (18 – 36)	**<0.001**

Onset to reperfusion, min [median (IQR)]	168 (117 – 269)	134 (104 – 191)	164 (117 – 241)	190 (128 – 310)	209 (133 – 422)	**<0.001**
Infarct location, n (%)						
Anterior	1,884 (38.9)	359 (29.3)	454 (37.8)	496 (41.1)	575 (47.4)	**<0.001**
Biochemical tests [median (IQR)]						
Pre-PCI haemoglobin, g/dL	13.9 (12.6 – 15)	14.2 (12.9 – 15.2)	13.9 (12.7 – 15)	13.6 (12.4 – 14.7)	13.8 (12.4 – 14.8)	**< 0.001**
Pre-PCI creatinine, μmol/L	86 (73 – 102)	85 (72 – 101)	85 (72 – 100)	83.5 (70 – 99)	91 (76 – 108)	**< 0.001**
Pre-PCI cTnT, ng/L	126 (34 – 672)	18 (12 – 24)	66 (48 – 88)	291 (184 – 452)	2,199 (1,162 – 6,074)	**< 0.001**
12h cTnT, ng/L	2,798 (786 – 8,092)	1,720 (356 – 5,756)	1,784 (440 – 5,576)	2,676 (639 – 6,339)	6,282 (2440 – 10,000)	**< 0.001**
Outcome						
In-hospital mortality, n (%)	167 (3.4)	16 (1.3)	25 (2.1)	36 (2.9)	90 (7.3)	**<0.001**
Longer-term mortality, n (%)	820 (17.3)	162 (13.2)	174 (14.6)	216 (18.2)	268 (23.6)	**<0.001**
Overall mortality, n (%)	987 (20.7)	178 (14.3)	199 (16.4)	252 (20.6)	358 (29.2)	**<0.001**

Table 3.1. Descriptive clinical characteristics of the study population. BP, blood pressure; CABG, coronary artery bypass graft; CAD, coronary artery disease; cTn, cardiac troponin; IQR, interquartile range; MI, myocardial infarction; PCI, percutaneous coronary intervention; TIMI, thrombolysis in myocardial infarction angiographic score. *Pre-procedural cardiac troponin quartiles

Variable	Entire cohort	1st cTn quartile (< 34 ng/L)	2nd cTn quartile (34 – 124.9 ng/L)	3rd cTn quartile (125 – 669.2 ng/L)	4th cTn quartile (> 669.2 ng/L)	*p* value
Arterial access, n (%)						
Radial	3,823 (77.9)	1,021 (82)	974 (80.1)	966 (79.1)	862 (70.4)	**< 0.001**
Femoral	1,077 (21.9)	223 (17.9)	241 (19.8)	253 (20.7)	360 (29.4)	**< 0.001**
Brachial	8 (0.2)	1 (0.1)	1 (0.1)	3 (0.3)	3 (0.2)	0.567
GPIIb/IIIa medication, n (%)	3,502 (71.7)	878 (71)	850 (70.2)	836 (68.8)	938 (76.9)	**< 0.001**
Contrast volume, mL	140 (100 – 170)	130 (100 – 160)	140 (100 – 170)	140 (108 – 175)	150 (110 -190)	**< 0.001**
TIMI flow pre-PCI, n (%)						
0	3,427 (72.1)	858 (71.5)	828 (70.5)	810 (68)	931 (78.2)	**< 0.001**
1	241 (5.1)	56 (4.7)	53 (4.5)	68 (5.7)	64 (5.4)	0.494
2	455 (9.6)	115 (9.6)	116 (9.9)	123 (10.3)	101 (8.5)	0.465
3	633 (13.3)	171 (14.3)	177 (15.1)	190 (16)	95 (8)	**< 0.001**
Thrombus aspiration	2,518 (51.4)	667 (53.6)	669 (55.1)	628 (51.5)	554 (45.2)	**< 0.001**
Number of stents						
0	281 (5.7)	55 (4.4)	66 (5.4)	61 (5)	99 (8.1)	**< 0.001**
1	2,654 (54)	709 (56.9)	697 (57.3)	658 (53.8)	590 (48)	**< 0.001**
2	1,393 (28.3)	340 (27.3)	321 (26.4)	353 (28.9)	379 (30.9)	0.072
3	427 (8.7)	104 (8.3)	98 (8.1)	116 (9.5)	109 (8.9)	0.607
> 3	157 (3.2)	37 (3)	35 (2.9)	35 (2.9)	50 (4.1)	0.251
Intra-procedural complications						
Coronary slow flow	84 (1.7)	5 (0.4)	22 (1.8)	20 (1.6)	37 (3)	**< 0.001**
Coronary dissection	83 (1.7)	26 (2.1)	15 (1.2)	20 (1.6)	22 (1.8)	0.421
Coronary perforation	15 (0.3)	5 (0.4)	2 (0.2)	4 (0.3)	4 (0.3)	0.751
Aortic dissection	5 (0.1)	0 (0)	1 (0.1)	2 (0.2)	2 (0.2)	0.527
Side branch occlusion	26 (0.5)	7 (0.6)	7 (0.6)	7 (0.6)	5 (0.4)	0.927
Heart block requiring pacing	7 (0.1)	2 (0.2)	1 (0.1)	3 (0.2)	1 (0.1)	0.666
Direct current cardioversion	53 (1.1)	18 (1.4)	12 (1)	13 (1.1)	10 (0.8)	0.481
TIMI flow post-PCI, n (%)						
0	107 (2.3)	21 (1.8)	30 (2.6)	22 (1.9)	34 (2.9)	0.180

1	47 (1)	8 (0.7)	7 (0.6)	9 (0.8)	23 (2)	**0.002**
2	187 (4)	22 (1.8)	31 (2.6)	48 (4.1)	86 (7.4)	**< 0.001**
3	4,349 (92.7)	1,140 (95.7)	1,103 (94.2)	1,090 (93.2)	1,016 (87.7)	**< 0.001**

Table 3.2. Periprocedural parameters. IQR, interquartile range; gpIIb/IIIa, glycoprotein IIb/IIIa inhibitors; PCI, percutaneous coronary intervention; TIMI, thrombolysis in myocardial infarction angiographic score

3.2.2. Higher pre-cTn levels are associated with increased mortality

In-hospital mortality rate was 3.4% and overall mortality was 20.7% (n=987 deaths) at a median follow-up period of 53 months (interquartile range 37 – 68 months) (**Table 3.1**). Patients in the highest quartile of pre-cTn had nearly a 6-fold higher in-hospital mortality rate compared to patients in the lowest quartile (7.3% vs. 1.3%, $p < 0.001$) (**Table 3.1**). Higher pre-cTn levels were also associated with an approximately 2-fold greater mortality rate after hospital discharge (23.6% vs. 13.2%, $p < 0.001$) (**Table 3.1)**. Both pre-cTn (log rank $p < 0.001$) and 12h post-PCI cTn (log rank $p = 0.003$) were associated with overall mortality by univariate Kaplan-Meier analysis (**Figures 3.1** and **3.2**). Although, curves for each pre-cTn quartile did not intersect, with ascending number of events across quartiles (**Figure 3.1**), whereas there was an overlap in Kaplan Meier curves for the 3 lower quartiles of 12h cTn (**Figure 3.2**).

Co-variables identified as determinants of high pre-cTn were (i) delay in PPCI for patients with inter-hospital transfer ($p = 0.001$), (ii) admission serum creatinine levels ($p < 0.001$), (iii) heart rate on admission ($p = 0.036$), (iv) cardiogenic shock on admission ($p < 0.001$), (v) previous history of myocardial infarction (0.023), (vi) presumed area at risk (anterior location, $p < 0.001$) and (vii) lack of spontaneous recanalization prior to PPCI (i.e. lack of TIMI 3 flow pre-PPCI, $p < 0.001$) (**Table 3.3**). In addition, age ($p < 0.001$), previous angina ($p = 0.037$), pre-PPCI haemoglobin ($p < 0.001$), pre-PPCI creatinine ($p < 0.001$), anterior infarct ($p < 0.001$), TIMI flow 3 pre-PPCI ($p < 0.001$), use of GPIIb/IIIa inhibitors ($p < 0.001$) were found to be independently associated to peak cTn levels (**Table 3.3**).

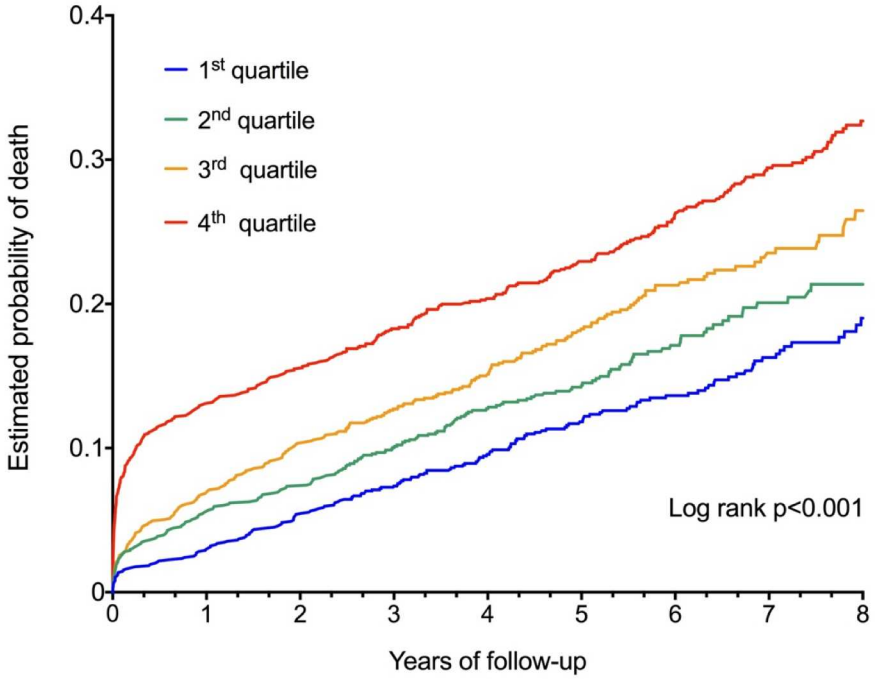

Number at risk

1st quartile	1246	1174	866	528	169
2nd quartile	1217	1122	781	382	112
3rd quartile	1223	1085	777	405	108
4th quartile	1228	1020	826	560	248

Figure 3.1. Kaplan-Meier curve displaying estimated probability of overall mortality according to pre-cTn quatiles.

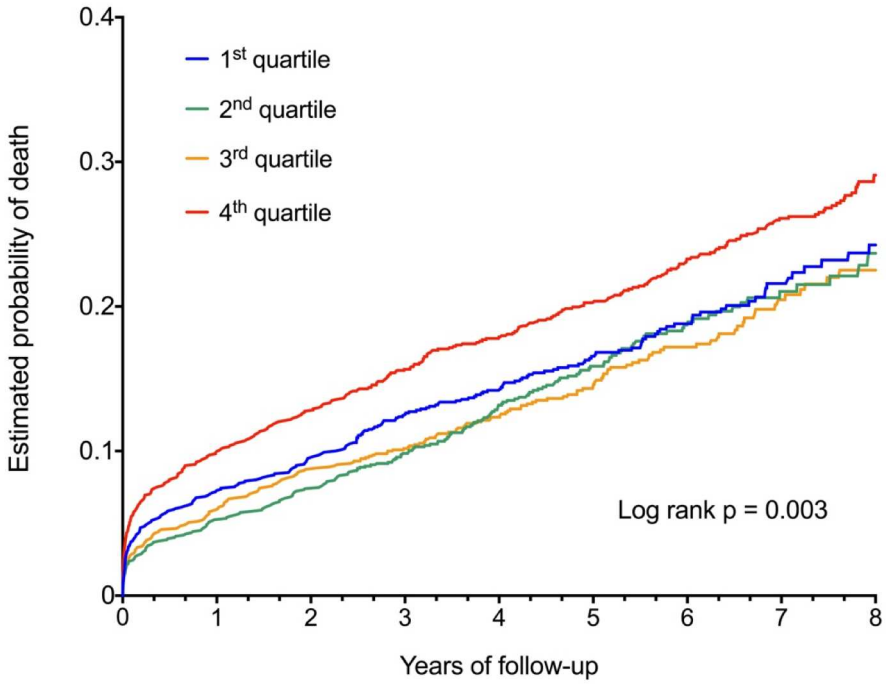

Number at risk

1st quartile	1209	1094	804	412	133
2nd quartile	1215	1125	794	379	86
3rd quartile	1223	1116	788	398	109
4th quartile	1222	1066	863	685	304

Figure 3.2. Kaplan-Meier curve displaying estimated probability of overall mortality according to post-cTn quatiles.

Variable	Pre-procedural cTn			Peak (12h post-PPCI) cTn		
	β	95% CI	p-value	β	95% CI	p-value
Age	1.676	-3.753 – 7.106	0.545	21.086	11.611 – 30.562	**< 0.001**
Previous angina	-91.642	-294.773 – 111.490	0.376	-308.969	-599.274 – -18.663	**0.037**
Previous MI	-250.507	-466.715 – -34.299	**0.023**	-27.507	-446.704 – 391.690	0.898
Previous PPCI	-58.207	-392.315 – 275.901	0.733	-339.710	-836.272 – 156.852	0.180
Pre-PCI haemoglobin	-8.168	-50.051 – 33.716	0.702	148.037	81.774 – 214.301	**< 0.001**
Pre-PCI creatinine	734.876	555.922 – 913.830	**< 0.001**	1287.806	1003.019 – 1572.594	**< 0.001**
Heart rate at admission	3.605	0.676 – 6.534	**0.036**	2.070	-3.386 – 7.526	0.457
Systolic BP at admission	0.570	-1.578 – 2.718	0.603	-0.180	-3.599 – 3.239	0.918
Cardiogenic shock	667.415	297.789 – 1037.04	**< 0.001**	518.986	-62.652 – 1100.624	0.080
Inter-hospital transfer	265.232	111.899 – 418.564	**0.001**	-84.166	-330.190 – 161.859	0.502
Onset to reperfusion	0.360	-0.007 – 0.079	0.102	-0.016	-0.089 – 0.058	0.678
Door to balloon	-0.002	-0.011 – 0.006	0.611	-0.006	-0.019 – 0.007	0.367
Anterior MI	405.940	263.932 – 547.948	**< 0.001**	847.175	622.261 – 1072.090	**< 0.001**
TIMI 3 Pre-PCI	-639.301	-846.756 – -431.846	**< 0.001**	-2023.167	-2357.173 – -1689.16	**< 0.001**
GP IIb/IIIa medication	-	-	**-**	885.806	636.027 – 1135.584	**< 0.001**
Thrombus aspiration	-	-	**-**	102.494	-123.181 – 328.168	0.373
TIMI flow 3 post-PPCI	-	-	**-**	-313.869	-748.872 – 121.134	0.157

Table 3.3. Predictors of pre-cTn and peak cTn levels. β, standardized regression coefficient; BP, blood pressure; CI, confidence interval; cTn, cardiac troponin; GPIIb/IIIa, glycoprotein IIb/IIIa; MI, acute myocardial infarction; PPCI, primary percutaneous coronary intervention; TIMI, thrombolysis in myocardial infarction angiographic score.

3.2.3. Pre-cTn is an independent predictor of mortality in STEMI patients

Multivariate Cox-regression analysis identified high pre-cTn (4th quartile) as an independent predictor of in-hospital mortality [Hazard ratio (HR) per highest to lowest quartile: 3.64; 95% Confidence Interval (CI): 1.86 – 7.10; p < 0.001] when adjusted for the variables in the core model of in-hospital mortality prediction (**Figure 3.3)**. In addition, pre-cTn levels were also independently associated with longer-term mortality (HR per highest to lowest quartile: 1.26; 95% CI: 1.01 – 1.57; p = 0.035) when adjusted for the core model of longer-term mortality prediction (**Figure 4.4**). In contrast, 12h post-PPCI cTn was not independently associated with either in-hospital or longer-term mortality in multivariate Cox-regression analysis (**Figures 3.3** and **3.4**).

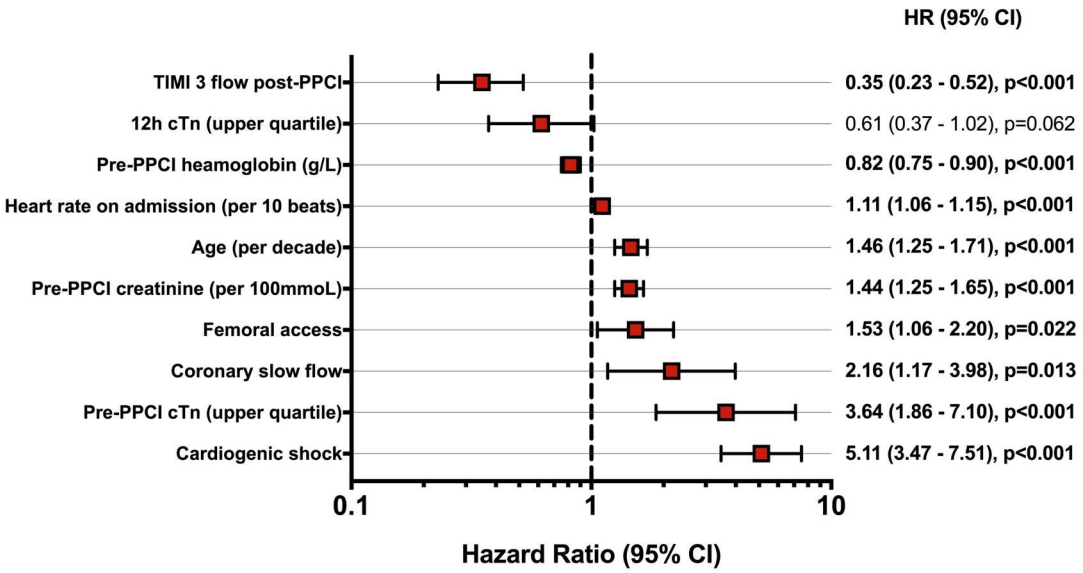

Figure 3.3. Pre-cTn is an independent predictor of in-hospital mortality.

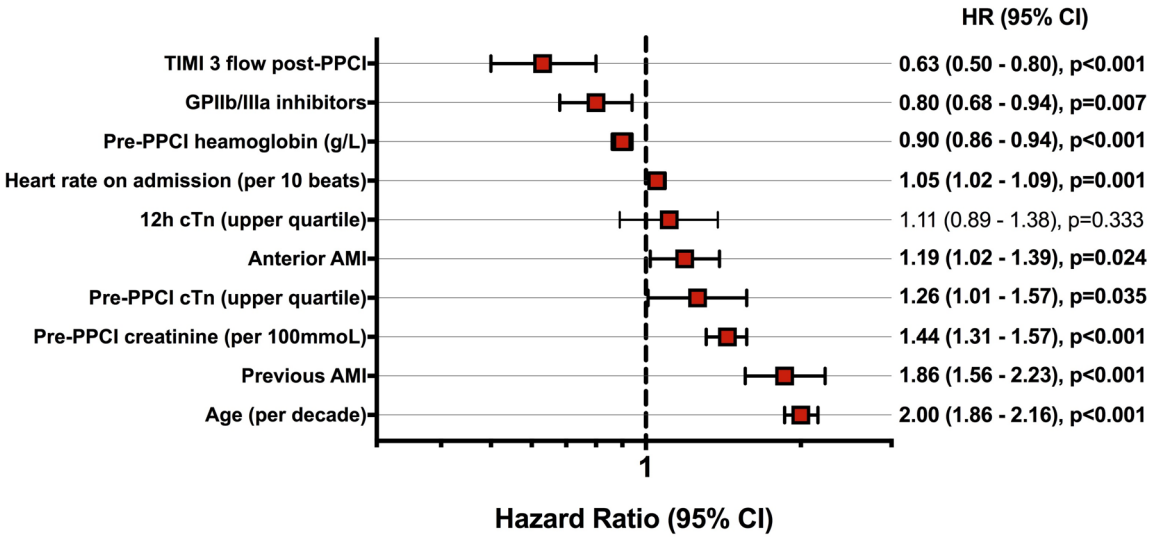

Figure 3.4. Pre-cTn is an independent predictor of longer-term mortality.

3.2.4. Pre-cTn confers incremental prognostic value over core predictive models of in-hospital and longer-term mortality

Pre-cTn in the highest quartile conferred significant but modest additive discrimination value over the core model of in-hospital mortality prediction (AUC:0.904; 95% CI: 0.876-0.932 vs. AUC:0.891; 95% CI: 0.861-0.922, respectively, p = 0.022) (**Table 3.4**). For longer-term mortality, the additive predictive value of pre-cTn in the highest quartile over the core predictive model was significant but weaker than that observed for in-hospital mortality (AUC:0.833; 95% CI: 0.818-0.848 vs. AUC:0.829, 95% CI: 0.814-0.845, respectively, p = 0.008) (**Table 3.4**). Similar results on the discriminative value of pre-cTn for both outcomes were derived from Harrell's C analysis (**Table 3.4**).

For reclassification performance, pre-cTn by ascending quartiles correctly reclassified 2,312 patients who were free of in-hospital death into lower risk categories while 20 patients who died were correctly reclassified into higher risk

category (overall catNRI = 65.6%, p < 0.001) (**Table 3.5**). Similarly, regarding longer-term mortality, the core model including pre-cTn by ascending quartiles correctly reclassified 1,499 subjects without the event into lower risk categories and 76 patients who died into higher risk categories (overall catNRI = 50.2%, p < 0.001) (**Table 3.6**).

	Discrimination			
	AUC (95% CI)	**p-value**	**Harrell's C index (95% CI)**	**p-value**
		In-hospital death		
***Core model**	0.891 (0.861-0.922)		0.884 (0.852-0.915)	
+Troponin (upper quartile)	0.904 (0.876-0.932)	0.022	0.899 (0.870-0.927)	0.012
		Long-term mortality		
****Core model**	0.829 (0.814-0.845)		0.801 (0.786-0.816)	
+Troponin (upper quartile)	0.833 (0.818-0.848)	0.008	0.804 (0.790-0.819)	0.004

Table 3.4. Incremental discrimination value of pre-cTn to core models of in-hospital and longer-term mortality prediction in STEMI patients.
Core model for in-hospital mortality prediction includes age, pre-PCI haemoglobin, pre-PCI creatinine, cardiogenic shock on admission, admission heart rate, femoral access, coronary flow slow, TIMI 3 flow post-PCI.
Core model for longer-term mortality prediction includes age, Hemoglobin, creatinine, admission heart rate, previous MI, anterior MI, GPIIb/IIIa inhibitors, TIMI 3 flow post-PCI.
AUC, area under the curve; 95% CI, 95% confidence interval.

Core model only	Core model + Pre-cTn			
Risk categories (in-hospital death)	<2% risk	2-5% risk	≥5% risk	Total
Subjects free of in-hospital death (n=4,398)				
<2% risk	1,110	41	11	1,162
2-5% risk	1,723	311	166	2,200
≥5% risk	533	274	229	1,036
Total	3,366	626	406	4,398
Subjects who died in-hospital (n=123)				
<2% risk	5	6	2	13
2-5% risk	5	6	33	44
≥5% risk	6	10	54	70
Total	16	18	89	123
catNRI	**Estimate**		**SE**	**p-value**
	0.656		0.063	<0.001

Table 3.5. Pre-cTn in ascending quartiles format reclassifies the risk for in-hospital mortality after STEMI over a core clinical model. The shaded values reflect subjects who were reclassified into lower-risk categories (light green) or higher-risk categories (red). Core model for in-hospital mortality prediction includes age, pre-PCI haemoglobin, pre-PCI creatinine, cardiogenic shock on admission, admission heart rate, femoral access, coronary flow slow, TIMI 3 flow post-PCI. catNRI, categorical net reclassification index; cTn, cardiac troponin.

Core model only	Core model + Pre-cTn			
Risk categories (longer-term death)	<15% risk	15-20% risk	≥20% risk	Total
Subjects alive (3,631)				
<15% risk	817	61	124	1,002
15-20% risk	673	86	175	934
≥20% risk	1,013	173	509	1,695
Total	2,503	320	808	3,631
Subjects who died (n = 853)				
<15% risk	51	14	88	153
15-20% risk	38	11	123	172
≥20% risk	65	46	417	528
Total	154	71	628	853
catNRI	**Estimate**		**SE**	**p-value**
	0.502		0.026	<0.001

Table 3.6. Pre-cTn in ascending quartiles format reclassifies the risk for longer-term mortality after STEMI over a core clinical model. The shaded values reflect subjects who were reclassified into lower-risk categories (light green) or higher-risk categories (red). Core model for longer-term mortality prediction includes age, Hemoglobin, Creatinine, admission heart rate, previous MI, anterior MI, GPIIb/IIIa inhibitors, TIMI 3 flow post-PCI. catNRI, categorical net reclassification index; cTn, cardiac troponin.

3.3. Discussion

This is the first large study to demonstrate the prognostic importance of pre-cTn assays for mortality prediction over a median 5 years follow up in a cohort of unselected STEMI patients treated with PPCI. Pre-cTn was independently associated with both in-hospital and longer-term mortality. In addition, pre-cTn improved the prognostic power of core clinical models to discriminate in-hospital and longer-term mortality. Finally, addition of pre-cTn to core clinical models of in-hospital and longer-term mortality prediction correctly reclassified patients into pre-established mortality risk categories based on the GRACE score.

Previous smaller studies have investigated whether admission cTn measurements had any prognostic value. Giannitsis et al.(Giannitsis et al., 2001) evaluated whether detection of cTnT by a rapid bedside assay at admission could predict 30-day and 9-month mortality in 140 consecutive patients. They reported higher rates of all-cause mortality in cTnT-positive in comparison to cTnT-negative patients both at 30 days (15.6% versus 3.9%, p = 0.02) and 9-months (18.8% versus 3.9%, p = 0.05) (Giannitsis et al., 2001). Similarly, Wang et al. (Wang et al., 2014a) observed that pre-catheterization hs-cTnT was an independent predictor of major adverse cardiovascular events (MACE), including death, myocardial infarction, and revascularisation, in a population of 173 consecutive patients at 30 days and 1 year of follow-up. In accordance with our findings, Giannitsis et al. demonstrated that cTnT-positive patients had more anterior infarcts (Giannitsis et al., 2001) and were less likely to achieve optimal coronary recanalization post-PPCI (TIMI flow < 3 post-PPCI) (Giannitsis et al., 2001). In addition, our study also shows that pre-cTn levels were independently associated with a delay in reperfusion, as reflected by higher frequency of patients being admitted by inter-hospital transfer in the upper pre-cTn quartile groups. Taken together, these findings suggest that pre-cTn is a marker that may cumulatively inform about the duration of ischaemia and the anatomical myocardial area at risk up until the time of PPCI. Therefore, pre-cTn may provide an early prediction for the success of the reperfusion procedure and for the prognostic outcomes thereafter. Nonetheless, because of the small sample sizes in these previous studies, the prognostic power of pre-cTn over traditional predictors of mortality in STEMI patients remained to be elucidated.

In this study, pre-cTn provided significant discrimination and reclassification value over core multivariable models for prediction of in-hospital and longer-term mortality. Its incremental discrimination value was stronger for in-hospital mortalilty than longer-term mortality. Considering that the markedly high discrimination accuracy of the core model may hinder C-statistics analysis from revealing the true clinical value of troponin in this population (Cook, 2007), reclassification statistics may estimate more accurately the clinical importance of pre-cTn. Indeed, pre-cTn conferred strong reclassification value for both in-hospital and longer-term mortality, especially for the prediction of in-hospital mortality (catNRI 65.5%). This is particularly valuable considering that cardiac mortality seems to be more prevalent within 30 days post-STEMI, with the majority of deaths within the 5 years following discharge being due to non-cardiac causes (<1.5% annual risk of cardiac death) (Pedersen et al., 2014). Interestingly, pre-cTn seemed to perform best in detecting truly low risk subjects both for in-hospital and longer-term mortality (correctly reclassified 2,312 and 1,499 patients who survived into lower risk categories, respectively). In contrast, reclassification value into higher risk categories was rather modest, which is not unexpected given the strong predictive ability of the core model for mortality. Overall, these results indicate a clear advantage of pre-cTn over established predictors in STEMI patients to improve risk stratification for in-hospital and longer-term mortality.

An important finding from this study was that peak (12h) cTn was not independently associated with in-hospital or longer-term mortality. A recent study by Cediel et al. (Cediel et al., 2017) also demonstrated that peak levels of both contemporary cTnI and hs-cTnT assays do not provide relevant prognostic information for the prediction of MACE at 30 days and 1 year of follow-up in consecutive STEMI patients undergoing PPCI (n = 1,260). In that study, pre-procedural hs-cTn levels were not included in the analysis (Cediel et al., 2017). In contrast, some previous investigations have shown associations between peak cTn levels and prognostic outcomes in STEMI patients (Boden et al., 2013, Buber et al., 2015, Hall et al., 2015). Boden et al. performed serial hs-cTnT measurements at fixed 6h intervals for 48h after PPCI in 188 consecutive STEMI patients and found that all measurements correlated with adverse outcomes during 1 year of follow-up (Boden et al., 2013). In addition, Buber et al. (Buber et al., 2015) observed that peak (8h) levels of cTnI were independently associated to the occurrence of all-cause death, recurrent infarct, or heart failure during hospitalisation in 175 STEMI patients. Finally, Hall et al. (Hall et

al., 2015) observed that post-PCI levels of cTnI provided incremental prognostic power over other outcome predictors in 1,066 patients in the PROTECTION AMI trial. Collectively, these studies provide important hypothesis generating data on the significance of cTn in STEMI. However, small sample sizes and use of strict selection criteria, which invariably excluded patients with more comorbidities, limit the generalization of these findings to the wide STEMI population and call for validation in larger cohorts. To that end, our findings derived from this large cohort of unselected STEMI patients resembling populations in routine clinical practice imply that serial measurements of cardiac troponin post-PPCI in STEMI patients is questionable, given that peak cTn does not seem to provide relevant prognostic information and brings an additional economic burden to health systems.

Although post-PCI cTn levels correlate with surrogate markers of worse prognosis, such as infarct size and left ventricular remodelling, better than pre-cTn in STEMI patients (Selvanayagam et al., 2005, Nguyen et al., 2015b, Reinstadler et al., 2016), it is possible to speculate why post-reperfusion cTn levels are not predictors of mortality in this population. First, the reperfusion process influences cTn kinetics, leading to an early cTn peak, resultant from rapid washout of cytosolic cTn (Katus et al., 1991, Bertinchant et al., 1996), which may potentially vary in amplitude and time of occurrence (8 – 12h post-PPCI) according to the quality of reperfusion therapy. In addition, the inter-personal variability of cTn concentration and distribution in cardiac tissue may contribute to absolute peak values that may not entirely reflect the extent of cardiac area at risk (Swaanenburg et al., 2001).

Some limitations are recognized in this study. First, conversion of cTnI values to the cTnT scale might potentially have added some degree of inaccuracy in terms of patient assignment into cTn quartile groups. In addition, specific data about cardiac death was not provided. Finally, because mortality data was retrieved from statistical records, misclassifications cannot entirely be excluded.

3.4. Conclusion

In conclusion, this chapter provides evidence to support an important role for pre-cTn levels in predicting prognosis in STEMI patients undergoing PPCI. We propose that pre-cTn could be used to better categorize risk in this population. Finally, we demonstrate that peak cTn levels do not seem to be useful for prognostic stratification of STEMI patients and therefore the cost-effectiveness of serial cTn measurements post-PPCI needs to be reconsidered.

Chapter 4. Overcoming Methodological Issues In Circulating miRNA Quantification In STEMI Patients

4.1. Introduction

Although cardiac troponins (cTn) are established biochemical markers of STEMI, technical limitations in their quantification methods (van der Linden et al., 2017) and only moderate correlations with infarct size (Cobbaert et al., 2014) prompt the identification of new markers of myocardial injury. In addition, as shown in **chapter 4**, cTn routinely quantified at 12 hours post-PPCI is not a predictor of in-hospital and longer-term mortality in STEMI patients. Therefore, investigation for relevant prognostic circulating biomarkers in STEMI patients is also warranted.

In the context of STEMI, circulating levels of several microRNAs (miRNA) have been shown to be deregulated by many studies (Viereck and Thum, 2017). Cardiac-enriched miRNAs attract special interest, as they are more likely to inform about the nature and extent of myocardial injury (Viereck and Thum, 2017). Nonetheless, lack of standardization in circulating miRNA quantification methods contributes to substantial inconsistencies and conflicting results among studies (Navickas et al., 2016). Notably, the lack of consensus regarding real time quantitative polymerase chain reaction (RT-qPCR) data normalization as well as the presence of RT-qPCR inhibitors, such as heparin, in STEMI patient samples represent critical limitations for the translation of miRNAs to daily clinical practice (Viereck and Thum, 2017, Santovito and Weber, 2017).

Currently, RT-qPCR is the preferred method for miRNA quantification given its specificity and broad dynamic range (Marabita et al., 2016). Data normalization is a critical step to reduce the effects of systematic errors and obtain biologically meaningful miRNA expression in RT-qPCR studies (Marabita et al., 2016). The most widely employed normalization strategy is the use of a stably expressed endogenous control. Nonetheless, there are no circulating miRNAs that have been systematically validated as endogenous controls in STEMI patients to date. To overcome this limitation, synthetic exogenous miRNAs, especially *Caenorhabditis elegans* miR-39 (cel-miR-39), have been used as alternatives for data normalization in most studies (Viereck and Thum, 2017). However, heparin, a medication that is routinely administered to STEMI patients during coronary intervention, has been shown to affect the detection of cel-miR-39 by RT-qPCR, which might compromise its use as a normalization control (Boeckel et al., 2013, Kaudewitz et al., 2013). Another

proposed normalization strategy is to use the mean expression of hundreds of quantified miRNAs in a sample (Kaudewitz et al., 2013). Yet, this approach is not feasible for clinical routine or large clinical studies focusing on few target miRNAs. In addition, the effect of RT-qPCR inhibitors on the global miRNA expression is unknown. Therefore, circulating miRNA quantification in STEMI patients undergoing PPCI remains an unmet challenge from a methodological perspective.

This chapter aimed to (i) identify and validate an endogenous circulating miRNA control for RT-qPCR data normalization in STEMI patients, (ii) assess the *in vitro* and *in vivo* effects of anticoagulant drugs administration, such as heparin and bivalirudin, on currently used normalization strategies; (iii) evaluate whether in vitro heparin inhibition with the addition of heparinase to RNA samples affects circulating cardiac-enriched miRNA detection by RT-qPCR.

4.2. Specific methods

4.2.1. Study design

The study described in this chapter was carried out in 3 consecutive phases (**Figure 4.1**). In phase 1, screening of 179 miRNAs using RT-qPCR panels was performed in STEMI patients across 6 time points prior to and post-PPCI as well as in stable CAD controls to identify candidate endogenous miRNA controls (**Figure 4.1A**). The 4 most stable miRNAs identified in phase 1 were subsequently quantified in 34 STEMI patients to assess expression stability for validation purposes (validation phase – **Figure 4.1B**). As part of the validation phase, the effects of heparin and bivalirudin administration on the three normalization approaches (global miRNA mean, cel-miR-39, and validated endogenous control) were also analysed (**Figure 4.1B**). Finally, the effect of the *in vitro* treatment of heparin-contaminated samples with heparinase on cardiac-enriched miRNA (miR-1 and miR-133b) quantification was evaluated in 70 STEMI patients (application phase - **Figure 4.1C**).

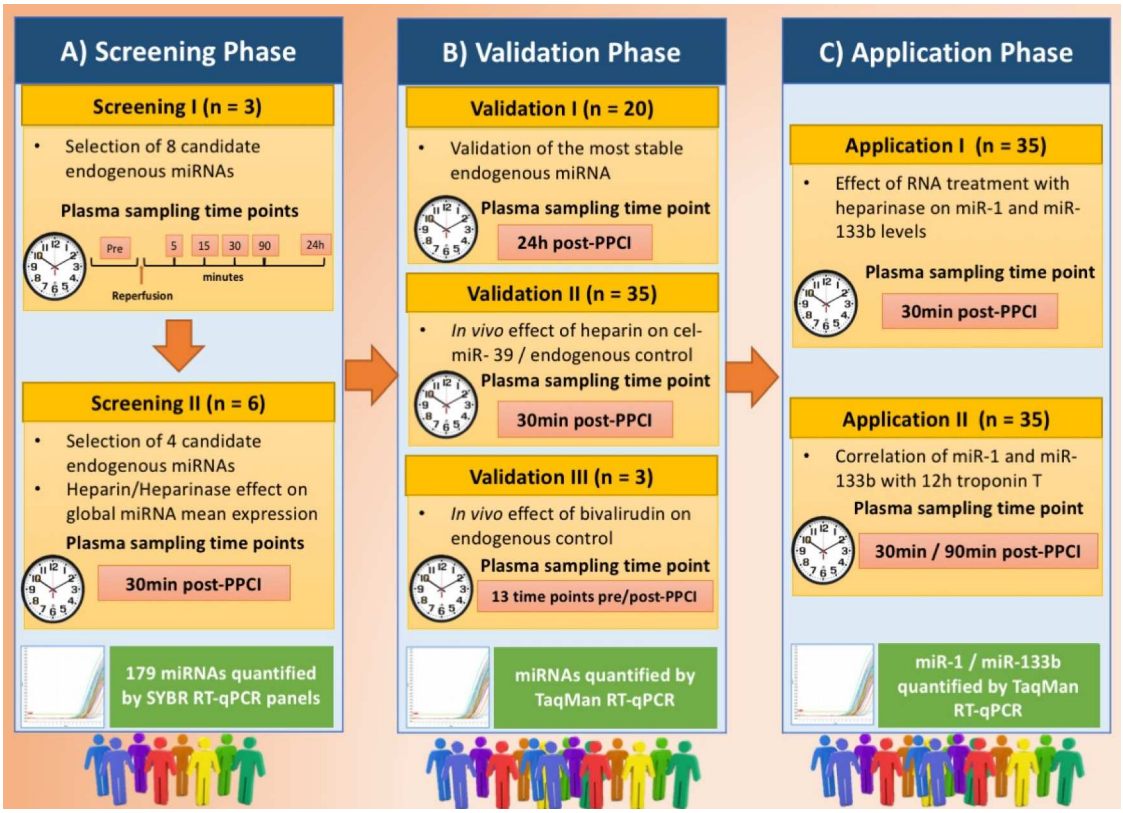

Figure 4.1. Study design. The study was carried out in three consecutive phases. In the screening phase (**A**), a total of 179 microRNAs were initially quantified in samples from 3 STEMI patients and 4 control samples using real time quantitative reverse transcription (RT-qPCR) panels to identify 8 candidate endogenous miRNA controls. In a second step of this phase, miRNA screening was performed in samples collected at 30min post-PCI from 6 STEMI patients and subsequently treated *in vitro* with heparinase to select the 4 most stable candidate endogenous miRNAs and to assess the effect of heparin and heparinase administration on the global miRNA mean expression (**B**), the 4 candidate miRNAs previously identified were quantified by TaqMan RT-qPCR in 20 STEMI samples collected 24h post-PCI (heparin-free) and miRNA stability was determined. In addition, cel-miR-39 and the validated endogenous miRNA control were quantified in a total of 35 STEMI samples (30min post-PCI) to evaluate the effect of *in vivo* administration of heparin on the miRNAs expression. To further assess the *in vivo* effect of bivalirudin on the exogenous spike-in and endogenous miRNA, these miRNAs were quantified in samples collected from STEMI patients (n = 3) at 13 time points prior to and following PCI. Finally, in the application phase (**C**), heparin-contaminated RNA samples from the same 35 STEMI patients (30min post-PCI) were then treated *in vitro* with heparinase and cardiac-enriched miRNAs (miR-1 and miR-133b) were quantified to assess the impact of heparin contamination and heparinase treatment on the levels of such miRNAs. Furthermore, correlation of cardiac-enriched miRNA levels with 12h Troponin T was also analysed.

4.3. Results

4.3.1. Patient baseline characteristics

Plasma samples were obtained from a total of 73 STEMI patients treated with PCI. Clinical baseline characteristics of the study population are displayed in **Table 4.1**. In summary, most patients were male (n = 61, 83%), with median age of 63 (55 – 71) years, and with a low to moderate prevalence of cardiovascular risk factors (<10% had diabetes or hypercholesterolaemia; 20 – 35% were current smokers, obese, or hypertensive). In terms of STEMI and procedural characteristics, most patients had non-anterior infarcts (69.4%), completely obstructed culprit coronary artery (TIMI flow 0 or 1) prior to PCI (97.2%), and achieved complete coronary perfusion (TIMI flow 3) post-PCI (93.1%) (**Table 4.1**).

Variable	Entire cohort (STEMI 1 + STEMI 2)	Endogenous miR control Cq values*			p-value
		1st tertile	2nd tertile	3rd tertile	
Number (male)	73 (61)	24 (20)	25 (20)	24 (21)	0.898
Age [years, median (IQR)]	63 (55 – 71)	65 (56 – 71)	65 (59 – 70)	61 (52 – 71)	0.396
Risk factors, n (%)					
Smoking status					
Never smoked	28 (38.9)	10 (41.7)	7 (29.2)	11 (45.8)	0.468
Ex-smoker	24 (33.3)	9 (37.5)	11 (45.8)	4 (16.7)	0.087
Current smoker	20 (27.8)	5 (20.8)	6 (25)	9 (37.5)	0.407
Hypertension	17 (23.6)	4 (16.7)	7 (29.2)	6 (25)	0.583
Diabetes mellitus	6 (8.3)	3 (12.5)	3 (12.5)	0 (0)	0.195
Hypercholesterolaemia	7 (9.7)	3 (12.5)	2 (8.3)	2 (8.3)	0.854
Obesity	25 (34.7)	8 (33.3)	12 (50)	5 (20.8)	0.104
Malignancies	0 (0)	0 (0)	0 (0)	0 (0)	-
Laboratory tests [median (IQR)]					
Admission eGFR, mL/min	83 (73 – 97)	82 (68 – 92)	83 (75 – 112)	83 (69 – 93)	0.441
Admission Troponin T, ng/L	49 (27 – 98)	33 (27 – 72)	61 (28 – 184)	46 (25 – 141)	0.346
Peak Troponin T, ng/L	3255 (1109 – 5658)	3422 (1712 – 6441)	2262 (745 – 6367)	3119 (1179 – 5152)	0.533
STEMI characteristics					
Onset to reperfusion (min)	157 (110 – 245)	144 (102 – 216)	225 (124 – 295)	147 (112 – 248)	0.156
Culprit vessel, n (%)					
LAD	22 (30.6)	6 (25)	10 (41.7)	6 (25)	0.351
LCx	13 (18)	5 (20.8)	3 (12.5)	5 (20.8)	0.687
RCA	37 (51.4)	13 (54.2)	11 (45.8)	13 (54.2)	0.801
Localization, n (%)					
Anterior	22 (30.6)	6 (25)	10 (41.7)	6 (25)	0.351
Non-anterior	50 (69.4)	18 (75)	14 (58.3)	18 (75)	0.351
TIMI flow pre PPCI, n (%)					
0	60 (83.3)	21 (87.5)	19 (79.2)	20 (83.3)	0.741
1	10 (13.9)	3 (12.5)	4 (16.7)	3 (12.5)	0.890
2	1 (1.4)	0 (0)	0 (0)	1 (4.2)	0.363
3	1 (1.4)	0 (0)	1 (4.2)	0 (0)	0.363
TIMI flow post PPCI, n (%)					
0	1 (1.4)	0 (0)	1 (4.2)	0 (0)	0.363
1	3 (4.2)	0 (0)	1 (4.2)	2 (8.3)	0.352
2	1 (1.4)	0 (0)	0 (0)	1 (4.2)	0.363
3	67 (93.1)	24 (100)	22 (91.7)	21 (87.5)	0.222
Medication during PPCI					
Heparin, n (%)	70 (95.8)	24 (100)	24 (96)	22 (91.7)	0.328
Bivalirudin, n (%)	3 (4.2)	0 (0)	1 (4)	2 (8.3)	0.328
Glycoprotein IIb/IIIa inhibitors, n (%)	48 (66.7)	15 (62.5)	18 (75)	15 (62.5)	0.570

Table 4.1. Clinical characteristics of the study population.eGFR, estimated glomerular filtration rate; LAD, left anterior descending; LCx, left circumflex; PPCI, primary percutaneous coronary intervention; RCA, right coronary artery; TIMI, thrombolysis in myocardial infarction; * endogenous miRNA control Cq values at 30 minutes post myocardial reperfusion (expression quantified in heparinase-treated RNA samples, except in samples from bivalirudin-treated patients)

4.3.2. Identification of candidate endogenous miRNA controls

From 179 quantified miRNAs, 60 presented Cq values < 35 across all time points in STEMI patients (n = 3) and controls (n = 4) and were selected for expression stability analysis by NormFinder and BestKeeper software (**Figure 4.2A and 4.2B**). Because each software uses a different algorithm, the four most stably expressed miRNAs identified by NormFinder and BestKeeper were selected and an additional screening performed in 6 STEMI patient samples was used to identify the four most stable miRNAs among this subgroup of eight miRNAs (miR-425-5p, miR-877-5p, miR-181a-5p, and miR-155-5p) for further validation (**Figure 4.2C**).

4.3.3. miR-425-5p is a stably expressed endogenous miRNA in STEMI patients

To validate the previously identified candidate endogenous miRNA controls, miRNA quantification was performed in samples from 34 STEMI patients collected at 24h post-PPCI, hence not contaminated with heparin. Amongst the 4 candidate miRNAs, miR-425-5p presented the best stability scores in NormFinder and BestKeeper and shared the best stability values in geNorm as well as the lowest CV with miR-181a-5p (**Table 4.2**). In the entire STEMI cohort (n = 70), miR-425-5p expression was not influenced by age, sex, traditional cardiovascular risk factors, renal function, magnitude of myocardial damage (as reflected by cardiac troponin levels), or antiplatelet agents (glycoprotein IIb/IIIa inhibitors) administered during PPCI (**Table 4.1**). In addition, miR-425-5p Cq values strongly and negatively correlated with total RNA concentration in patient samples (r = -0.744, p < 0.0001) (**Figure 4.3A**) but did not correlate with platelet count (r = 0.033, p = 0.786) (**Figure 4.3B**) or 12h cardiac troponin levels (r = -0.096, p = 0.429) (**Figure 4.3C**). Therefore, miR-425-5p was selected as an endogenous control for RT-qPCR normalisation.

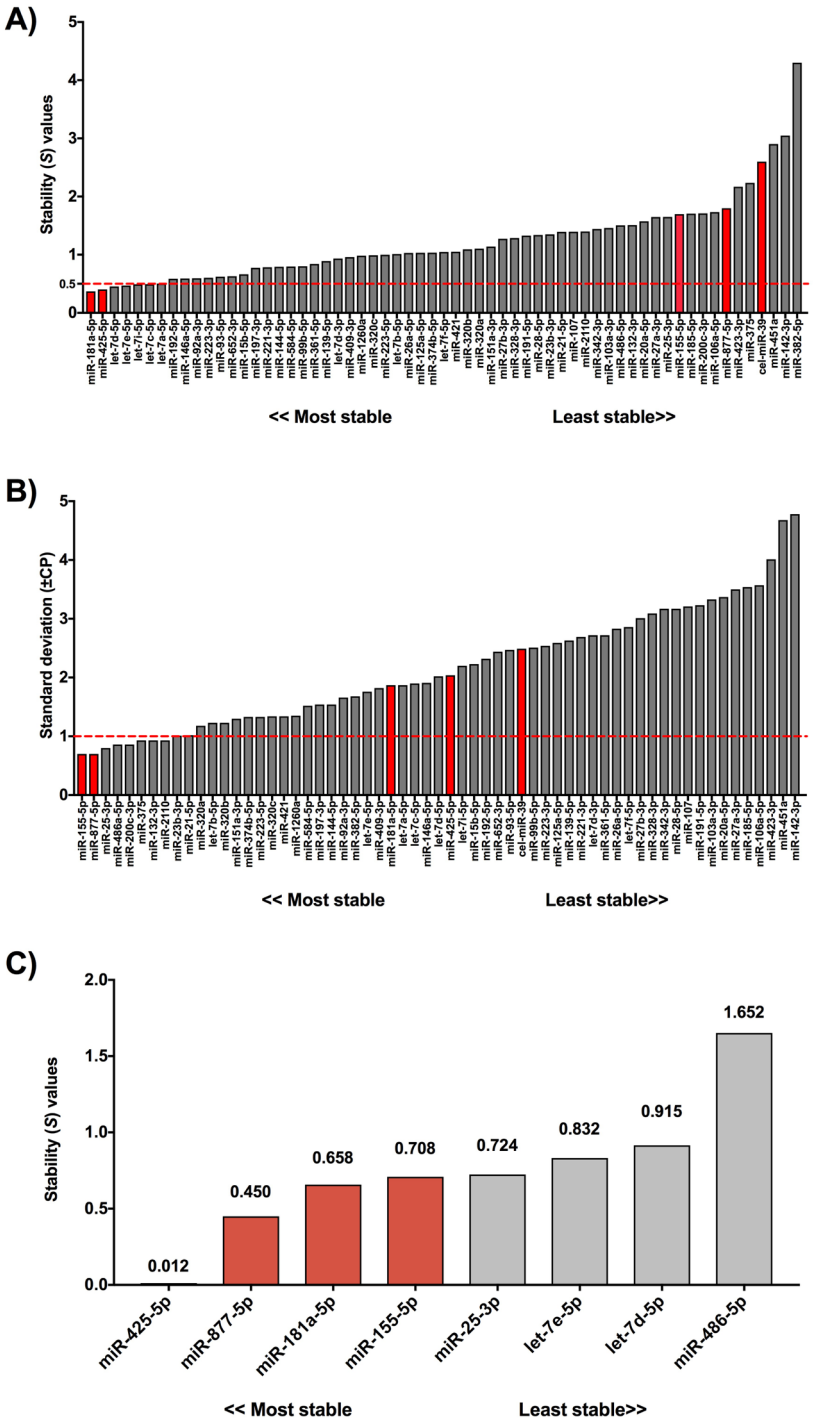

Figure 4.2. Selection of candidate endogenous miRNA controls following screening. After miRNA screening in 3 STEMI patients and 4 controls, 60 miRNAs presented Cq values < 35 across all time points and had their stability determined by NormFinder and BestKeeper. The four most stable miRNAs below the M score threshold of 0.5 identified by NormFinder **(A)** and the four most stable miRNAs with standard deviation < 1 in BestKeeper **(B)** were selected for further validation. Note that cel-miR-39 is amongst the least stable miRNAs in both algorithms. **(C)** Following screening of 179 circulating miRNAs in 6 samples collected from STEMI patients 30min post percutaneous coronary intervention (PCI), which were treated in vitro with 0.3U of heparinase, and 4 controls with stable coronary artery disease (CAD), the 4 most stably expressed endogenous miRNAs (miR-425-5p, miR-877-5p, miR-181a-5p, miR-155-5p - highlighted) were identified by NormFinder. The lower the stability (*S*) value in NormFinder the more stable the reference miRNA. These miRNAs were selected for further validation by TaqMan RT-qPCR assays in a larger cohort of STEMI patients.

microRNA	geNorm M score	Normfinder *S* score	Bestkeeper Std dev (±CP)	CV (%)
miR-425-5p	1.13	1.85	1.47	7
miR-181a-5p	1.13	2.09	1.51	7
miR-155-5p	2.62	2.04	4.03	14
miR-877-5p	2.72	2.18	3.97	13

Table 4.2. Candidate endogenous miRNA controls expression stability. CV, coefficient of variability; Std dev (±CP), standard deviation (±crossing point).

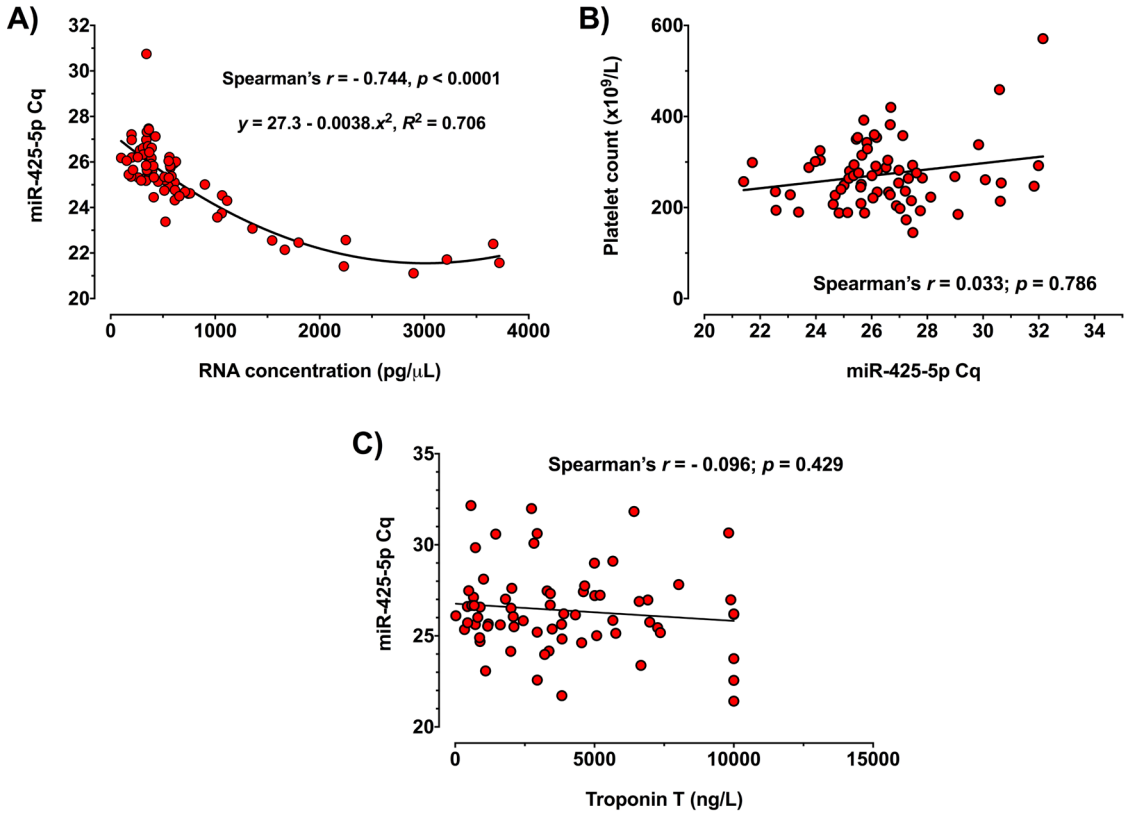

Figure 4.3. Correlation of miR-425-5p with sample RNA concentration and platelet count. (A) miR-425-5p expression strongly and negatively correlated with total RNA concentration in STEMI patient samples, n = 70. **(B)** miR-425-5p expression at 30min post-PPCI did not correlate with admission platelet count, n = 70. (**C**) miR-425-5p expression at 30min post-PPCI did not correlate with peak cardiac troponin T, n = 70.

4.3.4. Heparin concentration in RNA samples can be reduced by in vitro treatment with heparinase

Heparin was detected by ELISA in both plasma and plasma-derived RNA samples collected prior to myocardial reperfusion from the same STEMI patients (n = 10). Heparin concentration was similar between plasma [mean(±SEM) = 1,387(±266)pg/mL] and RNA samples [1,113(±167.4)pg/mL], p = 0.247 (**Figure 4.4A**), suggesting significant heparin resistance to the process of RNA extraction from plasma. Treatment of heparin-contaminated RNA samples with 0.25U, 0.5U, and 1U of heparinase resulted in approximate reduction of 7% (±0.2%, p = 0.337), 30% (±0.1%, p = 0.001), and 42% (±0.1%, p < 0.001) in heparin concentration, respectively (**Figure 4.4B**), indicating a dose-dependent inhibitory effect of heparinase on heparin levels in RNA samples.

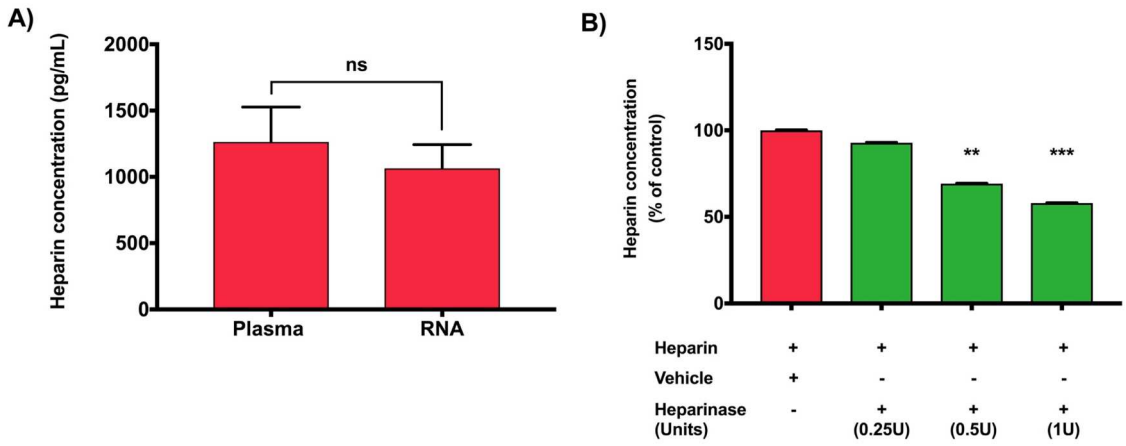

Figure 4.4. *In vitro* treatment with heparinase decreases heparin concentration in RNA samples from STEMI patients. Heparin was quantified in plasma and plasma-derived RNA samples collected prior to myocardial reperfusion from STEMI patients by ELISA. (**A**) Presence of heparin was confirmed in both plasma and RNA samples. Heparin concentration was similar between plasma [mean(±SEM) = 1,387(±266)pg/mL] and RNA samples [1,113(±167.4)pg/mL], p = 0.247; n = 10; ns, non-significant; paired t test. (**B**) Serial doses of heparinase I (0.25U, 0.5U, and 1U) were added to heparin contaminated samples from STEMI patients (n = 3), incubated for 1 hour at room temperature, and heparin concentration was subsequently assessed by ELISA. Addition of 0.5U and 1U were effective in reducing heparin concentration by approximately 30% and 42%, respectively, in relation to heparin-contaminated samples not treated with heparinase; **p=0.001 ***p<0.001 vs. control samples, one-way ANOVA and Dunnett's multiple comparison test.

4.3.5. Heparin inhibits the global miRNA mean, cel-miR-39, and miR-425-5p expression

In STEMI patients receiving heparin (n = 3), global miRNA mean Cq values remained significantly elevated by 4 cycles immediately after heparin administration until 30min post myocardial reperfusion in comparison to 24h post-reperfusion levels (**Figure 4.5A**). *In vitro* treatment of the same RNA samples from these STEMI patients with heparinase I prior to reverse transcription reduced the global miRNA mean by 4 cycles, bringing Cq values to similar levels of controls (**Figure 4.5B**).

Similarly, *in vitro* addition of heparin to RNA samples from non-heparinised STEMI patients resulted in significantly increased cel-miR-39 and miR-425-5p Cq values in a dose-dependent fashion (**Figures 4.6A and 4.6B**). In fact, a heparin dose of 2U completely inhibited the detection of such miRNAs by RT-qPCR. In contrast, *in vitro* treatment of heparin-contaminated RNA samples from STEMI patients with doses as low as 0.25U and 0.5U of heparinase I was effective in reducing Cq values of both cel-miR-39 (ΔCq = - 2.7, 95% CI: - 2.1 to - 3.3, $p<0.0001$) and miR-425-5p (ΔCq = - 1.6, 95% CI: - 0.5 to - 2.7, $p<0.01$), respectively (**Figures 4.6A and 4.6B**).

Furthermore, cel-miR-39 expression in heparin-contaminated RNA samples from STEMI patients (n = 35) was significantly inhibited by 1.5 cycles in comparison to non-heparinised samples from healthy and stable CAD controls (n = 12), which were spiked-in with the same number of cel-miR-39 copies (**Figure 4.7A**). Finally, *in vivo* administration of heparin to STEMI patients (n = 70) inhibited miR-425-5p expression by 2.4 cycles in comparison to heparinase-treated samples from the same patients (**Figures 4.7B**).

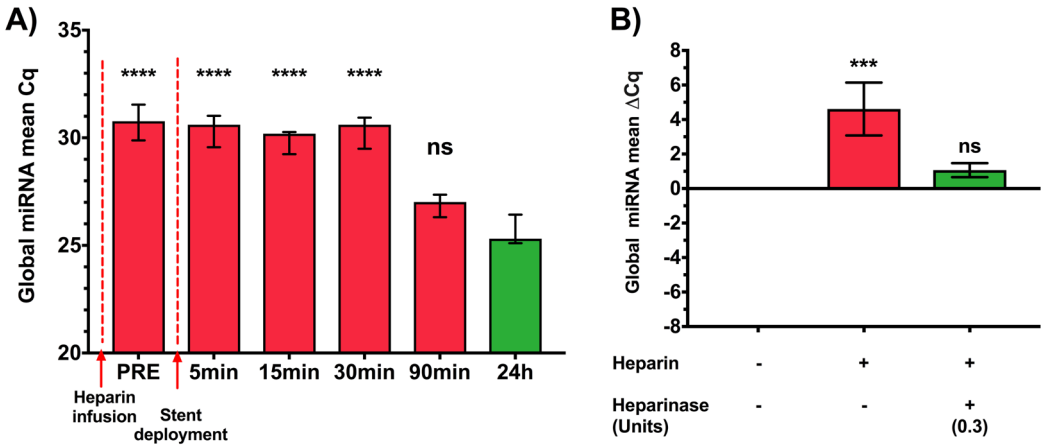

Figure 4.5. Heparin inhibitory effect on the global miRNA mean expression. (A) STEMI patients treated with heparin displayed significantly higher global miRNA mean Cq across the initial 30min following myocardial reperfusion in comparison to 24h values, when heparin was not present in the circulation; n = 3; ns, non-significant, ****p<0.0001 vs 24h; Repeated-measures one-way ANOVA and Dunnett's multiple comparison test; **(B)** To confirm *in vitro* whether heparin inhibits the global miRNA mean expression, heparin-contaminated RNA samples were treated with 0.3U of heparinase prior to reverse transcription and the difference in the global miRNA mean between these samples and non-heparinised, stable CAD controls (ΔCq) was calculated. Heparin-contaminated samples not treated with heparinase presented global miRNA mean 4 cycles higher than controls whereas samples from the same patients that were treated with heparinase had similar miRNA mean Cq to controls; n = 3; ns, non-significant, ****p<0.0001 vs stable CAD controls; one-way ANOVA and Dunnett's multiple comparison test .

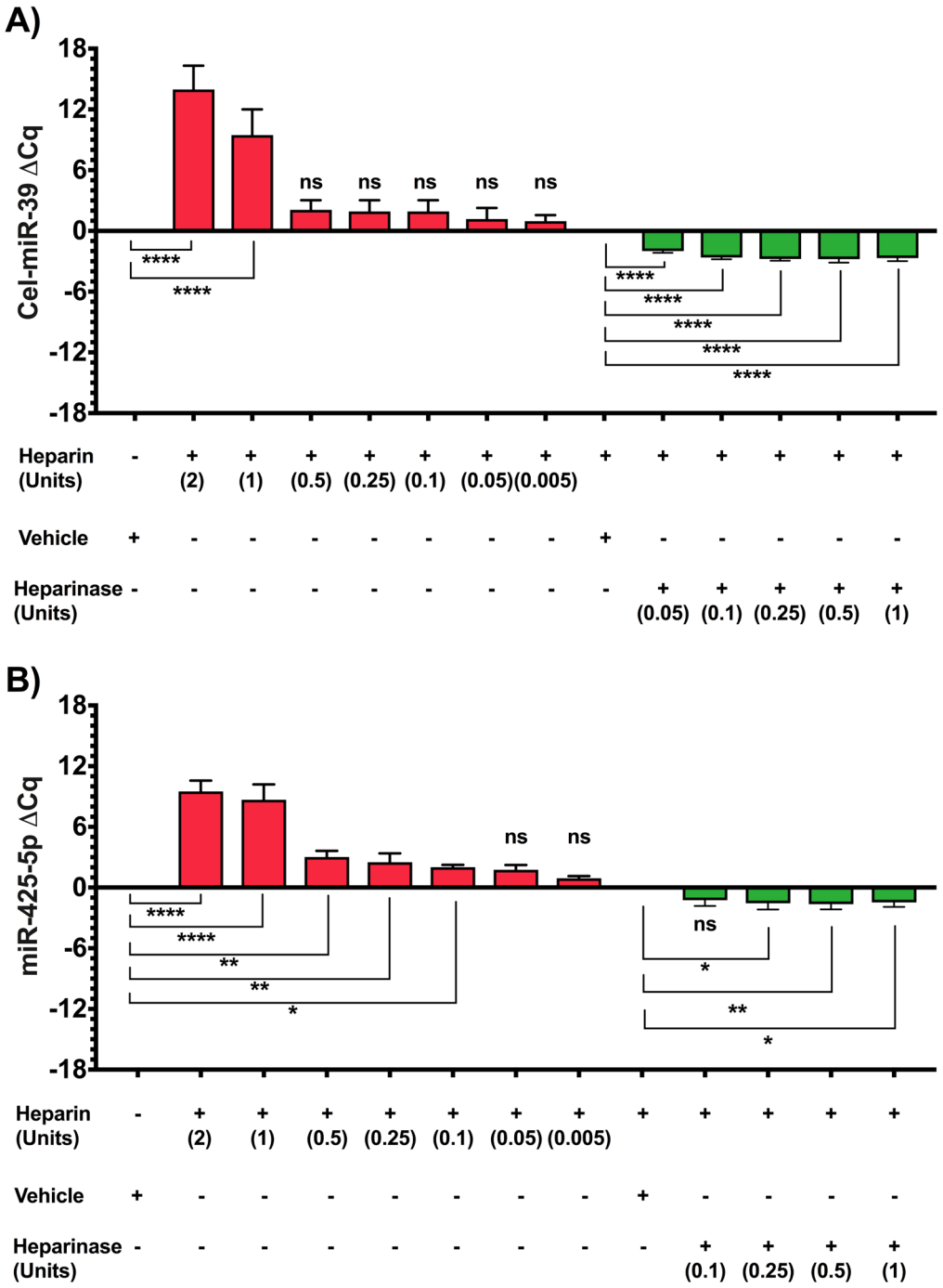

Figure 4.6. Effect of *in vitro* addition of serial doses of heparin or heparinase to RNA samples on cel-miR-39 and miR-425-5p expression. Seven different doses of heparin were added to RNA samples from STEMI patients not treated with heparin and changes on cel-miR-39 **(A)** and miR-425-5p **(B)** Cq were compared to the control, heparin-free samples (ΔCq). Heparin significantly inhibited both cel-miR-39 and miR-425-5p expression, whereas 2U completely inhibited miRNA detection by RT-qPCR. In contrast, treatment of heparin-contaminated samples from STEMI patients with 5 different doses of heparinase reduced Cq values, n = 3; ns, non-significant, *p<0.05, **p<0.01, ****p<0.0001; one-way ANOVA and Dunnett's multiple comparison test

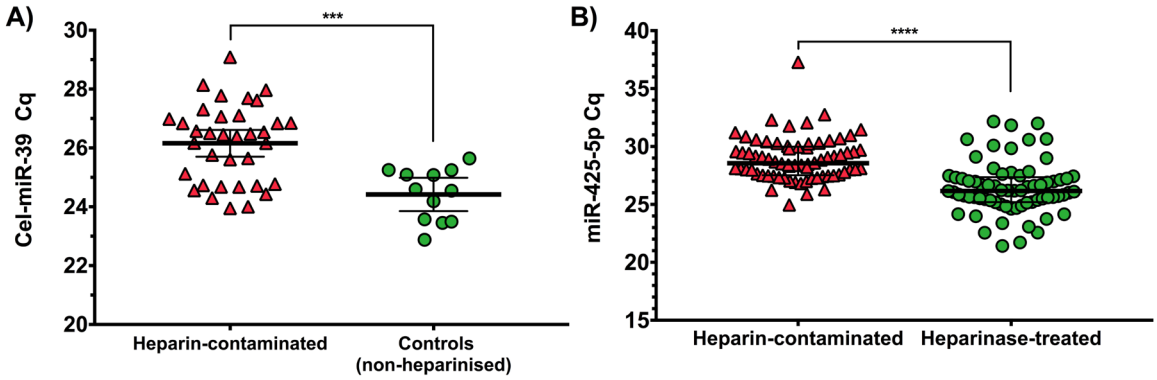

Figure 4.7. *In vivo* effect of heparin administration on cel-miR-39 and miR-425-5p expression. (A) Cel-miR-39 expression was significantly inhibited in heparin-contaminated STEMI samples (n = 35) in comparison to non-heparinised samples from healthy and stable CAD controls (n = 12), which were spiked-in with the same number of cel-miR-39 copies ***p<0.001, Mann-Whitney U test. **(B)** Similarly, miR-425-5p expression was inhibited by 2.4 cycles in heparin-contaminated versus heparinase-treated RNA samples from the same patients, n = 70; ****p<0.0001, Wilcoxon matched-pairs signed rank test.

4.3.6. Bivalirudin does not seem to affect cel-miR-39 or miR-425-5p expression

Given heparin interference with all RT-qPCR normalisation approaches, the effect of bivalirudin, an anticoagulant that can be used alternatively during PPCI, on miR-425-5p and cel-miR-39 expression was also investigated. *In vitro* addition of bivalirudin to RNA samples from control stable CAD patients (n = 3) did not affect miR-425-5p or cel-miR-39 detection by RT-qPCR (**Figure 4.8A and 4.8B**). The effect of *in vivo* bivalirudin administration on miRNA expression in STEMI patients was assessed by comparing miR-425-5p expression between patients who received bivalirudin prior to PPCI (n = 3) and heparinase-treated RNA samples from STEMI patients (n = 7) across 13 different time points prior to and after PPCI. No statistically significant difference in miR-425-5p expression was observed between these two groups at any time point (**Figure 4.8C**).

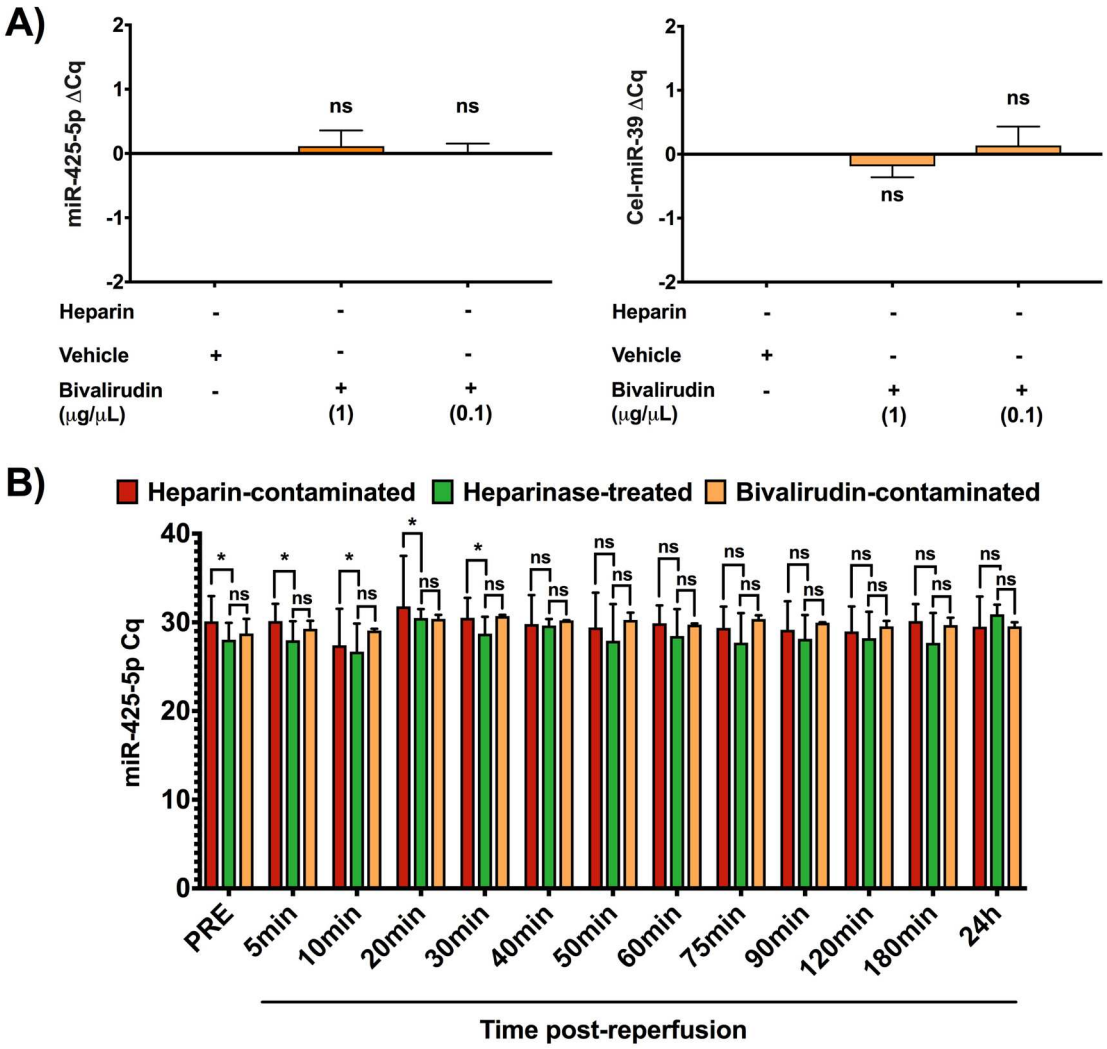

Figure 4.8. Bivalirudin does not affect miR-425-5p or cel-miR-39 expression. **(A)** *In vitro* addition of bivalirudin to RNA samples from patients with stable coronary artery disease did not result in changes on miR-425-5p or cel-miR-39 Cq values, n = 3; ns, non-significant, one-way ANOVA and Dunnett's multiple comparison test; **(B)** To evaluate the effect of bivalirudin on miR-425-5p *in vivo*, samples were obtained at 13 different time points from STEMI patients receiving either bivalirudin (n = 3) or heparin (n = 7). Aliquots from the heparin-contaminated RNA samples were treated with 0.3U of heparinase and miR-425-5p expression was compared between heparin-contaminated, heparinase-treated, and bivalirudin-contaminated samples. Significantly reduced Cq values were observed in heparinase-treated samples in comparison to heparin-contaminated samples from the same patients up to 30min post-PCI; *p<0.05, Wilcoxon matched-pairs signed rank test. No statistically significant differences were observed in miR-425-5p expression between heparinase-treated and bivalirudin-contaminated samples; ns, non-significant, Mann-Whitney U test.

4.3.7. Effect of RNA treatment with heparinase on cardiac-enriched miRNA expression

To test whether the inhibitory effect of heparin on RT-qPCR normalisation strategies had any impact on cardiac-enriched miRNA quantification, miR-1 and miR-133b were quantified in heparinase-treated (0.3U) and heparin-contaminated samples collected at 30min post-PPCI from the same patients (n = 70) and RT-qPCR data normalised to miR-425-5p. Median miR-1 and miR-133b levels were 3-fold and 1.5-fold higher in heparin-contaminated in comparison to heparinase-treated samples ($p<0.0001$), respectively (**Figure 4.9A**). This overestimation of cardiac-enriched miRNA levels in heparin-contaminated samples could partially be a result of the direct inhibition of heparin on the normalisation control (miR-425-5p) Cq values. Nonetheless, the different magnitudes of change in miR-1 and miR-133b expression after heparinase treatment suggested that heparin could also directly affect cardiac-enriched miRNA detection in distinct degrees. Indeed, miR-133b expression was significantly reduced by *in vitro* treatment with low doses of heparin whereas treatment of heparin-contaminated RNA samples with heparinase was effective in improving miR-133b expression (**Figure 4.9B**). In contrast, higher, supra-physiological *in vitro* doses of heparin were required to significantly inhibit miR-1 expression and therefore heparinase treatment had no significant effect in restoring miR-1 Cq values in heparin-contaminated patient samples (**Figure 4.9C**).

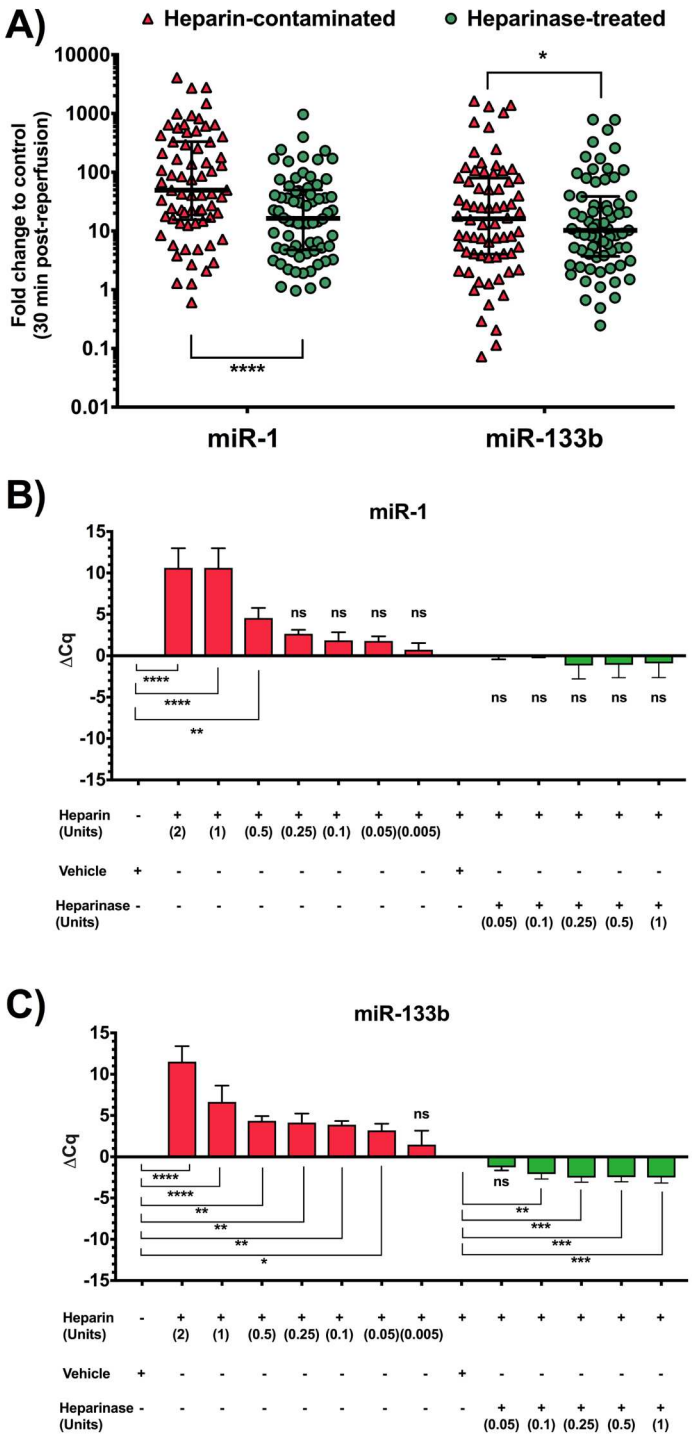

Figure 4.9. Effect of RNA sample treatment with heparinase on cardiac-enriched miRNA expression. (A) To assess whether RNA treatment with heparinase could affect cardiac-enriched miRNA quantification, miR-1 and miR-133b were quantified in heparinase-treated (0.3U) and heparin-contaminated samples collected at 30min post-PPCI from the same patients and data normalised to miR-425-5p. Expression of miR-1 and miR-133b in heparinase-treated sampled were 3-fold and 1.5-fold lower than that of heparin-contaminated samples; n = 70, ****p<0.0001; Wilcoxon matched-pairs signed rank test; **(B, C)** Effect of *in vitro* addition of serial doses of heparin or heparinase to RNA samples on miR-133b and miR-1 expression. Expression of miR-133b was affected by almost all tested doses of heparin and heparinase. In contrast, miR-1 Cq values were only affected by higher, supra-physiological doses of heparin and not significantly affected by heparinase in heparin-contaminated patient samples, n = 3; ns, non-significant, *p<0.05, **p<0.01, ****p<0.0001 vs controls; one-way ANOVA and Dunnett's multiple comparison test.

4.4. Discussion

This is the first study to (i) identify and systematically validate a circulating miRNA as an endogenous control for RT-qPCR normalisation in STEMI patients; (ii) demonstrate that heparin administration simultaneously affects all currently proposed RT-qPCR normalisation strategies; (iii) show that bivalirudin does not affect the expression of exogenous or endogenous miRNA normalisation controls; (iv) validate the treatment of heparin-contaminated RNA samples with heparinase combined with RT-qPCR normalisation to miR-425-5p as a suitable approach for circulating miRNA quantification in a cohort of STEMI patients.

4.4.1. miR-425-5p as an endogenous miRNA control for RT-qPCR normalization in STEMI patients

The paucity of standardized procedures for circulating miRNA quantification, especially regarding RT-qPCR data normalisation, might explain discrepancies or reproducibility issues amongst circulating miRNA studies (Lippi et al., 2013). Some studies in patients with acute myocardial infarction have used endogenous miRNAs, such as U6 snRNA (Ai et al., 2010, Wang et al., 2013, Zhang et al., 2015a, Zhang et al., 2015b), miR-16 (Peng et al., 2014), and miR-17 (D'Alessandra et al., 2010, Olivieri et al., 2013), as normalisation controls. However, these miRNAs are not stably detected in the blood (U6 snRNA) (Benz et al., 2013), are susceptible to haemolysis (miR-16) (McDonald et al., 2011), or were deemed stable based only on no statistical difference in expression between a small cohort of STEMI patients and controls (miR-17) (D'Alessandra et al., 2010). Selection of a reference miRNA solely on the basis of no statistically significant difference in expression between groups is not sufficient to establish that the miRNA is a stable reference and should involve more detailed *in silico* analysis (Marabita et al., 2016). Thus, an unequivocally stable circulating endogenous miRNA control remained to be validated.

In this chapter, miR-425-5p was identified as a stably expressed miRNA using a robust statistical approach based on 3 established gene stability assessment software. In addition, miR-425-5p expression reflected RNA sample concentration, allowing this miRNA to correct for differences in the input RNA quantity amongst samples. This is highly valuable for circulating miRNA quantification considering that

current miRNA reverse transcription protocols are based on same RNA input volume across different samples rather than same RNA concentration and that exogenous spike-in controls, although reflecting RNA extraction efficiency, are not able to correct for sources of variability such as input RNA quantity (Marabita et al., 2016). Interestingly, miR-425-5p has also been validated as an endogenous control in patients with breast cancer (McDermott et al., 2013). Circulating levels of miR-425-5p have otherwise been shown to be elevated in patients with colorectal (Zhu et al., 2017) and cervical cancer (Sun et al., 2017) as well as in patients with traumatic brain injury (Di Pietro et al., 2017), conditions that represented exclusion criteria for the present study. Data from miRNA tissue expression libraries (miRWalk 2.0, miRmine, miRGator 3.0) indicate high miR-425-5p expression in lymphoid cells, mammary glands, nasopharynx epithelium and mucosa, skin, brain, and testicular tissue (Min et al., 2013, Dweep and Gretz, 2015, Panwar et al., 2017). In the context of STEMI, the cellular or tissue sources of miR-425-5p remain to be elucidated in future studies. Our data suggest that miR-425-5p is not significantly expressed in or released from the myocardium in STEMI patients as there was no correlation between this miRNA plasmatic expression and circulating levels of cardiac troponin T. In contrast, strong correlations were observed between known cardiac-enriched miRNAs (miR-1 and miR-133b) and troponin T. In addition, data from validated miRNA tissue expression libraries showed irrelevant expression of miR-425-5p in the heart (Min et al., 2013, Dweep and Gretz, 2015, Panwar et al., 2017). Platelets have been previously shown to release their miRNA content, encapsulated in microparticles, following activation and aggregation in STEMI patients (Gidlof et al., 2013b). In addition, it has been recently postulated that accurate miRNA quantification in stored plasma samples relies on efficient removal of residual platelets prior to cryopreservation, as freezing of plasma samples resulted in release of platelet-derived microparticles containing miRNAs, including miR-425-5p, which expression strongly correlated with platelet count (Mitchell et al., 2016). However, in our study there was no correlation between miR-425-5p expression and baseline platelet count. Furthermore, miR-425-5p expression was not influenced by administration of antiplatelet aggregation medications (glycoprotein IIb/IIIa inhibitors) during PPCI in our cohort.

4.4.2. The inhibitory effect of heparin on miRNA detection by RT-qPCR

In STEMI patients undergoing PPCI, intravenous heparin administration represents a major obstacle for miRNA quantification, given its known interference with essential components of qPCR reactions, such as DNA polymerases and magnesium ions, resulting in qPCR inhibition (Satsangi et al., 1994, Yokota et al., 1999). Here, we demonstrate that heparin affects all currently proposed RT-qPCR normalisation strategies, including the global miRNA mean expression. This finding contradicts the study by Kaudewitz et al. (Kaudewitz et al., 2013), which reported that normalisation to the average Cq value of quantified miRNAs could overcome heparin-related cel-miR-39 inhibition and consequent overestimation of circulating miRNA levels in patients with acute coronary syndrome (ACS). In that study, however, miRNA mean expression was calculated based on the Cq values of only 14 miRNAs, some of which are known to be deregulated in patients with ACS. In accordance with our findings, inhibition of cel-miR-39 detection within the initial hour of heparin administration has been previously reported in smaller cohorts of patients undergoing coronary angiography (Boeckel et al., 2013, Kaudewitz et al., 2013).

A selective inhibitory effect of heparin on endogenous circulating cardiovascular-related miRNAs detection by RT-qPCR has also been reported by Boeckel et al. (Boeckel et al., 2013). In that study, miR-1, miR-92a, miR-126, miR-17, and miR-145 expression was not significantly altered after heparin administration to patients undergoing cardiac catheterisation (n = 11), whereas miR-133a, miR-34a, miR-378, and miR-499 detection was significantly reduced (Boeckel et al., 2013). Similarly, in our study, higher *in vitro* doses of heparin were required to inhibit miR-1 expression in non-heparinised STEMI samples when compared to miR-133b and miR-425-5p. This might explain why *in vitro* RNA treatment with heparinase was not effective in restoring miR-1 detection in heparin-contaminated samples from STEMI patients, in which heparin concentrations are lower than those necessary to inhibit miR-1 expression in our *in vitro* experiments. Consequently, following heparinase treatment of heparin-contaminated RNA samples from STEMI patients and PCR data normalisation to miR-425-5p, we observed different magnitudes of change in miR-1 and miR-133b expressions. A more pronounced reduction in miR-1 expression (3-fold) probably reflects the isolated effect of heparinase treatment in improving the endogenous normalisation control detection whereas the discreet reduction in miR-

133b expression (1.5 fold) might result from a synergistic effect of heparinase treatment on both the normaliser (miR-425-5p) and miR-133b detection. The mechanism behind this selective effect of heparin on miRNA detection is unknown. Future studies should investigate whether and how heparin interacts with the chemical structure of different miRNAs or plasmatic miRNA-binding proteins, such as Argonaute proteins (Turchinovich and Burwinkel, 2012).

4.4.3. Overcoming heparin-associated RT-qPCR inhibition for miRNA quantification in STEMI

Previous studies have also demonstrated that treatment of cellular and circulating RNA samples with heparinase could overcome heparin-induced RT-qPCR inhibition (Johnson et al., 2003, Plieskatt et al., 2014). Whilst this manuscript was under preparation, Li S et al. (Li et al., 2017) reported that heparinase treatment of RNA samples could abrogate heparin-induced impaired detection of cel-miR-39 in patients with CAD undergoing coronary intervention. Our data not only corroborate these findings but also show that treatment of heparin-contaminated RNA samples with heparinase improves the global miRNA mean and endogenous miRNA control (miR-425-5p) detection by RT-qPCR in STEMI patients post-PCI.

This study also sought to explore whether bivalirudin had any effect on the expression of endogenous and exogenous miRNA normalisation controls. Bivalirudin is an anti-thrombotic medication that can be used for anticoagulation therapy during PCI in STEMI patients, especially in those with heparin-induced thrombocytopenia (Ibanez et al., 2017). *In vitro* and *in vivo* bivalirudin administration did not interfere with miR-425-5p or cel-miR-39 expression. This suggests that RNA samples obtained from patients treated with bivalirudin could be an alternative to circumvent heparin interference with RT-qPCR normalisation for clinical studies of circulating miRNAs in STEMI patients.

This study presents some limitations. High throughput qPCR panels were used instead of microarray or RNA sequencing approaches for miRNA profiling and therefore could not identify novel miRNAs to be tested as stable endogenous controls. Furthermore, we did not evaluate whether miR-181a-5p, the second most stable endogenous miRNA, could produce similar results to miR-425-5p in terms of

cardiac-enriched miRNA normalization either separately or in association with miR-425-5p. Finally, we could not demonstrate a significant reduction in heparin concentration in RNA samples treated with 0.25U of heparinase by ELISA, whilst this dose was effective in restoring miRNA detection by RT-qPCR. We hypothesise that, due to RT-qPCR very high sensitivity, miRNA detection by RT-qPCR can be influenced by even small variations in heparin concentration in RNA samples, which ELISA might not be sensitive enough to detect.

4.5. Conclusion

In conclusion, this chapter addressed important methodological hurdles to accurate quantification of circulating miRNAs in STEMI patients. The results here described have also implications for circulating miRNA studies in other cohorts to which anticoagulation therapy is administered, e.g. patients undergoing organ transplantation or heart surgery. In addition, this study reinforces the evidence that levels of cardiac-enriched miRNAs early after myocardial reperfusion reflect the severity of cardiac injury. Finally, this chapter's results suggest that the use of samples from bivalirudin-treated patients or *in vitro* treatment of heparin-contaminated samples with heparinase, associated with normalisation to miR-425-5p, are suitable strategies for miRNA quantification in this STEMI patients, thus providing new tools to reduce variability and allow future detailed kinetics studies of circulating miRNAs in this population.

Chapter 5. Cardiac-enriched miRNA Release Following Myocardial Reperfusion

5.1. Introduction

Circulating levels of several microRNAs have been shown to be deregulated in STEMI patients both in relation to healthy individuals as well as to patients with other acute coronary syndrome manifestations (i.e. unstable angina and non-ST elevation acute myocardial infarction) (Viereck and Thum, 2017). Because almost all circulating miRNA studies in STEMI patients have focused on miRNA early diagnostic ability, they were designed to include mainly a single time point measurement, usually at patient admission to the emergency department or just prior to percutaneous coronary intervention. Therefore, little is known about miRNA expression following myocardial reperfusion in STEMI patients and how this process affects circulating miRNA levels.

The first insight into circulating miRNA kinetics following myocardial reperfusion in STEMI patients was provided by D'Alessandra et al. (D'Alessandra et al., 2010), who performed miRNA measurements at multiple time points after reperfusion (30 min, 3h, 9h, 15h, 21h, 33h, 45h, 69h). Peak miRNA levels were reported at 30 minutes after PPCI, followed by a significant, accentuated drop at 3 hours, and sustained lower levels in the remaining time points. In another study, Vogel et al. (Vogel et al., 2013) performed whole miRNome analysis in 6 STEMI patients at 5 different time points (pre-PPCI and 2h, 4h, 12h, and 24h post-PPCI). Interestingly, they observed that the most pronounced differences in miRNA expression in relation to controls happened at the first two initial time points (pre-PPCI and 2 hours post-PPCI) and that such differences were attenuated in the latter time points (Vogel et al., 2013). Combined, the findings from these two studies suggest that dynamic changes in circulating miRNA levels seem to happen predominantly within the initial 2 to 3 hours following reperfusion. Yet, no detailed serial miRNA measurement within the first 3 hours after PPCI has been performed.

As mentioned before, miRNAs can be carried in the circulation predominantly within extracellular vesicles or bound to argonaute proteins and HDL-cholesterol particles. Circulating microparticle (MP) levels have been shown to be increased in patients with ST-elevation acute myocardial infarction (Jung et al., 2012, Porto et al., 2012, Suades et al., 2016). However, the miRNA content of circulating MP and their

contribution to the total miRNA pool in plasma obtained from STEMI patients is unknown.

The aims of this study were to (i) identify candidate miRNA markers of failed myocardial reperfusion in STEMI patients; (ii) investigate the plasmatic kinetics of these candidate miRNAs within the initial 3 hours post-PPCI; (iii) assess miRNA expression in circulating microparticles; (iv) validate whether the expression of the candidate miRNAs is deregulated in a second STEMI cohort.

5.2. Results

5.2.1. Patient baseline characteristics

A total of 18 STEMI patients were included for a detailed study of miRNA release kinetics following myocardial reperfusion (STEMI cohort 2). Most patients (n = 17; 94.4%) presented completely obstructed culprit coronary arteries prior to PPCI, without angiographic evidence of coronary perfusion (TIMI flow 0 or 1) and achieved optimal coronary perfusion (TIMI flow 3) following PCI (n = 16; 94.4%). Baseline characteristics of this cohort are displayed in **table 5.1**. As for the second cohort of STEMI patients (STEMI cohort 3; n = 50), baseline characteristics are also displayed in **table 6.1**. In this cohort, all patients had TIMI flow 0 or 1 prior to PCI and 96% (n = 48) had TIMI flow 3 post-PCI.

Variable	STEMI cohort 2 (n = 18)	STEMI cohort 3 (n = 50)
Gender (male), n (%)	15 (83.3)	41 (82)
Age [years, mean (SD)]	58.3 (10)	65.2 (10.4)
Risk factors, n (%)		
Smoking status		
Never smoked	9 (50)	18 (36)
Ex-smoker	1 (5.6)	20 (40)
Current smoker	8 (44.4)	12 (24)
Diabetes mellitus	1 (5.6)	4 (8)
Hypertension	7 (38.9)	10 (20)
Hypercholesterolaemia	2 (11.1)	5 (10)
Obesity	4 (22.2)	19 (38.8)
Laboratory tests [median (IQR)]		
eGFR (mL/min)	83 (65.2 – 112)	83 (74 – 93.7)
Admission Troponin T (ng/L)	61.5 (14.5 – 156)	43 (27 – 80.7)
Peak Troponin T (ng/L)	2,752 (1,039 – 5,047)	3,447 (1,184 – 6,619)
STEMI clinical characteristics		
Onset to reperfusion (min)	131 (108 – 223)	173 (112 – 259)
Infarct location, n (%)		
Anterior	6 (33.3)	16 (32)
Non-anterior LCx	12 (66.7)	34 (68)
TIMI flow pre PPCI, n (%)		
0	16 (88.8)	42 (84)
1	1 (5.6)	8 (16)
2	1 (5.6)	0 (0)
3	0 (0)	0 (0)
TIMI flow post PPCI, n (%)		
0	0 (0)	0 (0)
1	1 (5.6)	2 (4)
2	1 (5.6)	0 (0)
3	16 (88.8)	48 (96)
Medication during PPCI		
Heparin, n (%)	15 (85)	50 (100)
Bivalirudin, n (%)	3 (15)	0 (0)
gpIIb/IIIa inhibitor, n (%)	13 (72.2)	33 (66)

Table 5.1. STEMI cohorts 2 and 3 baseline characteristics. eGFR, estimated glomerular filtration rate; gpIIb/IIIa, glycoprotein IIb/IIIa; IQR, interquartile range; PPCI, primary percutaneous coronary intervention; SD, standard deviation; TIMI, thrombolysis in myocardial infarction angiographic score.

5.2.2. Screening for selection of miRNA candidates of failed myocardial reperfusion

To explore the effect of myocardial reperfusion on circulating miRNA levels early after PPCI, screening of 179 miRNAs was performed in samples collected prior to and at 5 time points following PPCI from 3 STEMI patients. In relation to pre-reperfusion levels, a cluster of seven miRNAs (miR-1, miR-378a-3p, miR-30a-5p, miR-133b, miR-451a, miR-133a-3p, miR-125a-5p) presented increasing expression following reperfusion, with a peak at 90 min, followed by decrease at 24 hours, suggesting an association between these miRNAs and the reperfusion process (**Figure 5.1A**).

Subsequently, a second screening was performed in samples collected at 30min post-PPCI from STEMI patients with microvascular obstruction (n = 5) and age-matched stable CAD controls (n = 4) to identify the most highly expressed miRNAs in this subpopulation of STEMI patients. Except for miR-451a, all miRNAs identified in the initial screening were also amongst the 10 most up-regulated miRNAs in plasma from STEMI patients with microvascular obstruction (**Figure 5.1B**). Interestingly, the 3 most highly expressed miRNAs in this sub cohort (miR-133b, miR-1, and miR-133a-3p) are known to be enriched in muscular tissue, including the myocardium. Considering that failed myocardial reperfusion is strongly associated with myocardial damage, miR-133b and miR-1 were selected for a detailed release kinetics study and further validation in a larger cohort of STEMI patients.

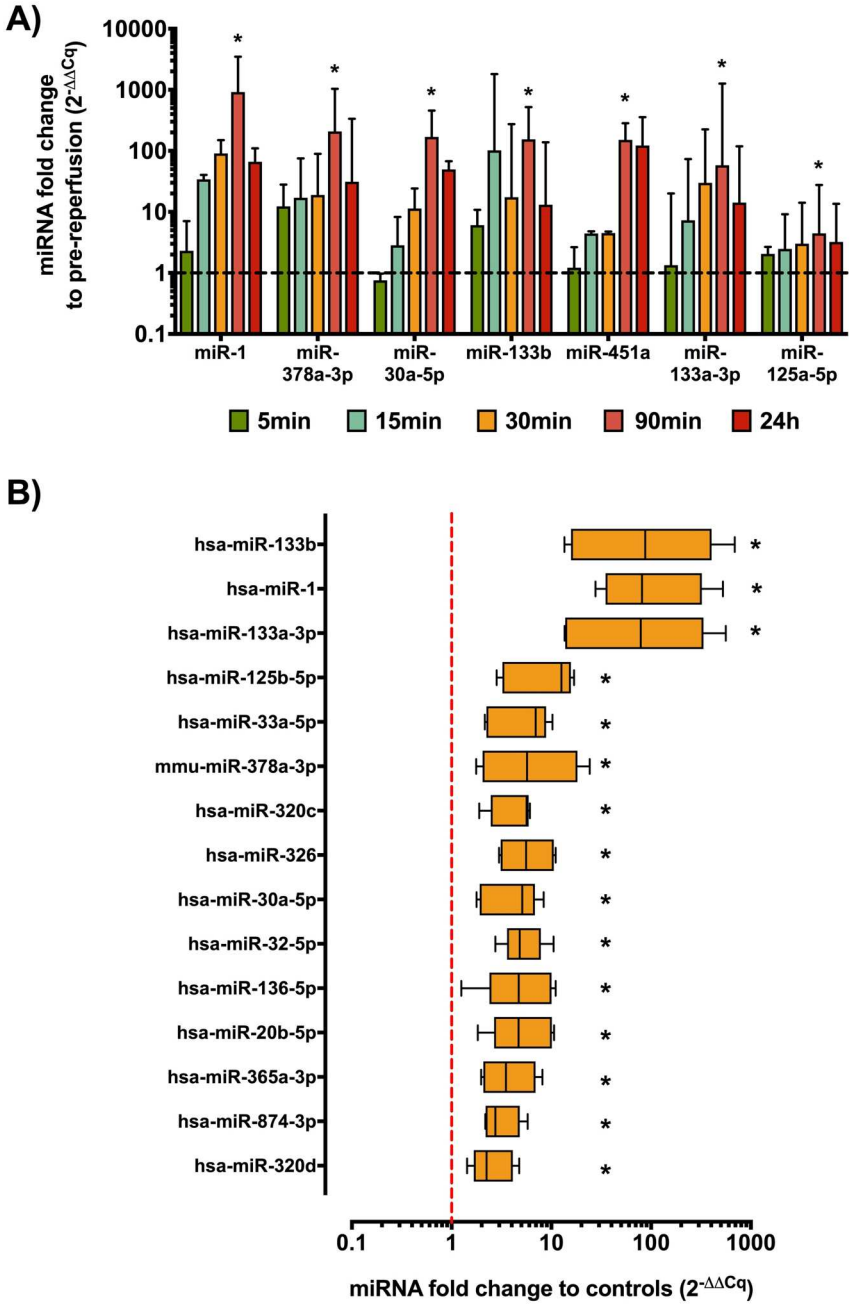

Figure 5.1. MicroRNA screening for selection of candidate markers of failed myocardial reperfusion. (A) Screening of 179 miRNAs using a PCR-based platform revealed a cluster of 7 miRNAs with progressive increase in expression across the initial 90 min post-reperfusion in STEMI patients. (n = 3). **(B)** The 15 most highly expressed miRNAs after screening of 179 miRNAs in 30 min post-reperfusion samples from STEMI patients with microvascular obstruction (n = 5). Note that all 7 miRNAs identified in (A) were also the highest expressed miRNAs in (B), except for miR-451a. In both screenings, samples from age-matched patients with stable coronary artery disease were used as controls (n = 4). In (A) data is presented as median (bar) and upper range (error bar). In (B) the boxplots depict median (central line), interquartile range (limits of the box) and range (error bars). Dashed lines represent reference pre-reperfusion (A) or control (B) levels. * $p < 0.05$, Kruskal-Wallis test with Dunn's correction for multiple comparisons (A) and Mann-Whitney U test (B).

5.2.3. Cardiac-enriched miRNA kinetics following myocardial reperfusion

Median miR-1 pre-reperfusion levels were approximately 4-fold higher in STEMI patients (n = 18) in comparison to miR-1 expression in healthy controls (n = 6) (**Table 5.2**). Gradually increasing median miR-1 levels were observed until a first peak was achieved at 30 min post-PPCI, when miR-1 levels were 49-fold higher than controls (**Table 5.2**). At 40 min post-PPCI, there was a slight drop in miR-1 expression followed by a steady increase until another peak was reached at 90 min (**Table 5.2**). After 90 min, circulating miR-1 expression decreased again until it returned to similar levels of pre-reperfusion at 24h post-PPCI (**Table 5.2**). Circulating miR-1 levels remained higher than those of controls across all measured time points and higher than pre-reperfusion levels from 20 min to 180 min post-reperfusion (**Figure 5.2A**). A very similar kinetics pattern was observed for miR-133b, except that miR-133b levels were lower than miR-1 and were not significantly higher than controls at pre-reperfusion and at 5 min, 10 min, and 24h post-PCI (**Table 5.2** and **Figure 5.2B**).

Time points	miR-1	miR-133b
Pre-reperfusion	3.8 (1.8 – 6.3)	2 (1 – 4.3)
5 min	8.7 (3.9 – 18)	3 (1 – 6.2)
10 min	14.6 (4.6 – 26.1)	3.4 (0.5 – 7.4)
20 min	31.8 (7 – 94.4)	11.5 (3.7 – 83.7)
30 min	49 (9.8 – 169.3)	32.6 (10.3 – 125)
40 min	33.5 (10.8 – 211.8)	16.3 (5.5 – 111.8)
50 min	38.9 (5.5 – 111.4)	11.2 (2.5 – 123.3)
60 min	47.8 (7.9 – 95.7)	12.2 (2.9 – 111.9)
75 min	45.7 (8.2 – 87.2)	12.1 (3 – 77)
90 min	53.1 (8.6 – 123.1)	28.8 (9.5 – 106)
120 min	28.8 (7.2 – 107.8)	10.5 (2.6 – 54.4)
180 min	33.7 (7 – 200.5)	21.8 (3.5 – 143.8)
24 hours	2.9 (1.2 – 6.35)	3.4 (1 – 10.8)

Table 5.2. miR-1 and miR-133b expression prior to and in the initial 3 hours post-PPCI. Values expressed as median (interquartile range) miRNA fold change to healthy controls. Fold change calculated using the $2^{-\Delta\Delta Ct}$.

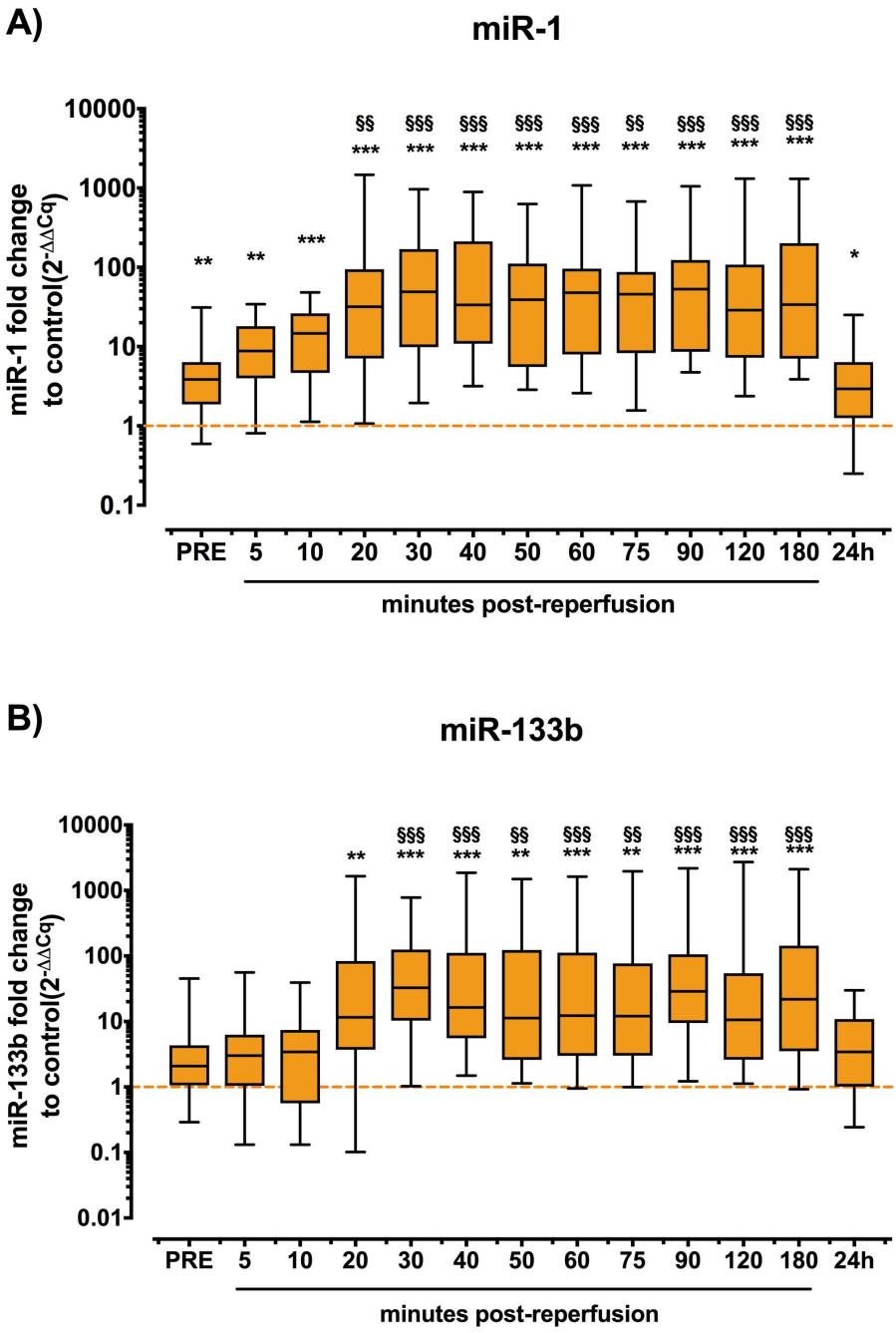

Figure 5.2. miR-1 and miR-133b plasmatic kinetics following myocardial reperfusion in STEMI patients. (A) miR-1 expression was higher than in healthy controls at all time points and increased in relation to pre-reperfusion levels between 20 min and 180 min post-PCI. **(B)** Kinetics analysis revealed that 20 min up to 180 min post-PCI miR-133b levels were elevated in relation to healthy controls. Also, 20 min up to 180 min post-reperfusion miR-133b expression was higher than pre-reperfusion levels. Data presented as median (central line in boxes), interquartile range (limits of the boxes), and range (error bars). Dashed lines represent reference control levels. n STEMI = 18; n controls = 6. Differences between STEMI patients and control miRNA levels were determined by Kruskal-Wallis test with Dunn's correction for multiple comparisons. Differences in miRNA expression among time points in STEMI patients were determined by Friedman test with Bonferroni's post hoc correction for multiple comparison. *$p < 0.05$ vs. healthy controls; **$p < 0.01$ vs. healthy controls; ***$p < 0.001$ vs. healthy controls; $^{§§}p < 0.01$ vs. pre-reperfusion; $^{§§§}p < 0.001$ vs. pre-reperfusion.

5.2.4. miR-1 and miR-133b kinetics patterns post-PCI

Considering the substantial variation in miRNA levels among patients at each time point, miRNA data for each patient was individually plotted to identify whether miRNA kinetics patterns were different at a single patient level. Indeed, it was possible to identify 2 distinct kinetics patterns for both miR-1 and miR-133b (data not shown). Such patterns became also evident after grouping these individuals accordingly: (i) monophasic, in which an early component of miRNA increase, peaking at 30 min post-PCI, was more prominent than miRNA levels in subsequent later time points (**Figure 5.3A**); (ii) biphasic, in which there seemed to be 2 components of miRNA increase – a first one with a peak at 30 min and a second one with a peak between 75 to 90 min post-PCI, which was higher in amplitude and followed by sustainably high miRNA levels until 180 min post-PCI (**Figure 5.3B**).

5.2.5. Impact of coronary perfusion status on miRNA release kinetics

To test a potential effect of the coronary artery perfusion status on miRNA release kinetics, miR-1 and miR-133b were quantified in (i) a patient undergoing TASH, hence with optimal coronary perfusion at the time of cardiomyocyte injury induction; (ii) a STEMI patient with TIMI flow 3 prior to PCI; (iii) a STEMI patient with TIMI flow 0 post-PCI.

In the TASH patient, miR-1 and miR-133b expressions were 9.1-fold and 4.8-fold higher than controls as early as 10 min after cardiomyocyte injury induction, respectively. MicroRNA expression gradually increased to reach maximum values of 231-fold (miR-1) and 195-fold (miR-133b) higher than controls at 180min (**Figure 5.4A**). In the STEMI patient with spontaneous coronary recanalization prior to PCI (TIMI flow 3), miR-1 and miR-133b expression barely changed from pre-reperfusion levels across the initial 90 min post-PCI and decreased to control levels at 120 min, 180 min and even below that at 24h post-PCI (**Figure 5.4B**). In contrast, miR-1 expression in the STEMI patient with TIMI flow 0 post-PCI increased steadily until 120 min post-PCI reaching maximum levels at 180 min post-PCI (171-fold) and remained elevated at 24h (**Figure 5.4C**). As for miR-133b expression, there was a discrete increase until 120 min followed by substantial elevation thereafter, reaching a peak at 24h post-PCI (45.9-fold) (**Figure 5.4C**).

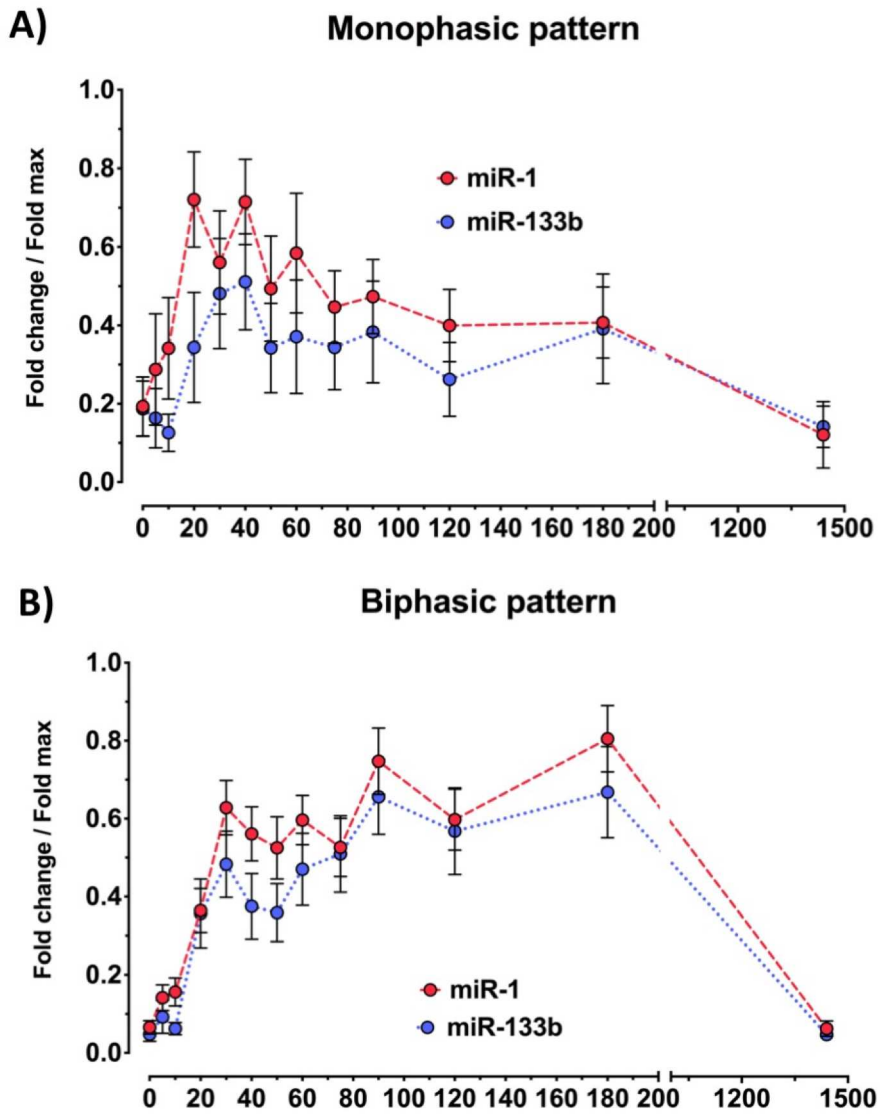

Figure 5.3. Post-reperfusion miR-1 and miR-133b kinetics patterns in STEMI patients. Graphical representation of the concept of distinct kinetics patterns, monophasic **(A)** and biphasic **(B),** for miR-**1** and miR-133b. Data presented as mean (dots) and standard error of the mean (error bars). *n* STEMI miR-1 (monophasic: 8 vs. biphasic: 9); *n* STEMI miR-133b (monophasic: 5 vs. biphasic: 12); *n* healthy controls = 4.

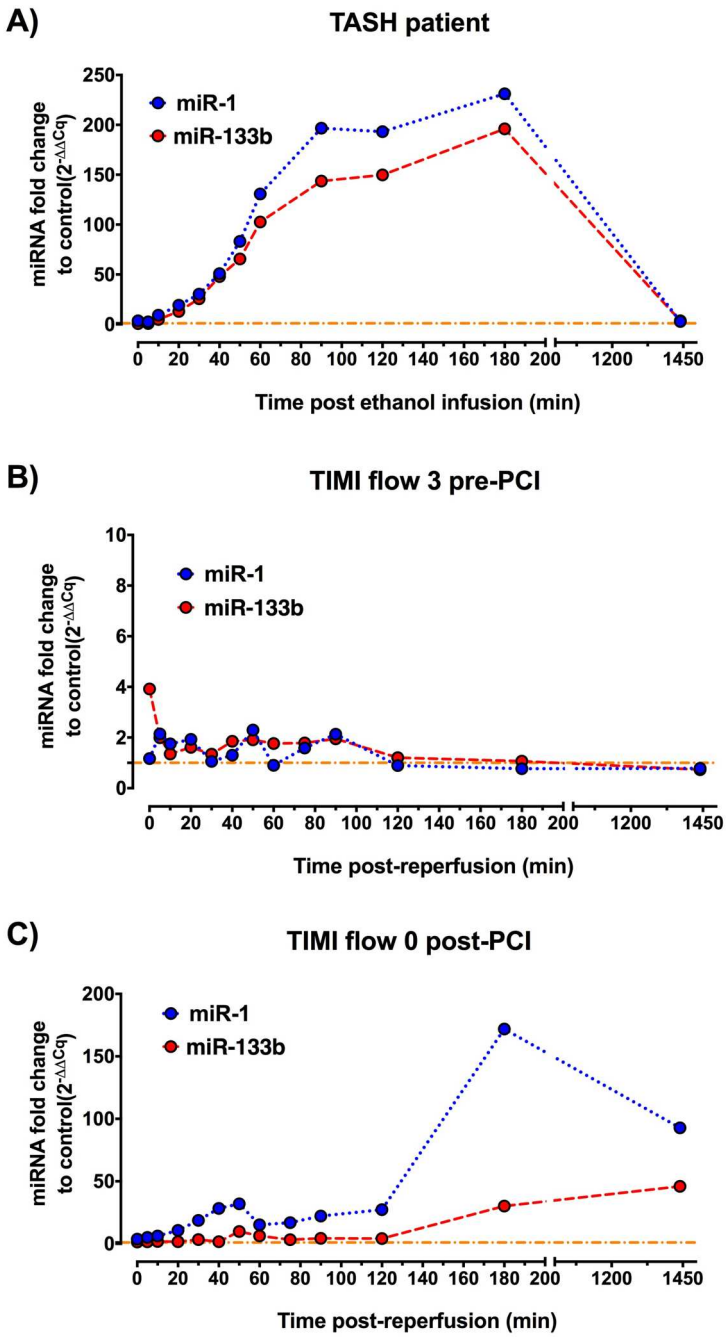

Figure 5.4. Proof of concept of the effect of coronary artery perfusion status on miRNA release kinetics. (A) miR-1 and miR-133b kinetics following ethanol-induced myocardial injury in a patient undergoing transcoronary ablation of septal hypertrophy. **(B)** miR-1 and miR-133b kinetics in a STEMI patient with spontaneous recanalization of the culprit coronary artery (TIMI flow 3) prior to PCI. **(C)** miR-1 and miR-133b kinetics in a STEMI patient with unsuccessful re-establishment of culprit coronary artery patency post-PCI (TIMI flow 0). Dots represent miRNA expression fold-change to healthy controls at each time point. Dashed lines represent reference control levels.

5.2.6. miRNA kinetics and the coronary microcirculatory function

To explore whether miR-1 or miR-133b release kinetics could be affected by the coronary microvascular function, patients who had invasive measurement of the index of microvascular resistance (n = 14) were divided according to IMR tertiles. Interestingly, miR-1 kinetics seemed to differ amongst IMR tertile groups, especially regarding the magnitude and timing of peak miRNA expression (**Figure 5.5A**). All IMR tertile groups presented an initial miR-1 peak, which occurred at 30 min post-PCI for the highest tertile group, at 40 min for the middle tertile, and at 60 min for the lowest tertile group (**Figure 5.5A**). As for a second peak, this was absent in the first tertile group, which presented a monophasic kinetics pattern (**Figure 5.5A**). A second miR-1 peak was observed at 90 min post-PCI in the middle tertile group, followed by sustained high levels until 180 min (**Figure 5.5A**). As for the highest tertile group, the second miR-1 peak was observed later at 180 min post-PCI (**Figure 5.5A**). Regarding miR-133b kinetics, all patient groups presented biphasic kinetics, however the association with IMR values was not so evident (**Figure 5.5B**).

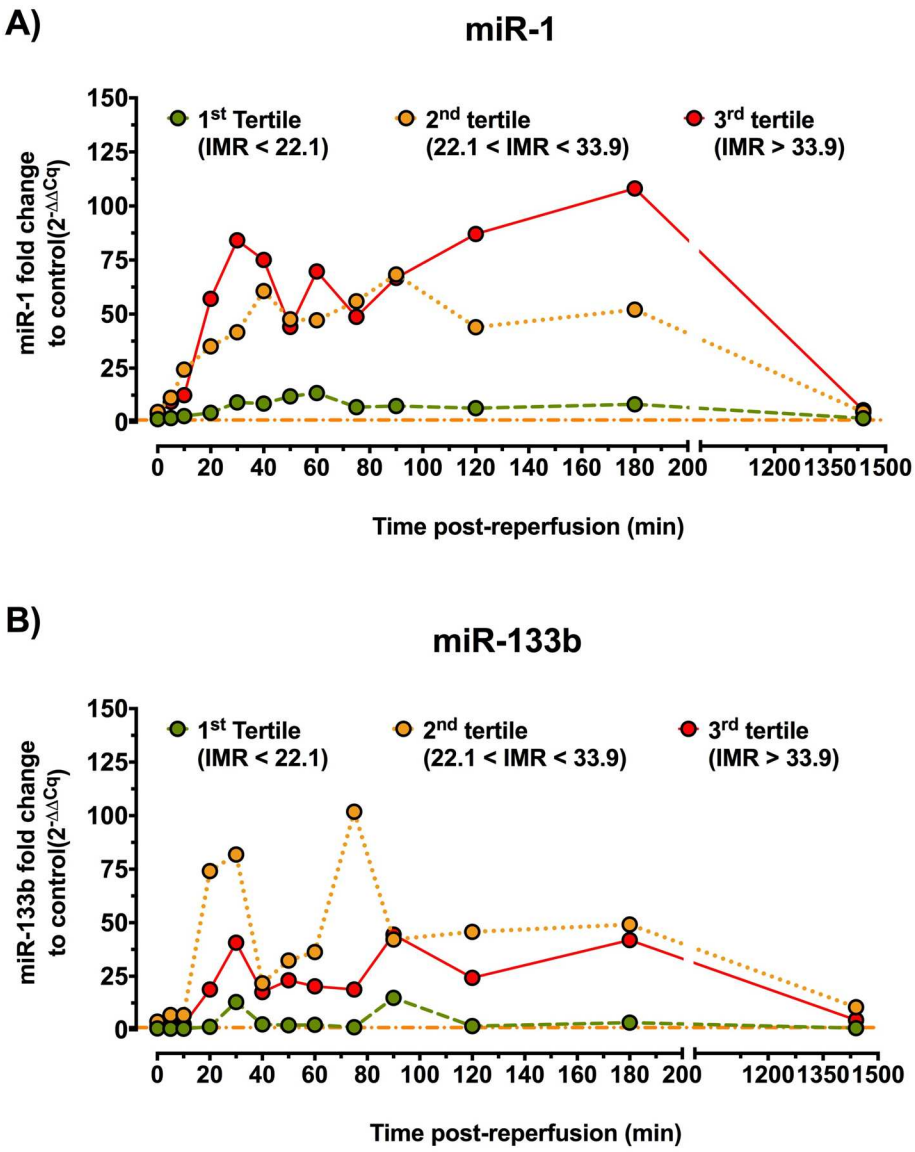

Figure 5.5. miR-1 and miR-133b kinetics according to index of microvascular resistance (IMR) tertiles. (A) miR-1 kinetics for each IMR tertile patient group. **(B)** miR-133b kinetics for each IMR tertile patient group. Data presented as median (dots) fold change to healthy controls. n STEMI = 14; n 1st tertile = 4; n 2nd tertile = 5; n 3rd tertile = 5.

5.2.7. miR-1 and miR-133b are carried in circulating microparticles

To gain an insight on miR-1 and miR-133b release mechanisms from the myocardium and transport in the blood stream following myocardial reperfusion, circulating microparticles were quantified in STEMI patients (n =10) as well as healthy controls (n = 3). In addition, miR-1 and miR-133b were measured in RNA samples isolated from microparticles. Circulating MP levels were significantly high at pre-reperfusion in the aorta (1,400 MP/μL, $p < 0.008$) and culprit coronary artery (1,385 MP/μL, $p = 0.024$) in STEMI patients compared to controls (526 MP/μL) (**Figure 5.6A**). In contrast, MP concentration decreased as early as 5 min as well as at 180 min post-reperfusion to similar levels of controls (**Figure 5.6A**).

Expression of miR-1 and miR-133b were 6-fold ($p = 0.014$) and 9.9-fold ($p = 0.007$) higher in MPs from STEMI patients at pre-reperfusion compared to controls, respectively (**Figure 5.6B**). Despite the decrease in circulating MP concentration post-PCI, both miR-1 and miR-133b expression in MP from STEMI patients remained elevated in relation to controls at 30 min (miR-1: 20-fold, $p = 0.007$; miR-133b: 29-fold, $p = 0.007$) and 90 min post-reperfusion (miR-1: 27-fold, $p = 0.007$; miR-133b: 69-fold, $p = 0.007$) (**Figure 5.6B**). No significant differences were observed between miR-1 and miR-133b expression in MP at pre-reperfusion or 30 min post-PCI, however miR-133b expression was 2.5-fold higher than miR-1 at 90 min post-reperfusion ($p = 0.019$).

Subsequently, miR-1 and miR-133b expression in plasma and MP from the same STEMI patients were compared to evaluate the contribution of circulating MPs to the total expression of these cardiac-enriched miRNAs in plasma. At pre-reperfusion, no difference in both miR-1 and miR-133b expression between plasma and MPs was observed (**Figures 5.6C and 5.6D**). Following myocardial reperfusion, miR-1 expression in MPs was significantly lower compared to plasma, accounting for only 16.2% of miR-1 total expression in plasma at 30 min ($p = 0.027$) and 34% at 90 min ($p = 0.027$). In contrast, miR-133b expression in MP remained similar to those observed in plasma at 30 min and 90 min post-reperfusion (**Figures 5.6C and 5.6D**).

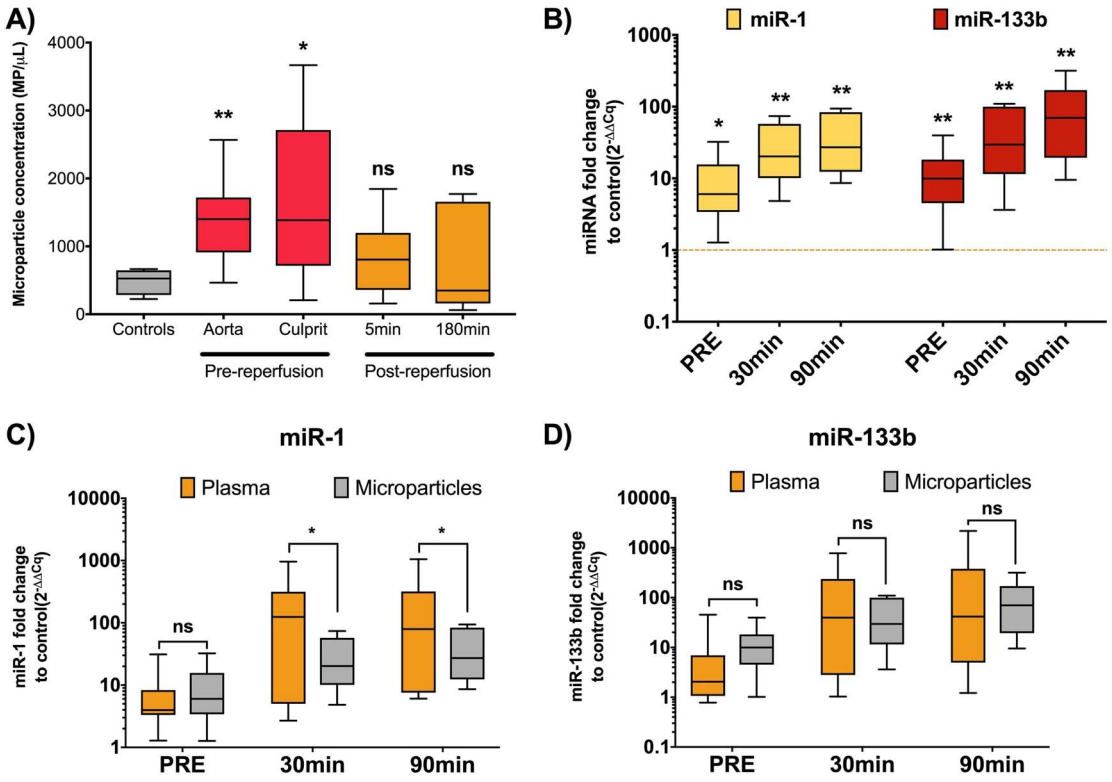

Figure 5.6. miR-1 and miR-133b expression in circulating microparticles isolated from STEMI patients. (A) Microparticle concentration in STEMI patients prior to and after coronary reperfusion. Microparticle concentration is significantly raised in the aorta and culprit coronary artery of STEMI patients compared to healthy controls. *p < 0.05 vs. controls; **p < 0.01 vs. controls; ns, non-significant. Kruskal-Wallis test with Dunn's correction for multiple comparisons. **(B)** miR-1 and miR-133b expression is increased in circulating microparticles isolated from STEMI patients at pre-reperfusion, 30 min and 90 min post-PCI. *p < 0.05 vs. healthy controls; **p < 0.01 vs. healthy controls, Mann-Whitney U test. **(C)** Comparative miR-1 expression between plasma and microparticles isolated from the same STEMI patients prior to and at 30 min and 90 min post-reperfusion. *p < 0.05, Wilcoxon matched-pairs signed rank test. **(D)** Comparative miR-133b expression between plasma and microparticles isolated from the same STEMI patients prior to and at 30 min and 90 min post-reperfusion. Data presented as median (central line in boxes), interquartile range (limits of the boxes), and range (error bars). *p < 0.05, Wilcoxon matched-pairs signed rank test.

5.2.8. *Post-reperfusion miR-1 and miR-133b levels are elevated in another STEMI cohort*

To validate whether miR-1 and miR-133b levels were indeed elevated after PCI, they were quantified in 48 STEMI patients with TIMI flow 3 post-PCI from a second cohort (STEMI cohort 3). MiR-1 expression was significantly higher in these patients in relation to control at 30 min (18.5-fold, $p < 0.0001$) and 90 min post-reperfusion (25.2-fold, $p < 0.0001$) (**Figure 5.7**). Likewise, miR-133b levels were also increased in this cohort compared to controls at 30 min (12-fold, $p < 0.0001$) and 90 min post-PCI (15-fold, $p < 0.001$) (**Figure 5.7**).

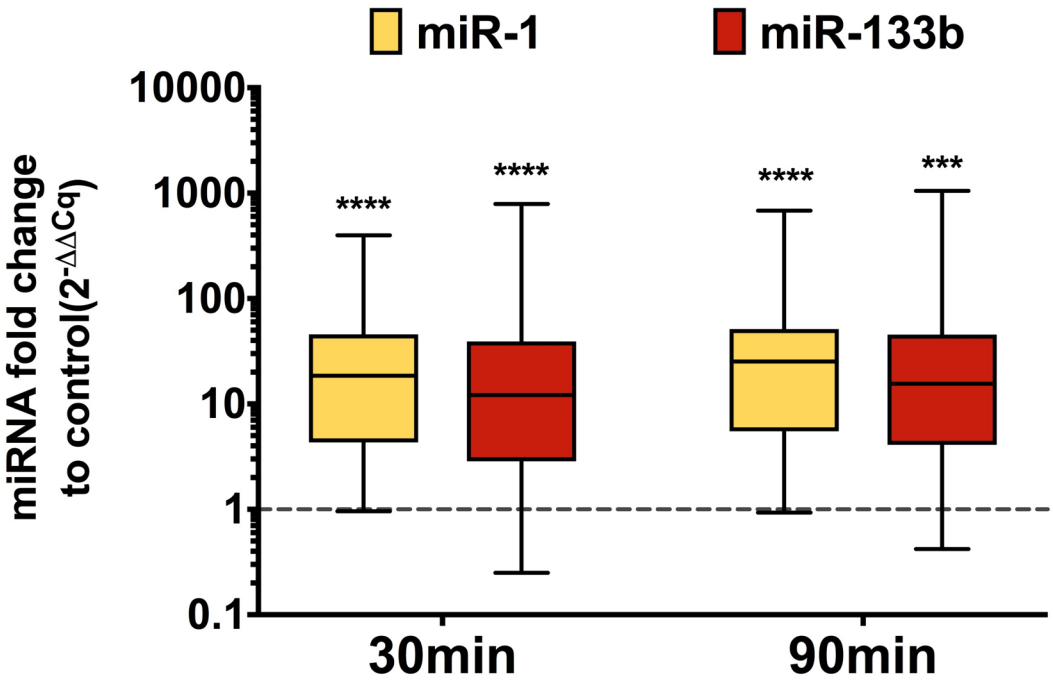

Figure 5.7. Post-reperfusion miR-1 and miR-133b levels in a validation STEMI cohort. MiR-1 and miR-133b levels were confirmed to be elevated at 30 min and 90 min post-reperfusion in a validation STEMI cohort. Data presented as median (central line in boxes), interquartile range (limits of the boxes), and range (error bars). n = 48. ***p < 0.001 vs. healthy controls; ****p < 0.0001 vs. healthy controls. Mann-Whitney U test.

5.3. Discussion

5.3.1. Biology of miR-1 and miR-133b

In this chapter, circulating miR-1 and miR-133b were found to be elevated in STEMI patients. MicroRNA-1 is encoded by two loci (miR-1-1 and miR-1-2) in the intron 2 of an uncharacterised gene C20ORF166 on the chromosome 20 and in the intron 12 of the E3 ubiquitin-protein ligase MIB1 on the chromosome 18 (Heidersbach et al., 2013), respectively. The miR-133b gene is located in the chromosome 6 (Ivey et al., 2008). In normal human tissues, miR-1 and miR-133b are highly expressed in cardiac and skeletal muscle as well as the thyroid, with less significant expression in the breast, oesophagus, prostate, bladder, and testicles (Liang et al., 2007, Chen et al., 2006). Deletion of either the miR-1-1 or miR-1-2 locus leads to variable lethality and subtle cardiac dysfunction but double miR-1 knockout invariably resulted in pre-natal death in mice demonstrating that miR-1 is fundamental for cardiac development and function (Heidersbach et al., 2013). MiR-1 has been shown to modulate the expression of genes involved in cardiovascular disease as well as different types of cancers. It has been shown that miR-1 overexpression leads to arrhythmogenic activity by inhibiting the expression of the protein phosphatase PP2A regulatory subunit B56α, resulting in increased calcium release (Terentyev et al., 2009), whereas miR-1 deletion results in overexpression of Irx5, a transcription factor that regulates cardiac repolarization (Zhao et al., 2007). In addition, miR-1 promotes cardiomyocyte anti-hypertrophic effects by targeting hypertrophy-associated genes such as ACTA1, calmodulin, MEF2a, Ras GTPase-activating protein (RasGAP) and cyclin-dependent kinase 9 (Cdk9) (Ikeda et al., 2009, Sayed et al., 2007). Finally, miR-1 expression was found to be reduced in rhabdomyosarcomas whilst the expression of its pro-oncogenic target, c-MET, was increased (Yan et al., 2009). The anti-oncogenic property of miR-1 has also been shown in bladder and prostate cancer in which down-regulation of miR-1 was associated with increased expression of TAGLN2 (Yoshino et al., 2011)and LASP1 as well as XPO6 (Ambs et al., 2008), respectively .

Similarly, miR-133b is involved in many stages of myocyte development, cell fate determination, apoptosis as well as gene programme regulation in cardiomyopathies (Sucharov et al., 2008). For example, miR-113b regulates the expression of the Rho subfamily of small GTP-binding proteins thus modulating cardiomyocyte hypertrophy

(Sucharov et al., 2008). In addition, miR-133b has been shown to exert a tumour-supressing role by targeting oncogenic genes involved in oesophageal (FSCN1), lung (MCL-1; BCL2L2), colorectal (MET), and gastric (FGFR1) cancers (Kano et al., 2010, Crawford et al., 2009, Hu et al., 2010, Wen et al., 2013).

5.3.2. Cardiac-enriched miRNA release in STEMI patients

Several studies demonstrated deregulation of circulating miR-1 and miR-133b levels following cardiac injury in both animal models and patients with acute myocardial infarction (AMI). In mice, serum miR-1 levels increased rapidly after coronary artery ligation concomitantly with downregulation of this miRNA in myocardial tissue, suggesting miR-1 release into the circulation (D'Alessandra et al., 2010). In patients with MI, elevated miR-1 levels could be detected at patient admission, between 6 and 12 hours after the onset of symptoms. Likewise, miR-133b levels were found to be significantly increased in plasma obtained from mice after 6 hours of AMI induction (D'Alessandra et al., 2010). Interestingly, hindlimb ischemia mouse models showed no deregulation in miR-1 or miR-133b circulating expression, suggesting a cardiac-specific release (D'Alessandra et al., 2010). Release from cardiac-specific miRNAs (miR-133a, miR-499 and miR-208a) from the myocardium in patients with myocardial infarction was confirmed by transcoronary gradient studies, which found increasing levels of such miRNAs across the coronary circulation (De Rosa et al., 2011).

In patients with STEMI, only few studies performed serial cardiac-enriched miRNA quantification. D'Alessandra et al. were the first to demonstrate peak levels of cardiac-enriched miRNAs (miR-1, miR-133a, and miR-133b) at 30 minutes after coronary intervention and accentuated drop in such levels after 3 hours in a cohort of 8 STEMI patients (D'Alessandra et al., 2010). Accordingly, miR-1 and miR-133b expression were shown to be significantly elevated only in plasma samples collected within 12 hours of symptoms onset but not after 12 hours (even if in the first day of presentation), 2 days, 3 days, or 1 month following STEMI (n = 25) (Gidlof et al., 2011). Furthermore, levels of miR-208a also peaked early after myocardial reperfusion (3h) and decreased at 6 and 12 hours later, reaching control levels at 24 hours in a cohort of 19 STEMI patients (Bialek et al., 2015). These findings suggest that the most pronounced changes in cardiac-enriched miRNA levels in STEMI

patients occur early after myocardial reperfusion, but no study had investigated in detail the expression of these miRNAs during this time frame.

In this study, a meticulous description of miR-1 and miR-133b release kinetics in the initial 3 hours following PPCI in STEMI patients, including 12 measurement time points, is displayed for the first time. In accordance with findings from the literature commented above, miR-1 levels were already elevated in STEMI patients prior to reperfusion. However, miR-133b expression was only significantly increased at 20 min post-PCI. Following reperfusion, they rapidly increased to achieve median levels of approximately 50-fold (miR-1) and 32-fold (miR-133b) those of controls after only 30 minutes following myocardial reperfusion.

5.3.3. Effect of coronary perfusion on cardiac-enriched miRNA release

Although there is evidence linking the release of cardiac-enriched miRNAs to cardiac injury due to MI, the effect of the degree of coronary artery perfusion on miRNA release kinetics in STEMI patients has not been studied. This chapter provided a proof of concept of how miR-1 and miR-133b kinetics might be affected by different coronary artery perfusion statuses.

Liebetrau et al. (Liebetrau et al., 2013) provided the first insight into the exact release kinetics of muscle-enriched miRNAs following cardiac damage. The authors used transcoronary ablation of septal hypertrophy (TASH) in patients with hypertrophic cardiomyopathy as a model to mimic AMI and assess muscle-enriched miRNA release kinetics after cardiomyocyte injury (Liebetrau et al., 2013). In TASH, a catheter is inserted in a branch of a septal artery, and alcohol is injected distal to an occluding balloon to provoke instant cardiomyocyte death. To evaluate biomarker kinetics, TASH is an excellent model as it allows an accurate monitoring of miRNA release since the very onset of cardiac damage. The authors measured miR-1, miR-133a, miR-208 and miR-21 levels in serum from 21 patients undergoing TASH at multiple time points (Liebetrau et al., 2013). They observed about 3-fold increased levels of miR-1 and miR-133a as early as 15 minutes after cardiomyocyte injury and maximum 65-fold increase for miR-1 at 75 minutes, followed by a plateau until 4 hours after TASH (Liebetrau et al., 2013). This suggests that cardiac-enriched miRNAs are released almost immediately after cardiac injury under optimal coronary

perfusion. In this chapter, similar findings were observed for miR-1 and miR-133b, which expression in the TASH patient was above control levels as early as 5 minutes and 10 minutes, respectively. However, TASH does not entirely mimic what happens in STEMI as there is no prolonged coronary occlusion followed by reperfusion and no involvement of the coronary microcirculation.

In animal models of MI, cardiac-enriched miRNA kinetics has been studied after permanent left anterior descending (LAD) artery ligation or after transient coronary occlusion (ischemia-reperfusion model). The kinetics differed significantly according to the model used. In rats submitted to LAD ligation, miR-1 levels started to increase 1 hour after ligation and reached a peak at 6 hours (Cheng et al., 2010, Wang et al., 2010). In mice also submitted to LAD ligation, cardiac-enriched miRNA levels only significantly increased in the circulation 6 hours post-ligation, with peak levels at 6 hours (miR-133b) or 18 hours (miR-1) (D'Alessandra et al., 2010). In both rodent models, sustained elevated miRNA levels were observed until 24 hours post-AMI (Cheng et al., 2010, D'Alessandra et al., 2010, Wang et al., 2010). In contrast, in a porcine model submitted to closed chest, transient coronary occlusion by balloon inflation for 40 minutes followed by myocardial reperfusion, miR-1 and miR-133b kinetics demonstrated much quicker dynamics. None of the miRNAs were detected during the occlusion period but started to increase in the circulation in only 20 minutes post myocardial reperfusion, peaking after 2 hours of ischaemia induction (or 80 minutes post-reperfusion) (Gidlof et al., 2011). This suggests that coronary reperfusion accelerates cardiac-enriched miRNA release kinetics.

Likewise, in this chapter, one STEMI patient with spontaneous coronary artery recanalization (TIMI flow 3) prior to PCI had slightly elevated miR-1 and miR-133b levels only until 90 min post-PCI followed by a drop below control levels afterwards. In contrast, in a STEMI patient with obstructed coronary artery post-PCI (TIMI flow 0) miRNA levels increased steadily until 120 min to achieve a late peak at 180 min (miR-1) or 24h (miR-133b). This suggests that the degree of coronary artery perfusion might influence miRNA kinetics and therefore future studies should take this into consideration.

5.3.4. miRNA release kinetics and failed reperfusion-associated injury

Finally, this study demonstrated for the first time that STEMI patients seem to have distinct miR-1 and miR-133b release kinetics patterns, i.e. monophasic (single peak at 30 min post-PCI) and biphasic ('early' peak at 30 min and 'late' peak at 90 min). In addition, miR-1 release kinetics seemed to be affected by coronary microvascular function, as the 'early' miR-1 peak magnitude as well as the occurrence and amplitude of the 'late' peak seemed to be dependent on IMR values. In a cohort of 281 STEMI patients, high IMR values (IMR > 34.9) were associated with increased MVO incidence and larger infarct size (Carrick et al., 2016a). Considering that (i) cardiac-enriched miRNAs are released almost immediately after cardiomyocyte injury under optimal coronary perfusion; (ii) all STEMI patients presented an 'early' peak; and (iii) the occurrence of the 'late' peak was associated with a surrogate marker of failed myocardial reperfusion, this study provides a hypothesis-generating concept that the 'early' miR-1 peak might reflect ischaemia-related myocardial injury whereas the 'late' miR-1 peak might be associated with cardiac injury due to failed myocardial reperfusion in STEMI patients who achieved TIMI 3 flow after PCI.

5.3.5. Microparticles as plasmatic carriers of cardiac-enriched miRNAs in STEMI patients

Corroborating data from previous studies, this work also observed increased levels of circulating microparticles prior to myocardial reperfusion followed by a rapid drop in MP levels immediately after PPCI (Morel et al., 2009, Min et al., 2013). In addition, circulating microparticles were found to express miR-1 and miR-133b, which levels were higher than controls prior to and at 30 min and 90 min after PCI. Prior to myocardial reperfusion, microparticle-associated miR-1 and miR-133b levels were similar to these miRNAs plasmatic expression. After reperfusion, miR-1 expression in MP was significantly lower than in plasma. In contrast, miR-133b expression in MP remained similar to plasma expression after reperfusion, despite a reduction in the concentration of circulating MP. This suggests a miR-133b enrichment in MP after reperfusion. Interestingly, very similar results were described by Deddens et al. (Deddens et al., 2016) in a porcine model of myocardial ischaemia and reperfusion, in which miR-1 and miR-133b were raised in plasma and circulating MP at 60 min post-reperfusion but only miR-133b expression was enriched in MP in relation to plasma. Combined, these results suggest that miR-133b might be mainly released and carried within MP prior to and after myocardial reperfusion. Differently, miR-1

might be mainly released within MP during the ischaemic period but other carriers (e.g. argonaute proteins) might play a more important role in the release and transport of this miRNA after reperfusion. Understanding in detail how these miRNAs are released might provide an important insight about the mechanism of cardiac injury that their circulating levels reflect. In this study, it was not possible to perform characterisation and isolation of cardiomyocyte-derived MPs due to the lack of reliable, specific surface markers. Future studies should investigate the contribution of other known miRNA carriers, such as argonaute proteins or lipoprotein particles, to the cardiac-enriched miRNA expression following myocardial reperfusion in STEMI patients.

5.4. Conclusion

This chapter provides several important new insights about cardiac-enriched miRNA kinetics and mechanisms of release from the myocardium. First, miR-1 and miR-133b were identified as the most highly expressed miRNAs in STEMI patients with failed myocardial reperfusion. In addition, a detailed miR-1 and miR-133b release kinetics analysis in the initial 3 hours post-PPCI revealed that levels of these miRNAs increased rapidly after myocardial reperfusion, following 2 different patters – monophasic and biphasic. Furthermore, cardiac-enriched miRNA kinetics seemed to be affected both by the status of epicardial coronary artery perfusion as well as by coronary microcirculatory function. Because of the association between high miR-1 levels at ‘late’ post-reperfusion time points (90 – 180 min) and high IMR, this study generates the hypothesis that miR-1 levels at these time points might reflect failed myocardial reperfusion-associated damage. Finally, quantification of miR-1 and miR-133b from circulating microparticles unveiled that these miRNAs are released in MP following STEMI. However, after reperfusion, whilst MP-related release seems to still be the predominant mechanism for miR-133b, other mechanisms seem to play a more important role for miR-1 release.

Chapter 6. Cardiac-enriched miRNAs and failed myocardial reperfusion

6.1. Introduction

The establishment of primary percutaneous coronary intervention (PPCI) as the first-line therapy for the management of ST-elevation myocardial infarction has significantly improved outcomes, with in-hospital mortality rates of under 7% in high-volume tertiary centres (Menees et al., 2013, Pedersen et al., 2014). However, while intra-hospital mortality post-PPCI has declined, 20% of patients who survive an anterior STEMI need to be readmitted due to heart failure in the first year, and 40% show adverse left ventricular (LV) remodelling (Cung et al., 2015). This may in part be a consequence of failed myocardial reperfusion, which manifests initially as microvascular obstruction (MVO) in cardiac MRI (Mangion et al., 2016). Microvascular obstruction is strongly associated with larger infarct size, LV remodelling, and worse clinical outcomes in STEMI patients (Hamirani et al., 2014). Although failed myocardial reperfusion occurs in up to 50% of PPCI patients (Wu, 2012), it usually passes undetected as it is not routinely screened for due to limitations in or lack of access to current diagnostic methods.

In **chapter 5**, miRNA screening, kinetics, and validation experiments revealed that the cardiac-enriched miRNAs miR-1 and miR-133b were consistently elevated early after myocardial reperfusion, with peak levels at 30 min and 90 min post-PCI. Although it is intuitive to think that circulating levels of these miRNAs could inform about the extent of myocardial damage and failed myocardial reperfusion, there is only scarce data to support this notion thus far. The previous chapter also demonstrated that the presence and amplitude of miR-1 peak between 90 min and 180 min post-PCI seemed to be related to a higher index of microvascular resistance, which has been shown to be associated with MVO (Carrick et al., 2016a). This lead to the hypothesis that miR-1 and miR-133b levels at 30min and 90min post-PCI could be associated with failed myocardial reperfusion.

This chapter aims to (i) investigate whether miR-1 and miR-133b are differentially expressed in patients with MVO; and (ii) assess whether miR-1 and miR-133b levels correlate with the extent of myocardial damage and are associated with LV remodelling, assessed by cardiac MRI.

6.2. Results

6.2.1. STEMI cohort 3 baseline characteristics

Cardiac MRI was performed in a total of 50 STEMI patients after PPCI to assess the presence of late MVO. Late MVO was detected in 21 patients (42%) (**Table 6.1**). Patients were divided into 2 groups according to the occurrence of MVO. Baseline characteristics for this cohort are displayed on **Table 6.1**. In summary, patients with MVO had a higher incidence of anterior myocardial infarction (52.4 vs. 17.2%, $p = 0.009$) and approximately 2.5-fold higher levels of peak cardiac troponin T levels ($p < 0.001$) when compared to patients without MVO. No statistically significant differences between the groups were observed for the other variables analysed, including age, gender, cardiovascular risk factors, co-morbidities, medical history, medications, laboratory tests, and procedural parameters (**Table 6.1**).

6.2.2. Association between MVO and other cardiac MRI parameters

A 'baseline' MRI was performed at an average of 3.1 (±1.72) days post-PCI in all patients, with no difference in time of MRI acquisition between MVO groups ($p = 0.603$) (**Table 6.2**). Out of 50 patients, 47 also had a 'follow-up' MRI performed at 3 months post-PPCI. Patients with MVO had twice as large acute infarct size ($p < 0.001$), a 11.9% reduced left ventricular ejection fraction (LVEF, $p < 0.001$), and higher end systolic volume (97mL vs 69.3mL, $p < 0.001$) in the baseline cardiac MRI compared to patients without MVO (**Table 6.2**). Similarly, occurrence of MVO in the baseline MRI remained associated with larger infarct size (10.6% vs 7.2%, $p = 0.005$), reduced LVEF (48.7% vs 58.6%, $p < 0.001$), and increased ESV (92.5mL vs 62.3mL, $p < 0.001$) at 3 months post-PPCI (**Table 6.2**). No differences in end diastolic volume (EDV) were observed between the groups on the baseline or 'follow-up' MRI (**Table 6.2**).

Variable	Cohort (n = 50)	MVO – (n = 29)	MVO + (n = 21)	p value
Gender, male [n (%)]	41 (82)	22 (75.8)	19 (90.4)	0.184
Age, years [mean, (SD)]	65.2 (10.4)	63.4 (10.2)	67.7 (10.3)	0.125
Risk factors, n (%)				
Smoking status				
Never smoked	18 (36)	9 (31)	9 (42.9)	0.390
Ex-smoker	20 (40)	7 (33.3)	13 (44.8)	0.413
Current smoker	12 (24)	7 (24.1)	5 (23.8)	0.979
Family history of IHD	17 (34)	11 (37.9)	6 (28.6)	0.490
Obesity	19 (38.8)	14 (48.3)	5 (25)	0.100
Co-morbidities, n (%)				
Diabetes Mellitus	4 (8)	4 (13.8)	0 (0)	0.076
COPD	2 (4)	1 (3.4)	1 (4.8)	0.815
Medical history, n (%)				
IHD	3 (6)	2 (6.9)	1 (4.8)	0.754
Past MI	0 (0)	0 (0)	0 (0)	-
Past Angiogram	1 (2)	0 (0)	1 (4.8)	0.235
CVA / TIA	0 (0)	0 (0)	0 (0)	-
Regular medication, n (%)				
Aspirin	3 (6)	2 (6.9)	1 (4.8)	0.754
ACE inhibitor / ARB	5 (10)	3 (10.3)	2 (9.5)	0.924
Beta-blocker	2 (4)	0 (0)	2 (9.5)	0.090
Calcium channel blocker	4 (8)	2 (6.9)	2 (9.5)	0.735
Diuretic	4 (8)	3 (10.3)	1 (4.8)	0.473
Statins	10 (20)	5 (17.2)	5 (23.8)	0.567
Laboratory tests [median (IQR)]				
eGFR	83	85	82	0.409
(mL/min)	(74 – 93.7)	(74.5 – 101.5)	(72 – 90)	
Pre-PPCI hs-cTnT	43	43	44	0.595
(ng/L)	(27 – 80.7)	(26.5 – 80)	(27.5 – 96.5)	
12h hs-cTnT	3447	2108	5765	**<0.001**
(ng/L)	(1184 – 6619)	(844 – 3826)	(3621 – 9946)	
STEMI and PCI parameters				
Onset to reperfusion, min	173	195	146	0.340
[median (IQR)]	(112 – 259)	(126 – 273)	(102 – 237)	
Door to balloon, min [median (IQR)]				
Infarct location, n (%)				
Anterior	16 (32)	5 (17.2)	11 (52.4)	**0.009**
Non-anterior	34 (68)	24 (82.8)	10 (47.6)	**0.009**
TIMI flow pre PPCI, n (%)				
0	42 (84)	23 (79.3)	19 (90.5)	0.288
1	8 (16)	6 (20.7)	2 (9.5)	0.288
Thrombus aspiration, n (%)	10 (20)	5 (17.2)	5 (23.8)	0.567
TIMI flow post PPCI, n (%)				
1	2 (4)	0 (0)	2 (9.5)	0.090
3	48 (96)	29 (100)	19 (90.5)	0.090
GPIIa/IIIb inhibitors, n (%)	33 (66)	21 (72.4)	12 (57.1)	0.261

Table 6.1. STEMI cohort 3 clinical characteristics. ACE, angiotensin-converting enzyme; MI, myocardial infarction; ARB, angiotensin receptor blocker; COPD, chronic obstructive pulmonary disease; CVA, cerebrovascular accident; eGFR, estimated glomerular filtration rate; hs-cTnT, high-

sensitivity cardiac troponin T; IHD, ischemic heart disease; IQR, interquartile range; MI, myocardial infarction; LVEF, left ventricular ejection fraction; MRI, magnetic resonance imaging; MVO, microvascular obstruction; PPCI, primary percutaneous coronary intervention; PVD, peripheral vein disease; RCA, right coronary artery; STEMI, ST-elevation myocardial infarction; TIA, transient ischaemic attack; TIMI, thrombolysis in myocardial infarction angiographic score

MRI parameters	Entire cohort	MVO – (n = 29)	MVO + (n = 21)	p value
Baseline MRI (n = 50)				
Time to MRI, days [mean(±SD)]	3.1 (±1.72)	3.2 (±1.85)	2.9 (±1.56)	0.603
Infarct size, % of LV	10.1 (4.1 – 15.3)	6.4 (2.3 – 10.7)	14.5 (11.9 – 22.1)	**<0.001**
LV ejection fraction, %	51.5 (40.5 – 56.9)	55.9 (51.3 – 58.1)	44 (42.4 – 35)	**<0.001**
End systolic volume, mL	76. 9 (66.4 – 97.1)	69.3 (59.3 – 73)	97 (80.5 – 113.6)	**<0.001**
End diastolic volume, mL	157 (138 – 173)	151 (137.9 – 169.8)	166 (147.9 – 182.5)	0.058
3-month MRI (n = 47)				
Infarct size, % of LV	9.3 (4.5 – 12.1)	7.2 (1.9 – 9.8)	10.6 (6.8 – 19.2)	**0.005**
LV ejection fraction, %	54.9 (49 – 61.4)	58.6 (52.8 – 64.1)	48.7 (38.5 – 52.7)	**<0.001**
End systolic volume, mL	73.4 (56.2 – 94.4)	63.2 (52.4 – 73.5)	92.5 (80.9 – 109.3)	**<0.001**
End diastolic volume, mL	168 (141 – 188)	150.9 (135.2 – 185.9)	174.3 (151.1 – 188.3)	0.132

Table 6.2. Microvascular obstruction association with other cardiac MRI parameters. EDV, end-diastolic volume; ESV, end-systolic volume; IS, infarct size; LV, left ventricle; LVEF, left ventricular ejection fraction; MRI, magnetic resonance imaging; MVO, microvascular obstruction. Data presented as median and interquartile range (IQR).

6.2.3. Circulating miR-1 and miR-133b levels are higher in patients with MVO

Considering the effect of reperfusion on miRNA kinetics shown in **chapter 5**, miR-1 and miR-133b measurements at 30min and 90min post-PPCI were compared between MVO groups including only patients who achieved TIMI flow 3 post-PCI (n = 48; n *MVO+/ve* = 19; n *MVO-/ve* = 29). At 30min post-PPCI, miR-1 and miR-133b levels were approximately 4.3-fold (p = 0.006) and 2.3-fold (p = 0.048) higher in patients with MVO, respectively (**Figure 6.1A**). Likewise, these miRNAs were also elevated in patients with MVO at 90min post-reperfusion [miR-1: 3-fold higher in MVO +/ve vs. MVO -/ve, p = 0.001; miR-133b: 4.4 fold-higher in MVO +/ve vs. MVO -/ve, p = 0.008).

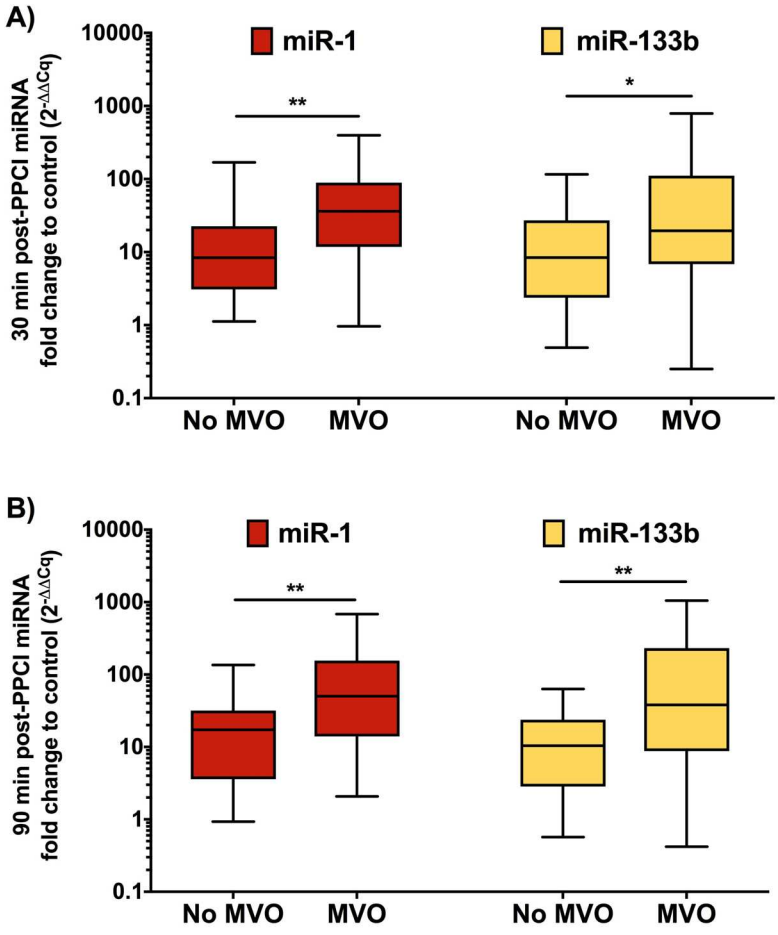

Figure 6.1. Post-reperfusion miR-1 and miR-133b levels are elevated in patients with MVO. A) 30min post-reperfusion miR-1 and miR-133b levels in patients with and without MVO determined by the baseline MRI; **B)** 90min post-reperfusion miR-1 and miR-133b levels in patients with and without MVO. Box plots depict median (central line), 25th and 75th percentiles (limits of the box), and range (error bars) fold change to healthy controls. Differences between MVO (n = 19) and no MVO (n = 29) patients were determined by Mann-Whitney U test. * $p < 0.05$; ** $p < 0.01$. MVO, microvascular obstruction.

6.2.4. miR-1 and miR-133b correlate with cardiac damage and function parameters

Given miR-1 and miR-133b association with MVO and their high expression in the myocardium, possible correlations between post-reperfusion miR-1 and miR-133b levels and markers of cardiac damage and function were evaluated. Firstly, miR-1 measurements at 30min and 90min post-reperfusion were found to be strongly correlated with 12h post-PPCI hs-cTnT levels (30min: $r = 0.676$, $p < 0.001$; 90min: $r = 0.727$, $p < 0.001$) (**Figures 6.2A and 6.2B**). Similarly, strong correlations between miR-133b and 12h post-PPCI hs-cTnT were observed (30min: $r = 0.541$, $p < 0.001$; 90min: $r = 0.672$, $p < 0.001$) (**Figures 6.2C and 6.2D**).

In addition, miR-1 at 90min post-PPCI positively correlated with acute infarct size ($r = 0.497$, $p < 0.001$) and ESV ($r = 0.293$, $p = 0.043$) as well as negatively correlated with LVEF ($r = - 0.343$, $p = 0.017$), as determined by the baseline MRI. Furthermore, 30min post-PPCI miR-1 only correlated with baseline MRI infarct size ($r = 0.420$, $p = 0.003$; $n = 48$) (**Table 6.3**). Such correlations remained significant at 3 months post-PCI, with 30min miR-1 levels additionally correlating with ESV ($r = 0.298$, $p = 0.046$; $n = 45$) (**Table 6.3**). A very similar pattern was observed for miR-133b. Positive correlations between 90min post-PCI levels, infarct size ($r = 0.445$, $p = 0.002$) and ESV (30min: $r = 0.304$, $p = 0.036$) whilst negative correlation with LVEF ($r = - 0.342$, $p = 0.018$) were observed at baseline (**Table 6.4**). Again, 30min miR-133b only correlated with infarct size ($r = 0.304$, $p = 0.036$) amongst baseline MRI parameters (**Table 6.4**). In addition, the same correlations persisted at 3-months post-PCI (**Table 6.4**). There were no significant correlations between miR-1 or miR-133b levels and EDV either at baseline or 3 months post-PCI (**Tables 6.3 and 6.4**).

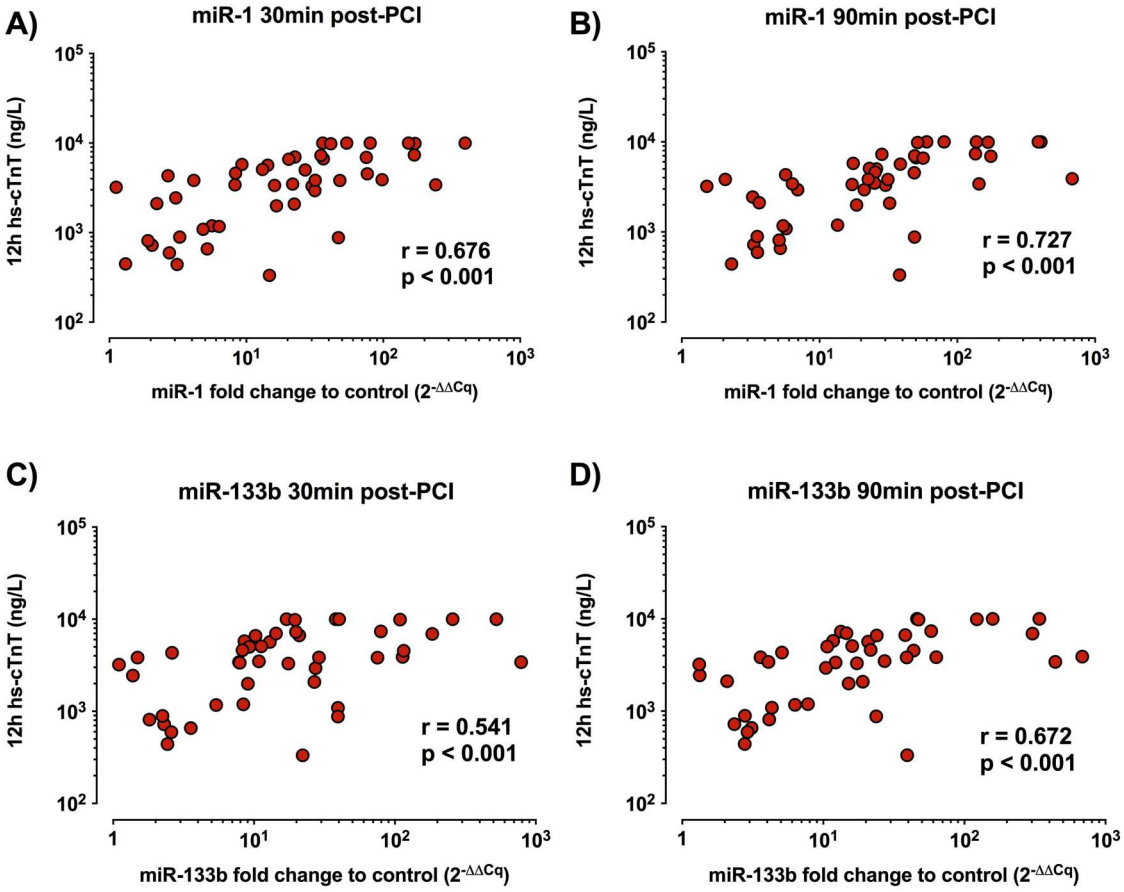

Figure 6.2. Post-reperfusion miR-1 and miR-133b levels strongly correlate with 12h post-PPCI hs-cTnT. A) Correlation between 30min post-PCI miR-1 and 12h hs-cTnT; **B)** Correlation between 90min post-PCI miR-1 and 12h hs-cTnT; **C)** Correlation between 30min post-PCI miR-133b and 12h hs-cTnT; **D)** Correlation between 90min post-PCI miR-133b and 12h hs-cTnT. Correlations calculated by Spearman's coefficient of correlation (r). n = 48. hs-cTnT, high-sensitivity troponin T.

MRI parameters	miR-1 (30min)	p value	miR-1 (90min)	p value
Baseline MRI (n = 48)				
Infarct size, % of LV	**0.420**	**0.003**	**0.497**	**<0.001**
LV ejection fraction, %	- 0.268	0.066	**- 0.343**	**0.017**
End systolic volume, mL	0.278	0.056	**0.293**	**0.043**
End diastolic volume, mL	0.139	0.347	0.091	0.537
3-month MRI (n = 45)				
Infarct size, % of LV	**0.449**	**0.002**	**0.546**	**<0.001**
LV ejection fraction, %	- 0.292	0.051	**- 0.389**	**0.008**
End systolic volume, mL	**0.298**	**0.046**	**0.390**	**0.008**
End diastolic volume, mL	0.147	0.335	0.182	0.232

Table 6.3. Correlation between miR-1 post-PPCI levels and cardiac MRI parameters. EDV, end-diastolic volume; ESV, end-systolic volume; IS, infarct size; LV, left ventricle; LVEF, left ventricular ejection fraction; MRI, magnetic resonance imaging. Spearman coefficient of correlation. n = 48 (baseline MRI); n = 45 (3-month MRI).

MRI parameters	miR-133b (30min)	p value	miR-133b (90min)	p value
Baseline MRI (n = 48)				
Infarct size, % of LV	**0.304**	**0.036**	**0.445**	**0.002**
LV ejection fraction, %	- 0.274	0.060	**- 0.342**	**0.018**
End systolic volume, mL	0.216	0.141	**0.322**	**0.026**
End diastolic volume, mL	0.029	0.847	0.118	0.423
3-month MRI (n = 45)				
Infarct size, % of LV	**0.357**	**0.017**	**0.538**	**<0.001**
LV ejection fraction, %	- 0.259	0.086	**- 0.300**	**0.045**
End systolic volume, mL	0.272	0.071	**0.332**	**0.026**
End diastolic volume, mL	0.132	0.388	0.167	0.273

Table 6.4. Correlation between miR-133b post-PPCI levels and cardiac MRI parameters. EDV, end-diastolic volume; ESV, end-systolic volume; IS, infarct size; LV, left ventricle; LVEF, left ventricular ejection fraction; MRI, magnetic resonance imaging. Spearman coefficient of correlation. n = 48 (baseline MRI); n = 45 (3-month MRI).

6.2.5. Patients in the highest baseline IS tertile have worse left ventricular functional recovery

Considering that the baseline infarct size is one of the most important determinants of cardiac function following myocardial infarction, patients were divided according to baseline IS tertiles (1st tertile: IS < 7%; 2nd tertile: IS 7% – 13.3%; 3rd tertile: IS > 13.3%) to analyse differences in final infarct size and changes in LVEF, ESV, and EDV across the first 3 months post-PPCI (baseline vs. follow-up MRI).

Acute infarct size was significantly different across baseline MRI IS tertiles ($p < 0.001$) (**Figure 6.3A**). At 3 months after of PPCI, the highest baseline IS tertile group still had the largest infarcts in relation to the lowest tertile but not the middle tertile (**Figure 6.3A**). In terms of LVEF, patients in the 2 lower baseline IS tertiles had a significant improvement at 3 months [1st tertile (n=16): 55.7% (baseline) vs. 57.9% (3-month), $p = 0.036$; 2nd tertile (n=16): 52.6% (baseline) vs. 58.4% (3-month), $p = 0.007$] (**Figure 6.3B**). In contrast, no significant difference in terms of LVEF was observed in the highest tertile group [3rd tertile (n=13): 44% (baseline) vs. 45.2% (3-month), $p = 0.249$] (**Figure 6.3B**).

This was accompanied by a trend towards ESV reduction at 3 months in relation to baseline for the first tertile group [68.6mL (baseline) vs. 57.2mL (3-month), $p = 0.056$] and a significant decrease for the middle tertile [78.3mL (baseline) vs. 68.8mL (3-month), $p = 0.020$] (**Figure 6.3C**). No difference in ESV was detected in the highest tertile group between baseline (91.8mL) and 3-month (92.5mL) measurements ($p = 0.600$) (**Figure 6.3C**). Finally, no differences in EDV were observed between the baseline and 3-month MRI for all tertile groups (**Figure 6.3D**). These findings suggest a worse left ventricular functional recovery in the 3 months following PPCI for the subgroup of patients with the largest baseline IS. Unsurprisingly, the incidence of MVO was greater in this patient subgroup [1st tertile: n = 2 (11.8%); 2nd tertile: n = 7 (41.2%); 3rd tertile: n = 12 (75%), $p = 0.001$].

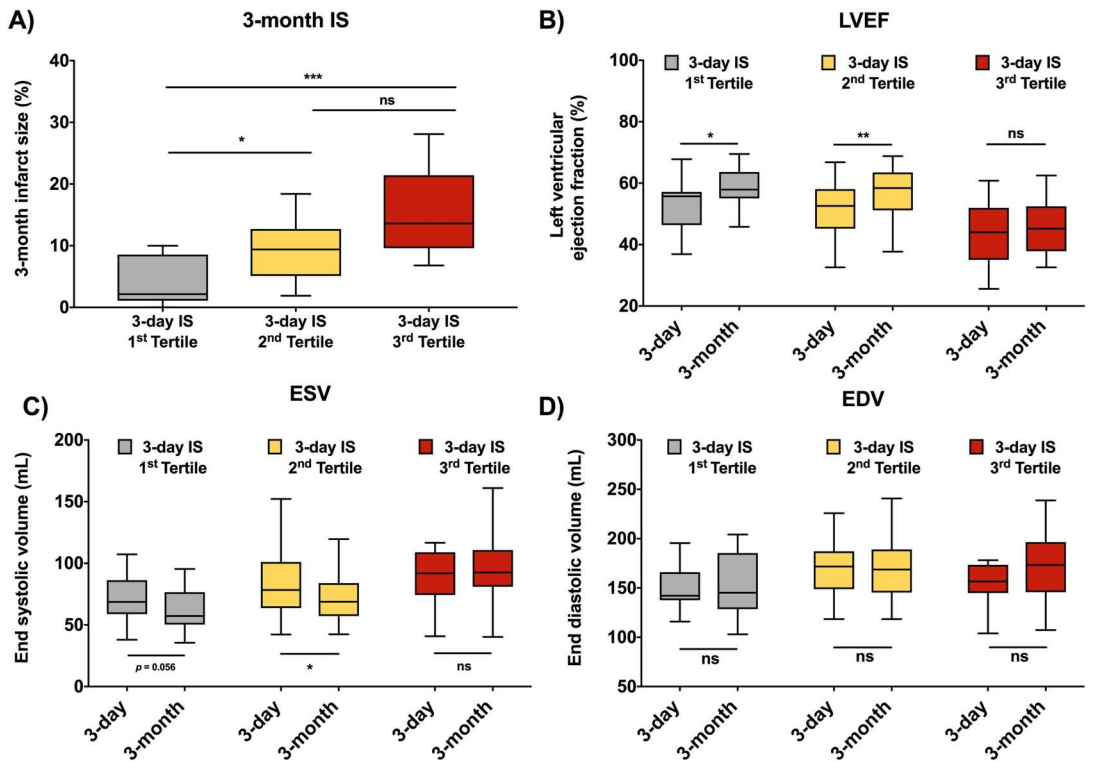

Figure 6.3. Final infarct size and 3-month post-PCI left ventricular functional recovery according to baseline IS tertiles. A) When patients were divided according to baseline IS tertiles, those in the highest tertile remained with the largest IS in relation to the lowest tertile at 3-months posr-PPCI; **B)** Patients in the two lower 3-day IS tertiles had significant improvements in LVEF over the initial 3 months following PCI. No changes in LVEF were observed for the highest tertile group; **C)** Compared to baseline levels, a trend in ESV reduction at 3 months post-PCI was observed for the lowest IS tertile group and a significant decrease for the middle tertile. There was no significant difference in ESV between baseline and 3-month measurements in the highest IS tertile. Box plots display median (central line), 25th and 75th percentiles (limits of the box), and range (error bars). Differences between 3-day and 3-month LVEF and ESV measurements were determined by paired Wilcoxon signed rank test. * $p < 0.05$; ** $p < 0.01$; ns, non-significant. n (1st tertile) = 16; n (2nd tertile) = 16; n (3rd tertile) = 13. IS, infarct size, ESV, end systolic volume; LVEF, left ventricular ejection fraction.

6.2.6. miR-1 is elevated in patients with worse left ventricular functional recovery

Median levels of miR-1 at 90min post-PPCI were significantly elevated in the highest baseline IS tertile compared to the lowest (3.3-fold, p = 0.013) and middle (2.7-fold, p = 0.031) tertile groups (**figure 6.4B**). Although miR-1 levels at 30min and miR-133b at 90min were also significantly elevated in the highest IS tertile group in relation to the lowest tertile (miR-1: 4.5-fold, p = 0.024; miR-133b: 4.4-fold, p = 0.013), they were not significantly raised compared to the middle tertile (miR-1: 2.7-fold, p = 0.103; miR-133b: 3.2-fold, p = 0.061) (**figures 6.4B and D**). In contrast, there was no difference in miR-133b levels at 30min post-PCI across baseline IS tertile groups (p = 0.063) (**figure 6.4C)**.

Interestingly, when the distribution of pre-PPCI hs-cTnT levels was analysed according to baseline IS tertiles, no difference between groups was observed (p = 0.459) (**figure 6.5A**). As for 12h post-PPCI hs-cTnT, levels in the highest IS tertile [4,601 (3,616 – 9,858) ng/L] were significantly increased only in relation to the lowest tertile group vs. [990 (674 – 4,275), p = 0.003] but not to the middle tertile group [3,620 (2,566 – 6,393), p = 0.859].

Taken together, these findings suggest that miR-1 levels at 90min post-reperfusion seem to be specifically elevated in STEMI patients with worse left ventricular functional recovery over the first 3 months following PPCI.

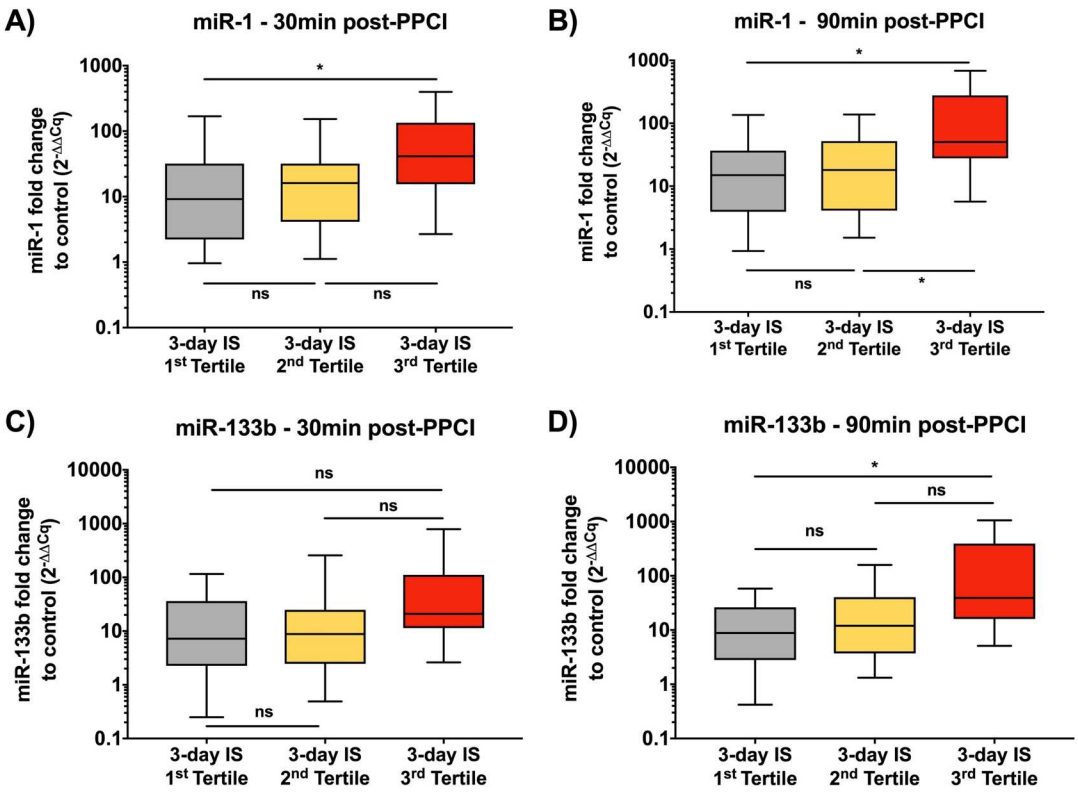

Figure 6.4. Post reperfusion miR-1 and miR-133b levels according to baseline IS tertiles. A) miR-1 levels at 30min post-PCI. Significantly higher miR-1 measurements were observed in the highest IS tertile in comparison to the lowest tertile; **B)** miR-1 levels at 90min post-PCI were significantly elevated in the highest tertile compared to the two lower tertile groups; **C)** No differences in miR-133b levels at 30min post-PCI amongst baseline IS tertile groups were observed. **D)** miR-133b levels at 90min post-PCI were significantly increased in the highest IS tertile in comparison to the lowest tertile. Box plots display median (central line), 25th and 75th percentiles (limits of the box), and range (error bars) fold change to healthy controls. Differences between groups were determined by Kruskall-Wallis test with Dunn's corrections for multiple comparisons. * $p < 0.05$; ns, non-significant. n (1st tertile) = 16; n (2nd tertile) = 16; n (3rd tertile) = 13. IS, infarct size.

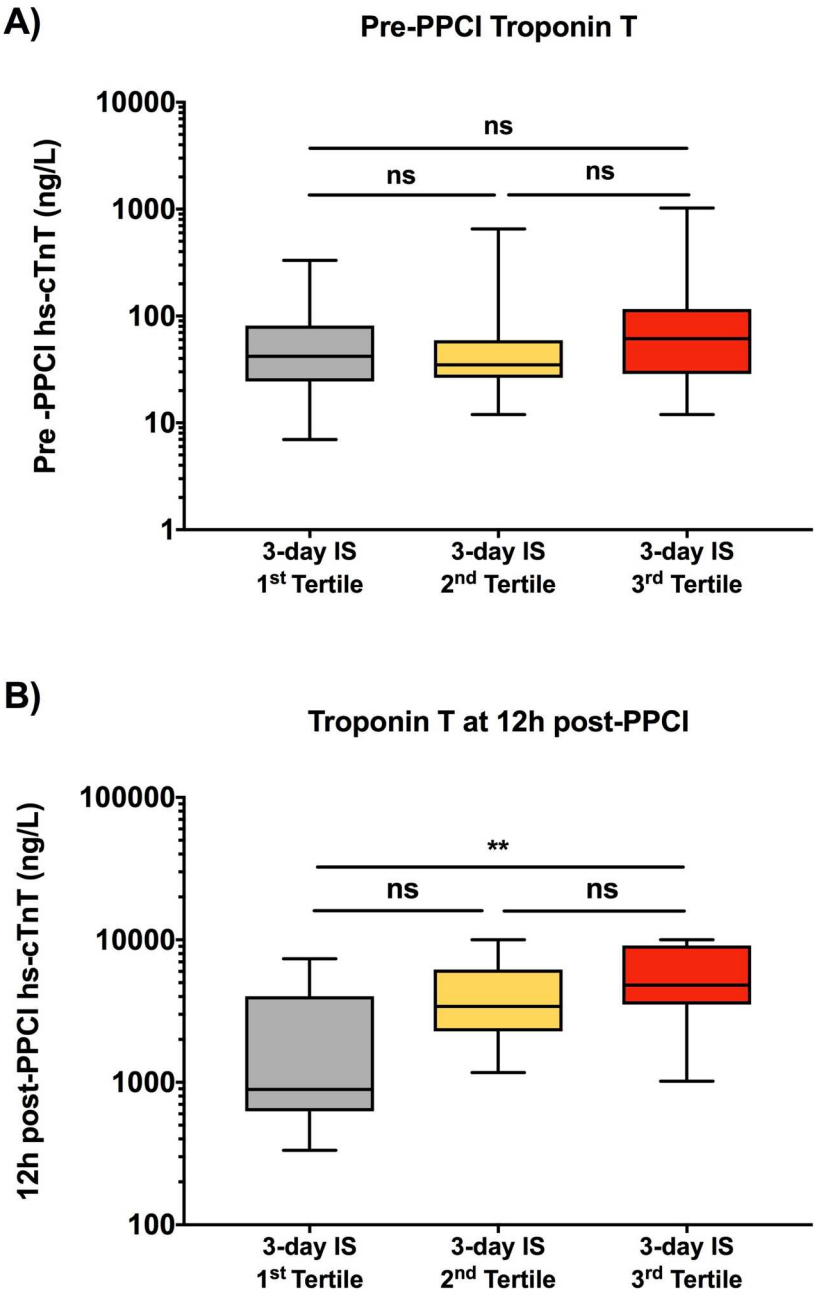

Figure 6.5. Pre-procedural and 12h post-PCI hs-cTnT levels according to baseline IS tertiles. **A)** No differences in pre-procedural hs-cTnT were observed between baseline IS tertile groups; **B)** 12h post-PCI hs-cTnT levels were significantly elevated in the highest IS tertile in relation to the lowest but not to the middle tertile. Box plots display median (central line), 25th and 75th percentiles (limits of the box), and range (error bars). Differences between groups were determined by Kruskall-Wallis test with Dunn's corrections for multiple comparisons. ** $p < 0.01$; ns, non-significant. n (1st tertile) = 16; n (2nd tertile) = 16; n (3rd tertile) = 13. hs-cTnT, high-sensitivity cardiac troponin T; IS, infarct size.

6.3. Discussion

6.3.1. Relationship between MVO, infarct size, and left ventricular function

In the cohort included in this study, the occurrence of late microvascular obstruction was associated with larger infarct size, reduced left ventricular ejection fraction, and increased left ventricular end systolic volume in the baseline (3-day) and follow-up (3-month) cardiac MRI. In addition, the incidence of late MVO was greater in a subgroup of patients with larger infarct size and lack of left ventricular functional improvement after 3 months of PCI. These findings are in accordance with previously published data, as shown by a meta-analysis including 33 studies that investigated the impact of MVO on infarct size and left ventricular remodelling in STEMI patients (Hamirani et al., 2014). These studies employed different cardiac MRI protocols for detection of MVO, especially regarding the timing of image acquisition post-contrast injection, with some identifying early MVO, late MVO, or both (Hamirani et al., 2014).

Early MVO has been shown to be associated with larger infarct size both in baseline (1st week) (de Waha et al., 2010, Klug et al., 2012, Bekkers et al., 2009) as well as follow-up (3 to 4-month) MRI (Bekkers et al., 2009). Although these studies reported a greater reduction in infarct size at follow-up in relation to baseline in patients with early MVO, both infarct extent and transmurality were increased in these patients (Weir et al., 2010). In addition, lower LVEF and increased left ventricular volumes have been reported in patients with early MVO (Orn et al., 2009, Bekkers et al., 2009, de Waha et al., 2010). Similarly, late MVO has been associated with larger infarct size in STEMI patients (Bogaert et al., 2007, de Waha et al., 2010). In fact, the study by Orn et al.(Orn et al., 2009), which performed serial MRIs at 2 days, 1 week, 2 months, and 1 year following PCI, found that 2-day baseline IS and MVO at 1 week were independent predictors of 1-year IS when adjusted for transmurality and infarct-related artery. Presence of late MVO has also been implicated with reduced LVEF, increased ESV (Bekkers et al., 2009, Nijveldt et al., 2009, Larose et al., 2010, Durante et al., 2017), and greater end diastolic volume even when correcting for infarct size (Nijveldt et al., 2008). In the studies that directly compared early and late MVO, late MVO seemed to be more specific to detect microvascular damage and presented a strongest relationship with left ventricular remodelling (Nijveldt et al., 2008, de Waha et al., 2010, Weir et al., 2010). Therefore, the findings described in

this chapter corroborate previous evidence of late MVO association with cardiac damage and function post-PPCI in STEMI patients.

6.3.2. Cardiac-enriched miRNA levels and MVO

This chapter shows for the first time an association between increased post-PCI cardiac-enriched microRNA (miR-1 and miR-133b) levels and the occurrence of MVO in STEMI patients.

To date, only the study by Eitel et al. (Eitel et al., 2012) investigated whether circulating levels of a miRNA (miR-133a) could be associated with MVO in STEMI patients undergoing PPCI. That study included 216 consecutive patients admitted to a single interventional cardiology centre who had a cardiac MRI performed at days 2 to 4 after the event. The authors reported that occurrence of MVO was significantly higher in the group of patients with admission miR-133a concentration $\geq$ median [miR-133a $\geq$ median: n = 72 (76%); miR-133a < median: n = 61 (63%); p = 0.002] (Eitel et al., 2012). This miRNA was the third mostly expressed in the miRNA screening performed in patients with MVO shown in **chapter 5** and is also a cardiac-enriched miRNA, from the same cluster as miR-133b. However, because only the top two candidates were chosen for validation as part of this PhD thesis, miR-133a was not quantified in the entire cohort here described. Given that MVO is a strong determinant of cardiac damage following reperfusion, it is not surprising that cardiac-enriched miRNAs are elevated in the presence of MVO. Nonetheless, considering that several miRNAs regulate mechanisms that have been implicated in the pathogenesis of MVO, such as oxidative stress (Gong et al., 2018), endothelial function (Caporali et al., 2011), leukocyte trafficking (Harris et al., 2008), and platelet reactivity (Sunderland et al., 2017), it is plausible to believe that future studies employing more comprehensive screening techniques might identify candidate circulating markers of MVO that are released from cell types other than cardiomyocytes and that may provide more specific information about pathological process affecting the coronary microcirculation.

6.3.3. Correlation between cardiac-enriched miRNAs and myocardial damage

This chapter also unveiled a previously unknown correlation between miR-1 and miR-133b 30min and 90min post-reperfusion levels and myocardial necrosis, as

assessed by 12h hs-cTnT levels and cardiac MRI. The correlation between circulating cardiac-enriched miRNA levels and cardiac troponins is still controversial in the literature. In the few studies that performed serial miRNA quantification post-PPCI, peak levels early after reperfusion (30 min – 4h) correlated with markers of cardiomyocyte necrosis, such as cardiac troponins or creatine kinase myocardial band (CK-MB) (D'Alessandra et al., 2010, Bialek et al., 2015, Wang et al., 2013). However, such correlations were not observed for miRNA levels prior to or several hours post-PPCI (Ai et al., 2010, Gidlof et al., 2011, Bauters et al., 2013). Collectively, these data suggest that the time window spanning up to a few hours after reperfusion might be particularly relevant to understand miR-1 and miR-133b association with cardiac damage.

Indeed, this study showed that higher miR-1 and miR-133b levels at 30min and 90min post-PCI correlated with larger infarct size at an average of 3 days and 3 months after the index event. Furthermore, in the study by Eitel et al. (Eitel et al., 2012), admission miR-133a concentration ≥ median was associated with larger area at risk and infarct size assessed by cardiac MRI. In that study, however, duration of ischaemia (symptom onset to reperfusion time) was significantly higher in the group of patients with pre-reperfusion miR-133b ≥ median ($p < 0.001$) and an independent predictor of pre-reperfusion miR-133a levels (Eitel et al., 2012), which might explain why infarct size was greater in that group.

Thus, the data here presented support the hypothesis that miR-1 and miR-133b early post-reperfusion levels may inform about the severity of cardiac damage both in the acute (3-day) and the convalescent (3-months) phases of STEMI.

6.3.4. Association of miR-1 and miR-133b with LV function and remodelling post-PCI

In the setting of STEMI, it seems logical that miRNAs that reflect myocardial injury may also serve as indicators of impaired cardiac function. Indeed, in this chapter, miR-1 and miR-133b levels at 90min post-PCI negatively correlated with LVEF as assessed by baseline and 3-month post-PCI cardiac MRI.

These findings are corroborated by previous studies in which cardiac-enriched miRNAs were associated with reduced LVEF in patients with acute myocardial

infarction or were deregulated in patients with advanced heart failure (Gidlof et al., 2013a, Eitel et al., 2012, Akat et al., 2014). In 424 patients with suspected acute coronary syndrome, increased levels of the cardiac-specific miR-208b and miR-499-5p measured between 24h to 72h after admission were associated with reduced LVEF and higher 30-day risk of heart failure or mortality (Gidlof et al., 2013a). In addition, LVEF assessed by cardiac MRI in the first week following STEMI was found to be lower in patients with higher admission miR-133a levels (Eitel et al., 2012). Using RNA sequencing, Akat et al. observed decreased miR-1 expression in myocardial tissue samples obtained from patients with advanced heat failure undergoing left ventricle assist device implantation compared to controls without heart disease (Akat et al., 2014). This was 'mirrored' by increased circulating levels of miR-1 and other cardiac-enriched miRNAs (miR-133b, miR-208a, miR-208b, miR-499) in this patient group (Akat et al., 2014). In contrast, no association between miR-1 and miR-133a and left ventricular function were reported in patients with acute myocardial infarction by other studies (Bauters et al., 2013, Gidlof et al., 2013a). This discrepancy might be explained by substantial differences in the timing of sample collection, as miRNAs were measured at 24 – 72h post-admission (Gidlof et al., 2013a) or at patient discharge (Bauters et al., 2013), which are late time points considering miR-1 and miR-133a kinetics described in this PhD thesis and previous exploratory studies. This highlights the importance of understanding the release kinetics of cardiac-enriched miRNAs following STEMI so that optimal time points for miRNA quantification and their correlation with clinical parameters can be identified.

In response to STEMI, structural changes in the left ventricle architecture aiming to preserve cardiac output despite myocardial tissue loss occur in the first weeks and months following the event (Bogaert et al., 1999, Choi et al., 2001, Hassell et al., 2017). The magnitude of this adaptive process, known as LV remodelling, is determined by infarct size and the presence of microvascular injury (MVO) at baseline (Solomon et al., 2001, Beek et al., 2003, Nijveldt et al., 2008). A recent study on cardiac MRI data from STEMI patients undergoing PCI proposed a classification for LV remodelling based on changes in ESV and EDV over time: (i) adverse remodelling, characterised by increase ≥12% in both ESV and EDV; (ii) no remodelling, defined by no changes in ESV and EDV; and (iii) reverse remodelling, characterised by decrease ≥12% in ESV and EDV or no EDV change (Bulluck et al., 2017). Adverse remodelling has been associated with worse clinical outcome (Cheng

and Vasan, 2011) whereas reverse remodelling been independently associated with decreased risk of long-term heart failure and cardiovascular events (Carrabba et al., 2012, Spinelli et al., 2013).

In this chapter, miR-1 and miR-133b levels at 90min post-PCI positively correlated with baseline and 3-month ESV. In addition, patients in the 2 lowest baseline IS tertile groups presented reverse LV remodelling 3 months after PCI whereas no LV remodelling was observed for the highest tertile, suggesting the latter had a less favourable risk profile. Among miR-1, miR-133b, and 12h hs-cTnT, only miR-1 levels at 90min post-PCI were found to be specifically elevated in the group of patients with worse LV functional recovery compared to patient with reverse remodelling. Previous studies that assessed LV remodelling in STEMI patients using echocardiography identified some other miRNAs (miR-21, miR-34a, miR-208a, miR-208b, and miR-150) associated with LV remodelling in this cohort (Zile et al., 2011, Devaux et al., 2013, Lv et al., 2014). Therefore, this is the first study to indicate that miR-1 levels at 90min post-reperfusion could also inform about LV remodelling assessed by cardiac MRI in STEMI patients. Nonetheless, due to the small sample size, future studies should investigate miR-1 association with LV remodelling and its prognostic relevance in larger STEMI cohorts.

6.4. Conclusion

This chapter provides evidence to support a clinically relevant role for the cardiac-enriched miRNAs miR-1 and miR-133b given their association with an early component of failed myocardial reperfusion (MVO) and the extent of cardiac damage following STEMI. Furthermore, miR-1 levels at 90min post-PPCI seem to be particularly informative regarding left ventricular remodelling and functional recovery in the first 3 months following PCI.

Chapter 7. General Discussion

7.1. Summary of the key findings

7.1.1. Introduction

The findings presented in this thesis significantly advance the current knowledge about the release of muscle-enriched miRNAs (miR-1 and miR-133b) from the myocardium as well as their clinical relevance in STEMI patients treated with PCI. Firstly, the prognostic importance of pre-PCI and peak cardiac troponins was retrospectively assessed in 4,914 consecutive STEMI patients treated with PPCI. Post-reperfusion troponin levels did not independently predict in-hospital or longer-term mortality in this population. These findings prompted the identification of new markers that may better inform about the reperfusion process and prognosis in this population, such as miRNAs. To improve miRNA quantification in plasma samples from STEMI patients, *in vitro* RNA sample treatment with heparinase and an endogenous circulating miRNA (miR-425-5p) were validated as strategies to tackle current issues related to RT-qPCR inhibition and normalization in this cohort, respectively. Subsequent miRNA screening and kinetics analyses revealed that the muscle-enriched miR-1 and miR-133b are rapidly released into the circulation following PCI, reaching an initial peak at 30min and a second peak at 90min post-PCI. The presence and amplitude of a second miRNA peak seemed to be associated with a higher index of microvascular resistance, a surrogate marker of coronary microcirculatory function. In addition, miR-1 and miR-133b levels at 30min and 90min post-PPCI were associated with microvascular obstruction measured by cardiac MRI. Finally, miR-1 and miR-133b levels were significantly elevated in a subgroup of STEMI patients with larger infarcts and worse left ventricular function and remodelling 3 months after PPCI.

7.1.2. Pre-PCI cTn, but not peak cTn, is an independent predictor of mortality in STEMI

In chapter 3, a retrospective analysis to determine the power of pre-PCI and 12h post-PCI cTn for mortality prediction in STEMI patients (n = 4,914) was displayed. This is the largest analysis of its kind reported to date. Univariate Kaplan-Meier survival analysis showed that both pre-cTn (log rank $p < 0.001$) and 12h cTn (log rank $p = 0.003$) were associated with mortality over a median follow-up period of 5

years. Multivariate Cox-regression analysis demonstrated that the highest pre-cTn quartile levels were independently associated with increased risk of both in-hospital (HR: 3.64; 95% CI: 1.86 – 7.10; p < 0.001) and longer-term (HR: 1.26; 95% CI: 1.01 – 1.57; p = 0.035) mortality when adjusted for core clinical models of mortality prediction. In contrast, 12h cTn was not independently associated with either in-hospital (HR: 0.61; 95% CI: 0.37 – 1.02; p < 0.001) or longer-term (HR: 1.11; 95% CI: 0.89 – 1.38; p = 0.333) mortality. In addition, ROC curve analysis revealed that the highest pre-cTn quartile levels improved the ability of core clinical models to discriminate patients who died in-hospital (AUC *model only*: 0.891 vs. AUC *model* + *pre-cTn*: 0.904, p = 0.022) or during follow-up (AUC *model only*: 0.829 vs. AUC *model* + *pre-cTn*: 0.833, p = 0.008). Interestingly, pre-cTn quartile levels reclassified 65% and 50% of the patients into correct risk categories for in-hospital and longer-term mortality risk, respectively, over core prediction models by net reclassification index analysis (p < 0.001). These findings are in accordance with previous, small studies that showed that admission cTn was associated with outcome in STEMI patients (Giannitsis et al., 2001, Wang et al., 2014a) and a recent large study including unselected STEMI patients which demonstrated that routine post-PCI cTn measurements were not predictive of outcome (Cediel et al., 2017). The prognostic relevance of pre-cTn levels seems to derive, however, from their ability to reflect the area at risk (p < 0.001) and ischaemic time (p = 0.001) prior to PCI rather than their ability to inform about the reperfusion process. Therefore, these results reinforced the need for identification of post-reperfusion biomarkers that could inform about the success of myocardial reperfusion and prognosis in STEMI patients.

7.1.3. In vitro heparin inhibition and RT-qPCR normalisation to miR-425-5p are suitable strategies to improve miRNA quantification in STEMI patients

Chapter 4 sought to identify and validate methodological strategies to overcome current limitation to accurate miRNA quantification by RT-qPCR in STEMI patient samples, namely (i) the lack of an endogenous circulating miRNA control for RT-qPCR normalization and (ii) heparin-induced RT-qPCR inhibition. Firstly, screening of 179 miRNAs in pre- and post-reperfusion samples followed by miRNA stability assessment identified a group of 4 miRNAs as the most stably expressed in a cohort of 6 STEMI patients (miR-425-5p, miR-877-5p, miR-181-a5p and miR-155-5p). Out of these 4 candidates, miR-425-5p was validated as the most stable miRNA in

samples collected at 24h post-PCI from 34 STEMI patients. In addition, the presence of heparin in RNA samples extracted from STEMI patients' plasma was confirmed by ELISA and *in vitro* treatment with heparinase significantly reduced heparin concentration in RNA samples. Heparin administration *in vitro* and *in vivo* was shown to affect all currently used RT-qPCR normalization strategies (global miRNA mean, cel-miR-39 and the endogenous control miR-425-5p) as well as the detection of muscle-enriched miRNAs (miR-1 and miR-133b). In contrast, heparinase addition to RNA samples restored miRNA detection by RT-qPCR. Finally, administration of bivalirudin instead of heparin as an alternative anticoagulant did not seem to affect miRNA detection. This is the first study to validate an endogenous miRNA control for RT-qPCR normalization in STEMI patients. Also, it provides original evidence that bivalirudin does not seem to interfere with miRNA quantification by RT-qPCR. This chapter corroborates previous literature about the use of heparinase to counteract heparin-induced RT-qPCR inhibition. Thus, this PhD thesis presents new tools to improve circulating miRNA quantification in STEMI patients, which may be helpful to achieve a higher level of standardisation and reproducibility among future studies.

7.1.4. Circulating miR-1 and miR-133b rapidly raise after PCI and their kinetics seem to be influenced by coronary microcirculatory function

In chapter 5, miRNA screening identified miR-1 and miR-133b as the top two candidate miRNAs to be most highly expressed after myocardial reperfusion in STEMI patients (n = 6) with microvascular obstruction. A detailed analysis of the plasmatic kinetics of these miRNAs in 18 STEMI patients prior to and in the initial 3 hours post-PCI showed that miR-1 and miR-133b presented 2 peaks in this time frame, which coincided at 30 min (miR-1: 49-fold vs. controls, $p < 0.001$; miR-133b: 32.6-fold, $p < 0.001$) and 90 min (miR-1: 53.1-fold, $p < 0.001$; miR-133b: 28.8-fold, $p < 0.001$) post-PCI. When miRNA kinetics were assessed separately for each patient, it was possible to group them into 2 kinetics patterns according to the presence of the second peak: (i) monophasic, with the presence of only the first peak at 30 min; and (ii) biphasic, with a first peak at 30 min and a second peak occurring at 75 – 90 min post-PCI. The release kinetics of miR-1 and miR-133b seemed to be influenced by the degree of epicardial coronary artery perfusion prior to and after PCI (TIMI angiographic flow grade), although are results are inconclusive as n = 2 only. In addition, the presence and amplitude of the second miRNA peak, especially for miR-

1, seemed to be associated with higher IMR values, which is associated with microvascular obstruction. Confirming the findings observed in the kinetics study, miR-1 and miR-133b levels were found to be elevated at 30 min (miR-1: 18.5-fold, $p < 0.0001$; miR-133b: 12-fold, $p < 0.0001$) and at 90 min (miR-1: 25.2-fold, $p < 0.0001$; miR-133b: 15-fold, $p < 0.001$) post-PCI in a validation cohort of 48 STEMI patients. Finally, miR-1 and miR-133b expressions were increased in circulating microparticles isolated prior to and at 30 min and 90 min post-PCI ($n = 10$) in relation to controls ($n = 3$). Microparticles seemed to be the main carriers of miR-133b prior to and after reperfusion but only represented the main carriers of miR-1 prior to reperfusion.

This chapter significantly contributed to the understanding of the kinetics and mechanisms of release of muscle-enriched miRNAs (miR-1 and miR-133b) in STEMI patients. In addition, it identified time points (30 min and 90 min) that may be useful for the investigation of the relationship between these miRNAs and clinical parameters. Furthermore, it generated the hypothesis that the presence of a second miRNA peak may reflect failed myocardial reperfusion-associated injury.

7.1.5. Circulating miR-1 and miR-133b are associated with failed myocardial reperfusion, cardiac damage, and LV function in STEMI patients

In chapter 6, the associations of miR-1 and miR-133b levels with microvascular obstruction as well as cardiac morphological and functional parameters assessed by a baseline (3-day post-PCI in average) and a follow-up (3-month post-PCI) cardiac MRI were investigated. Both miR-1 and miR-133b levels were significantly elevated in patients with microvascular obstruction at 30 min and 90 min post-PCI. In addition, miR-1 and miR-133b levels at both time points positively correlated with 12h cardiac troponin levels, acute (3-day) and final (3-month) infarct size, indicating that these miRNAs correlate with the extent of myocardial damage following STEMI. Furthermore, miR-1 and miR-133b at 90 min negatively correlated with baseline and 3-month left ventricular ejection fraction and end systolic volume, which suggests that higher post-PCI miR-1 and miR-133b are associated with impaired left ventricular function. Indeed, miR-1 levels at 90 min post-PCI, but not miR-133b or 12h hs-cTnT, were specifically elevated in a subgroup of STEMI patients who presented worse left ventricular remodelling (no remodelling as opposed to reverse remodelling in the other subgroups) over the initial 3 months following PCI. This is the first study to

demonstrate such correlations between miR-1 and miR-133b and these important prognostic parameters using cardiac MRI in STEMI patients.

7.2. Clinical Relevance

This PhD thesis unveiled the prognostic role of pre-cTn in a large cohort of consecutive STEMI patients. Pre-cTn was an independent predictor of in-hospital and longer-term mortality and prominently reclassified patients into lower mortality risk categories, meaning that it is a particularly valuable marker to identify low-risk patients over core prediction models. This is clinically important given that low-risk patients early (2-day) discharge post-PCI has been shown to be safe and to decrease future complications as well as costs associated with healthcare (Jones et al., 2012, Noman et al., 2013). As for 12h post-PCI cTn, the results from this thesis suggest that its application as a prognostic marker in STEMI patients is not justifiable. Therefore, this work questions the need for routine 12h cTn measurements in current clinical practice, which could save resources for healthcare systems. Although post-reperfusion cTn levels have been shown to be associated with late microvascular obstruction, correlations were stronger at later time points post-PCI, such as 72h (Younger et al., 2007) and 96h (Mayr et al., 2012), which might explain in part why 12h post-cTn lost association with mortality after adjustment to the core clinical models. Future studies could investigate whether post-cTn at those later time points are prognostically relevant. However, even if it is, the clinical feasibility of waiting 72h or 96h after PCI to quantify cTn is questionable given that most patients will have already been discharged at those time points.

Another clinically relevant finding from this thesis is the association between high miR-1 and miR-133b levels and microvascular obstruction, which suggests these miRNAs could potentially be used for the detection of MVO in clinical practice. Established methods to detect failed reperfusion such as electrocardiographic ST segment resolution and angiographic myocardial blush grade score lack sensitivity and reproducibility as routine tests (Nijveldt et al., 2008). Cardiac magnetic resonance imaging (MRI), the gold-standard technique for MVO detection, has prognostic importance (Eitel et al., 2014, Carrick et al., 2016b), however MRI is not feasible as a routine investigation, due to high costs, contraindications (Dill, 2008)

and lack of capacity. More recently, invasive assessment of coronary microcirculatory function with the IMR at the end of PCI has been shown to reliably inform about severe microvascular pathology, left ventricular remodelling (Carrick et al., 2016a), and mortality after STEMI (Fearon et al., 2013). Nevertheless, although in principle safe, IMR is a costly, invasive procedure that adds in the time of exposure to radiation, and is not available in all centres. Therefore, muscle-enriched miRNAs could represent novel non-invasive, affordable biochemical markers to detect MVO.

Although miRNA levels would not be readily available during PCI as there is currently no point-of-care technology for fast miRNA quantification, they could still be useful to guide clinical decisions, as MVO management is not only restricted to the acute setting in the catheterization laboratory. It has been shown that continued infusion of drugs after PPCI in the coronary care unit (CCU), such as glycoprotein IIb/IIIa inhibitors (Petronio et al., 2005), human atrial natriuretic peptide (Kitakaze et al., 2007), and exanatide (Lonborg et al., 2012), was beneficial and improved surrogate markers of reperfusion injury. Moreover, addition of cilostazol to dual antiplatelet therapy for 1 month post-PPCI improved 1-year outcome in patients with MVO (Lee et al., 2013). This suggests that a more aggressive pharmacological treatment following PPCI in patients with MVO, even if MVO is detected a few hours after the procedure, may still be important for the clinical management of the condition. In addition, miRNA smaller size and faster release kinetics following myocardial injury in comparison to other circulating biomarkers that have been associated with MVO, such as cardiac troponins and creatine-kinase muscle/brain (CK-MB), gives miRNAs an advantage in terms of time for detection of MVO.

An additional potential clinical application of muscle-enriched miRNAs could be the monitoring of therapeutic approaches for MVO. Failed myocardial reperfusion is a novel field of research, including pharmacological research. So far, there are no interventions for MVO prevention or treatment that have been validated by large randomized clinical trials with defined clinical end-points (Niccoli et al., 2016). Many of the studies that tested pharmacological interventions for MVO before, during, or after PCI have shown negative results in terms of MVO incidence or improvement in prognostic surrogate markers, such as infarct size and left ventricular remodelling (Niccoli et al., 2016). This highlights the need to better understand MVO pathophysiology so that precise therapeutic targets can be identified. Biomarkers of

failed reperfusion could provide valuable insight about the mechanisms underlying MVO and help monitoring the efficacy of novel therapeutic agents targeting MVO.

Finally, the results described in chapter 6 suggest that miR-1 levels at 90 min post-PCI could potentially be employed as a risk stratification tool in STEMI patients post-PCI. This miRNA was specifically elevated in a subgroup of patients with larger infarcts, higher incidence of MVO, and worse 3-month left ventricular remodelling, thus a higher-risk patient group in terms of prognosis. In this sense, miRNA levels could also guide clinical management post-MI. For example, low-risk patients would not require follow-up by cardiologists, whereas those at high risk could benefit from better follow-up, more aggressive secondary prevention measures, and rehabilitation strategies.

7.3. Study Limitations

This study presents several limitations that should be considered, many of which have been discussed in the respective chapters. First, in the retrospective analysis including 4,914 STEMI patients outlined in chapter 4, the conversion of cTnI values into the cTnT scale using a direct linear transformation might have introduced some degree of inaccuracy in patient assignment into cTn quatiles when cTnI values were close to the cut-off points for each quartile group. In addition, only data regarding all-cause death was available and, therefore, no sub-analysis referring to cardiac death specifically could be performed. Furthermore, due to the retrospective nature of mortality data collection from statistical records, misclassification cannot be entirely excluded.

Other important limitations of this study are the miRNA screening platform used and the small sample size. The RT-qPCR panels only allowed quantification of 179 circulating miRNAs, which represent a small fraction of the total number of known miRNAs to date. In addition, unlike other screening approaches such as RNA sequencing, it does not allow the identification of new miRNA transcripts that could be deregulated in patients with MVO. The small sample size of STEMI cohorts 2 and 3 did not confer this study with enough statistical power to draw more definitive conclusions regarding the association between miRNA kinetics patterns and the IMR

measurements and to test the predictive value of 30 min and 90 min miRNA levels for MVO detection. Also, the cohort 3 might not entirely reflect the demographic characteristics of a general STEMI population given the strict exclusion criteria used in the CAPRI trial. For example, large population trials of patients with acute coronary syndromes showed that the prevalence of diabetes ranged from 15.4% to 20% as opposed to only 8% in this study (Donahoe et al., 2007, Piccolo et al., 2016).

Finally, because of the cardiac MRI equipment available the image acquisition protocol did not include determination of parameters such as intramyocardial haemorrhage, myocardial oedema and myocardial salvage index, which are important for a more comprehensive assessment of failed myocardial reperfusion.

7.4. Future work

Although this PhD thesis proposed tools for the improvement of miRNA quantification in STEMI patients, the translation of these markers to clinical practice requires further technological developments. For example, the use of heparinase here described might introduce substantial variability in miRNA quantification across clinical laboratories. An emerging technology, digital droplet PCR (ddPCR), might be a suitable alternative to circumvent technical issues associated with RT-qPCR. Digital droplet PCR provides absolute quantification of nucleic acids based on the partitioning of individual template molecules into thousands of nanoliter-sized, aqueous-oily droplets, containing zero or one molecule per reaction, followed by PCR and rapid microfluidic analysis of individual droplets. The original nucleic acid copy number in a sample is then determined by Poisson statistical analysis including the number of reactions containing the amplified target (positive reactions) and not containing the amplified target (negative reactions), without the need for normalisation or external references (Vogelstein and Kinzler, 1999, Hindson et al., 2011). Partitioning of samples into droplets by digitization has been suggested to confer ddPCR with a higher tolerance to traditional PCR inhibitors, such as heparin and sodium dodecyl sulphate (SDS), in comparison to RT-qPCR for the detection of synthetic cytomegalovirus assays (Dingle et al., 2013). Digital droplet PCR has been validated for the absolute quantification of circulating miRNAs in cancer patients (Ferracin et al., 2015, Mangolini et al., 2015, Campomenosi et al., 2016, Beheshti et

al., 2017) and presented superior performance in terms of precision and reproducibility to RT-qPCR in this population (Hindson et al., 2013). A recent study that used ddPCR for miRNA (miR-21, miR-208, and miR-499) quantification in a small cohort of STEMI patients (n = 24) at 5h post-PCI reported superior limit of detection and coefficient of variation in relation to RT-qPCR but did not observe any correlation between these miRNAs and myocardial ischaemia and reperfusion injury, as assessed by ST-segment resolution in the ECG (Robinson et al., 2018). In addition, ddPCR tolerance to heparin inhibition for quantification of circulating miRNAs in heparin-contaminated patient samples has not yet been evaluated. To address this, my supervisor and I have been successful in securing a Heart Research UK Novel and Emerging Technologies grant (Grant reference number: RG2669/18/19) to investigate the effects of heparin and bivalirudin on ddPCR and how it compares to RT-qPCR in terms of miRNA kinetics quantification and correlation with MVO in a larger cohort of 75 STEMI patients. If validated, ddPCR could represent the next gold-standard technique for circulating miRNA quantification in this population and facilitate the insertion of miRNAs as markers of failed myocardial reperfusion in routine clinical practice.

Furthermore, future studies using high-throughput miRNA screening approaches, e.g. microarrays or RNA-sequencing, are warranted to unveil potential new candidate markers of failed myocardial reperfusion. It is possible that different miRNAs have distinct concentration and distribution in the heart and are differently expressed amongst patients, which is true for cardiac troponins and myoglobin, for example (Swaanenburg et al., 2001). By using several markers simultaneously, this could potentially provide more accurate information about underlying tissue injury mechanisms, myocardial area at risk and overcome inter-patient variability for single markers. Our group has just been awarded a research grant from the Newcastle upon Tyne hospitals NHS Trust to perform this work.

Also, considering the results from this PhD thesis, future studies employing a multiparametric analysis combining cardiac-enriched miRNA quantification, IMR measurements and a more detailed cardiac MRI protocol (including MVO, intramyocardial haemorrhage, myocardial oedema, and myocardial salvage index) simultaneously in larger STEMI patient populations could provide a more comprehensive picture of circulating miRNA relationship with the pathological

alterations associated with microvascular dysfunction and failed myocardial reperfusion. Finally, the deeper understanding of miR-1 and miR-133b kinetics provided in this PhD thesis might be very useful for future studies in choosing appropriate time points for the assessment of the prognostic role of these miRNAs.

7.5. Conclusions

In conclusion, this PhD thesis established a clinically relevant prognostic role for pre-cTn whilst demonstrating that routinely quantified 12h post-PCI cTn does not provide additional prognostic information over traditional clinical predictors in a large cohort of STEMI patients. Furthermore, it validated two methodological tools for circulating miRNA quantification in STEMI patients that may be useful for future studies: (i) miR-425-5p as a circulating endogenous miRNA control for RT-qPCR normalization and (ii) the use of heparinase or bivalirudin to overcome heparin-induced RT-qPCR inhibition. In addition, this study presented the most detailed description of cardiac-enriched miRNA (miR-1 and miR-133b) release kinetics in the initial 3h following PCI. This analysis revealed that miR-1 and miR-133b rapidly increase in the circulation after reperfusion following a monophasic or biphasic pattern, which seemed to be associated with the degree of coronary microcirculatory function. Finally, this PhD thesis provided evidence for the potential clinical usefulness of circulating miR-1 and miR-133b as early surrogate markers of failed myocardial reperfusion as well as cardiac remodelling and function after PCI in STEMI patients.

REFERENCES

AI, J., ZHANG, R., LI, Y., PU, J., LU, Y., JIAO, J., LI, K., YU, B., LI, Z., WANG, R., WANG, L., LI, Q., WANG, N., SHAN, H., LI, Z. & YANG, B. 2010. Circulating microRNA-1 as a potential novel biomarker for acute myocardial infarction. *Biochem Biophys Res Commun,* 391**,** 73-7.

AKAT, K. M., MOORE-MCGRIFF, D., MOROZOV, P., BROWN, M., GOGAKOS, T., CORREA DA ROSA, J., MIHAILOVIC, A., SAUER, M., JI, R., RAMARATHNAM, A., TOTARY-JAIN, H., WILLIAMS, Z., TUSCHL, T. & SCHULZE, P. C. 2014. Comparative RNA-sequencing analysis of myocardial and circulating small RNAs in human heart failure and their utility as biomarkers. *Proc Natl Acad Sci U S A,* 111**,** 11151-6.

ALPERT, J. S., THYGESEN, K., ANTMAN, E. & BASSAND, J. P. 2000. Myocardial infarction redefined--a consensus document of The Joint European Society of Cardiology/American College of Cardiology Committee for the redefinition of myocardial infarction. *J Am Coll Cardiol,* 36**,** 959-69.

AMABILE, N., JACQUIER, A., SHUHAB, A., GAUDART, J., BARTOLI, J. M., PAGANELLI, F. & MOULIN, G. 2012. Incidence, predictors, and prognostic value of intramyocardial hemorrhage lesions in ST elevation myocardial infarction. *Catheter Cardiovasc Interv,* 79**,** 1101-8.

AMBROSE, J. A. & SINGH, M. 2015. Pathophysiology of coronary artery disease leading to acute coronary syndromes. *F1000Prime Rep,* 7**,** 08.

AMBROSE, J. A., TANNENBAUM, M. A., ALEXOPOULOS, D., HJEMDAHL-MONSEN, C. E., LEAVY, J., WEISS, M., BORRICO, S., GORLIN, R. & FUSTER, V. 1988. Angiographic progression of coronary artery disease and the development of myocardial infarction. *J Am Coll Cardiol,* 12**,** 56-62.

AMBS, S., PRUEITT, R. L., YI, M., HUDSON, R. S., HOWE, T. M., PETROCCA, F., WALLACE, T. A., LIU, C. G., VOLINIA, S., CALIN, G. A., YFANTIS, H. G., STEPHENS, R. M. & CROCE, C. M. 2008. Genomic profiling of microRNA and messenger RNA reveals deregulated microRNA expression in prostate cancer. *Cancer Res,* 68**,** 6162-70.

ANDERSEN, C. L., JENSEN, J. L. & ORNTOFT, T. F. 2004. Normalization of real-time quantitative reverse transcription-PCR data: a model-based variance estimation approach to identify genes suited for normalization, applied to bladder and colon cancer data sets. *Cancer Res,* 64**,** 5245-50.

ANDERSEN, H. R., NIELSEN, T. T., RASMUSSEN, K., THUESEN, L., KELBAEK, H., THAYSSEN, P., ABILDGAARD, U., PEDERSEN, F., MADSEN, J. K., GRANDE, P., VILLADSEN, A. B., KRUSELL, L. R., HAGHFELT, T., LOMHOLT, P., HUSTED, S. E., VIGHOLT, E., KJAERGARD, H. K., MORTENSEN, L. S. & INVESTIGATORS, D.-. 2003. A comparison of coronary angioplasty with fibrinolytic therapy in acute myocardial infarction. *N Engl J Med,* 349**,** 733-42.

ARMSTRONG, P. W., GRANGER, C. B., ADAMS, P. X., HAMM, C., HOLMES, D., JR., O'NEILL, W. W., TODARO, T. G., VAHANIAN, A. & VAN DE WERF, F. 2007. Pexelizumab for acute ST-elevation myocardial infarction in patients undergoing primary percutaneous coronary intervention: a randomized controlled trial. *JAMA,* 297**,** 43-51.

ATKINS, G. B. & JAIN, M. K. 2007. Role of Kruppel-like transcription factors in endothelial biology. *Circ Res,* 100**,** 1686-95.

BANG, C., BATKAI, S., DANGWAL, S., GUPTA, S. K., FOINQUINOS, A., HOLZMANN, A., JUST, A., REMKE, J., ZIMMER, K., ZEUG, A., PONIMASKIN, E., SCHMIEDL, A., YIN, X., MAYR, M., HALDER, R., FISCHER, A., ENGELHARDT, S., WEI, Y., SCHOBER, A., FIEDLER, J. & THUM, T. 2014. Cardiac fibroblast-derived microRNA passenger strand-

enriched exosomes mediate cardiomyocyte hypertrophy. *J Clin Invest,* 124**,** 2136-46.

BAR, F. W., TZIVONI, D., DIRKSEN, M. T., FERNANDEZ-ORTIZ, A., HEYNDRICKX, G. R., BRACHMANN, J., REIBER, J. H., AVASTHY, N., TATSUNO, J., DAVIES, M., HIBBERD, M. G., KRUCOFF, M. W. & GROUP, C. S. 2006. Results of the first clinical study of adjunctive CAldaret (MCC-135) in patients undergoing primary percutaneous coronary intervention for ST-Elevation Myocardial Infarction: the randomized multicentre CASTEMI study. *Eur Heart J,* 27**,** 2516-23.

BARTON, P. J., BHAVSAR, P. K., BRAND, N. J., CHAN-THOMAS, P. S., DABHADE, N., FARZA, H., TOWNSEND, P. J. & YACOUB, M. H. 1992. Gene expression during cardiac development. *Symp Soc Exp Biol,* 46**,** 251-64.

BAUTERS, C., KUMARSWAMY, R., HOLZMANN, A., BRETTHAUER, J., ANKER, S. D., PINET, F. & THUM, T. 2013. Circulating miR-133a and miR-423-5p fail as biomarkers for left ventricular remodeling after myocardial infarction. *Int J Cardiol,* 168**,** 1837-40.

BEEK, A. M., KUHL, H. P., BONDARENKO, O., TWISK, J. W., HOFMAN, M. B., VAN DOCKUM, W. G., VISSER, C. A. & VAN ROSSUM, A. C. 2003. Delayed contrast-enhanced magnetic resonance imaging for the prediction of regional functional improvement after acute myocardial infarction. *J Am Coll Cardiol,* 42**,** 895-901.

BEEK, A. M., NIJVELDT, R. & VAN ROSSUM, A. C. 2010. Intramyocardial hemorrhage and microvascular obstruction after primary percutaneous coronary intervention. *Int J Cardiovasc Imaging,* 26**,** 49-55.

BEHESHTI, A., VANDERBURG, C., MCDONALD, J. T., RAMKUMAR, C., KADUNGURE, T., ZHANG, H., GARTENHAUS, R. B. & EVENS, A. M. 2017. A Circulating microRNA Signature Predicts Age-Based Development of Lymphoma. *PLoS One,* 12**,** e0170521.

BEKKERS, S. C., BACKES, W. H., KIM, R. J., SNOEP, G., GORGELS, A. P., PASSOS, V. L., WALTENBERGER, J., CRIJNS, H. J. & SCHALLA, S. 2009. Detection and characteristics of microvascular obstruction in reperfused acute myocardial infarction using an optimized protocol for contrast-enhanced cardiovascular magnetic resonance imaging. *Eur Radiol,* 19**,** 2904-12.

BEKKERS, S. C., YAZDANI, S. K., VIRMANI, R. & WALTENBERGER, J. 2010. Microvascular obstruction: underlying pathophysiology and clinical diagnosis. *J Am Coll Cardiol,* 55**,** 1649-60.

BENZ, F., RODERBURG, C., VARGAS CARDENAS, D., VUCUR, M., GAUTHERON, J., KOCH, A., ZIMMERMANN, H., JANSSEN, J., NIEUWENHUIJSEN, L., LUEDDE, M., FREY, N., TACKE, F., TRAUTWEIN, C. & LUEDDE, T. 2013. U6 is unsuitable for normalization of serum miRNA levels in patients with sepsis or liver fibrosis. *Exp Mol Med,* 45**,** e42.

BEREZIKOV, E. 2011. Evolution of microRNA diversity and regulation in animals. *Nat Rev Genet,* 12**,** 846-60.

BERTINCHANT, J. P., LARUE, C., PERNEL, I., LEDERMANN, B., FABBRO-PERAY, P., BECK, L., CALZOLARI, C., TRINQUIER, S., NIGOND, J. & PAU, B. 1996. Release kinetics of serum cardiac troponin I in ischemic myocardial injury. *Clin Biochem,* 29**,** 587-94.

BETGEM, R. P., DE WAARD, G. A., NIJVELDT, R., BEEK, A. M., ESCANED, J. & VAN ROYEN, N. 2015. Intramyocardial haemorrhage after acute myocardial infarction. *Nat Rev Cardiol,* 12**,** 156-67.

BIALEK, S., GORKO, D., ZAJKOWSKA, A., KOLTOWSKI, L., GRABOWSKI, M., STACHURSKA, A., KOCHMAN, J., SYGITOWICZ, G., MALECKI, M., OPOLSKI, G. & SITKIEWICZ, D. 2015. Release kinetics of circulating miRNA-208a in the early phase of myocardial infarction. *Kardiol Pol,* 73**,** 613-9.

BIGLANDS, J. D., RADJENOVIC, A. & RIDGWAY, J. P. 2012. Cardiovascular magnetic resonance physics for clinicians: Part II. *J Cardiovasc Magn Reson,* 14**,** 66.

BLEIER, J., VORDERWINKLER, K. P., FALKENSAMMER, J., MAIR, P., DAPUNT, O., PUSCHENDORF, B. & MAIR, J. 1998. Different intracellular compartmentations of cardiac troponins and myosin heavy chains: a causal connection to their different early release after myocardial damage. *Clin Chem,* 44**,** 1912-8.

BOAG, S. E., DAS, R., SHMELEVA, E. V., BAGNALL, A., EGRED, M., HOWARD, N., BENNACEUR, K., ZAMAN, A., KEAVNEY, B. & SPYRIDOPOULOS, I. 2015. T lymphocytes and fractalkine contribute to myocardial ischemia/reperfusion injury in patients. *J Clin Invest,* 125**,** 3063-76.

BODEN, H., AHMED, T. A., VELDERS, M. A., VAN DER HOEVEN, B. L., HOOGSLAG, G. E., BOOTSMA, M., LE CESSIE, S., COBBAERT, C. M., DELGADO, V., VAN DER LAARSE, A. & SCHALIJ, M. J. 2013. Peak and fixed-time high-sensitive troponin for prediction of infarct size, impaired left ventricular function, and adverse outcomes in patients with first ST-segment elevation myocardial infarction receiving percutaneous coronary intervention. *Am J Cardiol,* 111**,** 1387-93.

BOECKEL, J. N., THOME, C. E., LEISTNER, D., ZEIHER, A. M., FICHTLSCHERER, S. & DIMMELER, S. 2013. Heparin selectively affects the quantification of microRNAs in human blood samples. *Clin Chem,* 59**,** 1125-7.

BOERSMA, E., MAAS, A. C., DECKERS, J. W. & SIMOONS, M. L. 1996. Early thrombolytic treatment in acute myocardial infarction: reappraisal of the golden hour. *Lancet,* 348**,** 771-5.

BOGAERT, J., KALANTZI, M., RADEMAKERS, F. E., DYMARKOWSKI, S. & JANSSENS, S. 2007. Determinants and impact of microvascular obstruction in

successfully reperfused ST-segment elevation myocardial infarction. Assessment by magnetic resonance imaging. *Eur Radiol,* 17**,** 2572-80.

BOGAERT, J., MAES, A., VAN DE WERF, F., BOSMANS, H., HERREGODS, M. C., NUYTS, J., DESMET, W., MORTELMANS, L., MARCHAL, G. & RADEMAKERS, F. E. 1999. Functional recovery of subepicardial myocardial tissue in transmural myocardial infarction after successful reperfusion: an important contribution to the improvement of regional and global left ventricular function. *Circulation,* 99**,** 36-43.

BOGDANOV, V. Y., BALASUBRAMANIAN, V., HATHCOCK, J., VELE, O., LIEB, M. & NEMERSON, Y. 2003. Alternatively spliced human tissue factor: a circulating, soluble, thrombogenic protein. *Nat Med,* 9**,** 458-62.

BOHMER, E., HOFFMANN, P., ABDELNOOR, M., SELJEFLOT, I. & HALVORSEN, S. 2009. Troponin T concentration 3 days after acute ST-elevation myocardial infarction predicts infarct size and cardiac function at 3 months. *Cardiology,* 113**,** 207-12.

BOON, R. A., SEEGER, T., HEYDT, S., FISCHER, A., HERGENREIDER, E., HORREVOETS, A. J., VINCIGUERRA, M., ROSENTHAL, N., SCIACCA, S., PILATO, M., VAN HEIJNINGEN, P., ESSERS, J., BRANDES, R. P., ZEIHER, A. M. & DIMMELER, S. 2011. MicroRNA-29 in aortic dilation: implications for aneurysm formation. *Circ Res,* 109**,** 1115-9.

BUBER, J., LAISH-FARKASH, A., KOREN-MORAG, N., FEFER, P., SEGEV, A., HOD, H. & MATETZKY, S. 2015. Cardiac troponin elevation pattern in patients undergoing a primary percutaneous coronary intervention for ST-segment elevation myocardial infarction: characterization and relationship with cardiovascular events during hospitalization. *Coron Artery Dis,* 26**,** 503-9.

BULLUCK, H., GO, Y. Y., CRIMI, G., LUDMAN, A. J., ROSMINI, S., ABDEL-GADIR, A., BHUVA, A. N., TREIBEL, T. A., FONTANA, M., PICA, S., RAINERI, C., SIRKER, A., HERREY, A. S., MANISTY, C., GROVES, A., MOON, J. C. &

HAUSENLOY, D. J. 2017. Defining left ventricular remodeling following acute ST-segment elevation myocardial infarction using cardiovascular magnetic resonance. *J Cardiovasc Magn Reson,* 19**,** 26.

CAHILL, T. J. & KHARBANDA, R. K. 2017. Heart failure after myocardial infarction in the era of primary percutaneous coronary intervention: Mechanisms, incidence and identification of patients at risk. *World J Cardiol,* 9**,** 407-415.

CAMPOMENOSI, P., GINI, E., NOONAN, D. M., POLI, A., D'ANTONA, P., ROTOLO, N., DOMINIONI, L. & IMPERATORI, A. 2016. A comparison between quantitative PCR and droplet digital PCR technologies for circulating microRNA quantification in human lung cancer. *BMC Biotechnol,* 16**,** 60.

CAPORALI, A., MELONI, M., VOLLENKLE, C., BONCI, D., SALA-NEWBY, G. B., ADDIS, R., SPINETTI, G., LOSA, S., MASSON, R., BAKER, A. H., AGAMI, R., LE SAGE, C., CONDORELLI, G., MADEDDU, P., MARTELLI, F. & EMANUELI, C. 2011. Deregulation of microRNA-503 contributes to diabetes mellitus-induced impairment of endothelial function and reparative angiogenesis after limb ischemia. *Circulation,* 123**,** 282-91.

CAPPATO, R. 2009. Atrial fibrillation complicating acute myocardial infarction: how should it be interpreted and how should it be treated and prevented? *Eur Heart J,* 30**,** 1035-7.

CARO, C. G. 2009. Discovery of the role of wall shear in atherosclerosis. *Arterioscler Thromb Vasc Biol,* 29**,** 158-61.

CARRABBA, N., PARODI, G., VALENTI, R., MIGLIORINI, A., BELLANDI, B. & ANTONIUCCI, D. 2012. Prognostic value of reverse left ventricular remodeling after primary angioplasty for STEMI. *Atherosclerosis,* 222**,** 123-8.

CARRICK, D., HAIG, C., CARBERRY, J., MAY, V. T., MCCARTNEY, P., WELSH, P., AHMED, N., MCENTEGART, M., PETRIE, M. C., ETEIBA, H., LINDSAY, M., HOOD, S., WATKINS, S., MAHROUS, A., RAUHALAMMI, S. M., MORDI, I.,

FORD, I., RADJENOVIC, A., SATTAR, N., OLDROYD, K. G. & BERRY, C. 2016a. Microvascular resistance of the culprit coronary artery in acute ST-elevation myocardial infarction. *JCI Insight,* 1**,** e85768.

CARRICK, D., HAIG, C., RAUHALAMMI, S., AHMED, N., MORDI, I., MCENTEGART, M., PETRIE, M. C., ETEIBA, H., HOOD, S., WATKINS, S., LINDSAY, M., MAHROUS, A., FORD, I., TZEMOS, N., SATTAR, N., WELSH, P., RADJENOVIC, A., OLDROYD, K. G. & BERRY, C. 2016b. Prognostic significance of infarct core pathology revealed by quantitative non-contrast in comparison with contrast cardiac magnetic resonance imaging in reperfused ST-elevation myocardial infarction survivors. *Eur Heart J,* 37**,** 1044-59.

CECH, T. R. & STEITZ, J. A. 2014. The noncoding RNA revolution-trashing old rules to forge new ones. *Cell,* 157**,** 77-94.

CEDIEL, G., RUEDA, F., GARCIA, C., OLIVERAS, T., LABATA, C., SERRA, J., NUNEZ, J., BODI, V., FERRER, M., LUPON, J. & BAYES-GENIS, A. 2017. Prognostic Value of New-Generation Troponins in ST-Segment-Elevation Myocardial Infarction in the Modern Era: The RUTI-STEMI Study. *J Am Heart Assoc,* 6.

CHAN, W., TAYLOR, A. J., ELLIMS, A. H., LEFKOVITS, L., WONG, C., KINGWELL, B. A., NATOLI, A., CROFT, K. D., MORI, T., KAYE, D. M., DART, A. M. & DUFFY, S. J. 2012. Effect of iron chelation on myocardial infarct size and oxidative stress in ST-elevation-myocardial infarction. *Circ Cardiovasc Interv,* 5**,** 270-8.

CHEN, J. F., MANDEL, E. M., THOMSON, J. M., WU, Q., CALLIS, T. E., HAMMOND, S. M., CONLON, F. L. & WANG, D. Z. 2006. The role of microRNA-1 and microRNA-133 in skeletal muscle proliferation and differentiation. *Nat Genet,* 38**,** 228-33.

CHENDRIMADA, T. P., GREGORY, R. I., KUMARASWAMY, E., NORMAN, J., COOCH, N., NISHIKURA, K. & SHIEKHATTAR, R. 2005. TRBP recruits the

Dicer complex to Ago2 for microRNA processing and gene silencing. *Nature,* 436**,** 740-4.

CHENG, H. H., YI, H. S., KIM, Y., KROH, E. M., CHIEN, J. W., EATON, K. D., GOODMAN, M. T., TAIT, J. F., TEWARI, M. & PRITCHARD, C. C. 2013. Plasma processing conditions substantially influence circulating microRNA biomarker levels. *PLoS One,* 8**,** e64795.

CHENG, S. & VASAN, R. S. 2011. Advances in the epidemiology of heart failure and left ventricular remodeling. *Circulation,* 124**,** e516-9.

CHENG, Y., TAN, N., YANG, J., LIU, X., CAO, X., HE, P., DONG, X., QIN, S. & ZHANG, C. 2010. A translational study of circulating cell-free microRNA-1 in acute myocardial infarction. *Clin Sci (Lond),* 119**,** 87-95.

CHIA, S., SENATORE, F., RAFFEL, O. C., LEE, H., WACKERS, F. J. & JANG, I. K. 2008. Utility of cardiac biomarkers in predicting infarct size, left ventricular function, and clinical outcome after primary percutaneous coronary intervention for ST-segment elevation myocardial infarction. *JACC Cardiovasc Interv,* 1**,** 415-23.

CHOI, K. M., KIM, R. J., GUBERNIKOFF, G., VARGAS, J. D., PARKER, M. & JUDD, R. M. 2001. Transmural extent of acute myocardial infarction predicts long-term improvement in contractile function. *Circulation,* 104**,** 1101-7.

CLARKSON, T. B., PRICHARD, R. W., MORGAN, T. M., PETRICK, G. S. & KLEIN, K. P. 1994. Remodeling of coronary arteries in human and nonhuman primates. *JAMA,* 271**,** 289-94.

COBBAERT, C. M., BOOTSMA, M., BODEN, H., AHMED, T. A., HOOGSLAG, G. E., ROMIJN, F. P., BALLIEUX, B. E., WOLTERBEEK, R., HERMENS, W. T., SCHALIJ, M. J. & VAN DER LAARSE, A. 2014. Confounding factors in the relation between high sensitivity cardiac troponin T levels in serum and infarct

size of patients with first ST-elevation myocardial infarction. *Int J Cardiol,* 172**,** e3-5.

COOK, N. R. 2007. Use and misuse of the receiver operating characteristic curve in risk prediction. *Circulation,* 115**,** 928-35.

CRAWFORD, M., BATTE, K., YU, L., WU, X., NUOVO, G. J., MARSH, C. B., OTTERSON, G. A. & NANA-SINKAM, S. P. 2009. MicroRNA 133B targets pro-survival molecules MCL-1 and BCL2L2 in lung cancer. *Biochem Biophys Res Commun,* 388**,** 483-9.

CRENSHAW, B. S., WARD, S. R., GRANGER, C. B., STEBBINS, A. L., TOPOL, E. J. & CALIFF, R. M. 1997. Atrial fibrillation in the setting of acute myocardial infarction: the GUSTO-I experience. Global Utilization of Streptokinase and TPA for Occluded Coronary Arteries. *J Am Coll Cardiol,* 30**,** 406-13.

CUNG, T. T., MOREL, O., CAYLA, G., RIOUFOL, G., GARCIA-DORADO, D., ANGOULVANT, D., BONNEFOY-CUDRAZ, E., GUERIN, P., ELBAZ, M., DELARCHE, N., COSTE, P., VANZETTO, G., METGE, M., AUPETIT, J. F., JOUVE, B., MOTREFF, P., TRON, C., LABEQUE, J. N., STEG, P. G., COTTIN, Y., RANGE, G., CLERC, J., CLAEYS, M. J., COUSSEMENT, P., PRUNIER, F., MOULIN, F., ROTH, O., BELLE, L., DUBOIS, P., BARRAGAN, P., GILARD, M., PIOT, C., COLIN, P., DE POLI, F., MORICE, M. C., IDER, O., DUBOIS-RANDE, J. L., UNTERSEEH, T., LE BRETON, H., BEARD, T., BLANCHARD, D., GROLLIER, G., MALQUARTI, V., STAAT, P., SUDRE, A., ELMER, E., HANSSON, M. J., BERGEROT, C., BOUSSAHA, I., JOSSAN, C., DERUMEAUX, G., MEWTON, N. & OVIZE, M. 2015. Cyclosporine before PCI in Patients with Acute Myocardial Infarction. *N Engl J Med,* 373**,** 1021-31.

D'ALESSANDRA, Y., DEVANNA, P., LIMANA, F., STRAINO, S., DI CARLO, A., BRAMBILLA, P. G., RUBINO, M., CARENA, M. C., SPAZZAFUMO, L., DE SIMONE, M., MICHELI, B., BIGLIOLI, P., ACHILLI, F., MARTELLI, F., MAGGIOLINI, S., MARENZI, G., POMPILIO, G. & CAPOGROSSI, M. C.

2010. Circulating microRNAs are new and sensitive biomarkers of myocardial infarction. *Eur Heart J,* 31**,** 2765-73.

DAS, A., GANESH, K., KHANNA, S., SEN, C. K. & ROY, S. 2014. Engulfment of apoptotic cells by macrophages: a role of microRNA-21 in the resolution of wound inflammation. *J Immunol,* 192**,** 1120-9.

DAVIES, M. J. 1996. Stability and instability: two faces of coronary atherosclerosis. The Paul Dudley White Lecture 1995. *Circulation,* 94**,** 2013-20.

DAVIES, M. J. & THOMAS, A. C. 1985. Plaque fissuring--the cause of acute myocardial infarction, sudden ischaemic death, and crescendo angina. *Br Heart J,* 53**,** 363-73.

DE BOER, H. C., VAN SOLINGEN, C., PRINS, J., DUIJS, J. M., HUISMAN, M. V., RABELINK, T. J. & VAN ZONNEVELD, A. J. 2013. Aspirin treatment hampers the use of plasma microRNA-126 as a biomarker for the progression of vascular disease. *Eur Heart J,* 34**,** 3451-7.

DE ROSA, S., FICHTLSCHERER, S., LEHMANN, R., ASSMUS, B., DIMMELER, S. & ZEIHER, A. M. 2011. Transcoronary concentration gradients of circulating microRNAs. *Circulation,* 124**,** 1936-44.

DE WAHA, S., DESCH, S., EITEL, I., FUERNAU, G., ZACHRAU, J., LEUSCHNER, A., GUTBERLET, M., SCHULER, G. & THIELE, H. 2010. Impact of early vs. late microvascular obstruction assessed by magnetic resonance imaging on long-term outcome after ST-elevation myocardial infarction: a comparison with traditional prognostic markers. *Eur Heart J,* 31**,** 2660-8.

DEDDENS, J. C., VRIJSEN, K. R., COLIJN, J. M., OERLEMANS, M. I., METZ, C. H., VAN DER VLIST, E. J., NOLTE-'T HOEN, E. N., DEN OUDEN, K., JANSEN OF LORKEERS, S. J., VAN DER SPOEL, T. I., KOUDSTAAL, S., ARKESTEIJN, G. J., WAUBEN, M. H., VAN LAAKE, L. W., DOEVENDANS, P. A., CHAMULEAU, S. A. & SLUIJTER, J. P. 2016. Circulating Extracellular

Vesicles Contain miRNAs and are Released as Early Biomarkers for Cardiac Injury. *J Cardiovasc Transl Res,* 9**,** 291-301.

DEMER, L. L. 2002. Vascular calcification and osteoporosis: inflammatory responses to oxidized lipids. *Int J Epidemiol,* 31**,** 737-41.

DESTA, L., JERNBERG, T., LOFMAN, I., HOFMAN-BANG, C., HAGERMAN, I., SPAAK, J. & PERSSON, H. 2015. Incidence, temporal trends, and prognostic impact of heart failure complicating acute myocardial infarction. The SWEDEHEART Registry (Swedish Web-System for Enhancement and Development of Evidence-Based Care in Heart Disease Evaluated According to Recommended Therapies): a study of 199,851 patients admitted with index acute myocardial infarctions, 1996 to 2008. *JACC Heart Fail,* 3**,** 234-42.

DEVAUX, Y., VAUSORT, M., MCCANN, G. P., ZANGRANDO, J., KELLY, D., RAZVI, N., ZHANG, L., NG, L. L., WAGNER, D. R. & SQUIRE, I. B. 2013. MicroRNA-150: a novel marker of left ventricular remodeling after acute myocardial infarction. *Circ Cardiovasc Genet,* 6**,** 290-8.

DEY-HAZRA, E., HERTEL, B., KIRSCH, T., WOYWODT, A., LOVRIC, S., HALLER, H., HAUBITZ, M. & ERDBRUEGGER, U. 2010. Detection of circulating microparticles by flow cytometry: influence of centrifugation, filtration of buffer, and freezing. *Vasc Health Risk Manag,* 6**,** 1125-33.

DI GREGOLI, K., JENKINS, N., SALTER, R., WHITE, S., NEWBY, A. C. & JOHNSON, J. L. 2014. MicroRNA-24 regulates macrophage behavior and retards atherosclerosis. *Arterioscler Thromb Vasc Biol,* 34**,** 1990-2000.

DI PIETRO, V., RAGUSA, M., DAVIES, D., SU, Z., HAZELDINE, J., LAZZARINO, G., HILL, L. J., CROMBIE, N., FOSTER, M., PURRELLO, M., LOGAN, A. & BELLI, A. 2017. MicroRNAs as Novel Biomarkers for the Diagnosis and Prognosis of Mild and Severe Traumatic Brain Injury. *J Neurotrauma,* 34**,** 1948-1956.

DIEHL, P., FRICKE, A., SANDER, L., STAMM, J., BASSLER, N., HTUN, N., ZIEMANN, M., HELBING, T., EL-OSTA, A., JOWETT, J. B. & PETER, K. 2012. Microparticles: major transport vehicles for distinct microRNAs in circulation. *Cardiovasc Res,* 93**,** 633-44.

DILL, T. 2008. Contraindications to magnetic resonance imaging: non-invasive imaging. *Heart,* 94**,** 943-8.

DINGLE, T. C., SEDLAK, R. H., COOK, L. & JEROME, K. R. 2013. Tolerance of droplet-digital PCR vs real-time quantitative PCR to inhibitory substances. *Clin Chem,* 59**,** 1670-2.

DJEBALI, S., DAVIS, C. A., MERKEL, A., DOBIN, A., LASSMANN, T., MORTAZAVI, A., TANZER, A., LAGARDE, J., LIN, W., SCHLESINGER, F., XUE, C., MARINOV, G. K., KHATUN, J., WILLIAMS, B. A., ZALESKI, C., ROZOWSKY, J., RODER, M., KOKOCINSKI, F., ABDELHAMID, R. F., ALIOTO, T., ANTOSHECHKIN, I., BAER, M. T., BAR, N. S., BATUT, P., BELL, K., BELL, I., CHAKRABORTTY, S., CHEN, X., CHRAST, J., CURADO, J., DERRIEN, T., DRENKOW, J., DUMAIS, E., DUMAIS, J., DUTTAGUPTA, R., FALCONNET, E., FASTUCA, M., FEJES-TOTH, K., FERREIRA, P., FOISSAC, S., FULLWOOD, M. J., GAO, H., GONZALEZ, D., GORDON, A., GUNAWARDENA, H., HOWALD, C., JHA, S., JOHNSON, R., KAPRANOV, P., KING, B., KINGSWOOD, C., LUO, O. J., PARK, E., PERSAUD, K., PREALL, J. B., RIBECA, P., RISK, B., ROBYR, D., SAMMETH, M., SCHAFFER, L., SEE, L. H., SHAHAB, A., SKANCKE, J., SUZUKI, A. M., TAKAHASHI, H., TILGNER, H., TROUT, D., WALTERS, N., WANG, H., WROBEL, J., YU, Y., RUAN, X., HAYASHIZAKI, Y., HARROW, J., GERSTEIN, M., HUBBARD, T., REYMOND, A., ANTONARAKIS, S. E., HANNON, G., GIDDINGS, M. C., RUAN, Y., WOLD, B., CARNINCI, P., GUIGO, R. & GINGERAS, T. R. 2012. Landscape of transcription in human cells. *Nature,* 489**,** 101-8.

DONAHOE, S. M., STEWART, G. C., MCCABE, C. H., MOHANAVELU, S., MURPHY, S. A., CANNON, C. P. & ANTMAN, E. M. 2007. Diabetes and mortality following acute coronary syndromes. *JAMA,* 298**,** 765-75.

DORGE, H., NEUMANN, T., BEHRENDS, M., SKYSCHALLY, A., SCHULZ, R., KASPER, C., ERBEL, R. & HEUSCH, G. 2000. Perfusion-contraction mismatch with coronary microvascular obstruction: role of inflammation. *Am J Physiol Heart Circ Physiol,* 279**,** H2587-92.

DRIESEN, R. B., ZALEWSKI, J., VANDEN DRIESSCHE, N., VERMEULEN, K., BOGAERT, J., SIPIDO, K. R., VAN DE WERF, F. & CLAUS, P. 2012. Histological correlate of a cardiac magnetic resonance imaged microvascular obstruction in a porcine model of ischemia-reperfusion. *Cardiovasc Pathol,* 21**,** 129-31.

DURANTE, A., LARICCHIA, A., BENEDETTI, G., ESPOSITO, A., MARGONATO, A., RIMOLDI, O., DE COBELLI, F., COLOMBO, A. & CAMICI, P. G. 2017. Identification of High-Risk Patients After ST-Segment-Elevation Myocardial Infarction: Comparison Between Angiographic and Magnetic Resonance Parameters. *Circ Cardiovasc Imaging,* 10**,** e005841.

DWEEP, H. & GRETZ, N. 2015. miRWalk2.0: a comprehensive atlas of microRNA-target interactions. *Nature Methods,* 12**,** 697.

EITEL, I., ADAMS, V., DIETERICH, P., FUERNAU, G., DE WAHA, S., DESCH, S., SCHULER, G. & THIELE, H. 2012. Relation of circulating MicroRNA-133a concentrations with myocardial damage and clinical prognosis in ST-elevation myocardial infarction. *Am Heart J,* 164**,** 706-14.

EITEL, I., DE WAHA, S., WOHRLE, J., FUERNAU, G., LURZ, P., PAUSCHINGER, M., DESCH, S., SCHULER, G. & THIELE, H. 2014. Comprehensive prognosis assessment by CMR imaging after ST-segment elevation myocardial infarction. *J Am Coll Cardiol,* 64**,** 1217-26.

EITEL, I., NOWAK, M., STEHL, C., ADAMS, V., FUERNAU, G., HILDEBRAND, L., DESCH, S., SCHULER, G. & THIELE, H. 2010. Endothelin-1 release in acute myocardial infarction as a predictor of long-term prognosis and no-reflow assessed by contrast-enhanced magnetic resonance imaging. *Am Heart J,* 159**,** 882-90.

ELLIOT, D. & LADOMERY, M. 2016. Introduction to molecular biology of RNA. *Molecular Biology of RNA.* 2nd ed. New York: Oxford University Press.

EULALIO, A., HUNTZINGER, E. & IZAURRALDE, E. 2008. GW182 interaction with Argonaute is essential for miRNA-mediated translational repression and mRNA decay. *Nat Struct Mol Biol,* 15**,** 346-53.

FALK, E. 1985. Unstable angina with fatal outcome: dynamic coronary thrombosis leading to infarction and/or sudden death. Autopsy evidence of recurrent mural thrombosis with peripheral embolization culminating in total vascular occlusion. *Circulation,* 71**,** 699-708.

FALK, E., NAKANO, M., BENTZON, J. F., FINN, A. V. & VIRMANI, R. 2013. Update on acute coronary syndromes: the pathologists' view. *Eur Heart J,* 34**,** 719-28.

FANG, Y. & DAVIES, P. F. 2012. Site-specific microRNA-92a regulation of Kruppel-like factors 4 and 2 in atherosusceptible endothelium. *Arterioscler Thromb Vasc Biol,* 32**,** 979-87.

FANG, Y., SHI, C., MANDUCHI, E., CIVELEK, M. & DAVIES, P. F. 2010. MicroRNA-10a regulation of proinflammatory phenotype in athero-susceptible endothelium in vivo and in vitro. *Proc Natl Acad Sci U S A,* 107**,** 13450-5.

FAXON, D. P., GIBBONS, R. J., CHRONOS, N. A., GURBEL, P. A., SHEEHAN, F. & INVESTIGATORS, H.-M. 2002. The effect of blockade of the CD11/CD18 integrin receptor on infarct size in patients with acute myocardial infarction treated with direct angioplasty: the results of the HALT-MI study. *J Am Coll Cardiol,* 40**,** 1199-204.

FEARON, W. F., LOW, A. F., YONG, A. S., MCGEOCH, R., BERRY, C., SHAH, M. G., HO, M. Y., KIM, H. S., LOH, J. P. & OLDROYD, K. G. 2013. Prognostic value of the Index of Microcirculatory Resistance measured after primary percutaneous coronary intervention. *Circulation,* 127**,** 2436-41.

FERRACIN, M., LUPINI, L., SALAMON, I., SACCENTI, E., ZANZI, M. V., ROCCHI, A., DA ROS, L., ZAGATTI, B., MUSA, G., BASSI, C., MANGOLINI, A., CAVALLESCO, G., FRASSOLDATI, A., VOLPATO, S., CARCOFORO, P., HOLLINGSWORTH, A. B. & NEGRINI, M. 2015. Absolute quantification of cell-free microRNAs in cancer patients. *Oncotarget,* 6**,** 14545-55.

FICHTLSCHERER, S., DE ROSA, S., FOX, H., SCHWIETZ, T., FISCHER, A., LIEBETRAU, C., WEBER, M., HAMM, C. W., ROXE, T., MULLER-ARDOGAN, M., BONAUER, A., ZEIHER, A. M. & DIMMELER, S. 2010. Circulating microRNAs in patients with coronary artery disease. *Circ Res,* 107**,** 677-84.

FILATOV, V. L., KATRUKHA, A. G., BULARGINA, T. V. & GUSEV, N. B. 1999. Troponin: structure, properties, and mechanism of functioning. *Biochemistry (Mosc),* 64**,** 969-85.

FOX, K. A., FITZGERALD, G., PUYMIRAT, E., HUANG, W., CARRUTHERS, K., SIMON, T., COSTE, P., MONSEGU, J., GABRIEL STEG, P., DANCHIN, N. & ANDERSON, F. 2014. Should patients with acute coronary disease be stratified for management according to their risk? Derivation, external validation and outcomes using the updated GRACE risk score. *BMJ Open,* 4**,** e004425.

GALIUTO, L., GARRAMONE, B., SCARA, A., REBUZZI, A. G., CREA, F., LA TORRE, G., FUNARO, S., MADONNA, M., FEDELE, F., AGATI, L. & INVESTIGATORS, A. 2008. The extent of microvascular damage during myocardial contrast echocardiography is superior to other known indexes of post-infarct reperfusion in predicting left ventricular remodeling: results of the multicenter AMICI study. *J Am Coll Cardiol,* 51**,** 552-9.

GANAME, J., MESSALLI, G., DYMARKOWSKI, S., RADEMAKERS, F. E., DESMET, W., VAN DE WERF, F. & BOGAERT, J. 2009. Impact of myocardial haemorrhage on left ventricular function and remodelling in patients with reperfused acute myocardial infarction. *Eur Heart J,* 30**,** 1440-9.

GHORPADE, D. S., LEYLAND, R., KUROWSKA-STOLARSKA, M., PATIL, S. A. & BALAJI, K. N. 2012. MicroRNA-155 is required for Mycobacterium bovis BCG-mediated apoptosis of macrophages. *Mol Cell Biol,* 32**,** 2239-53.

GIANNITSIS, E., MULLER-BARDORFF, M., LEHRKE, S., WIEGAND, U., TOLG, R., WEIDTMANN, B., HARTMANN, F., RICHARDT, G. & KATUS, H. A. 2001. Admission troponin T level predicts clinical outcomes, TIMI flow, and myocardial tissue perfusion after primary percutaneous intervention for acute ST-segment elevation myocardial infarction. *Circulation,* 104**,** 630-5.

GIANNITSIS, E., STEEN, H., KURZ, K., IVANDIC, B., SIMON, A. C., FUTTERER, S., SCHILD, C., ISFORT, P., JAFFE, A. S. & KATUS, H. A. 2008. Cardiac magnetic resonance imaging study for quantification of infarct size comparing directly serial versus single time-point measurements of cardiac troponin T. *J Am Coll Cardiol,* 51**,** 307-14.

GIDLOF, O., ANDERSSON, P., VAN DER PALS, J., GOTBERG, M. & ERLINGE, D. 2011. Cardiospecific microRNA plasma levels correlate with troponin and cardiac function in patients with ST elevation myocardial infarction, are selectively dependent on renal elimination, and can be detected in urine samples. *Cardiology,* 118**,** 217-26.

GIDLOF, O., SMITH, J. G., MIYAZU, K., GILJE, P., SPENCER, A., BLOMQUIST, S. & ERLINGE, D. 2013a. Circulating cardio-enriched microRNAs are associated with long-term prognosis following myocardial infarction. *BMC Cardiovasc Disord,* 13**,** 12.

GIDLOF, O., VAN DER BRUG, M., OHMAN, J., GILJE, P., OLDE, B., WAHLESTEDT, C. & ERLINGE, D. 2013b. Platelets activated during

myocardial infarction release functional miRNA, which can be taken up by endothelial cells and regulate ICAM1 expression. *Blood,* 121**,** 3908-17, s1-26.

GJESING, A., GISLASON, G. H., KOBER, L., GUSTAV SMITH, J., CHRISTENSEN, S. B., GUSTAFSSON, F., OLSEN, A. M., TORP-PEDERSEN, C. & ANDERSSON, C. 2014. Nationwide trends in development of heart failure and mortality after first-time myocardial infarction 1997-2010: A Danish cohort study. *Eur J Intern Med,* 25**,** 731-8.

GODDARD, L. M. & IRUELA-ARISPE, M. L. 2013. Cellular and molecular regulation of vascular permeability. *Thromb Haemost,* 109**,** 407-15.

GOMES, A. V., POTTER, J. D. & SZCZESNA-CORDARY, D. 2002. The role of troponins in muscle contraction. *IUBMB Life,* 54**,** 323-33.

GONG, Y. Y., LUO, J. Y., WANG, L. & HUANG, Y. 2018. MicroRNAs Regulating Reactive Oxygen Species in Cardiovascular Diseases. *Antioxid Redox Signal,* 29**,** 1092-1107.

GREGORY, R. I., CHENDRIMADA, T. P., COOCH, N. & SHIEKHATTAR, R. 2005. Human RISC couples microRNA biogenesis and posttranscriptional gene silencing. *Cell,* 123**,** 631-40.

GREGORY, R. I., YAN, K. P., AMUTHAN, G., CHENDRIMADA, T., DORATOTAJ, B., COOCH, N. & SHIEKHATTAR, R. 2004. The Microprocessor complex mediates the genesis of microRNAs. *Nature,* 432**,** 235-40.

GROUP, F. T. T. F. C. 1994. Indications for fibrinolytic therapy in suspected acute myocardial infarction: collaborative overview of early mortality and major morbidity results from all randomised trials of more than 1000 patients. Fibrinolytic Therapy Trialists' (FTT) Collaborative Group. *Lancet,* 343**,** 311-22.

HAAF, P., REICHLIN, T., TWERENBOLD, R., HOELLER, R., RUBINI GIMENEZ, M., ZELLWEGER, C., MOEHRING, B., FISCHER, C., MELLER, B., WILDI, K.,

FREESE, M., STELZIG, C., MOSIMANN, T., REITER, M., MUELLER, M., HOCHGRUBER, T., SOU, S. M., MURRAY, K., MINNERS, J., FREIDANK, H., OSSWALD, S. & MUELLER, C. 2014. Risk stratification in patients with acute chest pain using three high-sensitivity cardiac troponin assays. *Eur Heart J,* 35**,** 365-75.

HAECK, J. D., KOCH, K. T., BILODEAU, L., VAN DER SCHAAF, R. J., HENRIQUES, J. P., VIS, M. M., BAAN, J., JR., VAN DER WAL, A. C., PIEK, J. J., TIJSSEN, J. G., KRUCOFF, M. W. & DE WINTER, R. J. 2009. Randomized comparison of primary percutaneous coronary intervention with combined proximal embolic protection and thrombus aspiration versus primary percutaneous coronary intervention alone in ST-segment elevation myocardial infarction: the PREPARE (PRoximal Embolic Protection in Acute myocardial infarction and Resolution of ST-Elevation) study. *JACC Cardiovasc Interv,* 2**,** 934-43.

HALL, T. S., HALLEN, J., KRUCOFF, M. W., ROE, M. T., BRENNAN, D. M., AGEWALL, S., ATAR, D. & LINCOFF, A. M. 2015. Cardiac troponin I for prediction of clinical outcomes and cardiac function through 3-month follow-up after primary percutaneous coronary intervention for ST-segment elevation myocardial infarction. *Am Heart J,* 169**,** 257-265.e1.

HALLEN, J. 2012. Troponin for the estimation of infarct size: what have we learned? *Cardiology,* 121**,** 204-12.

HALLEN, J., BUSER, P., SCHWITTER, J., PETZELBAUER, P., GEUDELIN, B., FAGERLAND, M. W., JAFFE, A. S. & ATAR, D. 2009. Relation of cardiac troponin I measurements at 24 and 48 hours to magnetic resonance-determined infarct size in patients with ST-elevation myocardial infarction. *Am J Cardiol,* 104**,** 1472-7.

HALLEN, J., JENSEN, J. K., BUSER, P., JAFFE, A. S. & ATAR, D. 2011. Relation of cardiac troponin I and microvascular obstruction following ST-elevation myocardial infarction. *Acute Card Care,* 13**,** 48-51.

HALLEN, J., JENSEN, J. K., FAGERLAND, M. W., JAFFE, A. S. & ATAR, D. 2010. Cardiac troponin I for the prediction of functional recovery and left ventricular remodelling following primary percutaneous coronary intervention for ST-elevation myocardial infarction. *Heart,* 96**,** 1892-7.

HAMIRANI, Y. S., WONG, A., KRAMER, C. M. & SALERNO, M. 2014. Effect of microvascular obstruction and intramyocardial hemorrhage by CMR on LV remodeling and outcomes after myocardial infarction: a systematic review and meta-analysis. *JACC Cardiovasc Imaging,* 7**,** 940-52.

HANGAUER, M. J., VAUGHN, I. W. & MCMANUS, M. T. 2013. Pervasive transcription of the human genome produces thousands of previously unidentified long intergenic noncoding RNAs. *PLoS Genet,* 9**,** e1003569.

HANSSON, G. K. & LIBBY, P. 2006. The immune response in atherosclerosis: a double-edged sword. *Nat Rev Immunol,* 6**,** 508-19.

HARRELL, F. E., JR., LEE, K. L. & MARK, D. B. 1996. Multivariable prognostic models: issues in developing models, evaluating assumptions and adequacy, and measuring and reducing errors. *Stat Med,* 15**,** 361-87.

HARRIS, T. A., YAMAKUCHI, M., FERLITO, M., MENDELL, J. T. & LOWENSTEIN, C. J. 2008. MicroRNA-126 regulates endothelial expression of vascular cell adhesion molecule 1. *Proc Natl Acad Sci U S A,* 105**,** 1516-21.

HASSELL, M. E., VLASTRA, W., ROBBERS, L., HIRSCH, A., NIJVELDT, R., TIJSSEN, J. G., VAN ROSSUM, A. C., ZIJLSTRA, F., PIEK, J. J. & DELEWI, R. 2017. Long-term left ventricular remodelling after revascularisation for ST-segment elevation myocardial infarction as assessed by cardiac magnetic resonance imaging. *Open Heart,* 4**,** e000569.

HEIDERSBACH, A., SAXBY, C., CARVER-MOORE, K., HUANG, Y., ANG, Y. S., DE JONG, P. J., IVEY, K. N. & SRIVASTAVA, D. 2013. microRNA-1 regulates

sarcomere formation and suppresses smooth muscle gene expression in the mammalian heart. *Elife,* 2**,** e01323.

HENKEL, D. M., WITT, B. J., GERSH, B. J., JACOBSEN, S. J., WESTON, S. A., MEVERDEN, R. A. & ROGER, V. L. 2006. Ventricular arrhythmias after acute myocardial infarction: a 20-year community study. *Am Heart J,* 151**,** 806-12.

HERGENREIDER, E., HEYDT, S., TREGUER, K., BOETTGER, T., HORREVOETS, A. J., ZEIHER, A. M., SCHEFFER, M. P., FRANGAKIS, A. S., YIN, X., MAYR, M., BRAUN, T., URBICH, C., BOON, R. A. & DIMMELER, S. 2012. Atheroprotective communication between endothelial cells and smooth muscle cells through miRNAs. *Nat Cell Biol,* 14**,** 249-56.

HINDSON, B. J., NESS, K. D., MASQUELIER, D. A., BELGRADER, P., HEREDIA, N. J., MAKAREWICZ, A. J., BRIGHT, I. J., LUCERO, M. Y., HIDDESSEN, A. L., LEGLER, T. C., KITANO, T. K., HODEL, M. R., PETERSEN, J. F., WYATT, P. W., STEENBLOCK, E. R., SHAH, P. H., BOUSSE, L. J., TROUP, C. B., MELLEN, J. C., WITTMANN, D. K., ERNDT, N. G., CAULEY, T. H., KOEHLER, R. T., SO, A. P., DUBE, S., ROSE, K. A., MONTESCLAROS, L., WANG, S., STUMBO, D. P., HODGES, S. P., ROMINE, S., MILANOVICH, F. P., WHITE, H. E., REGAN, J. F., KARLIN-NEUMANN, G. A., HINDSON, C. M., SAXONOV, S. & COLSTON, B. W. 2011. High-throughput droplet digital PCR system for absolute quantitation of DNA copy number. *Anal Chem,* 83**,** 8604-10.

HINDSON, C. M., CHEVILLET, J. R., BRIGGS, H. A., GALLICHOTTE, E. N., RUF, I. K., HINDSON, B. J., VESSELLA, R. L. & TEWARI, M. 2013. Absolute quantification by droplet digital PCR versus analog real-time PCR. *Nat Meth,* 10**,** 1003-1005.

HOMBACH, V., GREBE, O., MERKLE, N., WALDENMAIER, S., HOHER, M., KOCHS, M., WOHRLE, J. & KESTLER, H. A. 2005. Sequelae of acute myocardial infarction regarding cardiac structure and function and their

prognostic significance as assessed by magnetic resonance imaging. *Eur Heart J,* 26**,** 549-57.

HU, G., CHEN, D., LI, X., YANG, K., WANG, H. & WU, W. 2010. miR-133b regulates the MET proto-oncogene and inhibits the growth of colorectal cancer cells in vitro and in vivo. *Cancer Biol Ther,* 10**,** 190-7.

HUNDLEY, W. G., BLUEMKE, D. A., FINN, J. P., FLAMM, S. D., FOGEL, M. A., FRIEDRICH, M. G., HO, V. B., JEROSCH-HEROLD, M., KRAMER, C. M., MANNING, W. J., PATEL, M., POHOST, G. M., STILLMAN, A. E., WHITE, R. D. & WOODARD, P. K. 2010. ACCF/ACR/AHA/NASCI/SCMR 2010 expert consensus document on cardiovascular magnetic resonance: a report of the American College of Cardiology Foundation Task Force on Expert Consensus Documents. *J Am Coll Cardiol,* 55**,** 2614-62.

HUNG, J., TENG, T. H., FINN, J., KNUIMAN, M., BRIFFA, T., STEWART, S., SANFILIPPO, F. M., RIDOUT, S. & HOBBS, M. 2013. Trends from 1996 to 2007 in incidence and mortality outcomes of heart failure after acute myocardial infarction: a population-based study of 20,812 patients with first acute myocardial infarction in Western Australia. *J Am Heart Assoc,* 2**,** e000172.

IBANEZ, B., JAMES, S., AGEWALL, S., ANTUNES, M. J., BUCCIARELLI-DUCCI, C., BUENO, H., CAFORIO, A. L. P., CREA, F., GOUDEVENOS, J. A., HALVORSEN, S., HINDRICKS, G., KASTRATI, A., LENZEN, M. J., PRESCOTT, E., ROFFI, M., VALGIMIGLI, M., VARENHORST, C., VRANCKX, P., WIDIMSKY, P. & GROUP, E. S. C. S. D. 2017. 2017 ESC Guidelines for the management of acute myocardial infarction in patients presenting with ST-segment elevation: The Task Force for the management of acute myocardial infarction in patients presenting with ST-segment elevation of the European Society of Cardiology (ESC). *Eur Heart J*.

IBANEZ, B., JAMES, S., AGEWALL, S., ANTUNES, M. J., BUCCIARELLI-DUCCI, C., BUENO, H., CAFORIO, A. L. P., CREA, F., GOUDEVENOS, J. A.,

HALVORSEN, S., HINDRICKS, G., KASTRATI, A., LENZEN, M. J., PRESCOTT, E., ROFFI, M., VALGIMIGLI, M., VARENHORST, C., VRANCKX, P., WIDIMSKY, P. & GROUP, E. S. C. S. D. 2018. 2017 ESC Guidelines for the management of acute myocardial infarction in patients presenting with ST-segment elevation: The Task Force for the management of acute myocardial infarction in patients presenting with ST-segment elevation of the European Society of Cardiology (ESC). *Eur Heart J,* 39**,** 119-177.

IKEDA, S., HE, A., KONG, S. W., LU, J., BEJAR, R., BODYAK, N., LEE, K. H., MA, Q., KANG, P. M., GOLUB, T. R. & PU, W. T. 2009. MicroRNA-1 negatively regulates expression of the hypertrophy-associated calmodulin and Mef2a genes. *Mol Cell Biol,* 29**,** 2193-204.

INFUSINO, F., NICCOLI, G., FRACASSI, F., ROBERTO, M., FALCIONI, E., LANZA, G. A. & CREA, F. 2014. The central role of conventional 12-lead ECG for the assessment of microvascular obstruction after percutaneous myocardial revascularization. *J Electrocardiol,* 47**,** 45-51.

IVEY, K. N., MUTH, A., ARNOLD, J., KING, F. W., YEH, R. F., FISH, J. E., HSIAO, E. C., SCHWARTZ, R. J., CONKLIN, B. R., BERNSTEIN, H. S. & SRIVASTAVA, D. 2008. MicroRNA regulation of cell lineages in mouse and human embryonic stem cells. *Cell Stem Cell,* 2**,** 219-29.

JABBARI, R., ENGSTROM, T., GLINGE, C., RISGAARD, B., JABBARI, J., WINKEL, B. G., TERKELSEN, C. J., TILSTED, H. H., JENSEN, L. O., HOUGAARD, M., CHIUVE, S. E., PEDERSEN, F., SVENDSEN, J. H., HAUNSO, S., ALBERT, C. M. & TFELT-HANSEN, J. 2015a. Incidence and risk factors of ventricular fibrillation before primary angioplasty in patients with first ST-elevation myocardial infarction: a nationwide study in Denmark. *J Am Heart Assoc,* 4**,** e001399.

JABBARI, R., RISGAARD, B., FOSBOL, E. L., SCHEIKE, T., PHILBERT, B. T., WINKEL, B. G., ALBERT, C. M., GLINGE, C., AHTAROVSKI, K. A., HAUNSO, S., KOBER, L., JORGENSEN, E., PEDERSEN, F., TFELT-

HANSEN, J. & ENGSTROM, T. 2015b. Factors Associated With and Outcomes After Ventricular Fibrillation Before and During Primary Angioplasty in Patients With ST-Segment Elevation Myocardial Infarction. *Am J Cardiol,* 116**,** 678-85.

JANSEN, F., YANG, X., PROEBSTING, S., HOELSCHER, M., PRZYBILLA, D., BAUMANN, K., SCHMITZ, T., DOLF, A., ENDL, E., FRANKLIN, B. S., SINNING, J. M., VASA-NICOTERA, M., NICKENIG, G. & WERNER, N. 2014. MicroRNA Expression in Circulating Microvesicles Predicts Cardiovascular Events in Patients With Coronary Artery Disease. *J Am Heart Assoc,* 3.

JAZDZEWSKI, K., LIYANARACHCHI, S., SWIERNIAK, M., PACHUCKI, J., RINGEL, M. D., JARZAB, B. & DE LA CHAPELLE, A. 2009. Polymorphic mature microRNAs from passenger strand of pre-miR-146a contribute to thyroid cancer. *Proc Natl Acad Sci U S A,* 106**,** 1502-5.

JOHNSON, M. L., NAVANUKRAW, C., GRAZUL-BILSKA, A. T., REYNOLDS, L. P. & REDMER, D. A. 2003. Heparinase treatment of RNA before quantitative real-time RT-PCR. *Biotechniques,* 35**,** 1140-2, 1144.

JONES, D. A., RATHOD, K. S., HOWARD, J. P., GALLAGHER, S., ANTONIOU, S., DE PALMA, R., GUTTMANN, O., CLIFFE, S., COLLEY, J., BUTLER, J., FERGUSON, E., MOHIDDIN, S., KAPUR, A., KNIGHT, C. J., JAIN, A. K., ROTHMAN, M. T., MATHUR, A., TIMMIS, A. D., SMITH, E. J. & WRAGG, A. 2012. Safety and feasibility of hospital discharge 2 days following primary percutaneous intervention for ST-segment elevation myocardial infarction. *Heart,* 98**,** 1722-7.

JUNG, C., SORENSSON, P., SALEH, N., ARHEDEN, H., RYDEN, L. & PERNOW, J. 2012. Circulating endothelial and platelet derived microparticles reflect the size of myocardium at risk in patients with ST-elevation myocardial infarction. *Atherosclerosis,* 221**,** 226-31.

KANO, M., SEKI, N., KIKKAWA, N., FUJIMURA, L., HOSHINO, I., AKUTSU, Y., CHIYOMARU, T., ENOKIDA, H., NAKAGAWA, M. & MATSUBARA, H. 2010. miR-145, miR-133a and miR-133b: Tumor-suppressive miRNAs target FSCN1 in esophageal squamous cell carcinoma. *Int J Cancer,* 127**,** 2804-14.

KATUS, H. A., REMPPIS, A., SCHEFFOLD, T., DIEDERICH, K. W. & KUEBLER, W. 1991. Intracellular compartmentation of cardiac troponin T and its release kinetics in patients with reperfused and nonreperfused myocardial infarction. *Am J Cardiol,* 67**,** 1360-7.

KAUDEWITZ, D., LEE, R., WILLEIT, P., MCGREGOR, R., MARKUS, H. S., KIECHL, S., ZAMPETAKI, A., STOREY, R. F., CHANNON, K. M. & MAYR, M. 2013. Impact of intravenous heparin on quantification of circulating microRNAs in patients with coronary artery disease. *Thromb Haemost,* 110**,** 609-15.

KEELEY, E. C., BOURA, J. A. & GRINES, C. L. 2003. Primary angioplasty versus intravenous thrombolytic therapy for acute myocardial infarction: a quantitative review of 23 randomised trials. *Lancet,* 361**,** 13-20.

KIM, J. S., KIM, J., CHOI, D., LEE, C. J., LEE, S. H., KO, Y. G., HONG, M. K., KIM, B. K., OH, S. J., JEON, D. W., YANG, J. Y., CHO, J. R., LEE, N. H., CHO, Y. H., CHO, D. K. & JANG, Y. 2010. Efficacy of high-dose atorvastatin loading before primary percutaneous coronary intervention in ST-segment elevation myocardial infarction: the STATIN STEMI trial. *JACC Cardiovasc Interv,* 3**,** 332-9.

KINJO, K., SATO, H., SATO, H., OHNISHI, Y., HISHIDA, E., NAKATANI, D., MIZUNO, H., FUKUNAMI, M., KORETSUNE, Y., TAKEDA, H., HORI, M. & OSAKA ACUTE CORONARY INSUFFICIENCY STUDY, G. 2003. Prognostic significance of atrial fibrillation/atrial flutter in patients with acute myocardial infarction treated with percutaneous coronary intervention. *Am J Cardiol,* 92**,** 1150-4.

KITAKAZE, M., ASAKURA, M., KIM, J., SHINTANI, Y., ASANUMA, H., HAMASAKI, T., SEGUCHI, O., MYOISHI, M., MINAMINO, T., OHARA, T., NAGAI, Y., NANTO, S., WATANABE, K., FUKUZAWA, S., HIRAYAMA, A., NAKAMURA, N., KIMURA, K., FUJII, K., ISHIHARA, M., SAITO, Y., TOMOIKE, H., KITAMURA, S. & INVESTIGATORS, J. W. 2007. Human atrial natriuretic peptide and nicorandil as adjuncts to reperfusion treatment for acute myocardial infarction (J-WIND): two randomised trials. *Lancet,* 370**,** 1483-93.

KLONER, R. A., GANOTE, C. E. & JENNINGS, R. B. 1974. The "no-reflow" phenomenon after temporary coronary occlusion in the dog. *J Clin Invest,* 54**,** 1496-508.

KLONER, R. A., GIACOMELLI, F., ALKER, K. J., HALE, S. L., MATTHEWS, R. & BELLOWS, S. 1991. Influx of neutrophils into the walls of large epicardial coronary arteries in response to ischemia/reperfusion. *Circulation,* 84**,** 1758-72.

KLUG, G., MAYR, A., SCHENK, S., ESTERHAMMER, R., SCHOCKE, M., NOCKER, M., JASCHKE, W., PACHINGER, O. & METZLER, B. 2012. Prognostic value at 5 years of microvascular obstruction after acute myocardial infarction assessed by cardiovascular magnetic resonance. *J Cardiovasc Magn Reson,* 14**,** 46.

KONDKAR, A. A., BRAY, M. S., LEAL, S. M., NAGALLA, S., LIU, D. J., JIN, Y., DONG, J. F., REN, Q., WHITEHEART, S. W., SHAW, C. & BRAY, P. F. 2010. VAMP8/endobrevin is overexpressed in hyperreactive human platelets: suggested role for platelet microRNA. *J Thromb Haemost,* 8**,** 369-78.

KUMAR, A., GREEN, J. D., SYKES, J. M., EPHRAT, P., CARSON, J. J., MITCHELL, A. J., WISENBERG, G. & FRIEDRICH, M. G. 2011. Detection and quantification of myocardial reperfusion hemorrhage using T2*-weighted CMR. *JACC Cardiovasc Imaging,* 4**,** 1274-83.

LAFFONT, B., CORDUAN, A., PLE, H., DUCHEZ, A. C., CLOUTIER, N., BOILARD, E. & PROVOST, P. 2013. Activated platelets can deliver mRNA regulatory Ago2*microRNA complexes to endothelial cells via microparticles. *Blood,* 122**,** 253-61.

LANDRY, P., PLANTE, I., OUELLET, D. L., PERRON, M. P., ROUSSEAU, G. & PROVOST, P. 2009. Existence of a microRNA pathway in anucleate platelets. *Nat Struct Mol Biol,* 16**,** 961-6.

LAROSE, E., RODES-CABAU, J., PIBAROT, P., RINFRET, S., PROULX, G., NGUYEN, C. M., DERY, J. P., GLEETON, O., ROY, L., NOEL, B., BARBEAU, G., ROULEAU, J., BOUDREAULT, J. R., AMYOT, M., DE LAROCHELLIERE, R. & BERTRAND, O. F. 2010. Predicting late myocardial recovery and outcomes in the early hours of ST-segment elevation myocardial infarction traditional measures compared with microvascular obstruction, salvaged myocardium, and necrosis characteristics by cardiovascular magnetic resonance. *J Am Coll Cardiol,* 55**,** 2459-69.

LAUGAUDIN, G., KUSTER, N., PETITON, A., LECLERCQ, F., GERVASONI, R., MACIA, J. C., CUNG, T. T., DUPUY, A. M., SOLECKI, K., LATTUCA, B., CADE, S., CRANSAC, F., CRISTOL, J. P. & ROUBILLE, F. 2016. Kinetics of high-sensitivity cardiac troponin T and I differ in patients with ST-segment elevation myocardial infarction treated by primary coronary intervention. *Eur Heart J Acute Cardiovasc Care,* 5**,** 354-63.

LAUTAMAKI, R., SCHULERI, K. H., SASANO, T., JAVADI, M. S., YOUSSEF, A., MERRILL, J., NEKOLLA, S. G., ABRAHAM, M. R., LARDO, A. C. & BENGEL, F. M. 2009. Integration of infarct size, tissue perfusion, and metabolism by hybrid cardiac positron emission tomography/computed tomography: evaluation in a porcine model of myocardial infarction. *Circ Cardiovasc Imaging,* 2**,** 299-305.

LEE, K. H., AHN, Y., KIM, S. S., RHEW, S. H., JEONG, Y. W., JANG, S. Y., CHO, J. Y., JEONG, H. C., PARK, K. H., YOON, N. S., SIM, D. S., YOON, H. J., KIM,

K. H., HONG, Y. J., PARK, H. W., KIM, J. H., CHO, J. G., PARK, J. C., JEONG, M. H., CHO, M. C., KIM, C. J., KIM, Y. J. & INVESTIGATORS, K. 2013. Comparison of triple anti-platelet therapy and dual anti-platelet therapy in patients with acute myocardial infarction who had no-reflow phenomenon during percutaneous coronary intervention. *Circ J,* 77**,** 2973-81.

LEE, R. C., FEINBAUM, R. L. & AMBROS, V. 1993. The C. elegans heterochronic gene lin-4 encodes small RNAs with antisense complementarity to lin-14. *Cell,* 75**,** 843-54.

LEHTO, M., SNAPINN, S., DICKSTEIN, K., SWEDBERG, K., NIEMINEN, M. S. & INVESTIGATORS, O. 2005. Prognostic risk of atrial fibrillation in acute myocardial infarction complicated by left ventricular dysfunction: the OPTIMAAL experience. *Eur Heart J,* 26**,** 350-6.

LI, S., ZHANG, F., CUI, Y., WU, M., LEE, C., SONG, J., CAO, C. & CHEN, H. 2017. Modified high-throughput quantification of plasma microRNAs in heparinized patients with coronary artery disease using heparinase. *Biochem Biophys Res Commun,* 493**,** 556-561.

LIANG, Y., RIDZON, D., WONG, L. & CHEN, C. 2007. Characterization of microRNA expression profiles in normal human tissues. *BMC Genomics,* 8**,** 166.

LIBBY, P. 2002. Inflammation in atherosclerosis. *Nature,* 420**,** 868-74.

LIBBY, P. & THEROUX, P. 2005. Pathophysiology of coronary artery disease. *Circulation,* 111**,** 3481-8.

LIEBETRAU, C., MOLLMANN, H., DORR, O., SZARDIEN, S., TROIDL, C., WILLMER, M., VOSS, S., GAEDE, L., RIXE, J., ROLF, A., HAMM, C. & NEF, H. 2013. Release kinetics of circulating muscle-enriched microRNAs in patients undergoing transcoronary ablation of septal hypertrophy. *J Am Coll Cardiol,* 62**,** 992-8.

LIMA, J., JR., BATTY, J. A., SINCLAIR, H. & KUNADIAN, V. 2017. MicroRNAs in Ischemic Heart Disease: From Pathophysiology to Potential Clinical Applications. *Cardiol Rev,* 25**,** 117-125.

LIMBRUNO, U., DE CARLO, M., PISTOLESI, S., MICHELI, A., PETRONIO, A. S., CAMACCI, T., FONTANINI, G., BALBARINI, A., MARIANI, M. & DE CATERINA, R. 2005. Distal embolization during primary angioplasty: histopathologic features and predictability. *Am Heart J,* 150**,** 102-8.

LIPPI, G., MATTIUZZI, C. & CERVELLIN, G. 2013. Circulating microRNAs (miRs) for diagnosing acute myocardial infarction: meta-analysis of available studies. *Int J Cardiol,* 167**,** 277-8.

LOMBARDO, A., NICCOLI, G., NATALE, L., BERNARDINI, A., COSENTINO, N., BONOMO, L. & CREA, F. 2012. Impact of microvascular obstruction and infarct size on left ventricular remodeling in reperfused myocardial infarction: a contrast-enhanced cardiac magnetic resonance imaging study. *Int J Cardiovasc Imaging,* 28**,** 835-42.

LONBORG, J., VEJLSTRUP, N., KELBAEK, H., BOTKER, H. E., KIM, W. Y., MATHIASEN, A. B., JORGENSEN, E., HELQVIST, S., SAUNAMAKI, K., CLEMMENSEN, P., HOLMVANG, L., THUESEN, L., KRUSELL, L. R., JENSEN, J. S., KOBER, L., TREIMAN, M., HOLST, J. J. & ENGSTROM, T. 2012. Exenatide reduces reperfusion injury in patients with ST-segment elevation myocardial infarction. *Eur Heart J,* 33**,** 1491-9.

LOYER, X., POTTEAUX, S., VION, A. C., GUERIN, C. L., BOULKROUN, S., RAUTOU, P. E., RAMKHELAWON, B., ESPOSITO, B., DALLOZ, M., PAUL, J. L., JULIA, P., MACCARIO, J., BOULANGER, C. M., MALLAT, Z. & TEDGUI, A. 2014a. Inhibition of microRNA-92a prevents endothelial dysfunction and atherosclerosis in mice. *Circ Res,* 114**,** 434-43.

LOYER, X., VION, A. C., TEDGUI, A. & BOULANGER, C. M. 2014b. Microvesicles as cell-cell messengers in cardiovascular diseases. *Circ Res,* 114**,** 345-53.

LUMAN, P. F. 2014. *British Cardiovascular Intervention Society Audit for Adult Cardiovascular Interventions* [Online]. Available: http://www.bcis.org.uk/wp-content/uploads/2017/01/BCIS-audit-2014.pdf [Accessed October 1, 2018].

LV, P., ZHOU, M., HE, J., MENG, W., MA, X., DONG, S., MENG, X., ZHAO, X., WANG, X. & HE, F. 2014. Circulating miR-208b and miR-34a are associated with left ventricular remodeling after acute myocardial infarction. *Int J Mol Sci,* 15**,** 5774-88.

MAKSIMENKO, A. V. & TURASHEV, A. D. 2012. No-reflow phenomenon and endothelial glycocalyx of microcirculation. *Biochem Res Int,* 2012**,** 859231.

MANGION, K., CORCORAN, D., CARRICK, D. & BERRY, C. 2016. New perspectives on the role of cardiac magnetic resonance imaging to evaluate myocardial salvage and myocardial hemorrhage after acute reperfused ST-elevation myocardial infarction. *Expert Rev Cardiovasc Ther,* 14**,** 843-54.

MANGOLINI, A., FERRACIN, M., ZANZI, M. V., SACCENTI, E., EBNAOF, S. O., POMA, V. V., SANZ, J. M., PASSARO, A., PEDRIALI, M., FRASSOLDATI, A., QUERZOLI, P., SABBIONI, S., CARCOFORO, P., HOLLINGSWORTH, A. & NEGRINI, M. 2015. Diagnostic and prognostic microRNAs in the serum of breast cancer patients measured by droplet digital PCR. *Biomark Res,* 3**,** 12.

MANN, D. L., ZIPES, D. P., LIBBY, P., BONOW, O. P. & FABBRO-PERAY, P. 2015. *Braunwald's heart disease : a textbook of cardiovascular medicine*, Tenth edition. Philadelphia, PA : Elsevier/Saunders, [2015] ©2015.

MARABITA, F., DE CANDIA, P., TORRI, A., TEGNER, J., ABRIGNANI, S. & ROSSI, R. L. 2016. Normalization of circulating microRNA expression data obtained by quantitative real-time RT-PCR. *Brief Bioinform,* 17**,** 204-12.

MAXWELL, L. & GAVIN, J. B. 1991. The role of post-ischaemic reperfusion in the development of microvascular incompetence and ultrastructural damage in the myocardium. *Basic Res Cardiol,* 86**,** 544-53.

MAYR, A., KLUG, G., SCHOCKE, M., TRIEB, T., MAIR, J., PEDARNIG, K., PACHINGER, O., JASCHKE, W. & METZLER, B. 2012. Late microvascular obstruction after acute myocardial infarction: relation with cardiac and inflammatory markers. *Int J Cardiol,* 157**,** 391-6.

MAYR, A., MAIR, J., KLUG, G., SCHOCKE, M., PEDARNIG, K., TRIEB, T., PACHINGER, O., JASCHKE, W. & METZLER, B. 2011. Cardiac troponin T and creatine kinase predict mid-term infarct size and left ventricular function after acute myocardial infarction: a cardiac MR study. *J Magn Reson Imaging,* 33**,** 847-54.

MCDERMOTT, A. M., KERIN, M. J. & MILLER, N. 2013. Identification and validation of miRNAs as endogenous controls for RQ-PCR in blood specimens for breast cancer studies. *PLoS One,* 8**,** e83718.

MCDONALD, J. S., MILOSEVIC, D., REDDI, H. V., GREBE, S. K. & ALGECIRAS-SCHIMNICH, A. 2011. Analysis of circulating microRNA: preanalytical and analytical challenges. *Clin Chem,* 57**,** 833-40.

MCLAUGHLIN, M. G., STONE, G. W., AYMONG, E., GARDNER, G., MEHRAN, R., LANSKY, A. J., GRINES, C. L., TCHENG, J. E., COX, D. A., STUCKEY, T., GARCIA, E., GUAGLIUMI, G., TURCO, M., JOSEPHSON, M. E., ZIMETBAUM, P., CONTROLLED, A. & DEVICE INVESTIGATION TO LOWER LATE ANGIOPLASTY COMPLICATIONS, T. 2004. Prognostic utility of comparative methods for assessment of ST-segment resolution after primary angioplasty for acute myocardial infarction: the Controlled Abciximab and Device Investigation to Lower Late Angioplasty Complications (CADILLAC) trial. *J Am Coll Cardiol,* 44**,** 1215-23.

MEHTA, R. H., YU, J., PICCINI, J. P., TCHENG, J. E., FARKOUH, M. E., REIFFEL, J., FAHY, M., MEHRAN, R. & STONE, G. W. 2012. Prognostic significance of postprocedural sustained ventricular tachycardia or fibrillation in patients undergoing primary percutaneous coronary intervention (from the HORIZONS-AMI Trial). *Am J Cardiol,* 109**,** 805-12.

MENEES, D. S., PETERSON, E. D., WANG, Y., CURTIS, J. P., MESSENGER, J. C., RUMSFELD, J. S. & GURM, H. S. 2013. Door-to-balloon time and mortality among patients undergoing primary PCI. *N Engl J Med,* 369**,** 901-9.

MIN, P. K., KIM, J. Y., CHUNG, K. H., LEE, B. K., CHO, M., LEE, D. L., HONG, S. Y., CHOI, E. Y., YOON, Y. W., HONG, B. K., RIM, S. J. & KWON, H. M. 2013. Local increase in microparticles from the aspirate of culprit coronary arteries in patients with ST-segment elevation myocardial infarction. *Atherosclerosis,* 227**,** 323-8.

MISONO, S., SEKI, N., MIZUNO, K., YAMADA, Y., UCHIDA, A., ARAI, T., KUMAMOTO, T., SANADA, H., SUETSUGU, T. & INOUE, H. 2018. Dual strands of the miR-145 duplex (miR-145-5p and miR-145-3p) regulate oncogenes in lung adenocarcinoma pathogenesis. *J Hum Genet,* 63**,** 1015-1028.

MITCHELL, A. J., GRAY, W. D., HAYEK, S. S., KO, Y. A., THOMAS, S., ROONEY, K., AWAD, M., ROBACK, J. D., QUYYUMI, A. & SEARLES, C. D. 2016. Platelets confound the measurement of extracellular miRNA in archived plasma. *Sci Rep,* 6**,** 32651.

MOLDOVAN, L., BATTE, K. E., TRGOVCICH, J., WISLER, J., MARSH, C. B. & PIPER, M. 2014. Methodological challenges in utilizing miRNAs as circulating biomarkers. *J Cell Mol Med,* 18**,** 371-90.

MORAN, A. E., FOROUZANFAR, M. H., ROTH, G. A., MENSAH, G. A., EZZATI, M., FLAXMAN, A., MURRAY, C. J. & NAGHAVI, M. 2014a. The global burden of ischemic heart disease in 1990 and 2010: the Global Burden of Disease 2010 study. *Circulation,* 129**,** 1493-501.

MORAN, A. E., FOROUZANFAR, M. H., ROTH, G. A., MENSAH, G. A., EZZATI, M., MURRAY, C. J. & NAGHAVI, M. 2014b. Temporal trends in ischemic heart disease mortality in 21 world regions, 1980 to 2010: the Global Burden of Disease 2010 study. *Circulation,* 129**,** 1483-92.

MORAN, A. E., TZONG, K. Y., FOROUZANFAR, M. H., ROTHY, G. A., MENSAH, G. A., EZZATI, M., MURRAY, C. J. & NAGHAVI, M. 2014c. Variations in ischemic heart disease burden by age, country, and income: the Global Burden of Diseases, Injuries, and Risk Factors 2010 study. *Glob Heart,* 9**,** 91-9.

MOREL, O., PEREIRA, B., AVEROUS, G., FAURE, A., JESEL, L., GERMAIN, P., GRUNEBAUM, L., OHLMANN, P., FREYSSINET, J. M., BAREISS, P. & TOTI, F. 2009. Increased levels of procoagulant tissue factor-bearing microparticles within the occluded coronary artery of patients with ST-segment elevation myocardial infarction: role of endothelial damage and leukocyte activation. *Atherosclerosis,* 204**,** 636-41.

MORISHIMA, I., SONE, T., OKUMURA, K., TSUBOI, H., KONDO, J., MUKAWA, H., MATSUI, H., TOKI, Y., ITO, T. & HAYAKAWA, T. 2000. Angiographic no-reflow phenomenon as a predictor of adverse long-term outcome in patients treated with percutaneous transluminal coronary angioplasty for first acute myocardial infarction. *J Am Coll Cardiol,* 36**,** 1202-9.

MURRAY, C. J., RICHARDS, M. A., NEWTON, J. N., FENTON, K. A., ANDERSON, H. R., ATKINSON, C., BENNETT, D., BERNABE, E., BLENCOWE, H., BOURNE, R., BRAITHWAITE, T., BRAYNE, C., BRUCE, N. G., BRUGHA, T. S., BURNEY, P., DHERANI, M., DOLK, H., EDMOND, K., EZZATI, M., FLAXMAN, A. D., FLEMING, T. D., FREEDMAN, G., GUNNELL, D., HAY, R. J., HUTCHINGS, S. J., OHNO, S. L., LOZANO, R., LYONS, R. A., MARCENES, W., NAGHAVI, M., NEWTON, C. R., PEARCE, N., POPE, D., RUSHTON, L., SALOMON, J. A., SHIBUYA, K., VOS, T., WANG, H., WILLIAMS, H. C., WOOLF, A. D., LOPEZ, A. D. & DAVIS, A. 2013. UK health performance: findings of the Global Burden of Disease Study 2010. *Lancet,* 381**,** 997-1020.

NAGALLA, S., SHAW, C., KONG, X., KONDKAR, A. A., EDELSTEIN, L. C., MA, L., CHEN, J., MCKNIGHT, G. S., LOPEZ, J. A., YANG, L., JIN, Y., BRAY, M. S., LEAL, S. M., DONG, J. F. & BRAY, P. F. 2011. Platelet microRNA-mRNA coexpression profiles correlate with platelet reactivity. *Blood,* 117**,** 5189-97.

NAVICKAS, R., GAL, D., LAUCEVICIUS, A., TAPARAUSKAITE, A., ZDANYTE, M. & HOLVOET, P. 2016. Identifying circulating microRNAs as biomarkers of cardiovascular disease: a systematic review. *Cardiovasc Res,* 111**,** 322-37.

NAZARI-JAHANTIGH, M., WEI, Y., NOELS, H., AKHTAR, S., ZHOU, Z., KOENEN, R. R., HEYLL, K., GREMSE, F., KIESSLING, F., GROMMES, J., WEBER, C. & SCHOBER, A. 2012. MicroRNA-155 promotes atherosclerosis by repressing Bcl6 in macrophages. *J Clin Invest,* 122**,** 4190-202.

NEWSON, R. B. 2010. Comparing the predictive powers of survival models using Harrell's C or Somers' D. *Stata Journal,* 10**,** 339-358.

NGUYEN, T. L., FRENCH, J. K., HOGAN, J., HEE, L., MOSES, D., MUSSAP, C. J., RAJARATNAM, R., JUERGENS, C. P., DIMITRI, H. R., RICHARDS, D. A. B. & THOMAS, L. 2016. Prognostic value of high sensitivity troponin T after ST-segment elevation myocardial infarction in the era of cardiac magnetic resonance imaging. *Eur Heart J Qual Care Clin Outcomes,* 2**,** 164-171.

NGUYEN, T. L., PHAN, J. A., HEE, L., MOSES, D. A., OTTON, J., TERREBLANCHE, O. D., XIONG, J., PREMAWARDHANA, U., RAJARATNAM, R., JUERGENS, C. P., DIMITRI, H. R., FRENCH, J. K., RICHARDS, D. A. & THOMAS, L. 2015a. High-sensitivity troponin T predicts infarct scar characteristics and adverse left ventricular function by cardiac magnetic resonance imaging early after reperfused acute myocardial infarction. *Am Heart J,* 170**,** 715-725 e2.

NGUYEN, T. L., PHAN, J. A., HEE, L., MOSES, D. A., OTTON, J., TERREBLANCHE, O. D., XIONG, J., PREMAWARDHANA, U., RAJARATNAM, R., JUERGENS, C. P., DIMITRI, H. R., FRENCH, J. K., RICHARDS, D. A. & THOMAS, L. 2015b. High-sensitivity troponin T predicts infarct scar characteristics and adverse left ventricular function by cardiac magnetic resonance imaging early after reperfused acute myocardial infarction. *Am Heart J,* 170**,** 715-725.e2.

NICCOLI, G., COSENTINO, N., SPAZIANI, C., FRACASSI, F., TARANTINI, G. & CREA, F. 2013. No-reflow: incidence and detection in the cath-lab. *Curr Pharm Des,* 19**,** 4564-75.

NICCOLI, G., SCALONE, G., LERMAN, A. & CREA, F. 2016. Coronary microvascular obstruction in acute myocardial infarction. *Eur Heart J,* 37**,** 1024-33.

NIJVELDT, R., BEEK, A. M., HIRSCH, A., STOEL, M. G., HOFMAN, M. B., UMANS, V. A., ALGRA, P. R., TWISK, J. W. & VAN ROSSUM, A. C. 2008. Functional recovery after acute myocardial infarction: comparison between angiography, electrocardiography, and cardiovascular magnetic resonance measures of microvascular injury. *J Am Coll Cardiol,* 52**,** 181-9.

NIJVELDT, R., HOFMAN, M. B., HIRSCH, A., BEEK, A. M., UMANS, V. A., ALGRA, P. R., PIEK, J. J. & VAN ROSSUM, A. C. 2009. Assessment of microvascular obstruction and prediction of short-term remodeling after acute myocardial infarction: cardiac MR imaging study. *Radiology,* 250**,** 363-70.

NOMAN, A., ZAMAN, A. G., SCHECHTER, C., BALASUBRAMANIAM, K. & DAS, R. 2013. Early discharge after primary percutaneous coronary intervention for ST-elevation myocardial infarction. *Eur Heart J Acute Cardiovasc Care,* 2**,** 262-9.

O'REGAN, D. P., ARIFF, B., NEUWIRTH, C., TAN, Y., DURIGHEL, G. & COOK, S. A. 2010. Assessment of severe reperfusion injury with T2* cardiac MRI in patients with acute myocardial infarction. *Heart,* 96**,** 1885-91.

OHLMANN, P., MONASSIER, J. P., MICHOTEY, M. O., BERENGER, N., JACQUEMIN, L., LAVAL, G., ROUL, G. & SCHNEIDER, F. 2003. Troponin I concentrations following primary percutaneous coronary intervention predict large infarct size and left ventricular dysfunction in patients with ST-segment elevation acute myocardial infarction. *Atherosclerosis,* 168**,** 181-9.

OLIVIERI, F., ANTONICELLI, R., LORENZI, M., D'ALESSANDRA, Y., LAZZARINI, R., SANTINI, G., SPAZZAFUMO, L., LISA, R., LA SALA, L., GALEAZZI, R., RECCHIONI, R., TESTA, R., POMPILIO, G., CAPOGROSSI, M. C. & PROCOPIO, A. D. 2013. Diagnostic potential of circulating miR-499-5p in elderly patients with acute non ST-elevation myocardial infarction. *Int J Cardiol,* 167**,** 531-6.

OMURA, T., TERAGAKI, M., TANI, T., YAMAGISHI, H., YANAGI, S., NISHIKIMI, T., YOSHIYAMA, M., TODA, I., AKIOKA, K., TAKEUCHI, K. & ET AL. 1993. Estimation of infarct size using serum troponin T concentration in patients with acute myocardial infarction. *Jpn Circ J,* 57**,** 1062-70.

ORN, S., MANHENKE, C., GREVE, O. J., LARSEN, A. I., BONARJEE, V. V., EDVARDSEN, T. & DICKSTEIN, K. 2009. Microvascular obstruction is a major determinant of infarct healing and subsequent left ventricular remodelling following primary percutaneous coronary intervention. *Eur Heart J,* 30**,** 1978-85.

PAN, Y., LIANG, H., LIU, H., LI, D., CHEN, X., LI, L., ZHANG, C. Y. & ZEN, K. 2014. Platelet-secreted microRNA-223 promotes endothelial cell apoptosis induced by advanced glycation end products via targeting the insulin-like growth factor 1 receptor. *J Immunol,* 192**,** 437-46.

PANWAR, B., OMENN, G. S. & GUAN, Y. 2017. miRmine: a database of human miRNA expression profiles. *Bioinformatics,* 33**,** 1554-1560.

PAYNE, A. R., BERRY, C., KELLMAN, P., ANDERSON, R., HSU, L. Y., CHEN, M. Y., MCPHADEN, A. R., WATKINS, S., SCHENKE, W., WRIGHT, V., LEDERMAN, R. J., ALETRAS, A. H. & ARAI, A. E. 2011. Bright-blood T(2)-weighted MRI has high diagnostic accuracy for myocardial hemorrhage in myocardial infarction: a preclinical validation study in swine. *Circ Cardiovasc Imaging,* 4**,** 738-45.

PEDERSEN, F., BUTRYMOVICH, V., KELBAEK, H., WACHTELL, K., HELQVIST, S., KASTRUP, J., HOLMVANG, L., CLEMMENSEN, P., ENGSTROM, T., GRANDE, P., SAUNAMAKI, K. & JORGENSEN, E. 2014. Short- and long-term cause of death in patients treated with primary PCI for STEMI. *J Am Coll Cardiol,* 64**,** 2101-8.

PEDERSEN, S. F., THRYSOE, S. A., ROBICH, M. P., PAASKE, W. P., RINGGAARD, S., BOTKER, H. E., HANSEN, E. S. & KIM, W. Y. 2012. Assessment of intramyocardial hemorrhage by T1-weighted cardiovascular magnetic resonance in reperfused acute myocardial infarction. *J Cardiovasc Magn Reson,* 14**,** 59.

PENCINA, M. J., D'AGOSTINO, R. B., PENCINA, K. M., JANSSENS, A. C. & GREENLAND, P. 2012. Interpreting incremental value of markers added to risk prediction models. *Am J Epidemiol,* 176**,** 473-81.

PENCINA, M. J., D'AGOSTINO, R. B., SR. & STEYERBERG, E. W. 2011. Extensions of net reclassification improvement calculations to measure usefulness of new biomarkers. *Stat Med,* 30**,** 11-21.

PENG, L., CHUN-GUANG, Q., BEI-FANG, L., XUE-ZHI, D., ZI-HAO, W., YUN-FU, L., YAN-PING, D., YANG-GUI, L., WEI-GUO, L., TIAN-YONG, H. & ZHEN-WEN, H. 2014. Clinical impact of circulating miR-133, miR-1291 and miR-663b in plasma of patients with acute myocardial infarction. *Diagn Pathol,* 9**,** 89.

PERAZZOLO MARRA, M., LIMA, J. A. & ILICETO, S. 2011. MRI in acute myocardial infarction. *Eur Heart J,* 32**,** 284-93.

PERNET, K., ECARNOT, F., CHOPARD, R., SERONDE, M. F., PLASTARAS, P., SCHIELE, F. & MENEVEAU, N. 2014. Microvascular obstruction assessed by 3-tesla magnetic resonance imaging in acute myocardial infarction is correlated with plasma troponin I levels. *BMC Cardiovasc Disord,* 14**,** 57.

PETRONIO, A. S., DE CARLO, M., CIABATTI, N., AMOROSO, G., LIMBRUNO, U., PALAGI, C., DI BELLO, V., ROMANO, M. F. & MARIANI, M. 2005. Left ventricular remodeling after primary coronary angioplasty in patients treated with abciximab or intracoronary adenosine. *Am Heart J,* 150**,** 1015.

PFAFFL, M. W., TICHOPAD, A., PRGOMET, C. & NEUVIANS, T. P. 2004. Determination of stable housekeeping genes, differentially regulated target genes and sample integrity: BestKeeper--Excel-based tool using pair-wise correlations. *Biotechnol Lett,* 26**,** 509-15.

PICCOLO, R., FRANZONE, A., KOSKINAS, K. C., RABER, L., PILGRIM, T., VALGIMIGLI, M., STORTECKY, S., RAT-WIRTZLER, J., SILBER, S., SERRUYS, P. W., JUNI, P., HEG, D. & WINDECKER, S. 2016. Effect of Diabetes Mellitus on Frequency of Adverse Events in Patients With Acute Coronary Syndromes Undergoing Percutaneous Coronary Intervention. *Am J Cardiol,* 118**,** 345-52.

PILLAI, R. S., BHATTACHARYYA, S. N. & FILIPOWICZ, W. 2007. Repression of protein synthesis by miRNAs: how many mechanisms? *Trends Cell Biol,* 17**,** 118-26.

PINTO, D. S., FREDERICK, P. D., CHAKRABARTI, A. K., KIRTANE, A. J., ULLMAN, E., DEJAM, A., MILLER, D. P., HENRY, T. D., GIBSON, C. M. & NATIONAL REGISTRY OF MYOCARDIAL INFARCTION, I. 2011. Benefit of transferring ST-segment-elevation myocardial infarction patients for percutaneous coronary intervention compared with administration of onsite fibrinolytic declines as delays increase. *Circulation,* 124**,** 2512-21.

PLIESKATT, J. L., FENG, Y., RINALDI, G., MULVENNA, J. P., BETHONY, J. M. & BRINDLEY, P. J. 2014. Circumventing qPCR inhibition to amplify miRNAs in plasma. *Biomark Res,* 2**,** 13.

PORTO, I., BIASUCCI, L. M., DE MARIA, G. L., LEONE, A. M., NICCOLI, G., BURZOTTA, F., TRANI, C., TRITARELLI, A., VERGALLO, R., LIUZZO, G. &

CREA, F. 2012. Intracoronary microparticles and microvascular obstruction in patients with ST elevation myocardial infarction undergoing primary percutaneous intervention. *Eur Heart J,* 33**,** 2928-38.

RAPOSO, G. & STOORVOGEL, W. 2013. Extracellular vesicles: exosomes, microvesicles, and friends. *J Cell Biol,* 200**,** 373-83.

RATHORE, S. S., BERGER, A. K., WEINFURT, K. P., SCHULMAN, K. A., OETGEN, W. J., GERSH, B. J. & SOLOMON, A. J. 2000. Acute myocardial infarction complicated by atrial fibrillation in the elderly: prevalence and outcomes. *Circulation,* 101**,** 969-74.

REFFELMANN, T. & KLONER, R. A. 2006. The no-reflow phenomenon: A basic mechanism of myocardial ischemia and reperfusion. *Basic Res Cardiol,* 101**,** 359-72.

REINSTADLER, S. J., FEISTRITZER, H. J., KLUG, G., MAIR, J., TU, A. M., KOFLER, M., HENNINGER, B., FRANZ, W. M. & METZLER, B. 2016. High-sensitivity troponin T for prediction of left ventricular function and infarct size one year following ST-elevation myocardial infarction. *Int J Cardiol,* 202**,** 188-93.

REZKALLA, S. H., DHARMASHANKAR, K. C., ABDALRAHMAN, I. B. & KLONER, R. A. 2010. No-reflow phenomenon following percutaneous coronary intervention for acute myocardial infarction: incidence, outcome, and effect of pharmacologic therapy. *J Interv Cardiol,* 23**,** 429-36.

ROBBERS, L. F., EERENBERG, E. S., TEUNISSEN, P. F., JANSEN, M. F., HOLLANDER, M. R., HORREVOETS, A. J., KNAAPEN, P., NIJVELDT, R., HEYMANS, M. W., LEVI, M. M., VAN ROSSUM, A. C., NIESSEN, H. W., MARCU, C. B., BEEK, A. M. & VAN ROYEN, N. 2013. Magnetic resonance imaging-defined areas of microvascular obstruction after acute myocardial infarction represent microvascular destruction and haemorrhage. *Eur Heart J,* 34**,** 2346-53.

ROBINSON, S., FOLLO, M., HAENEL, D., MAULER, M., STALLMANN, D., TEWARI, M., DUERSCHMIED, D., PETER, K., BODE, C., AHRENS, I. & HORTMANN, M. 2018. Droplet digital PCR as a novel detection method for quantifying microRNAs in acute myocardial infarction. *Int J Cardiol,* 257**,** 247-254.

ROFFI, M., PATRONO, C., COLLET, J. P., MUELLER, C., VALGIMIGLI, M., ANDREOTTI, F., BAX, J. J., BORGER, M. A., BROTONS, C., CHEW, D. P., GENCER, B., HASENFUSS, G., KJELDSEN, K., LANCELLOTTI, P., LANDMESSER, U., MEHILLI, J., MUKHERJEE, D., STOREY, R. F., WINDECKER, S. & GROUP, E. S. C. S. D. 2016. 2015 ESC Guidelines for the management of acute coronary syndromes in patients presenting without persistent ST-segment elevation: Task Force for the Management of Acute Coronary Syndromes in Patients Presenting without Persistent ST-Segment Elevation of the European Society of Cardiology (ESC). *Eur Heart J,* 37**,** 267-315.

SAEED, M., HETTS, S. & WILSON, M. 2010. Reperfusion injury components and manifestations determined by cardiovascular MR and MDCT imaging. *World J Radiol,* 2**,** 1-14.

SAKUMA, T., LEONG-POI, H., FISHER, N. G., GOODMAN, N. C. & KAUL, S. 2003. Further insights into the no-reflow phenomenon after primary angioplasty in acute myocardial infarction: the role of microthromboemboli. *J Am Soc Echocardiogr,* 16**,** 15-21.

SANTOVITO, D. & WEBER, C. 2017. Zooming in on microRNAs for refining cardiovascular risk prediction in secondary prevention. *Eur Heart J,* 38**,** 524-528.

SATSANGI, J., JEWELL, D. P., WELSH, K., BUNCE, M. & BELL, J. I. 1994. Effect of heparin on polymerase chain reaction. *Lancet,* 343**,** 1509-10.

SAYED, D., HONG, C., CHEN, I. Y., LYPOWY, J. & ABDELLATIF, M. 2007. MicroRNAs play an essential role in the development of cardiac hypertrophy. *Circ Res,* 100**,** 416-24.

SCHWARTZ, B. G. & KLONER, R. A. 2012. Coronary no reflow. *J Mol Cell Cardiol,* 52**,** 873-82.

SCHWARTZ, R. S., BURKE, A., FARB, A., KAYE, D., LESSER, J. R., HENRY, T. D. & VIRMANI, R. 2009. Microemboli and microvascular obstruction in acute coronary thrombosis and sudden coronary death: relation to epicardial plaque histopathology. *J Am Coll Cardiol,* 54**,** 2167-73.

SELVANAYAGAM, J. B., PORTO, I., CHANNON, K., PETERSEN, S. E., FRANCIS, J. M., NEUBAUER, S. & BANNING, A. P. 2005. Troponin elevation after percutaneous coronary intervention directly represents the extent of irreversible myocardial injury: insights from cardiovascular magnetic resonance imaging. *Circulation,* 111**,** 1027-32.

SEO, H., YOON, S. J., YOON, J., KIM, D., GONG, Y., KIM, A. R., OH, I. H., KIM, E. J. & LEE, Y. H. 2015. Recent trends in economic burden of acute myocardial infarction in South Korea. *PLoS One,* 10**,** e0117446.

SKYSCHALLY, A., SCHULZ, R., ERBEL, R. & HEUSCH, G. 2002. Reduced coronary and inotropic reserves with coronary microembolization. *Am J Physiol Heart Circ Physiol,* 282**,** H611-4.

SOLECKI, K., DUPUY, A. M., KUSTER, N., LECLERCQ, F., GERVASONI, R., MACIA, J. C., CUNG, T. T., LATTUCA, B., CRANSAC, F., CADE, S., PASQUIE, J. L., CRISTOL, J. P. & ROUBILLE, F. 2015. Kinetics of high-sensitivity cardiac troponin T or troponin I compared to creatine kinase in patients with revascularized acute myocardial infarction. *Clin Chem Lab Med,* 53**,** 707-14.

SOLOMON, S. D., GLYNN, R. J., GREAVES, S., AJANI, U., ROULEAU, J. L., MENAPACE, F., ARNOLD, J. M., HENNEKENS, C. & PFEFFER, M. A. 2001. Recovery of ventricular function after myocardial infarction in the reperfusion era: the healing and early afterload reducing therapy study. *Ann Intern Med,* 134**,** 451-8.

SON, D. J., KUMAR, S., TAKABE, W., KIM, C. W., NI, C. W., ALBERTS-GRILL, N., JANG, I. H., KIM, S., KIM, W., WON KANG, S., BAKER, A. H., WOONG SEO, J., FERRARA, K. W. & JO, H. 2013. The atypical mechanosensitive microRNA-712 derived from pre-ribosomal RNA induces endothelial inflammation and atherosclerosis. *Nat Commun,* 4**,** 3000.

SPINELLI, L., MORISCO, C., ASSANTE DI PANZILLO, E., IZZO, R. & TRIMARCO, B. 2013. Reverse left ventricular remodeling after acute myocardial infarction: the prognostic impact of left ventricular global torsion. *Int J Cardiovasc Imaging,* 29**,** 787-95.

STEEN, H., GIANNITSIS, E., FUTTERER, S., MERTEN, C., JUENGER, C. & KATUS, H. A. 2006. Cardiac troponin T at 96 hours after acute myocardial infarction correlates with infarct size and cardiac function. *J Am Coll Cardiol,* 48**,** 2192-4.

SUADES, R., PADRO, T., CRESPO, J., RAMAIOLA, I., MARTIN-YUSTE, V., SABATE, M., SANS-ROSELLO, J., SIONIS, A. & BADIMON, L. 2016. Circulating microparticle signature in coronary and peripheral blood of ST elevation myocardial infarction patients in relation to pain-to-PCI elapsed time. *Int J Cardiol,* 202**,** 378-87.

SUCHAROV, C., BRISTOW, M. R. & PORT, J. D. 2008. miRNA expression in the failing human heart: functional correlates. *J Mol Cell Cardiol,* 45**,** 185-92.

SUN, C., ALKHOURY, K., WANG, Y. I., FOSTER, G. A., RADECKE, C. E., TAM, K., EDWARDS, C. M., FACCIOTTI, M. T., ARMSTRONG, E. J., KNOWLTON, A. A., NEWMAN, J. W., PASSERINI, A. G. & SIMON, S. I. 2012. IRF-1 and

miRNA126 modulate VCAM-1 expression in response to a high-fat meal. *Circ Res,* 111**,** 1054-64.

SUN, L., JIANG, R., LI, J., WANG, B., MA, C., LV, Y. & MU, N. 2017. MicoRNA-425-5p is a potential prognostic biomarker for cervical cancer. *Ann Clin Biochem,* 54**,** 127-133.

SUN, Y. 2009. Myocardial repair/remodelling following infarction: roles of local factors. *Cardiovasc Res,* 81**,** 482-90.

SUNDERLAND, N., SKROBLIN, P., BARWARI, T., HUNTLEY, R. P., LU, R., JOSHI, A., LOVERING, R. C. & MAYR, M. 2017. MicroRNA Biomarkers and Platelet Reactivity: The Clot Thickens. *Circ Res,* 120**,** 418-435.

SWAANENBURG, J. C., VISSER-VANBRUMMEN, P. J., DEJONGSTE, M. J. & TIEBOSCH, A. T. 2001. The content and distribution of troponin I, troponin T, myoglobin, and alpha-hydroxybutyric acid dehydrogenase in the human heart. *Am J Clin Pathol,* 115**,** 770-7.

TERENTYEV, D., BELEVYCH, A. E., TERENTYEVA, R., MARTIN, M. M., MALANA, G. E., KUHN, D. E., ABDELLATIF, M., FELDMAN, D. S., ELTON, T. S. & GYORKE, S. 2009. miR-1 overexpression enhances Ca(2+) release and promotes cardiac arrhythmogenesis by targeting PP2A regulatory subunit B56alpha and causing CaMKII-dependent hyperphosphorylation of RyR2. *Circ Res,* 104**,** 514-21.

THYGESEN, K., ALPERT, J. S., JAFFE, A. S., CHAITMAN, B. R., BAX, J. J., MORROW, D. A., WHITE, H. D. & GROUP, E. S. C. S. D. 2018. Fourth universal definition of myocardial infarction (2018). *Eur Heart J*.

TOWNSEND, N., WILLIAMS, J., BHATNAGAR, P., WICKRAMASINGHE, K. & RAYNER, M. 2014. *Cardiovascular Disease statistics 2014,* London, British Heart Foundation.

TURCHINOVICH, A. & BURWINKEL, B. 2012. Distinct AGO1 and AGO2 associated miRNA profiles in human cells and blood plasma. *RNA Biol,* 9**,** 1066-75.

TZIVONI, D., KOUKOUI, D., GUETTA, V., NOVACK, L., COWING, G. & INVESTIGATORS, C. S. 2008. Comparison of Troponin T to creatine kinase and to radionuclide cardiac imaging infarct size in patients with ST-elevation myocardial infarction undergoing primary angioplasty. *Am J Cardiol,* 101**,** 753-7.

VALADI, H., EKSTROM, K., BOSSIOS, A., SJOSTRAND, M., LEE, J. J. & LOTVALL, J. O. 2007. Exosome-mediated transfer of mRNAs and microRNAs is a novel mechanism of genetic exchange between cells. *Nat Cell Biol,* 9**,** 654-9.

VAN DER LINDEN, N., STRENG, A. S., BEKERS, O., WODZIG, W., MEEX, S. J. R. & DE BOER, D. 2017. Large Variation in Measured Cardiac Troponin T Concentrations after Standard Addition in Serum or Plasma of Different Individuals. *Clin Chem,* 63**,** 1300-1302.

VAN KRANENBURG, M., MAGRO, M., THIELE, H., DE WAHA, S., EITEL, I., COCHET, A., COTTIN, Y., ATAR, D., BUSER, P., WU, E., LEE, D., BODI, V., KLUG, G., METZLER, B., DELEWI, R., BERNHARDT, P., ROTTBAUER, W., BOERSMA, E., ZIJLSTRA, F. & VAN GEUNS, R. J. 2014. Prognostic value of microvascular obstruction and infarct size, as measured by CMR in STEMI patients. *JACC Cardiovasc Imaging,* 7**,** 930-9.

VANDESOMPELE, J., DE PRETER, K., PATTYN, F., POPPE, B., VAN ROY, N., DE PAEPE, A. & SPELEMAN, F. 2002. Accurate normalization of real-time quantitative RT-PCR data by geometric averaging of multiple internal control genes. *Genome Biol,* 3**,** RESEARCH0034.

VASILE, V. C., BABUIN, L., GIANNITSIS, E., KATUS, H. A. & JAFFE, A. S. 2008. Relationship of MRI-determined infarct size and cTnI measurements in patients with ST-elevation myocardial infarction. *Clin Chem,* 54**,** 617-9.

VICKERS, K. C., PALMISANO, B. T., SHOUCRI, B. M., SHAMBUREK, R. D. & REMALEY, A. T. 2011. MicroRNAs are transported in plasma and delivered to recipient cells by high-density lipoproteins. *Nat Cell Biol,* 13**,** 423-33.

VIERECK, J. & THUM, T. 2017. Circulating Noncoding RNAs as Biomarkers of Cardiovascular Disease and Injury. *Circ Res,* 120**,** 381-399.

VILLARROYA-BELTRI, C., GUTIERREZ-VAZQUEZ, C., SANCHEZ-CABO, F., PEREZ-HERNANDEZ, D., VAZQUEZ, J., MARTIN-COFRECES, N., MARTINEZ-HERRERA, D. J., PASCUAL-MONTANO, A., MITTELBRUNN, M. & SANCHEZ-MADRID, F. 2013. Sumoylated hnRNPA2B1 controls the sorting of miRNAs into exosomes through binding to specific motifs. *Nat Commun,* 4**,** 2980.

VION, A. C., RAMKHELAWON, B., LOYER, X., CHIRONI, G., DEVUE, C., LOIRAND, G., TEDGUI, A., LEHOUX, S. & BOULANGER, C. M. 2013. Shear stress regulates endothelial microparticle release. *Circ Res,* 112**,** 1323-33.

VIRMANI, R., BURKE, A. P., FARB, A. & KOLODGIE, F. D. 2006. Pathology of the vulnerable plaque. *J Am Coll Cardiol,* 47**,** C13-8.

VOGEL, B., KELLER, A., FRESE, K. S., KLOOS, W., KAYVANPOUR, E., SEDAGHAT-HAMEDANI, F., HASSEL, S., MARQUART, S., BEIER, M., GIANNITIS, E., HARDT, S., KATUS, H. A. & MEDER, B. 2013. Refining diagnostic microRNA signatures by whole-miRNome kinetic analysis in acute myocardial infarction. *Clin Chem,* 59**,** 410-8.

VOGELSTEIN, B. & KINZLER, K. W. 1999. Digital PCR. *Proc Natl Acad Sci U S A,* 96**,** 9236-41.

WANG, F., LONG, G., ZHAO, C., LI, H., CHAUGAI, S., WANG, Y., CHEN, C. & WANG, D. W. 2013. Plasma microRNA-133a is a new marker for both acute myocardial infarction and underlying coronary artery stenosis. *J Transl Med,* 11**,** 222.

WANG, G., YANG, H. J., KALI, A., COKIC, I., TANG, R., XIE, G., YANG, Q., FRANCIS, J., LI, S. & DHARMAKUMAR, R. 2019. Influence of Myocardial Hemorrhage on Staging of Reperfused Myocardial Infarctions With T2 Cardiac Magnetic Resonance Imaging: Insights Into the Dependence on Infarction Type With Ex Vivo Validation. *JACC Cardiovasc Imaging,* 12**,** 693-703.

WANG, G. K., ZHU, J. Q., ZHANG, J. T., LI, Q., LI, Y., HE, J., QIN, Y. W. & JING, Q. 2010. Circulating microRNA: a novel potential biomarker for early diagnosis of acute myocardial infarction in humans. *Eur Heart J,* 31**,** 659-66.

WANG, T. K., SNOW, T. A., CHEN, Y., ROSTOM, H., WHITE, J. M., STEWART, J. T., WEBSTER, M. W., RUYGROK, P. N., WATSON, T. & WHITE, H. D. 2014a. High-sensitivity troponin level pre-catheterization predicts adverse cardiovascular outcomes after primary angioplasty for ST-elevation myocardial infarction. *Eur Heart J Acute Cardiovasc Care,* 3**,** 118-25.

WANG, X., HUANG, W., LIU, G., CAI, W., MILLARD, R. W., WANG, Y., CHANG, J., PENG, T. & FAN, G. C. 2014b. Cardiomyocytes mediate anti-angiogenesis in type 2 diabetic rats through the exosomal transfer of miR-320 into endothelial cells. *J Mol Cell Cardiol,* 74**,** 139-50.

WEBER, C. & NOELS, H. 2011. Atherosclerosis: current pathogenesis and therapeutic options. *Nat Med,* 17**,** 1410-22.

WEI, Y., NAZARI-JAHANTIGH, M., CHAN, L., ZHU, M., HEYLL, K., CORBALAN-CAMPOS, J., HARTMANN, P., THIEMANN, A., WEBER, C. & SCHOBER, A. 2013. The microRNA-342-5p fosters inflammatory macrophage activation through an Akt1- and microRNA-155-dependent pathway during atherosclerosis. *Circulation,* 127**,** 1609-19.

WEIR, R. A., MURPHY, C. A., PETRIE, C. J., MARTIN, T. N., BALMAIN, S., CLEMENTS, S., STEEDMAN, T., WAGNER, G. S., DARGIE, H. J. & MCMURRAY, J. J. 2010. Microvascular obstruction remains a portent of adverse remodeling in optimally treated patients with left ventricular systolic

dysfunction after acute myocardial infarction. *Circ Cardiovasc Imaging,* 3**,** 360-7.

WEN, D., LI, S., JI, F., CAO, H., JIANG, W., ZHU, J. & FANG, X. 2013. miR-133b acts as a tumor suppressor and negatively regulates FGFR1 in gastric cancer. *Tumour Biol,* 34**,** 793-803.

WHITE, H. D. 2000. Thrombolytic therapy in the elderly. *Lancet,* 356**,** 2028-30.

WILLEIT, P., ZAMPETAKI, A., DUDEK, K., KAUDEWITZ, D., KING, A., KIRKBY, N. S., CROSBY-NWAOBI, R., PROKOPI, M., DROZDOV, I., LANGLEY, S. R., SIVAPRASAD, S., MARKUS, H. S., MITCHELL, J. A., WARNER, T. D., KIECHL, S. & MAYR, M. 2013. Circulating microRNAs as novel biomarkers for platelet activation. *Circ Res,* 112**,** 595-600.

WILLIAMS, K. J. & TABAS, I. 1998. The response-to-retention hypothesis of atherogenesis reinforced. *Curr Opin Lipidol,* 9**,** 471-4.

WITWER, K. W., BUZAS, E. I., BEMIS, L. T., BORA, A., LASSER, C., LOTVALL, J., NOLTE-'T HOEN, E. N., PIPER, M. G., SIVARAMAN, S., SKOG, J., THERY, C., WAUBEN, M. H. & HOCHBERG, F. 2013. Standardization of sample collection, isolation and analysis methods in extracellular vesicle research. *J Extracell Vesicles,* 2.

WU, A. H. B. 2017. Release of cardiac troponin from healthy and damaged myocardium. *Frontiers in Laboratory Medicine,* 1**,** 144-150.

WU, K. C. 2012. CMR of microvascular obstruction and hemorrhage in myocardial infarction. *J Cardiovasc Magn Reson,* 14**,** 68.

WU, W., XIAO, H., LAGUNA-FERNANDEZ, A., VILLARREAL, G., JR., WANG, K. C., GEARY, G. G., ZHANG, Y., WANG, W. C., HUANG, H. D., ZHOU, J., LI, Y. S., CHIEN, S., GARCIA-CARDENA, G. & SHYY, J. Y. 2011a. Flow-

Dependent Regulation of Kruppel-Like Factor 2 Is Mediated by MicroRNA-92a. *Circulation,* 124**,** 633-41.

WU, X., MINTZ, G. S., XU, K., LANSKY, A. J., WITZENBICHLER, B., GUAGLIUMI, G., BRODIE, B., KELLETT, M. A., JR., DRESSLER, O., PARISE, H., MEHRAN, R., STONE, G. W. & MAEHARA, A. 2011b. The relationship between attenuated plaque identified by intravascular ultrasound and no-reflow after stenting in acute myocardial infarction: the HORIZONS-AMI (Harmonizing Outcomes With Revascularization and Stents in Acute Myocardial Infarction) trial. *JACC Cardiovasc Interv,* 4**,** 495-502.

YAN, D., DONG XDA, E., CHEN, X., WANG, L., LU, C., WANG, J., QU, J. & TU, L. 2009. MicroRNA-1/206 targets c-Met and inhibits rhabdomyosarcoma development. *J Biol Chem,* 284**,** 29596-604.

YANCY, C. W., JESSUP, M., BOZKURT, B., BUTLER, J., CASEY, D. E., JR., DRAZNER, M. H., FONAROW, G. C., GERACI, S. A., HORWICH, T., JANUZZI, J. L., JOHNSON, M. R., KASPER, E. K., LEVY, W. C., MASOUDI, F. A., MCBRIDE, P. E., MCMURRAY, J. J., MITCHELL, J. E., PETERSON, P. N., RIEGEL, B., SAM, F., STEVENSON, L. W., TANG, W. H., TSAI, E. J., WILKOFF, B. L., AMERICAN COLLEGE OF CARDIOLOGY, F. & AMERICAN HEART ASSOCIATION TASK FORCE ON PRACTICE, G. 2013. 2013 ACCF/AHA guideline for the management of heart failure: a report of the American College of Cardiology Foundation/American Heart Association Task Force on Practice Guidelines. *J Am Coll Cardiol,* 62**,** e147-239.

YOKOTA, M., TATSUMI, N., NATHALANG, O., YAMADA, T. & TSUDA, I. 1999. Effects of heparin on polymerase chain reaction for blood white cells. *J Clin Lab Anal,* 13**,** 133-40.

YOSHINO, H., CHIYOMARU, T., ENOKIDA, H., KAWAKAMI, K., TATARANO, S., NISHIYAMA, K., NOHATA, N., SEKI, N. & NAKAGAWA, M. 2011. The tumour-suppressive function of miR-1 and miR-133a targeting TAGLN2 in bladder cancer. *Br J Cancer,* 104**,** 808-18.

YOUNGER, J. F., PLEIN, S., BARTH, J., RIDGWAY, J. P., BALL, S. G. & GREENWOOD, J. P. 2007. Troponin-I concentration 72 h after myocardial infarction correlates with infarct size and presence of microvascular obstruction. *Heart,* 93**,** 1547-51.

ZAMPETAKI, A., WILLEIT, P., TILLING, L., DROZDOV, I., PROKOPI, M., RENARD, J. M., MAYR, A., WEGER, S., SCHETT, G., SHAH, A., BOULANGER, C. M., WILLEIT, J., CHOWIENCZYK, P. J., KIECHL, S. & MAYR, M. 2012. Prospective study on circulating MicroRNAs and risk of myocardial infarction. *J Am Coll Cardiol,* 60**,** 290-9.

ZELLER, T., KELLER, T., OJEDA, F., REICHLIN, T., TWERENBOLD, R., TZIKAS, S., WILD, P. S., REITER, M., CZYZ, E., LACKNER, K. J., MUNZEL, T., MUELLER, C. & BLANKENBERG, S. 2014. Assessment of microRNAs in patients with unstable angina pectoris. *Eur Heart J,* 35**,** 2106-14.

ZHANG, L., CHEN, X., SU, T., LI, H., HUANG, Q., WU, D., YANG, C. & HAN, Z. 2015a. Circulating miR-499 are novel and sensitive biomarker of acute myocardial infarction. *J Thorac Dis,* 7**,** 303-8.

ZHANG, R., LAN, C., PEI, H., DUAN, G., HUANG, L. & LI, L. 2015b. Expression of circulating miR-486 and miR-150 in patients with acute myocardial infarction. *BMC Cardiovasc Disord,* 15**,** 51.

ZHAO, Y., RANSOM, J. F., LI, A., VEDANTHAM, V., VON DREHLE, M., MUTH, A. N., TSUCHIHASHI, T., MCMANUS, M. T., SCHWARTZ, R. J. & SRIVASTAVA, D. 2007. Dysregulation of cardiogenesis, cardiac conduction, and cell cycle in mice lacking miRNA-1-2. *Cell,* 129**,** 303-17.

ZHOU, J., WANG, K. C., WU, W., SUBRAMANIAM, S., SHYY, J. Y., CHIU, J. J., LI, J. Y. & CHIEN, S. 2011. MicroRNA-21 targets peroxisome proliferators-activated receptor-alpha in an autoregulatory loop to modulate flow-induced endothelial inflammation. *Proc Natl Acad Sci U S A,* 108**,** 10355-60.

ZHU, M., HUANG, Z., ZHU, D., ZHOU, X., SHAN, X., QI, L. W., WU, L., CHENG, W., ZHU, J., ZHANG, L., ZHANG, H., CHEN, Y., ZHU, W., WANG, T. & LIU, P. 2017. A panel of microRNA signature in serum for colorectal cancer diagnosis. *Oncotarget,* 8**,** 17081-17091.

ZIJLSTRA, F., HOORNTJE, J. C., DE BOER, M. J., REIFFERS, S., MIEDEMA, K., OTTERVANGER, J. P., VAN 'T HOF, A. W. & SURYAPRANATA, H. 1999. Long-term benefit of primary angioplasty as compared with thrombolytic therapy for acute myocardial infarction. *N Engl J Med,* 341**,** 1413-9.

ZILE, M. R., MEHURG, S. M., ARROYO, J. E., STROUD, R. E., DESANTIS, S. M. & SPINALE, F. G. 2011. Relationship between the temporal profile of plasma microRNA and left ventricular remodeling in patients after myocardial infarction. *Circ Cardiovasc Genet,* 4**,** 614-9.

APPENDIX

Following submission of this thesis, a more comprehensive miRNA screening was performed to identify possible new candidate miRNA markers of MVO. The HTG EdgeSeq miRNA Whole Transcriptome Assay (miRNA WTA; HTG Molecular, Tucson, AZ, USA) was used to quantify 2,083 human miRNA transcripts using next-generation sequencing (NGS) in plasma collected prior to and at 90 min post-PPCI from STEMI patients with (n = 6) and without MVO (n = 6).

The HTG EdgeSeq miRNA Whole Transcriptome Assay (miRNA WTA) measures the expression of 2,083 human miRNA transcripts using next-generation sequencing (NGS). For each sample, 15µl of plasma was lysed with 15µl of HTG plasma lysis buffer and 3ul proteinase K (both HTG Molecular, Tucson, AZ, USA), then incubated for 180 minutes at 50°C with orbital shaking. From each prepared sample, 25µL were added per well to a 96-well sample plate and run on an HTG EdgeSeq Processor using the HTG EdgeSeq miRNA WTA (HTG Molecular, Tucson, AZ, USA). Sample miRNAs are protected with proprietary protection probes, while all non-hybridized probes and non-targeted RNA are degraded by S1 nuclease, resulting in a 1:1 stoichiometric ratio of probes to targeted RNA. Samples were subsequently individually barcoded by PCR with adapters and dual molecular barcodes via tailed primers. For PCR, 3ul sample was incubated with 6µl OneTaq PCR GC buffer, 2.4µl Hemo KlenTaq enzyme (both New England Biolabs), 0.2mM dNTPs, and 3µl F and R primers (HTG Molecular) in a 30µl reaction. Samples were heated at 95°C for 4 minutes, followed by 16 cycles of: 95°C for 15 seconds, 56°C for 45 seconds and 68°C for 45 seconds; then 68°C for 10 minutes. Barcoded samples were individually purified using AMPure XP beads (Beckman Coulter), quantitated using a KAPA Library Quantification kit (KAPA Biosystem, Wilmington, MA, USA) then pooled at a concentration of 4pM. The library was sequenced on an Illumina NextSeq (Illumina,

Inc., San Diego, CA) using a NextSeq 500/550 High Output Kit v2.5 (75 cycles) kit with two index reads and 5% PhiX spike-in as standard. Data were returned from the sequencer in the form of demultiplexed FASTQ files, with one file per original well of the assay. The HTG EdgeSeq Parser (HTG Molecular, Tucson, AZ, USA) was used to align the FASTQ files to the probe list to provide raw sequencing reads per miRNA.

A group of 17 miRNAs were expressed at least 2-fold higher in patients with MVO compared to patients without MVO (**Appendix Figure 1**). Notably, miR-133b was the most highly expressed miRNA in patients with MVO. Interestingly, miR-1 was not amongst this group of miRNAs. This might suggest that miR-133b might be a more specific marker for microvascular damage than miR-1. This needs to be investigated in further studies.

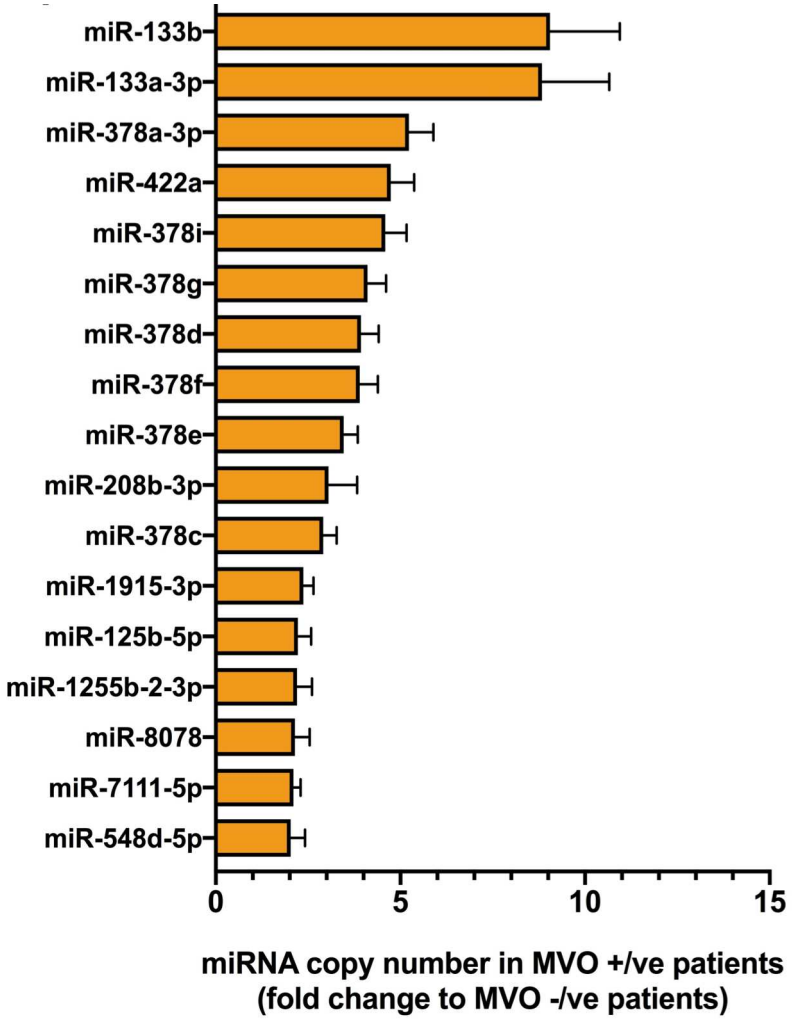

Appendix Figure 1. MiR-133b is the most highly expressed miRNA in patients with MVO. Group of 17 miRNAs presenting copy number at least two-fold higher in patient with MVO compared to patients without MVO at 90 min post-reperfusion (MVO +/ve n = 6; MVO -/ve n = 6) after screening of 2,083 miRNAs.